UNIVERSITAT DE BARCELONA

Spatio-temporal dynamics of intercellular Notch signaling: a modeling approach

Juan Camilo Luna-Escalante

Universitat de Barcelona

Ph.D. Thesis

Spatio-temporal dynamics of intercellular Notch signaling: a modeling approach

Author:
Juan Camilo Luna-Escalante

Advisor:
Dra. Marta Ibañes Miguez
Tutor:
Prof. José María Sancho Herrero

Memoria presentada para optar al título de Doctor en el Programa de Doctorado en Física de la Universidad de Barcelona

Departamento de Física de la Materia Condensada
Facultad de Física

July 2016

Declaration of Authorship

I, Juan Camilo Luna-Escalante, declare that this thesis titled, *Spatio-temporal dynamics of intercellular Notch signaling: a modeling approach*, and the work presented in it are my own. I confirm that:

- This work was done wholly or mainly while in candidature for a doctorate degree at this University.
- Where any part of this thesis has previously been submitted for a degree or any other qualification at this University or any other institution, this has been clearly stated.
- Where I have consulted the published work of others, this is always clearly attributed.
- Where I have quoted from the work of others, the source is always given. With the exception of such quotations, this thesis is entirely my own work.
- I have acknowledged all main sources of help.
- Where the thesis is based on work done by myself jointly with others, I have made clear exactly what was done by others and what I have contributed myself.

Signed: _____

Date: _____

A mi hermana y a mis padres

Acknowledgements

Writing this PhD Thesis is the culmination of four years of scientific and academic work. To me, my doctoral studies represent the accomplishment of a dream that I had back in school, but also the very first step of my career. It has been and intense and satisfactory experience, from which I have learned a lot (inside and outside my office). I could have not achieved any of this without the guidance, help and support of the people around me. I want to dedicate a few words to acknowledge those people.

My parents gave me the means and the meaning for pursuing my PhD studies. I do not have words to express my gratitude to them. I can only dedicate to them, and my sister, all the work done here.

First, I want to express my most sincere respect and gratitude to Dra. Marta Ibañes for the immense work you spent on my formation. Thank you very much for accepting me as your student during the master and the PhD. Both periods were very inspiring and developed inside me the motivation for continuing an academic career. You have deeply influenced the way in which I look at problems and understand explanations. Watching at the details is the first step to a work well done. ¡*Moltes gracies*!

I want to thank Prof. José María Sancho for being my tutor. Thanks a lot for the support along these years.

Thank you very much Pau (Dr. Pau Formosa-Jordan) for all the time you dedicated to the work we've done together. To me, you are an example of professionalism and hard work kindly done.

I want to thank the people with whom I was able to collaborate. Specially, Prof. Fernando Giráldez at the University Pompeu Fabra. I enjoyed and learned a lot from our discussions together with Jelena, Joana, Gina and Hector. Thank you all.

I also want to thank Dra. Ana I. Caño-Delgado and the other members of her group at the Centre de Recerca en Agrigenómica (CRAG). Lab meetings always were a source for new ideas and inspiration.

For the people at the Library of the Faculty of Pharmacy, with whom I was working these last two years, my most loving appreciation.

To the staff of the Department of *Estructura y Constituyentes de la Materia* and *Física de la Materia Condensada*, thank you for your work.

To the members of the evaluation committee, thank you very much for taking the time and effort in the evaluation of my work.

Last but not least, I want to thank all the people outside the faculty (although some of them did extra hours inside) for your support. It's been an incredible experience only because you were there. David and Sara, you were very important people to me along these years and I hope you remain being important in the coming years.

Contents

Declaration of Authorship ii

Acknowledgements v

Contents vii

List of Figures xi

List of Tables xv

1 Introduction 1
- 1.1 Systems biology and biophysics . . . 1
- 1.2 Metazoan development as a case of study of self-organization . . 2
  - 1.2.1 Early models of morphogenesis . . . 3
  - 1.2.2 Cell-to-cell communication in Metazoan: Juxtacrine signaling . . . 4
- 1.3 Juxtacrine signaling mediated by Notch . . . 6
  - 1.3.1 Notch signaling activation . . . 7
- 1.4 Lateral inhibition and periodic patterning in development . . . 8
  - 1.4.1 Collier et al. [1996] model of lateral inhibition . . . 9
  - 1.4.2 Other abstractions of lateral regulation mediated by Notch signaling . . . 10
  - 1.4.3 Lateral induction . . . 13
- 1.5 Scope of this Thesis . . . 14
  - 1.5.1 Different types of ligands can trigger Notch signaling . . . 14
  - 1.5.2 Lateral inhibition with self-activation of Atoh1 . . . 16
  - 1.5.3 Differential signaling efficiency between two co-expressed ligands triggering Notch signaling . . . 17

2 Notch signaling mediated by two co-expressing ligands 21

2.1 Introduction: lateral communication meditated by more than one type of Notch ligand . . . 21
2.1.1 Lateral inhibition and periodic pattern formation . . . 22
2.1.2 Lateral induction and ligand propagation . . . 25
2.1.3 Statement of the problem . . . 28
2.2 Modeling approach . . . 28
2.3 Results . . . 31
2.3.1 Equivalent ligands can drive either redundant or impaired responses . . . 31
2.3.1.1 Equally strong signaling ligands driving redundant states . . . 31
2.3.1.2 The co-expression of two equally regulated ligands can prevent the emergence of the functional response, even if one of the ligands signals weakly 34
2.3.2 Ligands equivalently regulated drive emergent responses when one of the ligands acts as a partial agonist . . . 41
2.3.2.1 The type of lateral regulation mediated by ligand2 changes to its opposite when it acts as a partial agonist . . . 41
2.3.2.2 The partial agonist can drive emergent responses when co-expressed with ligand1 . . . 44
2.3.3 Ligands oppositely regulated by Notch signaling can drive concerted responses functional when the ligand2 acts as a partial agonist . . . 48
2.3.3.1 The partial agonist cooperates to drive the same response driven by ligand1 expressed in isolation 48
2.3.3.2 Cooperation between ligands to drive pattern formation involves faster patterning dynamics . 55
2.3.4 Oppositely regulated ligands can drive oscillations . . . 60
2.3.5 The inner ear as a case of study . . . 67
2.4 Discussion . . . 73

3 Lateral inhibition and self-activation of Atoh1 77
3.1 Introduction: Lateral inhibition in the developing inner ear . . . 77
3.1.1 Atoh1 drives hair cell differentiation . . . 77
3.1.2 Hair cell differentiation and patterning can be robust to miss-expression of Delta1 *in vivo* . . . 79
3.1.3 Statement of the problem . . . 79
3.2 Modeling approach . . . 81
3.3 Results . . . 83
3.3.1 The outcome of the two models to miss-expression of Dl1 induced after differentiation is opposite . . . 83
3.3.2 Cell-autonomous multistability can drive irreversible differentiation and robust periodic patterning . . . 88

3.3.2.1 The self-activation of Atoh1 can drive irreversible HC differentiation . . . 89
3.3.2.2 The self-activation of Atoh1 drives robust HC periodic patterning . . . 94
3.3.3 Self-activation of Atoh1 can account for reported *in vivo* phenotypes . . . 98
3.3.3.1 The model with self-activation of Atoh1 can account for the role of Dl1 mediating lateral inhibition in the inner ear of the chick . . . 98
3.3.3.2 Errors in patterning can be explained by low Notch signaling at the onset of differentiation . . . 105
3.4 Discussion . . . 106

4 Characterization of the differential signaling efficiency between co-expressed Notch ligands 111
4.1 Introduction . . . 111
4.1.1 Statement of the problem . . . 112
4.2 Modeling approach . . . 113
4.2.1 Model with trans-interaction only. Reactions . . . 113
4.2.2 Model with trans-interaction only. Dynamic equations . . . 115
4.2.3 Model with cis-interactions . . . 116
4.2.4 Model assumptions . . . 117
4.2.4.1 Parameter values . . . 117
4.2.4.2 Relative signaling efficiency between ligands . . . 119
4.3 Results . . . 119
4.3.1 Complex-processing is essential to modulate the relative signaling efficiency between ligands . . . 120
4.3.2 Low values of the relative signaling efficiency can drive trans-inhibition of the signal by over-expression of the less efficient ligand . . . 122
4.3.3 Differential signaling efficiency only arises when intermediary complexes degrade . . . 123
4.3.4 The role of the ligand with slower dynamics of complex-processing can change in time . . . 127
4.3.5 The less efficient signaling ligand sequesters the receptor and enhances its degradation . . . 129
4.3.6 Cis-interactions can modulate the value of the relative signaling efficiency between ligands . . . 131
4.4 Discussion . . . 134

5 Conclusions 137
5.1 Overview . . . 137
5.2 Summary of the results . . . 138
5.2.1 Two co-expressed ligands can drive functional responses . . . 138

5.2.2 Lateral inhibition with self-activation of Atoh1 can drive robust hair cell differentiation . . . 140
5.2.3 Emergence of the differential efficiency between two ligands on Notch signaling activation . . . 141
5.3 Future perspectives . . . 142

A Linear stability analysis **145**
A.1 Linear stability analysis: One ligand . . . 145
A.2 Stability of the homogeneous state in the two and three ligands-scenario . . . 151

B Details on numerical analysis and simulations **155**
B.1 Phase diagrams . . . 155
B.2 Numerical simulations . . . 156
B.3 Basins of attraction . . . 157
B.4 Numerical corroboration of the phase diagrams . . . 158

C Resumen **163**
C.1 Introducción . . . 163
C.1.1 Contexto biológico . . . 163
C.1.2 Aproximación matemática . . . 164
C.2 Resumen de los resultados y conclusiones . . . 166
C.2.1 Respuestas funcionales en un sistema de comunicación inter-celular mediada por dos ligandos . . . 166
C.2.1.1 Motivación . . . 166
C.2.1.2 Aproximación y resultados . . . 166
C.2.2 Inhibición lateral mediada por la vía de Notch y auto-activación de Atoh1 . . . 168
C.2.2.1 Motivación . . . 168
C.2.2.2 Aproximación y resultados . . . 169
C.2.3 Estudio de un modelo detallado de la activación de la señal de Notch . . . 170
C.2.3.1 Motivación . . . 170
C.2.3.2 Aproximación y resultados . . . 170

Bibliography **173**

List of Figures

1.1 Reaction diffusion mechanism a pattern formation. 4
1.2 Juxtacrine signaling. 6
1.3 Notch signaling. 8
1.4 Abstractions of lateral regulation mediated by Notch signaling. . 12

2.1 Functional response mediated by a ligand repressed by Notch . . 24
2.2 Functional response mediated by a ligand activated by Notch . . 27
2.3 Periodic patterning in a system of equivalent ligands repressed by Notch 32
2.4 Ligand propagation in a system of equivalent ligands activated by Notch 33
2.5 Activity levels of the signal in the homogeneous steady state for ligands signaling equivalently 35
2.6 Periodic patterning in a system of ligands that signal differently and that are transcriptionally repressed by Notch 36
2.7 Bistability and ligand propagation in a system of ligands that signal differently and that are transcriptionally activated by Notch 38
2.8 Activity levels of the signal in the homogeneous steady state for ligands signaling differently 39
2.9 Signaling states after the over-expression of one of the ligands . . 40
2.10 Strength of the lateral regulation mediated by ligand2 when ligands are repressed by Notch 42
2.11 Strength of the lateral regulation mediated by ligand2 when ligands are activated by Notch 43
2.12 Ligand propagation and periodic patterning driven by the partial agonist 45
2.13 Ligand propagation driven by the partial agonist when ligands are respressed by Notch 46
2.14 Periodic patterning driven by the partial agonist when the transcription of the ligands is activated by Notch 47
2.15 Periodic patterning and ligand propagation driven by equivalent ligands oppositely regulated by Notch 49
2.16 Lateral communication mediated by oppositely regulated ligands 50

2.17 Bistability of homogeneous states and ligand propagation driven cooperatively by the two ligands 51
2.18 Types of ligand propagation occurring in the regime of trans-inhibition when ligand1 is activated and ligad2 is repressed by Notch 52
2.19 Signaling states involved in each emergent ligand propagation . . 52
2.20 Periodic patterning driven cooperatively by the two ligands . . . 53
2.21 Types of patterned states that arise in the regime of trans-inhibition when ligand1 is repressed and ligad2 is activated by Notch 54
2.22 Patterning dynamics driven by co-expressing ligands in the linear regime 57
2.23 59
2.23 Patterning dynamics driven by co-expressing ligands inferred from numerical simulations 60
2.24 Antagonistic ligands driving oscillations 61
2.25 Oscillatory dynamics of the inter-cellular signaling system (short time) 62
2.26 Oscillatory dynamics of the inter-cellular signaling system (long time) 63
2.27 Oscillation of the inhomogeneous state in the two cells system . . 64
2.28 Functional response of the two cell system for decreasing levels of the mutual trans-activation of the signal (r_2) 66
2.29 Oscillation of the inhomogeneous state in the two cells system . . 67
2.30 Regime of spontaneous hair cell patterning for the system with 3 co-expressed ligands 69
2.31 Regime of predicted Hair Cell patterning when Jag2, Dl1 and Jag1 are co-expressed 70
2.32 Signaling states driven by 3 co-expressed 72

3.1 Schematic representation of the Notch signaling with self-activation of Atoh1. 78
3.2 Our schematic summary of results of the *in vivo* experiments in the inner ear of the chick. 80
3.3 Hair cell differentiation dynamics and patterning in the LI and SA models 84
3.4 *In silico* electroporation with exogenous Dl1. 85
3.5 Effect of d_{ex} in cell fate determination in the LI and SA models . 86
3.6 Effect of d_{ex} in cell fate determination in the LI and SA models . 87
3.7 Trans-differentiation events after d_{ex} induction in the LI and SA models 88
3.8 Dl1-Notch regulation in the one cell scenario 89
3.9 Stable steady states of Atoh1 activity in the one cell scenario . . 90
3.10 Dl1-Notch regulation in the two coupled cells scenario 90
3.11 Stable steady states in the two coupled cells scenario 92
3.12 Induction of d_{ex} in cell 1 after cell 2 differentiates into HC 93

3.13 Spatial organization of HCs and SCs. 94
3.14 Cartoon of the reduced cell type model 95
3.15 Cell fate determination in the reduced model of hexagonal cells . 96
3.16 Periodic patterning when exogenous Dl1 is homogeneously expressed 97
3.17 Differentiation of HCs on large arrays of hexagonal cells 100
3.18 102
3.18 Miss-expression of Dl1 trough type I electroporation in large arrays of hexagonal cells. 103
3.19 104
3.19 Miss-expression of Dl1 trough type II electroporation in large arrays of hexagonal cells. 105
3.20 Errors in patterning by contacts between adjacent 106
3.21 Bistability driven by a self-activation loop 107

4.1 Schematic representation of the two cell scenario. 113
4.2 Relative signaling efficiency of ligand2 with respect to ligand1 (ε_s). 121
4.3 Concentration of the signal in the stationary state as a function of the production rate of ligand2. 123
4.4 Complex formation, processing and leaking pathways during signal activation. 124
4.5 Relative signaling efficiency (ε_s) at the stationary state as a function of the rate of active complexes degradation (γ_{C^*}). 126
4.6 Concentration of the signal at the stationary state as a function of the production rate of ligand2 (variable complexes degradation). 127
4.7 Concentration of the signal as a function of the production rate of ligand2, evaluated at early and late times. 128
4.8 Effect of over-expression of ligand2 on the concentration of the signal for variable time of evaluation and enzyme concentration. 130
4.9 Receptor occupancy at the stationary state with and without a differential signaling efficiency between the ligands. 132
4.10 Relative signaling efficiency at the stationary state as a function of the binding rates of ligand2 to the receptor in cis and trans. . 133
4.11 Concentration of the signal at the stationary state as a function of the production rate of ligand2 in a model with cis-interactions. 134

C.1 Respuestas en un tejido mediadas por la vía de Notch 165

List of Tables

2.1 Summary of the values of the signaling efficiency of Dl1 and Jag1 in Fig. 2.31 69

4.1 Parameter values for the numerical simulations. 118

B.1 Numerical corroboration of Fig. 2.3C 159
B.2 Numerical corroboration of Fig. 2.12A 159
B.3 Numerical corroboration of Fig. 2.12B 160
B.4 Numerical corroboration of Fig. 2.17B 160
B.5 Numerical corroboration of Fig. 2.20B 161

Chapter 1

Introduction

1.1 Systems biology and biophysics

In the last decades, cell and molecular biologists have described in impressive detail the molecular scaffold above which living beings are built [Alberts et al., 2013]. Given the great number of factors involved in biological processes, i.e., proteins, genes and small molecules among others, it remains difficult to associate this complex structures with the systems behavior. A systemic approach can be useful to understand the principles by which this molecular scaffold functions.

Systems biology is a field of research that uses mathematical modeling and computational methods, among other approaches, to address complex phenomena in biology arising at the system-level [Alon, 2006, Kitano, 2002, Kitano et al., 2001]. The realm of these observations and analysis is focused mainly on the biological domain. This approach has lead to a better understanding of several biological processes, spanning from cells and tissues to organisms. Biophysics involves the study of the physical attributes of biological systems. In some cases, these attributes arise at a system-level. For instance, the degree of organization of a tissue can be seen as a physical aspect that can not be defined locally (i.e., by exploring the individual cells forming the tissue), but requires information of the entire system (in this case, the tissue). The main framework of this Thesis is grounded both in biophysics and systems biology. Our

approach combines mathematical modeling and analysis with numerical simulations to describe and understand processes occurring by the interaction between macromolecules (proteins) at the intra-cellular levels, but also between cells at the inter-cellular level. Using this modeling proposal, we studied and measured physical properties of developing cell arrays, as the degree of organization and the stability of the arising states. But also, our analysis is important to obtain conclusions on the realm of developmental biology as will be describe below.

1.2 Metazoan development as a case of study of self-organization

Self-organized phenomena involve spatial and/or temporal spontaneous coordination without the presence of long-range driving forces mediating such coordination [Nicolis et al., 1989]. Simple, yet non-linear interactions between the components can account for the self-organization of a system [Prigogine, 1987]. The dynamics of self-organized phenomena occur under non-equilibrium conditions. Temporal self-organized phenomena can be exemplified by an oscillatory dynamics arising in a system of chemical components interacting far from equilibrium [Gray and Scott, 1985].

Living systems exhibit complex behavior and self-organizing phenomena [Kauffman, 1993, Smith and Morowitz, 2004]. This type of behavior arises at different levels, scaling from populations of organisms to tissues and cells [Karsenti, 2008, Lehn, 2002, Strogatz, 2014]. Metazoan development stands as an important example of collective, self-organized behavior in biology [Kauffman, 1987, Müller and Newman, 2003]. During development, specific cell types arise upon the spatial-temporal coordinated interplay between cell proliferation, migration and differentiation. For instance, during the formation of neural-sensory organs of vertebrates, cells follow a temporal sequence of differentiation such that neurons differentiate first inhomogeneously [Fekete and Wu, 2002, Neves et al., 2013a]. After differentiation, neurons migrate and relocate at the cortex and the remaining cells adopt a prosensory phenotype homogeneously. Later, this homogeneous tissue undergoes inhomogeneous differentiation of sensory and non-sensory cells.

Despite biological systems comprise an overwhelming ensemble of molecular components and biochemical interactions, the basic mechanisms underlying self-organized phenomena in these systems can be expected to be accounted in terms of few components and simple interactions.

1.2.1 Early models of morphogenesis

An example of spatial self-organization is spontaneous periodic patterning. With the focus on morphogenesis of developing tissues, Alan Turing developed a theoretical approach from which it can be established under what conditions periodic patterning can arise spontaneously in a system of interacting chemicals of different nature[1] [Turing, 1952]. Turing modeling is based on a *reaction-diffusion* system, in which there are two types of chemical components, an inhibitor and an activator. These components interact mutually such that the activator activates the inhibitor while the inhibitor inhibits the activator, as described in Fig. 1.1A. The activator can also promote its own production, in a process called *auto-catalysis*. This type of auto-regulatory processes and interaction introduce non-linear terms in the equations that describe the dynamics of the chemical reactants[2]. In addition, the model assumes that the two reactants diffuse differently, such that the inhibitor diffuse faster than the activator, and that they are produced and destroyed with constant rates (Fig. 1.1).

Turing work is based on the linear analysis of the stability of the homogeneous state, which in infinite spatially extended systems involves translational invariance. Turing found that when the components interact without diffusion, then the homogeneous state is expected to be stable [Murray, 2001]. Interestingly, when the chemical components diffuse, the homogeneous state can become unstable to small perturbations such that certain periodic structures can arise (Fig. 1.1B). In this system there is no long-range driving force taking place, and the emergence of long range spatial structures is due to the interaction between the components, of which the auto-catalytic step is of great relevance.

This model has been used as a theoretical tool to understand periodic patterns arising in Metazoan developing tissues [Green and Sharpe, 2015, Kondo and

[1] A detailed explanation of the Turing analysis can be found in [Murray, 2001]. Here we only outline the most relevant aspects of that approach to our purposes.

[2] Although important, self-regulating processes are not the only source of non-linearity in chemical reactions.

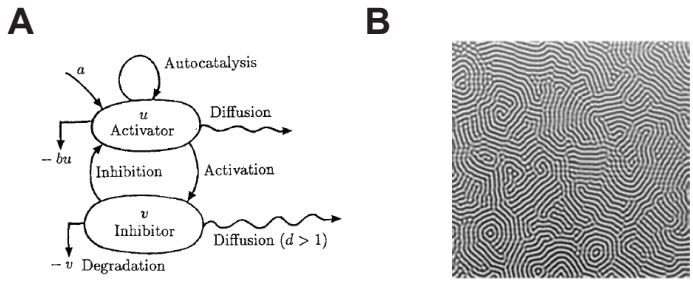

Figure 1.1 Reaction diffusion mechanism a pattern formation. A) Schematic representation of a reaction-diffusion like mechanism as that B) Real photography of an patterned state obtained by a chemical reaction-diffusion mechanism. These images are taken from [Murray, 2001] without modifications.

Miura, 2010, Marcon and Sharpe, 2012, Painter et al., 1999]. In fact, Turing himself hypothesized that the chemical components described in his idealized model could be seen as *morphogens* taking place in living organisms during their development [Turing, 1952]. Despite the material identification of these morphogens remains elusive, Turing framework constitutes a relevant mathematical basis for the study of patterning in developmental biology [Kondo and Miura, 2010]. It is a great example of how simple interactions between few components can drive the formation of complex structures.

1.2.2 Cell-to-cell communication in Metazoan: Juxtacrine signaling

How spatial-temporal coordination in cell differentiation arises is a problem of great relevance in developmental biology. Cell-to-cell communication is a mechanism that can account for the coordinated events occurring between cells in Metazoan [3] [Singh and Harris, 2005]. This type of communication can be mediated by[4]:

[3] Different forms of cell-to-cell communication also arise in unicellular organisms and Bacteria as well [Bassler, 2002, Miller and Bassler, 2001].

[4] The examples listed below are only illustrative and in any case are an extensive list of all possible types of cell-to-cell communication mechanisms observed.

1. paracrine signaling by soluble factors released in the extra-cellular matrix within a tissue, as occurs during the segmentation of the *Drosophila* embryo [Lewis, 1978],

2. Cell-Adhesion Molecules (CAM), which are involved for instance in axon orientation and migration, but also can stimulate neurite growth [Doherty et al., 1990], and

3. juxtacrine signaling mediated by ligand[5] –receptor physical interactions at the cell membrane of neighboring cells [Fagotto and Gumbiner, 1996, Singh and Harris, 2005, Zimmerman et al., 1993].

In this Thesis we focus on juxtacrine signaling. This type of signaling occurs upon physical contacts between neighboring cells trough proteins attached to the cell membrane, which typically are membrane-attached ligands and receptors. Because of this, cells can only interact with their closest adjacent neighbors, in contrast to those mechanisms that involve soluble factors. These interactions involve the formation of a ligand–receptor complex (Fig. 1.2). In turn, this complex engages directly or indirectly signaling pathways that mediate the activity of transcription factors in the receptor-carrying cell.

Given the scale length at which these juxtacrine interactions occur they are considered as *short-range* interactions. However, in some cases cells can generate prolongations of the plasmic membrane, extending the range of the physical interactions[6]. In this thesis we only address juxtacrine signaling involving short range interactions. In the following we will describe how this type of interactions can drive complex behavior, i.e., coordination and self-organization of cell-fate commitment at the tissue level.

There are several membrane proteins that can drive juxtacrine signaling [Massague and Pandiella, 1993]. In some cases, cell communication occurs trough proteins that can be found in a membrane-attached or in a soluble form, such that the same kind of molecules are driving juxtacrine and paracrine signaling concomitantly. For instance, Activation of the Tumor Necrosis Factor receptor

[5] Herein after, we refer to ligands within a biochemical context. In this regard, ligand refers to a protein forming a complex with another protein, which we will call receptor according to standard terminology.

[6] These prolongations are known as *filopodia*. It has been shown that filopodia are relevant to determine the spatial periodicity in the bristle patterning, at which sensory cells arise during the development of the eye of *Drosophila* [Cohen et al., 2010].

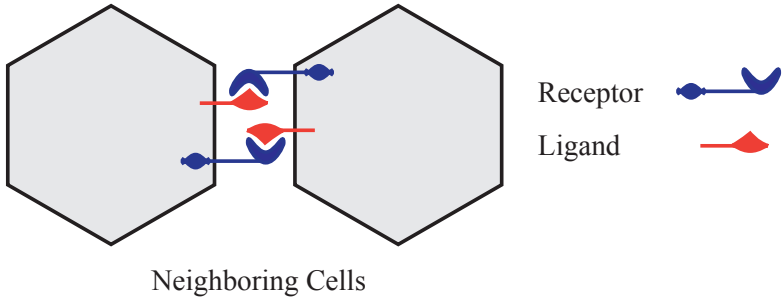

Figure 1.2 Juxtacrine signaling. Schematic representation of two neighboring cells mutually communicating through juxtacrine signaling. Membrane-attached ligand and receptor mediate the physical interaction.

(rTNF) can occur by binding both to membrane-attached or soluble forms of TNF. In other cases, the primary source of signal activation is attributed to ligands attached to the cell membrane. This is the case of Notch signaling. In the following section we describe in detail the activation of Notch signaling from a biochemical standpoint, since it is the biological reference in which is based the majority of the approach presented in this Thesis.

1.3 Juxtacrine signaling mediated by Notch

Notch signaling is an example of juxtacrine signaling occurring during metazoan development. Genetic studies have shown that Notch receptor and ligands are expressed at different stages during development in vertebrates and *Drosophila*. Notch signaling mediates several coordinated cell fate decisions, orchestrating the development of sensory organs in vertebrates Chitnis [1995], the imaginal disk of the eye in *Drosophila* [Roignant and Treisman, 2009], pancreas [Apelqvist et al., 1999], intestine [VanDussen et al., 2012] and immune cells [Radtke et al., 2004], among others. The role of Notch signaling during development can be sometimes difficult to unravel as different outcomes can be obtained by blocking Notch. For instance, the disruption of Notch signaling during the development of the inner ear of vertebrates can lead either to depletion or overproduction of sensory cells, depending on the stage at which the blockage is done [Brooker et al., 2006]. These opposite outcomes are due to the complexity of Notch signaling, which can be attributed to the wide genetic

battery which is transcriptionaly regulated by Notch signaling (reviewed in [Fortini, 2009]), the post-transcriptional modifications of Notch receptor, which can modulate its interaction with ligands [Hicks et al., 2000, LeBon et al., 2014, Panin et al., 1997, Yang et al., 2005] or the repertory of different ligand types triggering Notch signaling differently (reviewed in [D'souza et al., 2008]), among other factors.

1.3.1 Notch signaling activation

Juxtacrine signaling mediated by Notch follows the trans-interaction between the transmembrane Notch receptor with membrane-bound DSL (Delta/Serrate also known as Jagged/Lag2) ligands anchored on the membranes of neighboring cells [Kopan and Ilagan, 2009]. Different type of ligands can bind to Notch receptor with different affinity. It has been shown that glycosiltransferase proteins Fringe can modulate differently the binding rate of each type of ligand to Notch receptor [Hicks et al., 2000, Panin et al., 1997]. After this trans-interaction, the cytoplasmic portion of Notch receptor undergoes consecutive cleavage events (Fig. 1.3). These are mediated by proteases, whose activity is dependent on the conformational state of Notch. Upon ligand-receptor binding, Notch receptor undergoes a conformational change in which the binding site for the proteases is exposed. It has been shown that effective Notch signaling requires endocytosis of the ligand in the signaling cell[7]. This process in turn could be different for each type of ligand, but more experimental evidences are needed in this direction. In addition, it has been shown that Fringe can also be involved in the modulation of the effective rate of signaling mediated by each ligand. This rate is independent of the affinity of the ligand to bind to Notch [Yang et al., 2005]. After cleaving, the Notch intracellular domain (NICD, hereafter referred to as the signal) is released and translocates to the nucleus (recently reviewed in [Fortini, 2009]). Notch signal can associate with other transcription factors to regulate the transcription of target genes involved in cell differentiation and proliferation among others. In particular, Notch signaling is known to activate basic Helix Loop Helix transcription factors Hes and Hey, which are repressors of the proneural genes (reviewed in [Fischer and Gessler, 2007]). In this regard, Notch signaling can prevent neural-sensory differentiation. It has been shown

[7] In this context, *signaling cells* are those cells triggering Notch signaling on their neighbors through ligand expression. In Chapter 2 we definin more detail this concept.

that the repressor Hes and Hey can act as repressors of its own transcription as well. In contrast, genes involved in sensory cells differentiation, as Atoh1, can drive the activation of its own transcription.

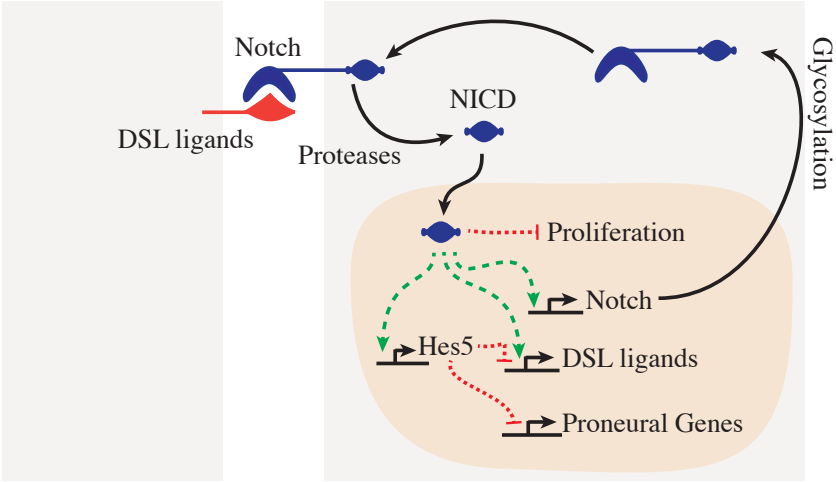

Figure 1.3 Notch signaling. Schematic representation of the Notch signaling activated upon binding with ligands attached to the membrane of neighboring cells. Canonical signal activation requires the activity of proteases. Upon proteolysis, the cytoplasmic domain of Notch translocates to the nucleus to regulate genetic transcription. The genes of the ligands that activate the signal in the first place and the gene of Notch receptor are among the targets of Notch signal.

1.4 Lateral inhibition and periodic patterning in development

Notch signaling is known to regulate the transcription of the ligands which in first place are responsible for signaling activation. This establishes a feedback mechanisms in the process of lateral regulation (i.e., that regulation a cell exerts on its adjacent neighbors) mediated by Notch signaling. Ligands transcription can be either activated or repressed by Notch. Examples of ligands repressed by Notch signaling are Delta in the ommatidial crystal of *Drosophila* [Lubensky et al., 2011], Delta4 in angiogenesis [Benedito et al., 2009], and Delta 1 (Dl1) and Jagged2 (Jag2) in the developing inner ear of vertebrates [Kiernan et al.,

2001, Neves et al., 2011]. In turn, Jagged1 is a type of ligand that can be activated by Notch signaling.

The type of regulation that Notch signaling exerts on the ligand transcription has been associated to the type of lateral regulation mediated by Notch. When the ligand triggering Notch signaling is repressed by the signal, then it is said to act in lateral inhibition. In this type of lateral regulation, a cell inhibits an adjacent cell to adopt its same cell fate [Pickles and van Heumen, 2000, Zine et al., 2000]. When all adjacent cells are competent to trigger signaling, lateral inhibition becomes mutual between cells. Lateral inhibition with feedback has been proposed to account for cell fate determination and periodic patterning arising during development of neural-sensory organs [Collier et al., 1996]. For instance, the regular selection of few cells to become neurons among surrounding non-neurogenic cells during vertebrate retina development [Formosa-Jordan et al., 2013, Harris, 1997, Livesey and Cepko, 2001, Marquardt and Gruss, 2002], or the specification of hair cells, surrounded by supporting cells during the development of sensory organs [Daudet and Lewis, 2005, Neves et al., 2012, Zine et al., 2000].

1.4.1 Collier et al. [1996] model of lateral inhibition

Notice that lateral regulation and communication mediated by Notch signaling can be reduced to two main steps; (i) signal activation mediated by the ligand and (ii) transcriptional regulation of the ligand mediated by the signal. In this regard, the state of a cell within an array can be described using only two variables, one accounting for the levels of the signal activity and the other for the ligand activity. This was indeed the proposal made by Collier et al. [1996] of a model of juxtacrine signaling mediated by the Delta-Notch system based on two regulatory steps[8]. In this model, the signal activity in one cell is promoted by the ligands in neighboring cells, while the activity of the ligand is repressed by the signal, i.e., the ligand acts in *lateral inhibition*[9].

[8] Details on the model equations and on the linear stability analysis of the Collier et al. [1996] model can be found in Chapter 2 and Appendix A.

[9] In Chapter 2 we present our mathematical interpretations of lateral inhibition.

Collier et al. [1996], performed a study of the stability of the homogeneous stationary state[10] to small perturbations of any wavelength, within the limits of the cell array, evaluated within the linear regime of the dynamics. When the homogeneous state results unstable to one or several periodic perturbations, then the array of cells is expected to evolve to a periodic patterned state dictated partially by the periodicity of the fastest growing perturbation[11]. This analysis revealed that if mutual lateral inhibition between neighboring cells is sufficiently strong (i.e., if cells are sufficiently sensitive to inhibition by their neighbors), then a positive feedback loop on ligand activity can arise that unstabilizes the homogeneous steady state and drives periodic patterning. Interestingly, the periodicity of the perturbations which is expected to first unstabilize the homogeneous state is consistent to that observed in developing sensory organs [Goodyear and Richardson, 1997].

Since this type of stability analysis evaluates the growth of the perturbations in the linear regime, then very small perturbations are expected to be sufficient to drive patterning [Collier et al., 1996]. In cell systems, these variations are expected to be due to random fluctuations on the transcriptional activity of the ligand from cell to cell or in the degradation of the ligand and the signal[12] (see for instance [Blake et al., 2003]).

1.4.2 Other abstractions of lateral regulation mediated by Notch signaling

Despite the model of Collier *et al* involves a significant simplification of the Notch signaling pathway, simpler models can also account for periodic patterning in cell arrays. In this regard, mutual inhibition between neighboring cells can be modelled through one single regulatory step (Fig. 1.4A). These simpler versions of lateral inhibition have been used to address other processes relevant for periodic pattern formation. For instance, it has been shown that cell proliferation and migration can enhance the ordering degree of the arising pattern mediated by lateral inhibition [Pers et al., 2012]. Models of lateral inhibition

[10] In this case, the homogeneous state is defined as that where the activity levels of the signal and the ligand are the same in all the cells within the array.

[11] In Appendix A we describe mathematically the linear stability analysis and the conditions for spontaneous pattern formation.

[12] The geometry of the cells can also be a source of fluctuations between cells [Gibson et al., 2006].

involving a single variable has been used also to address the effect of time delays in the dynamics and structure of the patterning. For instance, Momiji and Monk [2009] showed that when cells mutually interact, such that they inhibit each other (by a single state variable), and there is a time delay in the process of inhibition then either transient or stable oscillations can arise at the onset of patterning or cells can oscillate steadily in phase. Additionally, signaling delays in lateral inhibition can mediate error-free patterned states [Glass et al., 2016], i.e., patterned states in which the expected periodicity predicted from the linear stability analysis realizes without defects. Cell-to-cell interactions can involve more than one communicating pathway. In turn, the activation of each pathway can be modeled by a single regulatory step. For instance, de Back et al. [2013] modeled the interaction between neighboring cells using both Notch-pathway elements mediating lateral inhibition together with gap junctions molecules mediating *lateral stabilization*[13]. They showed that lateral stabilization can modulate the periodicity of the patterned states, such that cell differentiation can occur in a more scattered way than that driven by lateral inhibition alone.

Other modeling approaches use the two regulatory steps proposed by Collier et al. [1996] to describe lateral regulation (Fig. 1.4B). For instance, a recent work [Formosa-Jordan and Ibañes, 2014] propose an extension of the model of Collier et al. [1996] to include the interactions of the ligand with Notch receptor in the same cell, which are known as cis interactions [Jacobsen et al., 1998, Schweisguth, 2004]. The authors showed that cis-inhibition (i.e., when the interaction in cis prevent Notch signaling activation) can modulate the ratio of cell differentiation within the cell array, and allows pattern localization (i.e., there can be an arising patterned state which does not propagate along the array) [Formosa-Jordan and Ibañes, 2014]. In addition, the model of Collier et al. [1996] can be extended such that Notch signaling is activated either by juxtacrine or paracrine interactions, or both. In this regard, the ligand can exist both membrane-anchored and in soluble form. By modelling Notch signaling through two steps (signal activation and ligand repression), Formosa-Jordan and Ibañes [2009] showed that when the ligand can exist in soluble form, which effectively triggers Notch signaling, then patterning is prevented as the diffusion

[13] In the context of this work [de Back et al., 2013], the authors termed lateral stabilization the positive feedback loop between neighboring cells, formed by mutual activating interactions.

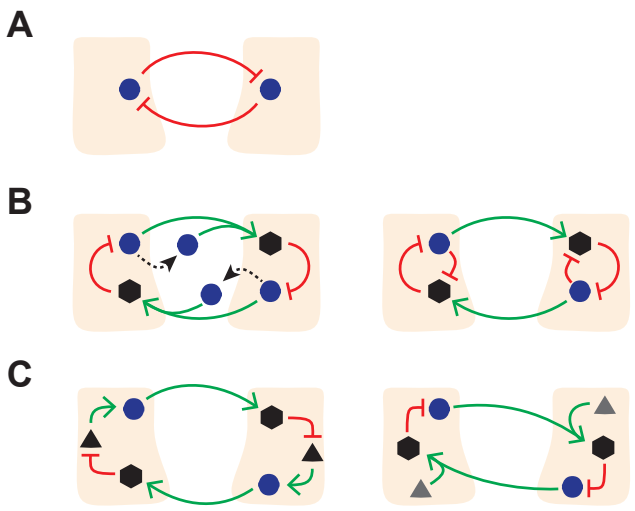

Figure 1.4 Abstractions of lateral regulation mediated by Notch signaling. Schematic representation of the topology of interactions used to model lateral inhibition mediated by Notch signaling. Signal to ligand inhibition A) in one regulatory step, B) in two regulatory steps or C) in three regulatory steps. A) A single variable describes the state of each cell and there is mutual inhibition between cells. This variable can be interpreted both as the ligand of the Notch signal activity. B) The ligand (blue disc) present in one cell activates the formation of the signal (black rhombus) in a neighboring cell, which in turn represses the ligand activity. We have represented the cases in which the ligand can attached in the cell membrane or as soluble factor (left), as described by [Formosa-Jordan and Ibañes, 2009], and the case in which the ligand acts also in cis inhibition (right), as described by [Formosa-Jordan and Ibañes, 2014]. C) The ligand is activated by an intermediary species (black triangle) which in turn is repressed by the signal, as described by [Petrovic et al., 2014] (left). The ligand and the receptor (gray triangle) form an intermediary species which regulates the transcription of the ligand, as described by [Owen et al., 2000, Wearing et al., 2000].

rate of the soluble form of the ligand increases [Formosa-Jordan and Ibañes, 2009].

Finally, lateral regulation has been modeled detailing more elements on the Notch pathway (Fig. 1.4C). For instance, the model proposed by Wearing et al. [2000] considers explicitly the dynamics of the ligand and receptor binding and unbinding. Upon ligand-receptor binding, there is the formation of an intermediary molecule which regulates the transcription of the ligand. This type of modeling involves more richness in the dynamics of the ligand since it considers the degradation of the ligand after binding to the receptor. This model

has been also extended in order to account for cis-interactions [Sprinzak et al., 2010]. The authors showed that cis-inhibition can facilitate periodic pattern formation and enhances the patterning dynamics Sprinzak et al. [2010, 2011]. The effect of post-translational modifications of the receptor have also been modelled (see for instance Boareto et al. [2015]). While including multiple steps of Notch signaling enables a more detailed description of the dynamics, it also entails a much larger set of yet unknown parameters. Therefore, a fundamental task of the modeller is to decide which level of description is appropriate for the question posed and for the available information of the system under study.

1.4.3 Lateral induction

When Notch signaling promotes the transcription of the ligands, the type of lateral regulation in which the ligand is acting is termed lateral induction[14] (see for example [Hartman et al., 2010]). When the ligand is acting in lateral induction, cells can induce their neighbors to adopt its same cell fate [Hartman et al., 2010, Neves et al., 2011]. Lateral induction is proposed to underlie the specification of prosensory patches during development of the inner ear in vertebrates [Daudet and Lewis, 2005, Hartman et al., 2010, Neves et al., 2011], the differentiation of the lens fiber in rats [Saravanamuthu et al., 2009], and muscle differentiation in mice [Manderfield et al., 2012], as well as embryonic endocrine epithelial-to-mesenchymal transitions and oncogenic transformation [Timmerman et al., 2004]. *In vitro* experiments have shown that lateral induction mediated by mutual ligand-signal activation can results in Notch signaling propagation, following a wave-like behavior [Matsuda et al., 2012]. Yet, up to now little attention has been devoted to lateral induction, possibly because fewer type of ligands ligands activated by Notch are known [D'souza et al., 2008]. Because of this, examples of lateral inhibition phenomena arising *in vivo* could be less frequent.

Regarding modeling, lateral induction can be described as a single-step [de Back et al., 2013], two-step [Matsuda et al., 2012, Owen et al., 2000, Petrovic et al., 2014] or multiple-steps [Boareto et al., 2015] process. In Chapter 2 we describe in more detail the modeling approach to lateral induction and the functional response at the tissue level that it can drive.

[14] In Chapter 2 we introduce a mathematical definition of *lateral induction* as used in this Thesis.

1.5 Scope of this Thesis

In this Thesis we addressed three aspects of Notch signaling. First, we addressed Notch signaling when it is activated by several ligands (two or three) under different regulatory scenarios (Chapter 2). Second, we evaluated the effect of the dynamics of Atoh1, which self-activates its production and the production of ligand Dl1, on patterning robustness. Third, we studied a more detailed model of Notch signaling activation and addressed which processes can be relevant to modulate the signaling efficiency of each ligand type. Below we briefly review the motivation of these extensions.

1.5.1 Different types of ligands can trigger Notch signaling

Notch signaling is commonly activated by several co-expressed ligands [Benedito et al., 2009, Gama-Norton et al., 2015, Kiernan et al., 2005, Petrovic et al., 2014, Preuße et al., 2015]. For instance, Dl1 and Jag2 ligands are co-expressed during the hair cell specification stage in the development of sensory organs in mice, and both drive Notch signaling and are repressed by it [Kiernan et al., 2005]. Nascent hair cells in mice co-express Dl1 and Jag2, which are repressed by Notch signaling, but also co-express Jag1, which is activated by Notch [Zine, 2003, Zine et al., 2000].

When each of the co-expressed types of ligands triggers a different signaling pathway (i.e., canonical or non-canonical[15]), the overall state of the array may be expected to be a superposition of the states mediated by each type of ligands. However, Notch ligands typically activate the same canonical pathway such that the processes of lateral communication each type of ligand mediates are coupled at the level of signal activation.

In addition, it has been shown that different types of Notch ligands activate the same canonical signal at different extents. On the one hand, there are differences on binding affinity to Notch, which are ligand dependent [Hicks et al., 2000, Panin et al., 1997, Yang et al., 2005]. On the other hand, upon binding to Notch, different ligands drive Notch signaling at distinct activity levels, which

[15] See [Andersen et al., 2012] for a recent review on the regulatory mechanisms displayed in the non-canonical Notch signaling pathway.

could translate into distinct maximal signaling levels produced at saturation of the Notch receptor by each ligand [Benedito et al., 2009, Petrovic et al., 2014, Yang et al., 2005]. It has been shown that differences in signaling enable to modulate the levels of Notch signaling in a more complex manner. Specifically, co-expressing a weakly efficient ligand in a tissue which already exhibits Notch signaling by a stronger ligand can drive an overall reduction of Notch signaling, as it has been reported in angiogenesis [Benedito et al., 2009], in inner ear development [Petrovic et al., 2014] and in the development of haematopoietic stem cells [Gama-Norton et al., 2015]. These differences are expected to come from different efficiencies rather than binding affinities since these data come from experiments in which the amount of ligand is considered to be very large (for instance, as described in [Petrovic et al., 2014]). Thus, the most inefficient ligand behaves like a partial agonist. This reduction happens when the two types of ligand share resources that can become limiting [Petrovic et al., 2014]. Therefore, differential activation of the signaling by each ligand is a relevant aspect to take into account and the sharing of limiting resources adds additional couplings between the lateral communication each ligand mediates.

Theoretical studies to understand the general effect of two ligands have focused on antagonistically regulated ligands, like Dl1 and Jag1 [Boareto et al., 2015, Jolly et al., 2015]. As part of a previous work of ours[16] [Petrovic et al., 2014], we studied a model in which Notch signaling is triggered by Jag1 and Dl1 during the development of the inner ear. Our results showed that the differential efficiency between these ligands, being Jag1 the weakly efficient one, could account for the the type of signal and ligand activities found in the inner ear of chick embryos [Petrovic et al., 2014]. Our model predicted that Jag1 mediates different types of lateral regulation depending on whether it acts in isolation or it drives signaling together with Dl1 [Petrovic et al., 2014].

This background brings the following questions

- Which type of lateral regulation arises (i.e., between lateral induction and lateral inhibition) when there are several ligands are triggering Notch signal?

[16]The results in [Petrovic et al., 2014] are not shown within the content of this Thesis. My participation there, together with Dr. Pau Formosa-Jordan and Dra. Marta Ibañes, included the proposal, discussion and computational analysis of the mathematical model. The conclusions obtained in previous work motivated the study depicted in Chapters 2 and 3.

- How is the contribution of the lateral regulation mediated by each type of ligand on the spatial organization of the tissue?

These questions are addressed in Chapter 2.

1.5.2 Lateral inhibition with self-activation of Atoh1

It has been shown that Notch signaling is involved in sensory cell differentiation during the development of the inner ear of the chick. Also, it has been shown that Dl1 acts in lateral inhibition, driving hair cell (HC) patterning [Adam et al., 1998, Haddon et al., 1998, Zine et al., 2000]. In [Petrovic et al., 2014], we have shown that self-activation of Atoh1 can be important to mediate robustness of sensory HC patterning and differentiation in the inner ear to loss and gain of function of Notch ligand Jag1, which is activated by Notch signaling. The self-activation of Atoh1 is a conserved motif occurring in mouse, chick [Neves et al., 2013b], zebra-fish [Millimaki et al., 2007] and *Drosophila* [Lubensky et al., 2011], but it is typically neglected in lateral inhibition models despite the expression of Atoh1 is tightly bounded to Notch signaling. Activation of Atoh1 is necessary and sufficient to drive sensory hair cells (HC) differentiation, and cells that fail to activate Atoh1 adopt non-sensory cell fate [Bermingham et al., 1999, Kelley, 2006].

Intriguingly, *in vivo* experiments have shown that HC differentiation and patterning can be to some extent robust to miss-expression of Dl1, which is repressed by Notch signaling. *In vivo* electroporations of exogenous Dl1 at the onset of HC differentiation in the *basilar papilla* of the chick revealed that exogenous Dl1 prevented most of the HC differentiation, but there can be HC differentiation of cells that are in contact with other cells expressing exogenous Dl1 [Chrysostomou et al., 2012]. Despite the transcription of the exogeneous Dl1 is extended along the tissue, some clusters still remained where HC differentiation occurred normally.

Taking into account this experimental background and the theoretical work we have done in the inner ear in regard to Jag1 loss and gain of function [Petrovic et al., 2014], we ask

- What is the effect of the self-activation of Atoh1 on HC differentiation and patterning?

This question is addressed in Chapter 3.

1.5.3 Differential signaling efficiency between two co-expressed ligands triggering Notch signaling

In the last part of this Thesis, we have addressed a more detailed model of Notch signaling activation where we consider how the ligand–receptor complex is processed for signaling (Chapter 4). Notch receptor can be subjected to post-translational modifications, which may alter signal activity. Glycosylation mediated by Fringe proteins is an important example of these type of modifications [Haines and Irvine, 2003, Stanley, 2007]. It has been shown that the effect of Notch glycosylation mediated by Fringe proteins can have different effects on signaling activation depending on the type of ligand binding to Notch. For instance, Lunatic Fringe enhances the binding of Delta-like ligands to Notch while hinders Jagged-like ligand binding to Notch [Haines and Irvine, 2003, Yang et al., 2005]. A similar behavior has been associated to Maniatic Fringe, but Radical Fringe can have the opposite effect and enhance the binding of Jagged-like ligands to Notch [Yang et al., 2005]. These processes result in a different rate of Notch signaling activation. Interestingly, it has been suggested that Fringe-mediated glycosylation might also affect Notch signaling without altering the ligand–receptor binding rates. In particular, it has been suggested that Jagged–Notch complexes might be less prone to signal provided that they cannot be properly processed when Notch receptor is glycosylated by Lunatic Fringe [Yang et al., 2005]. This is because these complexes could be less stable and will tend to dissociate after ligand endocytosis, which is a process that occurs upon complex formation and that is necessary for proper Notch signaling activation [Glittenberg et al., 2006].

As a consequence of Notch glycosylation, we can hypothesize that different types of ligands could trigger signaling with different efficiency. In addition, when different ligands are co-expressed they can compete for common resources to trigger signaling. Interestingly, in a context of competition for common resources to signal, the overall signaling level is lower than that from the more

efficient signaling ligand when ligands with different efficiency of signaling are co-expressed [Benedito et al., 2009, Petrovic et al., 2014]. Hence, inhibition of the signal upon over-expression of one of the ligands can suggest that there is a differential signaling efficiency between ligands. However, the mechanism by which Fringe might mediate the emergence of a differential signaling efficiency between the ligands remains elusive.

Taking into account this context, we ask

- How a differential signaling efficiency between ligands (mediated by Fringe) can arise, such that the less efficient signaling ligand trans-inhibits signal formation?

This question is addressed in Chapter 4.

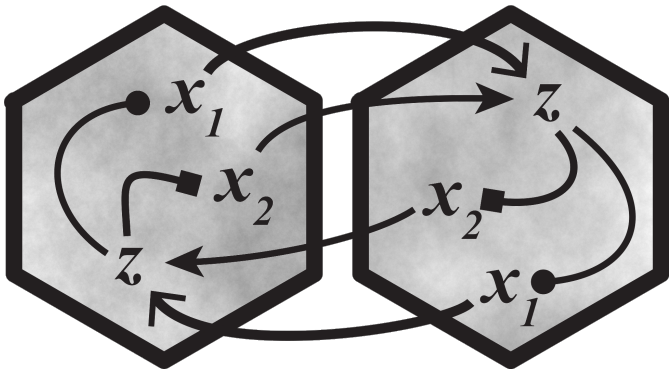

"Pues creo que la evolución que se hace delante de nosotros es el paso de una ciencia como geometría a una ciencia como narración."

I. Prigogine

Chapter 2

Notch signaling mediated by two co-expressing ligands

2.1 Introduction: lateral communication mediated by more than one type of Notch ligand

In most cases, theoretical studies of Notch signaling assumed that only one type of ligand is binding Notch receptor [Barad et al., 2010, Collier et al., 1996, Owen et al., 2000, Sprinzak et al., 2010, Wearing et al., 2000, Webb and Owen, 2004]. As described in the previous chapter, Notch signaling can either repress or activate the transcription of the ligand, which brings two different processes of lateral regulation. In this context, the process of lateral regulation is specific of the type of regulation exerted by Notch on the transcription of the ligand. However, different types of Notch ligands are found to be co-expressed within tissues. For instance, in the developing inner ear in mice Dl1 and Jag2 and Jag1 co-express [Adam et al., 1998, Lanford et al., 1999, Morrison et al., 1999] (nascent hair cells express Dl1 and Jag2, while supporting cells express Jag1). Likewise, during angiogenesis Dl4 and Jag1 are found to be co-expressed [Benedito et al., 2009]. These evidences prompt to study Notch signaling beyond

the one ligand type scenario. In this chapter we make a first approach to understand what type of lateral regulation circuit arises when Notch signaling is mediated by two or more type of ligands.

In the context of one type of ligand triggering Notch signal, there are two well studied functional responses that can arise, periodic patterning and ligand propagation. Each of these responses is driven by the feedback established by the lateral regulation processes mediated by Notch. To study the emergence of these responses (periodic patterning and ligand propagation), we proposed a model in which Notch signaling can be activated by two or three different type of ligands. In turn, these ligands can be different because of: (i) their transcriptional regulation, i.e., the type of regulation that Notch signaling exerts on their transcription (positive or negative), and/or (ii) their signaling strength (or affinity) which is defined by the maximal signal activity levels that each type of ligand can activate when expressed in isolation.

In the following we discuss a model of Notch signaling activated by a single ligand type and showed how the analysis of this model can predict the emergence of a functional response.

2.1.1 Lateral inhibition and periodic pattern formation

First, we discuss the case in which the Notch signaling activity represses the transcription of the ligand within an array of equivalent cells[1].

Assuming that the state of the cell can be described by two variables (i.e., the signal and ligand activity, s and l, respectively), and that both the signal activation and ligand regulation are one-step processes, we can write the dynamics of the signal activity in cell i as

$$\frac{\mathrm{d}s_i}{\mathrm{d}t} = \underbrace{\frac{r\langle l_i\rangle}{1+r\langle l_i\rangle} - s_i}_{F_s(\langle l_i\rangle, s_i)} \tag{2.1}$$

where $\langle l_i\rangle \equiv \frac{1}{\omega}\sum_{j\in NN} l_j$ is the average ligand activity in the $\omega = 6$ Nearest Neighboring cells (NN), within a perfect array of hexagonal cells. In turn, r

[1] This case corresponds to that studied by Collier et al. [1996]. By equivalent we mean that the parameter values are assumed equal for every cell within the array.

defines the strengths of trans-interactions mediated by the ligand. Accordingly, the dynamics of the activity of the ligand in cell i reads

$$\frac{\mathrm{d}l_i}{\mathrm{d}t} = \underbrace{v\left(\frac{1}{1+bs_i^h} - l_i\right)}_{F_l(s_i,l_i)} \tag{2.2}$$

where $b^{-1/h}$ is the signal activity threshold of the ligand activity regulation, h stands for the effective cooperativity of the process and v is the ratio of the characteristic time scale dynamics of the ligand over that of the signal. Eqns. 2.1 and 2.2 correspond to the model defined by Collier et al. [1996].

In order to determine what is the effect of the ligand activity on the signal activity levels at the homogeneous stationary state, we can calculate the partial derivative of the dynamics of the signal activity with respect to the ligand, evaluated at the homogeneous stationary state (s^{st}, l^{st})[2]:

$$R_{s,\langle l\rangle} \equiv \left.\frac{\partial F_s}{\partial\langle l\rangle}\right|_{s^{st},l^{st}} = \frac{r}{(1+l^{st}r)^2} \tag{2.3}$$

Notice that for any choice in the parameter values we have that $R_{s,\langle l\rangle} > 0$. This means that the effect of the activity of the ligand on the activity levels of the signal is positive, i.e., the ligand promotes the activation of the signal. Accordingly, the effect of the signal activity on the activity levels of the ligand at the homogeneous stationary state reads

$$R_{l,s} \equiv \frac{1}{v}\left.\frac{\partial F_l}{\partial s}\right|_{s^{st},l^{st}} = -\frac{hb(s^{st})^{h-1}}{\left(1+b(s^{st})^h\right)^2} \tag{2.4}$$

Again, notice that $R_{l,s} < 0$ for any value of the parameters, which means that the signal represses the production of the ligand. Finally, notice that the feedback on the transcription of the ligand is negative, i.e.,

$$R_{s,\langle l\rangle}R_{l,s} < 0 \tag{2.5}$$

[2]See Appendix A for further details on the definition of the homogeneous stationary state.

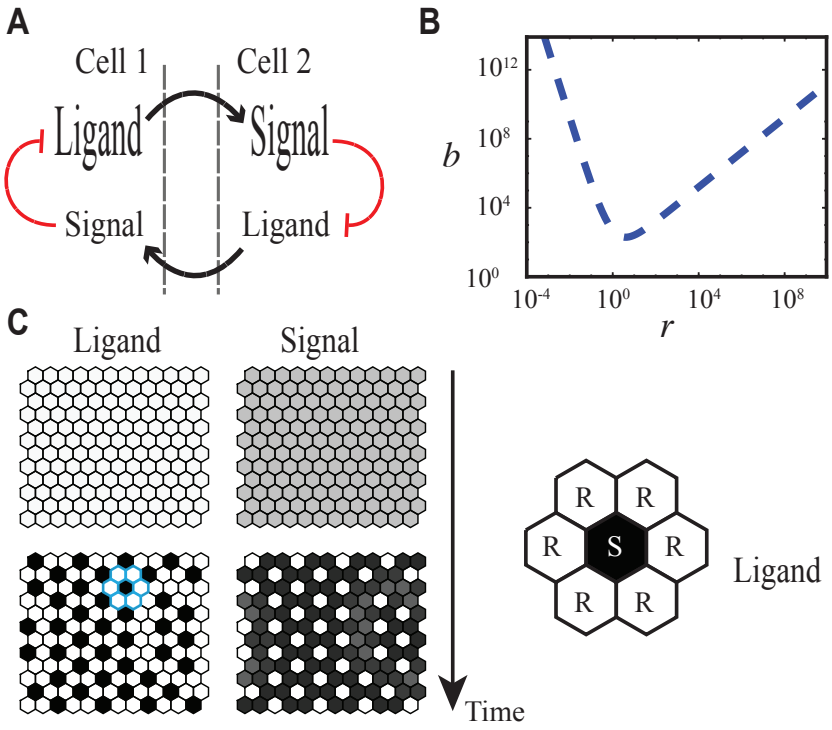

Figure 2.1 Functional response mediated by a ligand repressed by Notch. A) Schematic representation of the interactions and activity states of the ligand and the signal of two neighboring cells. The font size stands for the levels of each species (ligand and the signal), the blunt red arrows for the inhibition of the transcription of the ligand and the black arrow for the trans-activation of the signal mediated by the ligand. B) Regime of periodic pattern formation in the parametric space b, where $b^{-1/h}$ is the threshold of the ligand activity regulation, and r which is the strength of trans-interactions mediated by the ligand. Spontaneous patterning occurs inside the region bounded by the blue-dashed line. C) Snapshots of the dynamics of the ligand and the signal acting in lateral inhibition within an array of hexagonal cells. The activity levels for the ligand and the signal in each cell (hexagon) is shown in a linear gray-scale from the lowest (white) to the highest (black) levels. This notation is conserved in the rest of the figures. The parameter values for the phase diagrams and the simulations are $h = 4$ and $v = 1$. (Right) Schematic representation of the signaling states in a the cluster of 7 cells depicted with blue borders in B. The activity of the ligand is denoted in gray-scale. Pattern is formed by signal sending (S) and signal receiving (R) cells.

This means that the lateral effect of the ligand on its neighbors results in inhibition of ligand production. This interpretation comes from the fact that the partial derivative $R_{s,\langle l\rangle}$ is obtained with respect to $\langle l\rangle$, which is the variable that accounts for the lateral coupling between adjacent cells. The sign establishes whether the effect is positive (activation) or negative (repression).

Hereafter, we say that the ligand is acting in lateral inhibition when condition 2.5 is met[3].

It has been shown that this model (Eqns. 2.1 and 2.2) can drive periodic pattern formation, arising from a linear unstability of the homogeneous state [Collier et al., 1996]. Within an array of hexagonal cells, the condition for which the homogeneous state is unstable to inhomogenous perturbations (driving spontaneous periodic patterning) reads (see appendix A and [Collier et al., 1996])

$$R_{s,\langle l\rangle} R_{l,s} < -2 \tag{2.6}$$

Applying the linear stability analysis across the parameter space r and b it is easy to note that the regime where a pattern can arise becomes wider when the threshold of the ligand regulation by Notch ($\frac{1}{b}^{\frac{1}{h}}$) becomes lower (i.e., for high sensitivity of the transcription to regulation by Notch) [Fig. 2.1B].

In the pattern that arises has two different cell types: (i) one cell type has high ligand activity levels while low levels of the signal activity and (ii) another cell type that has high levels of the signal activity while low levels of the ligand activity (Fig. 2.1C). In accordance to the nomenclature proposed by other authors [Sprinzak et al., 2010, 2011], we define the cell type expressing high levels of the ligand as signal sending, S. Accordingly, the cell type with high levels of the signal is termed signal receiving, R.

2.1.2 Lateral induction and ligand propagation

When the production of the ligand is activated by Notch signaling (Fig. 2.2A), then we set the dynamics of the ligand activity of cell i to be

[3]Notice that this definition takes into account the sign of the complete regulatory feedback, not only how the signal regulates the transcription of the ligand.

$$\frac{\mathrm{d}l_i}{\mathrm{d}t} = v\left(\delta_l + (1-\delta_l)\frac{bs_i^h}{1+bs_i^h} - l_i\right) \tag{2.7}$$

where δ_l stands for the basal constant production of the ligand. The dynamics of the signal activity is the same as in the previous case (i.e., Eqn. 2.1).

In this case of a ligand activated by the signal activity, the effect of the signal on ligand activity follows

$$R_{l,s} \equiv \left.\frac{\partial F_l}{\partial s}\right|_{s^{st},l^{st}} = \frac{hb(s^{st})^{h-1}}{(1+b(s^{st})^h)^2} \tag{2.8}$$

which is non-negative for any choice in the parameter values. Notice that when the ligand activating Notch signaling is positively regulated by the signal, the overall regulation of the circuit is positive (i.e., $R_{s,\langle l\rangle}R_{l,s} > 0$) for any choice in the parameter values. Hence, we say that the ligand is acting in lateral induction.

A recent theoretical and experimental work has shown that lateral induction can drive a wave-like propagation of the expression of the ligand that is activated by Notch signaling [Matsuda et al., 2012]. It has been proposed that lateral induction could be underlying the specification of the prosensory domains in the developing sensory organs of vertebrates [Kiernan et al., 2001]. For our analysis, we assumed that ligand propagation occurs when there is a transition from a linearly stable homogeneous state with low activity levels of the ligand to a homogeneous linearly stable state with higher activity levels upon a non-linear perturbation given by a local increase in the activity level of the ligand within a small cluster of cells (Fig. 2.2B). Because of this, we expect that ligand propagation occurs when there are two linearly stable homogeneous states. However, it remains to be tested experimentally whether transient transitions are enough to account for ligand propagation *in vivo*[4].

According to the linear stability analysis (see Appendix A for details) a homogeneous steady state is linearly stable to *any* type of perturbation when the condition

[4] In case that the propagation occurs transiently, the condition of bistability is not required. In our analysis however we are imposing a more restrictive condition, such that bistability is necessary for ligand propagation to arise.

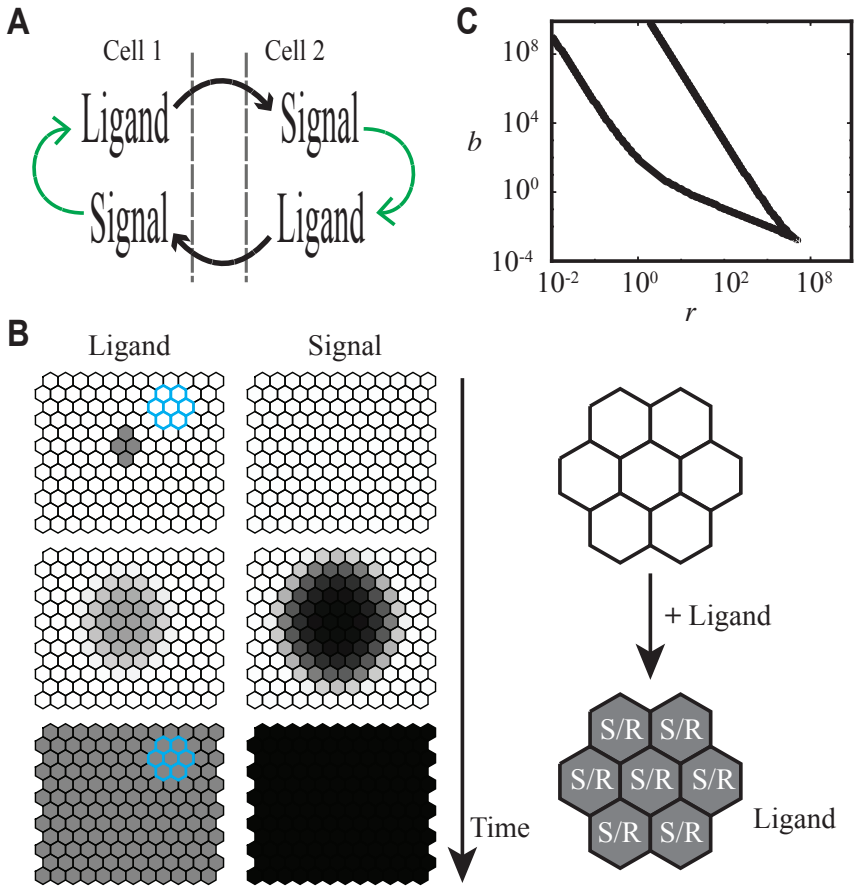

Figure 2.2 Functional response mediated by a ligand activated by Notch. A) Schematic representation of the interaction and the activity levels of the ligand and the signal in two neighboring cells. Green arrows describe transcriptional activation and the font size and black arrows have the same meaning as in Fig. 2.1. B) Snapshots showing the dynamic from a state of low levels of the species to a state of high levels of ligand and the signal acting in lateral induction after the induction of high activity levels of the ligand in four cells in the center of the array. The activity levels for the ligand and the signal in each cell are shown as described in Fig. 2.1. C) Regime of bistability of homogeneous states in the parametric space b and r, as described in Fig. 2.1. Bistability and ligand propagation occurs inside the region bounded by the black line. The parameter values for the phase diagrams and the simulations are $h = 4$ and $v = 1$. (Right) Schematic representation of the signaling states of a small cluster of cells. After ligand propagation the state cells are both signal sending and receiving (S/R).

$$-2 < R_{s,\langle l\rangle} R_{l,s} < 1 \tag{2.9}$$

is met. Hence, when there are two homogeneous stationary states following this condition (2.9), then we say that the system is bistable. An inspection of this condition in the parameter space b and r shows that the regime where bistability of homogeneous states arises becomes wider when the propensity of the ligand to bind to Notch decreases and the sensitivity of the ligand to regulation by Notch increases (Fig. 2.2C).

2.1.3 Statement of the problem

Lateral communication mediated by Notch can drive two types of functional responses, among others, i.e., periodic patterning and ligand propagation. These responses, and the signaling states that arise in each type of response, are well understood when there is only one ligand mediating lateral communication. However, it has been shown repeatedly that different types of Notch ligands can be found co-expressed in developing tissues. In this chapter we aim to characterize which functional response arises, and the corresponding signaling states of the cells, when Notch is triggered by two ligands co-expressed. We explore different regulatory scenarios of ligands repressed and/or activated by Notch signaling which in turn can trigger the signal with the same or different efficiency.

2.2 Modeling approach

To address the situation in which Notch signaling is triggered by two ligands, we extended the model proposed by Collier et al. [1996] to account for the contribution of the second ligand to signal production. In this chapter we addressed two variations of this extension, depending on whether ligands use independent resources to signal or not. In this case, the signal dynamics reads

$$\frac{\mathrm{d}s_i}{\mathrm{d}t} = \frac{r_1\langle l_{1,i}\rangle}{1 + r_1\langle l_{1,i}\rangle} + \varepsilon\frac{\varepsilon_r r_1\langle l_{2,i}\rangle}{1 + \varepsilon_r r_1\langle l_{2,i}\rangle} - s_i \tag{2.10}$$

In contrast, when ligands use shared resources the signal dynamics reads

$$\frac{\mathrm{d}s_i}{\mathrm{d}t} = \frac{r_1\langle l_{1,i}\rangle + \varepsilon\varepsilon_r r_1\langle l_{2,i}\rangle}{1 + r_1\langle l_{1,i}\rangle + \varepsilon_r r_1\langle l_{2,i}\rangle} - s_i \tag{2.11}$$

In both cases, the propensity of ligand2 to bind to Notch, r_2, is set as $r_2 \equiv \varepsilon_r r_1$ and ε stands for the relative signaling strength or efficiency of ligand2 with respect to that of ligand1. In this regard, if $\varepsilon = 1$ then we say that both ligands are equivalently strong signaling ligands. In contrast, if $\varepsilon < 1$ then we say that ligand2 is less efficient or a weaker signaling ligand than ligand1.

We explored different regulatory scenarios, such that the activity of the ligands can be equivalently regulated (i.e., both activated or both repressed) or antagonistically regulated (i.e., one activated and the other repressed) by Notch signaling activity. The dynamics of each type of ligand corresponds to Eqn. 2.2 in case the ligand is repressed by the Notch signal activity or to Eqn. 2.8 in case it is activated. Unless stated otherwise, the parameter values used are $b_l = 10^4$ and $h_l = 4$, when the ligand(s) is (are) repressed by the signal and $b_l = 1$ and $h_l = 4$, when the ligand(s) is (are) repressed, where $l = 1$ and $l = 2$ for ligand1 and ligand2 respectively. For these parameter values each type of ligand expressed in isolation is expected to drive its corresponding functional response, i.e., if the ligand activity is repressed by the signal then periodic patterning is expected (Fig. 2.1) while if the ligand activity is activated by the signal then ligand propagation is expected (Fig. 2.2). However, the emergence of these responses is not restricted by this specific set of parameter values, i.e., the responses are robust to variations in the value of the parameters. Without loss of generality, we assumed that $v = 1$[5].

In the case of ligands using independent resources, the effect of the activity of ligand1 and ligand2 on the signal activity in the homogeneous steady state (s^{st}, l_1^{st}, l_2^{st}) reads

$$\begin{aligned} R_{s,\langle l_1\rangle} &\equiv \left.\frac{\partial F_s}{\partial\langle l_1\rangle}\right|_{s^{st},l_1^{st},l_2^{st}} = \frac{r_1}{(1 + r_1 l_1^{st})^2} \\ R_{s,\langle l_2\rangle} &\equiv \left.\frac{\partial F_s}{\partial\langle l_2\rangle}\right|_{s^{st},l_1^{st},l_2^{st}} = \varepsilon\varepsilon_r \frac{r_1}{(1 + \varepsilon_r r_1 l_2^{st})^2} \end{aligned} \tag{2.12}$$

[5]Notice that the stability conditions do not depend in the value of v as long as it is the same for both ligands.

respectively, where $F_s = \frac{r_1\langle l_{1,i}\rangle}{1+r_1\langle l_{1,i}\rangle} + \varepsilon\frac{\varepsilon_r r_1\langle l_{2,i}\rangle}{1+\varepsilon_r r_1\langle l_{2,i}\rangle} - s_i$. Notice that both expressions are non-negative for any choice in the parameter values, similarly to the case in which there is only one type of ligand triggering Notch signaling.

In contrast, in the case of ligands sharing resources to signal, the effect of ligand2 activity on signal activity reads

$$R_{s,\langle l_2\rangle} \equiv \left.\frac{\partial F_s}{\partial\langle l_2\rangle}\right|_{s^{st},l_1^{st},l_2^{st}} = r_1\varepsilon_r\frac{\varepsilon - r_1 l_1^{st}(1-\varepsilon)}{\left(1+r_1 l_1^{st}+\varepsilon_r r_1 l_2^{st}\right)^2} \tag{2.13}$$

where $F_s = \frac{r_1\langle l_{1,i}\rangle+\varepsilon\varepsilon_r r_1\langle l_{2,i}\rangle}{1+r_1\langle l_{1,i}\rangle+\varepsilon_r r_1\langle l_{2,i}\rangle} - s_i$. Notice that in this case the sign of $R_{s,\langle l_2\rangle}$ can be positive or negative, unlike previous cases.

According to the linear stability analysis detailed in Appendix A, when there are two co-expressed ligands periodic patterned states arise when

$$R_{s,\langle l_1\rangle}R_{l_1,s} + R_{s,\langle l_2\rangle}R_{l_2,s} \leq -2 \tag{2.14}$$

where $R_{l_1,s}$ and $R_{l_2,s}$ are defined equivalently as in the one ligand scenario.

In addition, bistability of homogeneous states and ligand propagation is expected to arise when there are two homogeneous stationary states for which the condition

$$-2 < R_{s,\langle l_1\rangle}R_{l_1,s} + R_{s,\langle l_2\rangle}R_{l_2,s} < 1. \tag{2.15}$$

is met (see Appendix A for details).

We explored the parameter space ε_r and r_1 and characterized the regions in which periodic patterning and ligand propagation arise, by evaluating conditions 2.14 and 2.15, respectively. In all figures, these regions are enclosed by the dashed-blue line (for periodic patterning) and by the solid-black line (for ligand propagation). We also studied the regions of the parameter space where ligand1 and ligand2 drive sufficiently strong lateral regulation, such that they could drive periodic patterning if expressed in isolation. Hence, ligand1 (or ligand2) is said to be sufficiently strong to drive patterning if $R_{s,\langle l_1\rangle}R_{l_1,s} \leq -2$ ($R_{s,\langle l_2\rangle}R_{l_2,s} \leq -2$). These regions are represented in red for ligand1 (or gray

for ligand2). Notice that a ligand can be sufficiently strong (in the sense described before) to drive patterning, but still patterning might not arise. For instance, ligand1 can be sufficiently strong (i.e., $R_{s,\langle l_1\rangle}R_{l_1,s} \leq -2$), but overall $R_{s,\langle l_1\rangle}R_{l_1,s} + R_{s,\langle l_2\rangle}R_{l_2,s} > -2$ (i.e., $R_{s,\langle l_2\rangle}R_{l_2,s} > 0$). This aspect will be described in more detail in the following sections.

The details on the numerical methods used for the calculation of these phase diagrams are described in Appendix B. Additionally, we used numerical simulations to corroborate the results of linear stability analysis in specific points of the phase diagrams, as described in Appendix B (see the tables in that Appendix for the parameter values in which corroborations were done). The following subsections describe the results from this analysis across the parameter space an for different scenarios of ligand regulation and efficiency of signaling.

2.3 Results

2.3.1 Equivalent ligands can drive either redundant or impaired responses

2.3.1.1 Equally strong signaling ligands driving redundant states

We consider the case in which two equivalent ligands drive Notch signaling using either independent (Eqn. 2.10) or shared (Eqn. 2.11) resources to signal. This equivalence between ligands refers to two separate properties:

1. The efficiency of signaling of the ligands is the same, i.e., both ligands can drive the same amount of signaling when expressed in isolation such that $\varepsilon = 1$.

2. The regulation that Notch exerts on the production of the ligands is of the same type, i.e., the activity levels of both ligands can be repressed (following Eqn. 2.2) or activated (following Eqn.2.7) by the signal activity.

According to our model, when the production of the ligands is repressed by the activity of Notch signaling (Fig. 2.3A, B), then periodic patterning is the only type of functional response arising. As expected, co-expression of both ligands

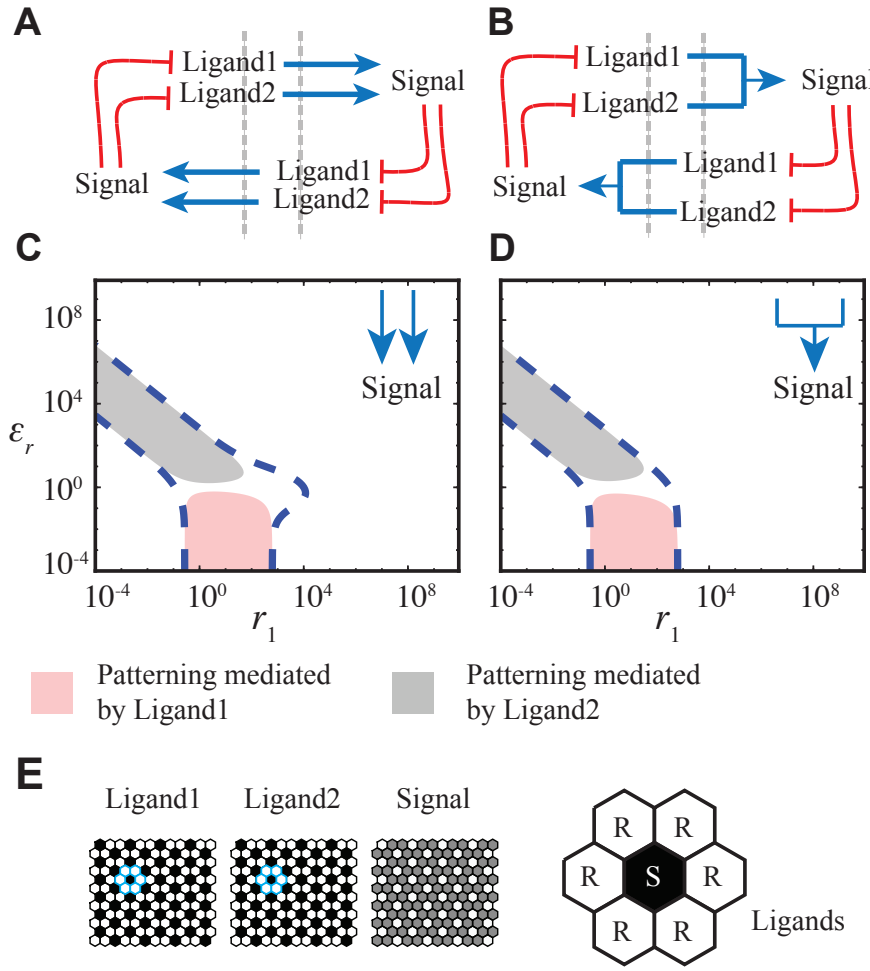

Figure 2.3 Periodic patterning in a system of equivalent ligands repressed by Notch. Schematic representation of the of the transcriptional regulation of the ligands (red blunt arrows) and the trans-activation of the signal when ligands use independent resources (A) or shared resources (B) to signal. Regime of spontaneous periodic pattern formation according to Eqn. 2.14, in the parameter space ε_r and r_1. The value of the rest of the parameters is described in the text (with $\varepsilon = 1$). Ligands can use independent resources (C) or shared resources(D) to signal. E) Snapshots of the numerical simulations calculated when ligands use independent resources to signal. Simulations are calculated for $r_1 = 10$ and $\varepsilon_r = 1$. (Right) Representation of the signaling states that arise in the patterned state, where the activity levels of the ligands is depicted. The pattern is composed by signal sending cells (S) and signal receiving cells (R).

is not necessary for pattern formation to arise since each ligand in isolation can drive patterning (Fig. 2.3C, D). In addition, both ligands can drive the same periodic patterned state, occurring in the one type of ligand scenario, in which two different signaling states arise. One state has high levels of the ligands activity (and low levels of the signal) which can trigger Notch signaling in their neighbors, i.e., signal sending (S). The other state has high levels of the signal activity (and low levels of the ligands), i.e., signal receiving (R). Notice that the type of functional response and the signaling state of the cells are driven redundantly by the ligands, since no differences were found with respect to the case in which there is only one type of ligand expressed (e.g., Figs. 2.1 and 2.2). This situation is similar in both scenarios where ligands use shared or independent resources to signal (Fig. 2.3).

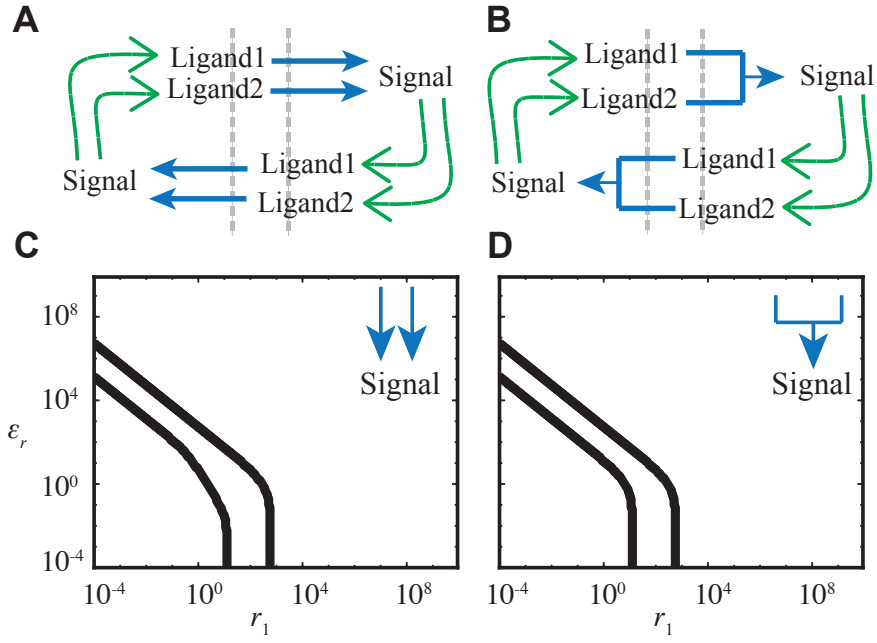

Figure 2.4 Ligand propagation in a system of equivalent ligands activated by Notch. Schematic representation of the of the transcriptional regulation of the ligands (green arrows) and the trans-activation of the signal when ligands use independent resources (A) or shared resources (B) to signal. Regime of ligand propagation according to Eqn. 2.15, in the parameter space ε_r and r_1. The value of the rest of the parameters is described in the text (with $\varepsilon = 1$). Ligands can use independent resources (C) or shared resources(D) to signal.

We also studied the case in which the equivalent ligands are activated by Notch (Fig. 2.4A, B). In this case the only functional response that arises is bistability of homogeneous states and ligand propagation. Similar to the previous regulatory scenario, when equivalent ligands are activated by Notch signal they can drive ligand propagation redundantly. This behavior is independent of whether ligands share resources for signaling or not (Fig. 2.4C, D).

Notice that the over-expression of either ligand (i.e., $r_1 \gg 1$ or $\varepsilon_r \gg 1$, while $r_1 \geqslant 1$ in Figs. 2.3C, D and 2.4C, D), disrupted the functional response (i.e., periodic patterning or ligand propagation) of the system. We reasoned that this can be due to saturation of the signal production upon over-expression of the ligands (Fig. 2.5). This is because the functional responses are expected to arise only when the levels of the signal activity can be regulated by ligands, i.e., $\left|R_{s,\langle li\rangle}\right| > 0$. In contrast, if the production of the signal saturates due to over-expression of the ligands, then the signal activity levels become non-responsive to variation on the levels of the ligands, i.e., $R_{s,\langle li\rangle} = 0$ for $i = 1$ and $i = 2$. Under this condition we have that $R_{s,\langle li\rangle}R_{li,s} \approx 0$ and therefore none of the conditions described above for periodic patterning (Eqn. 2.14) or ligand propagation (Eqn. 2.15) are fulfilled.

2.3.1.2 The co-expression of two equally regulated ligands can prevent the emergence of the functional response, even if one of the ligands signals weakly

We explored the case in which ligands are equally regulated by Notch, but in this case the maximal level of signal activity that can be triggered by ligand2 when expressed in isolation is lower than that of ligand1 (i.e., $\varepsilon < 1$). We considered as before that ligands can use independent (Eqn. 2.10) or shared (Eqn. 2.11) resources to signal.

In the regulatory scenario in which the transcription of the ligands is repressed by Notch signaling, the regime where spontaneous patterning arises is restricted to the region where the overall regulation associated to ligand1 is sufficiently strong to drive patterning[6] (i.e., $R_{s,\langle l_2\rangle}R_{l_2,s} \leq -2$). The maintenance of the functional response (periodic patterning) upon co- and over-expression of

[6]Note that the lateral feedback mediated by ligand2 (i.e., $R_{s,\langle l_2\rangle}R_{l_2,s}$) is not sufficiently strong to drive patterning even when expressed in isolation (i.e., for $r_1 \ll 1$) given that its signaling efficiency is low compared to that of ligand1.

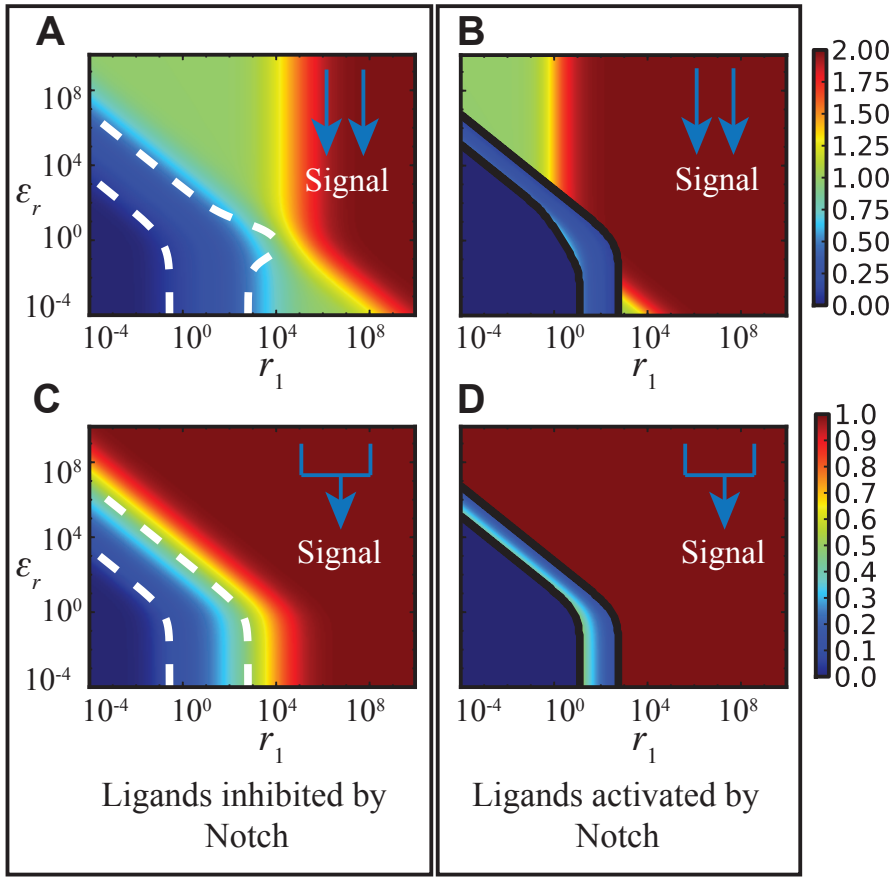

Figure 2.5 Activity levels of the signal in the homogeneous steady state for ligands signaling equivalently (i.e., $\varepsilon = 1$). Heat map showing the level of the signal in the parameter space ε_r and r_1 when the transcription of the two ligands is equally repressed (A, C) or activated (B, D) by the signal. Ligands can use independent resources (A, B) or shared resources (C, D) to signal. Spontaneous patterning occurs inside the region bounded by the white-dashed line.

ligand2 depends crucially on whether ligands use shared or independent resources to signal (Fig. 2.6). When ligands use independent resources, the over-expression of ligand2 only has a mild effect on the regime of periodic patterning driven by ligand1 (Fig. 2.6A, C). Notice that this is in contrast to what occurred when the ligands were equally efficient at signaling and the over-expression of either ligand disrupted the functional response (Fig. 2.5). This difference can be understood at the light of the effect of ligand2 on the signal activity in the homogeneous stationary state, $R_{s,\langle l_2 \rangle}$. When ligands use independent resource

to signal, then as $\varepsilon \to 0$ follows that $R_{s,\langle l_2 \rangle} \to 0$, according to Eqn. 2.12.

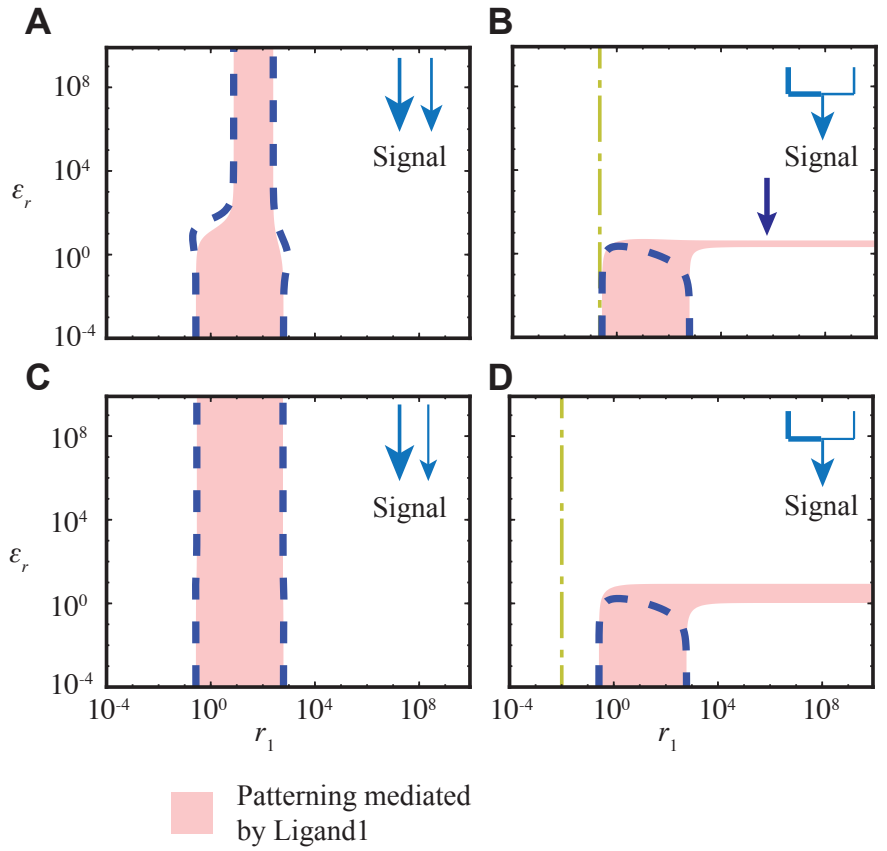

Figure 2.6 Periodic patterning in a system of ligands that signal differently (i.e., $\varepsilon < 1$) and that are transcriptionally repressed by Notch. Regime of periodic pattern formation when the two ligands use independent resources (A, C) or shared resources (B, D) to signal. Ligands signal differently, with a signaling efficiency ratio of $\varepsilon = 0.1$ (A, B) or $\varepsilon = 0.01$ (C, D). In C and D, ligand2 acts as a partial agonist (i.e., $R_{s,\langle l_2 \rangle} < 0$) at the right of the yellow-dashed line.

In contrast, when ligands use shared resources to signal, the co- or over-expression of ligand2 disrupts the regime of periodic patterning and drives a single homogeneous state (Fig. 2.6B, D). To understand why patterning is disrupted in this scenario of shared resources, despite ligand2 has a smaller efficiency of signaling compared to ligand1 (i.e., $\varepsilon < 1$), we analyzed the effect of ligand2 on the signal activity in the homogeneous stationary state (i.e., $R_{s,\langle l_2 \rangle}$). In this case of ligands using shared resources, as $\varepsilon \to 0$ we have that[7]

[7]This can be seen easily from Eqn. 2.13.

$$R_{s,\langle l_2\rangle} \to -\frac{\varepsilon_r l_1^{st} r_1^2}{(1 + l_1^{st} r_1 + l_2^{st} r_1 \varepsilon_r)^2} < 0 \tag{2.16}$$

Hence, when the relative signaling efficiency of ligand2 compared to ligand1 is negligible ($\varepsilon \to 0$), ligand2 has a negative effect on the signal activity (only in the case in which ligands share resources to signal). Hereafter, we termed this kind of regulation of the signal activity by ligand2 as *trans-inhibition*.

This type of behavior is observed as well in the regulatory scenario in which the two ligands are both activated by Notch signaling, but they have different signaling efficiency $\varepsilon < 1$ (Fig. 2.7). In this context, the over-expression of ligand2 (which is the weak signaling ligand) has little or no effect on the functional response driven by ligand1 (ligand propagation) when ligands use independent resources for signaling (Fig. 2.7A, C), but disrupts the response when ligands share resources (Fig. 2.7B, D).

These results show that co-expression of two equivalently regulated ligands can have an effect on the response driven by the strong signaling ligand only in the scenario in which ligands share resources to signal. In this scenario (i.e., assuming that ligands share resources and signal differently such that $\varepsilon < 1$), ligand2 is expected to trans-inhibit the formation of the signal when the condition [Formosa Jordan, 2013, Petrovic et al., 2014]:

$$\varepsilon < \frac{l_1^{st} r_1}{1 + l_1^{st} r_1} \tag{2.17}$$

is met[8]. Hereafter, when ligand2 trans-inhibits the formation of the signal we say that it behaves as a *partial agonist*.

We evaluated the activity levels of the signal in the homogeneous stationary state and we found that upon over-expression of ligand2 the levels of the signal decrease if ligands use shared resources to signal (Fig. 2.8C, D). Such reduction occurs in the regime where ligand2 can act as a partial agonist (in the right of yellow dotted-dashed line shown in Fig. 2.8C, D).

[8]Notice that condition 2.17 only holds when the ligands are co-expressed, i.e., when $l_1^{st} r_1 > 0$.

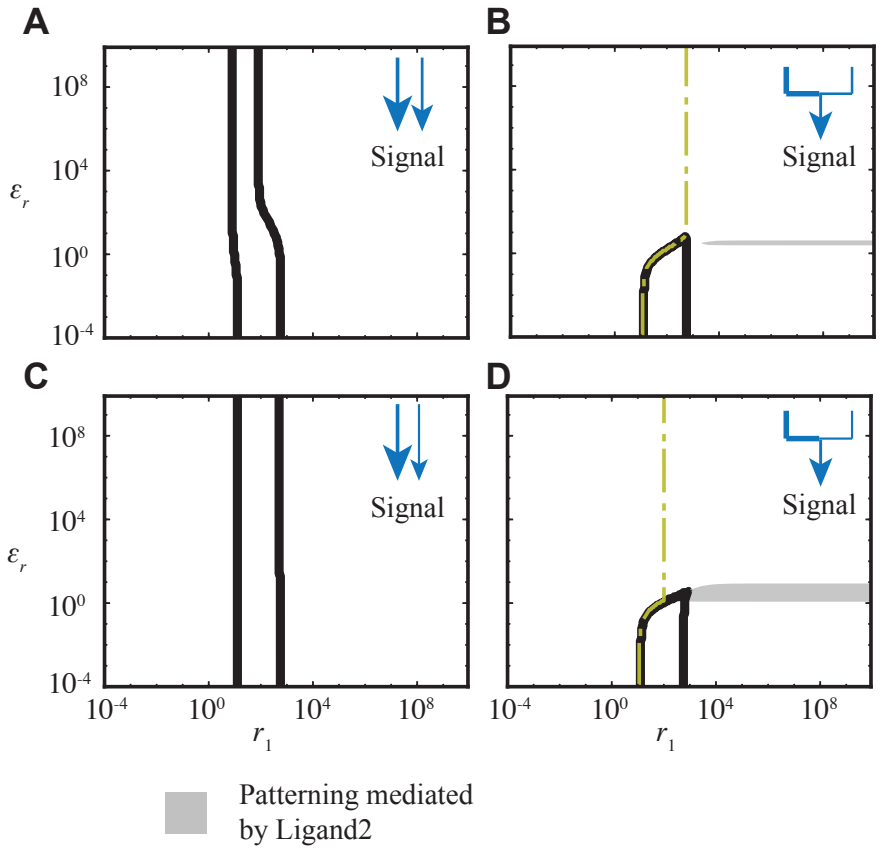

Figure 2.7 Bistability and ligand propagation in a system of ligands that signal differently and that are transcriptionally activated by Notch. Regime of istability of homogeneous states and ligand propagation when the two ligands use independent resources (A, C) or shared resources (B, D) to signal. Ligands signal differently, with a signaling efficiency ratio of $\varepsilon = 0.1$ (A, B) or $\varepsilon = 0.01$ (C, D). In C and D, ligand2 acts as a partial agonist at the right of the yellow-dashed line.

Conversely, when ligands use independent resources to signal then ligand2 can act only as an activator of the signal (Fig. 2.8A, B). In a special case when $\varepsilon = 0$, ligand2 is expected to have no effect on signal activation.

Taken together, our results show that the co-expression of two ligands equally regulated by the signal can drive either redundant or impaired responses. This disruption occurs upon over-expression of the ligands. When ligands share resources to signal, the disruption of the response can be explained by two different processes. On the one hand, if both ligands are equivalently strong at

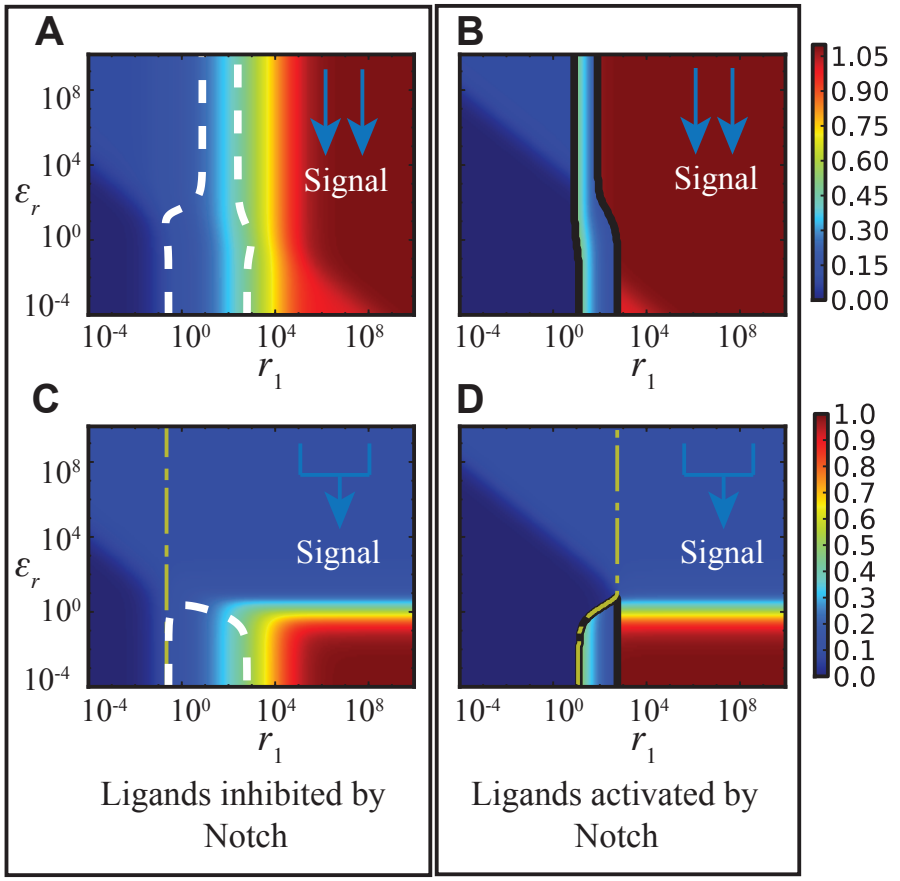

Figure 2.8 Activity levels of the signal in the homogeneous steady state for ligands signaling differently. Heat map showing the level of the signal in the parameter space ε_r and r_1 when the two ligands are repressed (A, C) or activated (B, D) by the signal. Ligands can use independent resources (A, B) or shared resources (C, D) to signal. Spontaneous pattern formation occurs inside the region bounded by the white-dashed line. In A-D, ligand2 is a weak signaling ligand and activate the signal in isolation to a maximal value $\varepsilon = 0.1$

signaling then the over-expression of ligand2 saturates the signal leading to a single homogeneous S/R state (Fig. 2.9A). On the other hand, when ligand2 acts as a partial agonist then the over-expression of this ligand prevents signaling and drives a single homogeneous state of cells mutually blocking the signal (Fig. 2.9B).

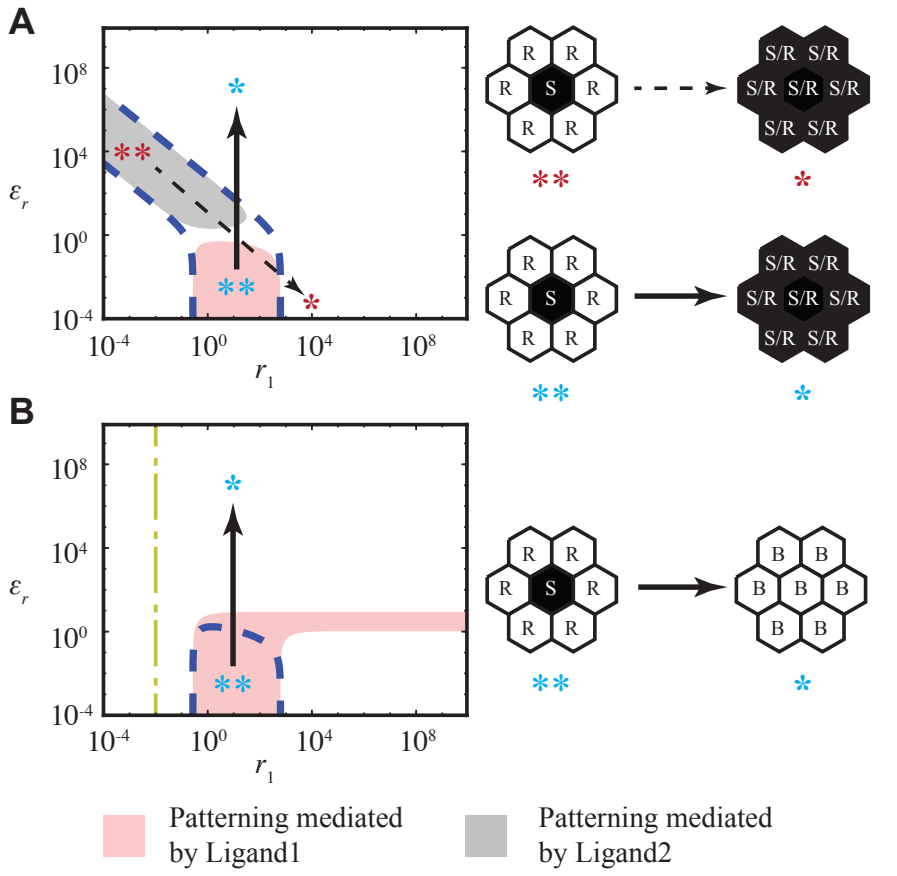

Figure 2.9 Signaling states after the over-expression of one of the ligands. A) Regime of spontaneous patterning as described in Fig. 2.3D. Over-expression of ligand1 occurs when $r_1 \gg 1$ (dashed line) while over-expression of ligand2 occurs when $\varepsilon_r \gg 1$, while r_1 is maintained constant (solid line). Both over-expression events entail a homogeneous state of signal sending and signal receiving (S/R) in which cells have high levels of the signal.

2.3.2 Ligands equivalently regulated drive emergent responses when one of the ligands acts as a partial agonist

In this section we addressed the functional response that arises when Notch signaling regulates the ligands activities equivalently[9].

2.3.2.1 The type of lateral regulation mediated by ligand2 changes to its opposite when it acts as a partial agonist

We evaluated the lateral regulation mediated by ligand2 in the homogeneous stationary state (i.e., $R_{s,\langle l_2\rangle}R_{l_2,s}$) when the ligands are repressed by the signal in two situations: 1) both ligands are equally strong signaling (i.e., $\varepsilon = 1$) and 2) ligand2 can act as a partial agonist (i.e., $\varepsilon < 1$). Notice that the sign of $R_{s,\langle l_2\rangle}R_{l_2,s}$ will tell whether ligand2 is acting in lateral inhibition or lateral induction, as defined in previous sections, while its magnitude will tell whether this lateral regulation can drive a functional response (this will be addressed in the next subsection).

When both ligands are equally strong signaling, the lateral regulation mediated by ligand2 is negative ($R_{s,\langle l_2\rangle}R_{l_2,s} < 0$) and thereby this ligand is said to act in lateral inhibition, as expected for a ligand being repressed by Notch signaling (Fig. 2.10A). In contrast, when ligand2 behaves as a partial agonist it can act in lateral induction, i.e., $R_{s,\langle l_2\rangle}R_{l_2,s} > 0$ (Fig. 2.10B). This is because when acting as a partial agonist the effect of ligand2 changes from trans-activation ($R_{s,\langle l_2\rangle} > 0$) to trans-inhibition ($R_{s,\langle l_2\rangle} < 0$), but the effect of the signal on the ligand activity remains the same ($R_{l_2,s} < 0$). Interestingly, there is a region in which the strength of the lateral regulation mediated ligand2 is remarkably strong ($R_{s,\langle l_2\rangle}R_{l_2,s} \approx 2.8$).

We found that the equivalent type of behavior arises in the regulatory scenario in which the transcription of the ligands is activated by Notch signaling. In particular, when both ligands are equally strong signaling ligands (i.e., $\varepsilon = 1$) then ligand2 acts in lateral induction (Fig. 2.11A), as expected, but it changes

[9]Note that here we refer to the regulation of the ligands as *equivalent*, but not equal since we assume different values of the parameters in the dynamics of each ligands. Below we reasoned that this difference might be necessary for the functional responses driven by the partial agonist to arise.

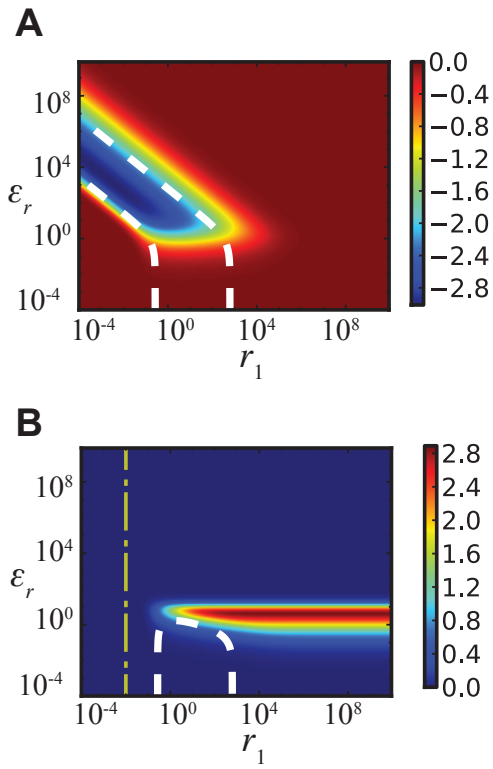

Figure 2.10 Strength of the lateral regulation mediated by ligand2 when ligands are repressed by Notch. Heat maps showing the strength of the lateral regulation of ligand2 in the homogeneous steady state when (i.e., $R_{s,\langle l_2\rangle}R_{l_2,s}$) when A) Ligands are repressed by Notch and they are equivalently strong signaling ligands (i.e., $\varepsilon = 1$) or B) ligand2 induce weaker signaling than ligand1 (i.e., $\varepsilon = 0.01$). Here, the region shown in blue at both sides of the critical line have opposite sign, but are very low and hence they are show as if they were ≈ 0 due to the resolution of the scale.

to act in lateral inhibition (Fig. 2.11B) when it behaves as a partial agonist (i.e., for $\varepsilon < 1$). Notice that this kind of lateral inhibition mediated by ligand2 can be as well significantly strong locally ($R_{s,\langle l_2\rangle}R_{l_2,s} \approx -2.8$).

These results show that the type of lateral regulation mediated by a ligand (i.e., either lateral induction or lateral inhibition) when is co-expressed with a stronger signaling ligand, can be independent of the type of transcriptional regulation it is being subjected to by the signal. This is in contrast to the one ligand scenario in which the type of lateral regulation mediated by that

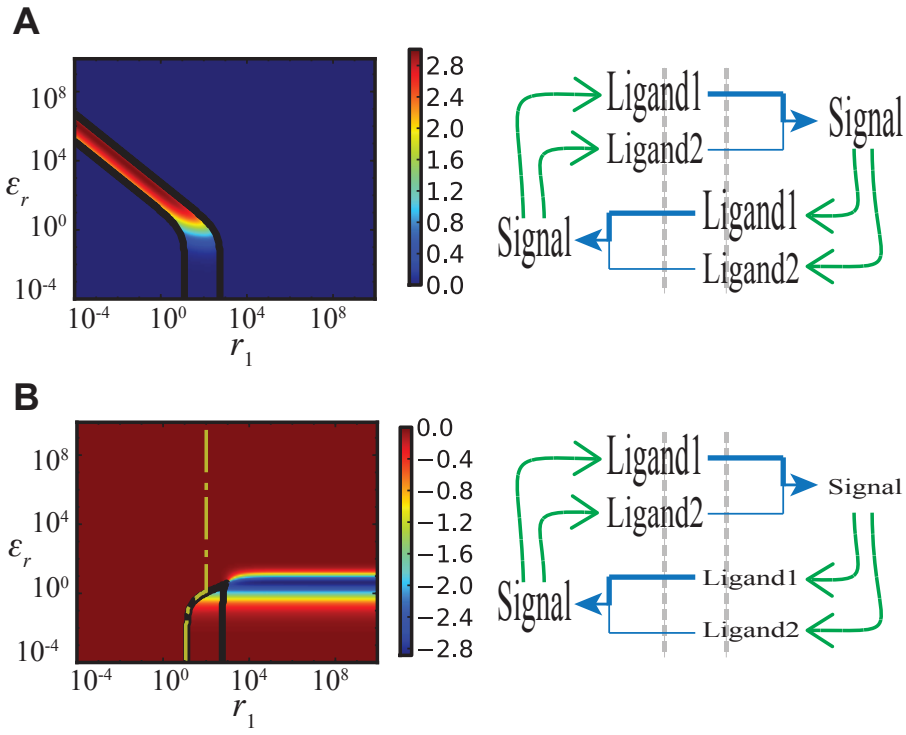

Figure 2.11 Strength of the lateral regulation mediated by ligand2 when ligands are activated by Notch. Heat maps showing the strength of the lateral regulation of ligand2 in the homogeneous steady state (i.e., $R_{s,\langle l_2\rangle}R_{l_2,s}$) when A) both ligands are activated by Notch and they are equivalently strong signaling ligands (i.e., $\varepsilon = 1$) or B) ligand2 induce weaker signaling than ligand1 (i.e., $\varepsilon = 0.01$). (right) Schematic representation of the activity of the ligands and the signal in two neighboring cells within the regime where A) ligand2 activates the formation of the signal or B) ligand2 acts as a partial agonist (i.e., $R_{s,\langle l_2\rangle} < 1$). The levels of each specie is denoted by the font size. Here, the region shown in red at both sides of the critical line have opposite sign, but are very low and hence they are show as if they were ≈ 0 due to the resolution of the scale. In A, the scheme of the right shows that ligand2 can be less efficient than ligand1 at signaling (represented by arrow lines of different width) but still is sufficiently efficient to drive signaling activation.

ligand depends exclusively on the type of regulation exerted by the signal on the production of the ligand.

2.3.2.2 The partial agonist can drive emergent responses when co-expressed with ligand1

In this subsection we addressed whether the lateral regulation mediated by ligand2 acting as a partial agonist can drive a functional response. When both ligands have the same threshold of regulation (i.e., $b_1 = b_2$), we could not find a functional response driven by the partial agonist despite the magnitude of the lateral regulation was high. Therefore, we evaluated the functional response (periodic patterning and ligand propagation) across the parameter space r_1 and ε_r assuming that ligands have different thresholds of regulation (i.e., $b_1 \neq b_2$) and that ligand2 can act as a partial agonist (i.e., $\varepsilon < 1$).

In the case of two ligands repressed by the signal, we found that the partial agonist (ligand2) can drive ligand propagation when $b_2 > b_1$ (Fig. 2.12A). Interestingly, there is a constant regime of ε_r for which this functional response is not disrupted upon over-expression of ligand1 (i.e., for $r_1 \gg 1$), unlike previous cases in which the over-expression of either ligand disrupted the functional response of the system. We explored systematically this relation between the thresholds of regulation of each ligand (i.e., $b_2 > b_1$) and we found that ligand propagation only arises when this condition is met (Fig. 2.12C).

The regime of ligand propagation mediated by ligand2 is characterized by two homogeneous stationary states with low and high levels of the two ligands, respectively (Fig. 2.13A). Yet, in the homogeneous stationary state in which the activity levels of the two ligands is low, the activity level of ligand1 is sufficiently high to activate Notch signaling. Hence, the signaling state of cells can be defined as signal sending/signal receiving, S/R (Fig. 2.13B). After a non-linear perturbation[10] this state evolves to a homogeneous state where both ligands have high activity levels while the signal activity is low. In this state, ligand2 acts as a partial agonist and prevents signaling mediated by ligand1. Therefore we termed this state as signal blocking, B (Fig. 2.13B).

[10] In this context, the non-linear perturbation is done by increasing the activity level of ligand2 locally, in a small cluster of cells within the array (i.e., $l_i = 1$, for each cell i in the cluster).

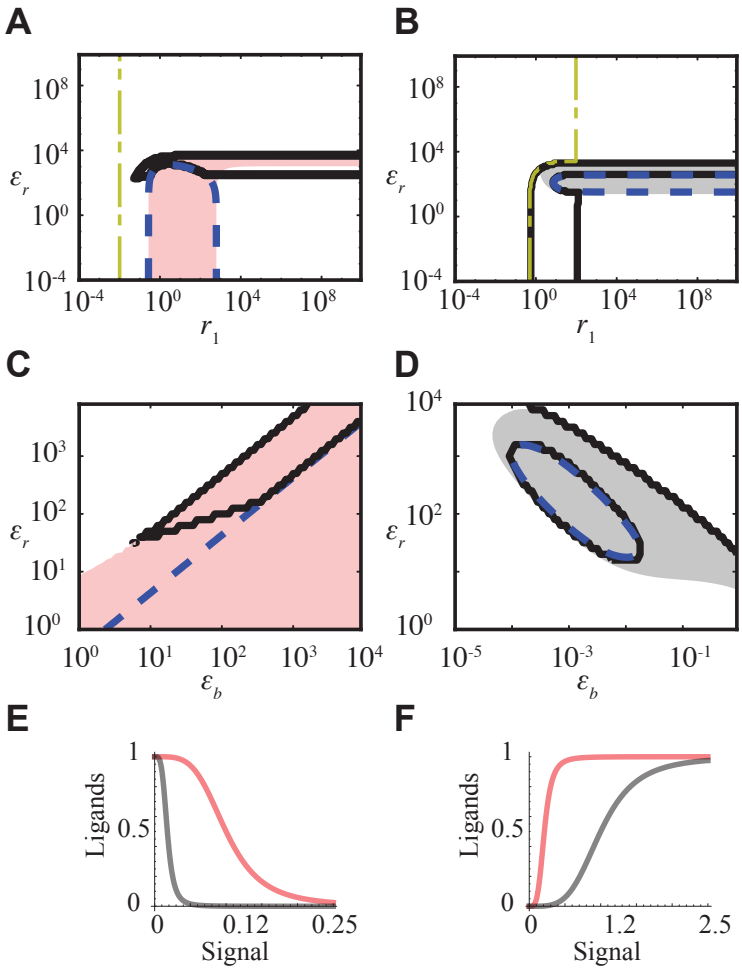

Figure 2.12 Ligand propagation and periodic patterning driven by the partial agonist. Regime of bistability of homogeneous states and ligand propagation when the transcription of the ligands is A) repressed or B) activated by the signal. Ligand2 acts as a partial agonist (i.e., $R_{s,\langle l_2\rangle} < 1$) at the right of the yellow-dashed line. Variable thresholds regulation of the ligands. Regime of bistability of homogeneous states and ligand propagation driven by the ligand2 acting as a partial agonist (i.e., $R_{s,\langle l_2\rangle} < 0$) when $\varepsilon = 0.01$ in C) a regulatory scenario in which the transcription of the two ligands is repressed by Notch and D) in the regulatory scenario in which the transcription of the ligands is activated by notch. We defined $\varepsilon_b = b_2/b_1$. E, F) Schematic repressentation of the response of the ligand activity upon regulation by Notch signaling when the ligands are repressed o activated by the signal. Red and gray curves describes the behavior of ligand1 and ligand2, respectively.

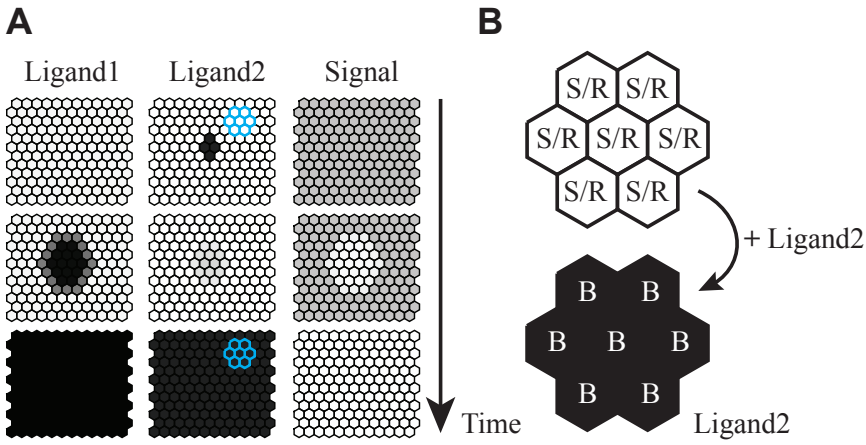

Figure 2.13 Ligand propagation driven by the partial agonist when ligands are respressed by Notch. A) Snapshots of the numerical simulations show the transition from a homogeneous state of low levels of the ligands to a homogeneous state of high levels of the ligands upon the induction of ligand2 in four cell in the center of the array. B) Representation of the signaling states that arise during ligand propagation of the partial agonist (ligand2), depicting the levels of ligand2 in gray scale. Ligand propagation occurs from a homogeneous state where cells are both signal sending and signal receiving (S/R), to a state where cells are signal blocking (B).

When the two ligands are activated by Notch, the partial agonist acting in lateral inhibition (i.e., $R_{s,\langle l_2\rangle}R_{l_2,s} < 0$) can drive periodic patterning for $b_2 < b_1$ (Fig. 2.12B). For a constant regime of ε_r this response can be robust to overexpression of ligand1 (i.e., for $r_1 \gg 1$). Again, we explored systematically this condition and we found that pattern formation only arises when $b_1 > b_2$ (Fig. 2.12D).

We used numerical simulations to confirm the periodicity of the patterned state that arises and which are the cell types that compose this pattern (Fig. 2.14). We found that the patterned state that arises has two different cell types organized according to the proportion $\frac{1}{3}$ and $\frac{2}{3}$ (Fig. 2.14A), which is characteristic of the lateral inhibition-patterned state driven by a single ligand (Fig. 2.1C)[11]. However, the cell types are different in this case compared to those arising in the one ligand scenario. In one of the cell types (I) the activity levels of ligand1 and the signal are low and intermediate, respectively, while there is no activity of ligand2. Therefore, this cell type can send signal (through ligand1, which is

[11] See Appendix A for further details on this.

weakly expressed) but also receive signal, S/R. In the other cell type (II), the activity levels of the ligands and the signal are high. Despite the activity levels of ligand1 are higher in cell type II than in I, the activity levels of the signal are higher in II than in I. This can be explained by the role of ligand2 in cell type II, where this ligand acts as a partial agonist blocking signaling activity in neighboring cells. Because of this, cell type II can be defined both as signal blocking and signal receiver, B/R (Fig. 2.14B).

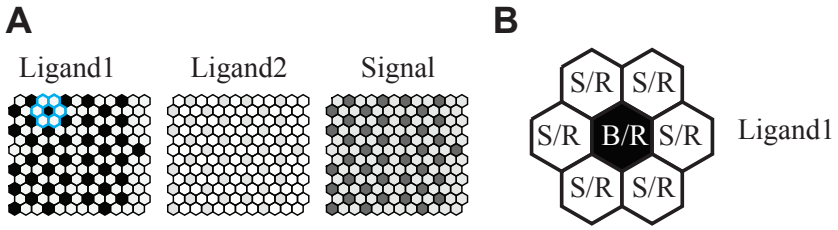

Figure 2.14 Periodic patterning driven by the partial agonist when the transcription of the ligands is activated by Notch. A) Snapshots of the steady state of the numerical simulations showing the periodic patterned state arise when ligand2 acts as a partial agonist. B) Representation of the patterned state shown in A, Depicting the levels of ligand1 in gray scale. Cells with high levels of ligand1 and intermediate to low levels of ligand2 partially block the signal on their neighbors (B/R) which in turn have low levels of the signal and ligand1, sufficient to induce Notch signal on adjacent cells. Thereby, these are signal sending and receiving (S/R).

We reasoned that the differences between the regulatory thresholds of the ligands for which the functional responses arise serves to produce alternative states in which one of the ligands is expressed, but not both simultaneously (Fig. 2.12E, F). Alternative cell types are necessary both for periodic patterning or ligand propagation. When both ligands are repressed by the signal, the partial agonist is more sensitive to repression and therefore it will be repressed by low levels of the signal while activity of ligand1 can be maintained. On the other hand, when both ligands are activated by Notch, ligand1 is more sensitive to activation such that low activity levels of the signal can trigger the transcription of ligand1 but not the transcription of ligand2.

Taken together, these results show that when ligands share resources to signal and they have different signaling efficiency (i.e., $\varepsilon \neq 1$), the overall response of the system can be very different from that expected in the one ligand scenario. In the regulatory scenario discussed in this section, the partial agonist can drive

a response opposite to that expected from the type of regulation of the ligand production (which is the same for both ligands) and requires the co-expression of both ligands. In terms of signaling states, when ligand2 acts as a partial agonist it entails the formation of a novel blocking signaling state, B. In turn, this partial agonist requires the co-expression of a stronger signaling ligand to arise. In this regard, both ligands are equally necessary for the emergent states described in this section to arise. These properties and states can not be envisaged from the one ligand scenario.

2.3.3 Ligands oppositely regulated by Notch signaling can drive concerted responses functional when the ligand2 acts as a partial agonist

In this section we studied which functional response (periodic patterning or ligand propagation) arises when the ligands are oppositely regulated by Notch signaling. In contrast to previous sections, herein one ligand is activated by Notch signaling while the other is repressed. Similarly as in previous cases, ligands are equally strong signaling (i.e., $\varepsilon = 1$) or they signal with different efficiency (i.e., $\varepsilon < 1$)[12], and they use shared or independent resources to signal.

2.3.3.1 The partial agonist cooperates to drive the same response driven by ligand1 expressed in isolation

Since each ligand is oppositely regulated by Notch signaling, with respect to the other, when both ligands are equally efficient at triggering signaling (i.e., $\varepsilon = 1$) different functional responses arise if each ligand is expressed in isolation. The ligand that is repressed by Notch drives periodic patterning while the ligand that is activated drives ligand propagation. However, when they are co-expressed at equivalent levels both functional responses vanish. Since both ligands signal with the same efficiency, they are said to be symmetric in the sense that the outcome of the system is independent on the type of regulation of each ligand as long as there is one ligand being activated and the other ligand being repressed by Notch signaling. This behavior is independent of whether ligands use independent resources to signal or not (Fig. 2.15).

[12]This condition implies that ligand2 is the weaker signaling ligand.

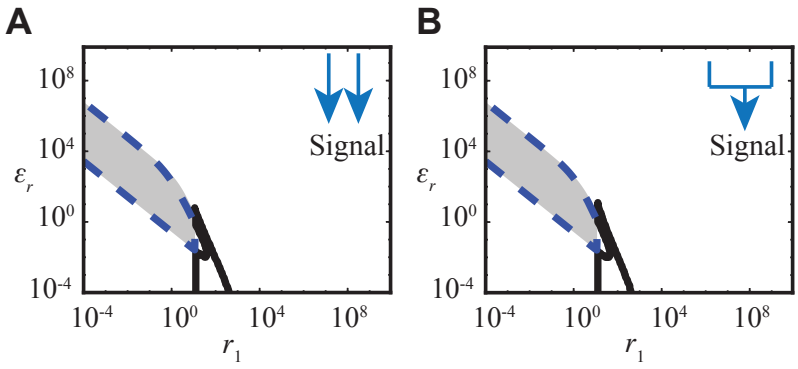

Figure 2.15 Periodic patterning and ligand propagation driven by equivalent ligands oppositely regulated by Notch. Regime of ligand propagation and spontaneous patterning driven by ligand1 and ligand2, respectively, in the parameter space ε_r and r_1. Ligand1 is activated by the signal, while ligand2 is repressed and they activate the signal with the same efficiency (i.e., $\varepsilon = 1$) either using A) independent resources or B) shared resources to signal. Parameter values as described in the text for ligands activated and repressed by the signal.

In the case in which ligands signal differently ($\varepsilon < 1$), they are not symmetric and hence there are two different regulatory scenarios depending on whether the weak signaling ligand is being repressed or activated by the signal (Fig. 2.16). We assumed that the efficiency of signaling of ligand2 is low such that there is no functional response arising when this ligand is expressed in isolation (i.e., for $r_1 \ll 1$). In contrast, the strong signaling ligand can drive a functional response depending on the type of regulation that Notch signaling exerts on its production.

We found that the type of functional response driven by ligand1 in isolation results enhanced upon co-expression with ligand2. This occurs in the region of the parameter space r_1 and ε_r in which ligand2 acts as a partial agonist. For instance, in the regulatory scenario in which ligand1 and ligand2 are activated and repressed by Notch signaling, respectively (Fig. 2.16A), ligand propagation is enhanced a becomes robust to over-expression of ligand1 (i.e., the response is maintained despite having that $r_1 \gg 1$) for a constant regime of ε_r (Fig. 2.17). In previous sections we show that over-expression of the partial agonist (i.e., $\varepsilon_r \gg 1$ for constant r_1) disrupts the functional response when ligands are equivalently regulated by Notch signaling. This also occurs when ligands are oppositely regulated by Notch (Fig. 2.17). However, the region in the parameter

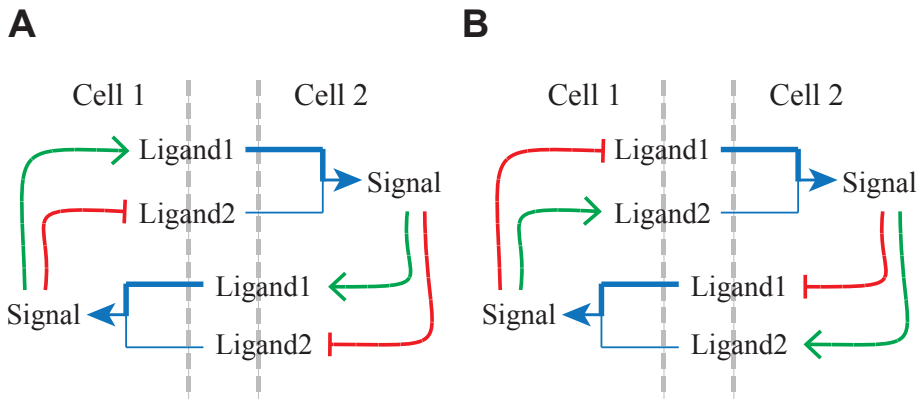

Figure 2.16 Lateral communication mediated by oppositely regulated ligands. A) Schematic representation of the regulatory interactions between two neighboring cells. Ligands binds the same receptor to activate the signal, but they have different signaling efficiency (denoted by the thickness of the arrow). The transcription of ligand1 and ligand2 is activated (green arrow) and repressed (red-blunt arrow) by the signal, respectively. B) The same as in A, but in this case the transcription of ligand1 and ligand2 is repressed and activated by the signal, respectively.

space for which ligand propagation arises becomes wider when the ligands are co-expressed (Fig. 2.17). This effect on the regime where the functional response (ligand propagation) arises upon co-expression is what we call *enhancement* of the response.

In addition, we explored a related case in which ligand1 is a strong signaling ligand, but it is not able to drive ligand propagation when expressed in isolation given that its Hills coefficient is low (i.e., we assumed that $h_1 = 1$ instead of $h_1 = 4$). In this case, we found that ligand propagation can still arise only when both ligands are co-expressed (Fig. 2.17C). We concluded that the functional response is driven cooperatively by both ligands in the sense that both are needed in order that the response can arise.

We explored which signaling states can be formed in this type of response mediated cooperatively by both ligands. We found two homogeneous stationary states differentiated by the activity levels of the ligands and the signal in each state. In one, cells have high activity levels of ligand2 and low activity levels of ligand1 and the signal. Despite the levels of ligand1 are low, they could drive high signal activity levels if this ligand was expressed in isolation. However,

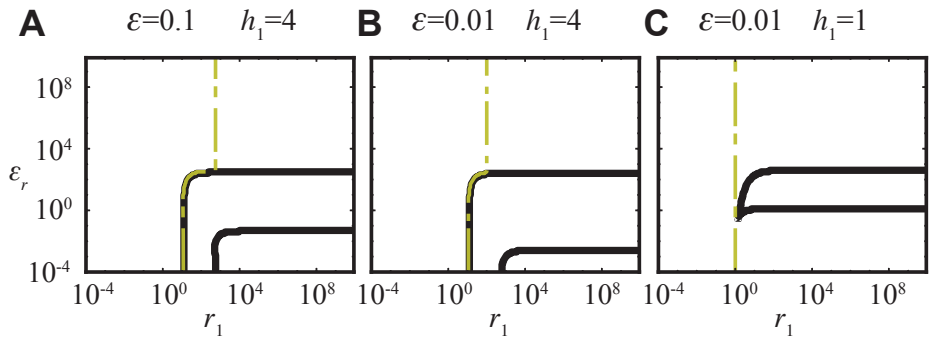

Figure 2.17 Bistability of homogeneous states and ligand propagation driven cooperatively by the two ligands. Regime of bistability of homogeneous states and ligand propagation when ligand1 is activated by the signal and ligand2 is repressed, as described in Fig. 2.16A, in the parameter space ε_r and r_1. Ligand2 acts as a partial agonist of the signal in the region at the right of the yellow-dashed line. The diagrams depict ligand propagation either when ligand1 is able to drive it expressed in isolation (i.e., panels A and B for $h_1 = 4$) or not (i.e., panel C for $h_1 = 1$).

this is not the case due to the co-expression with ligand2 which acts as a partial agonist. Therefore, the expression of this ligand drives a signal blocking state, B (Fig. 2.19). In the other homogeneous state, cells have high levels of ligand1 and the signal and low levels of ligand2. Therefore, this state can be termed as signal sending and receiving state[13], S/R (Fig. 2.19). There can be two types of ligand propagation events, each associated to a different ligand (Fig. 2.18A, B). These propagation events involve the transition from one to other of the homogeneous stationary states described above, upon non-linear perturbations[14] (Figs. 2.18 and 2.19).

Likewise, in the regulatory scenario in which ligand1 and ligand2 are repressed and activated by Notch signaling, respectively (Fig. 2.16B), we found that periodic patterning becomes insensitive to over-expression of ligand1 within a constant regime of ε_r when ligand2 acts as a partial agonist (Fig. 2.20A-C). For a very similar model this result is shown in [Formosa Jordan, 2013, Petrovic et al., 2014]. In addition, we found that three different patterned states can arise (Fig. 2.21). These are composed by two or three different cell types, where each

[13] Using the notation of Boareto et al. [2015].

[14] Non-linear perturbations in this case consists in the increase of the activity levels of one of the ligands locally in a small cluster of cells within the array.

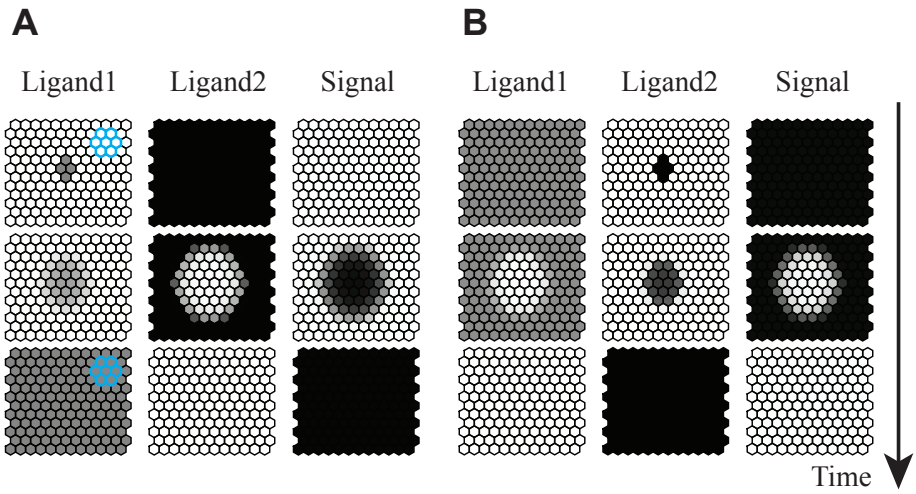

Figure 2.18 Types of ligand propagation occurring in the regime of trans-inhibition when ligand1 is activated and ligad2 is repressed by Notch. A) Snapshots of the numerical simulations showing the ligand1 propagation in an array of hexagonal cells after induction of this ligands in four cells in the middle of the array. The dimensional levels of the species are described in gray scale as in Fig. 2.1C. B) Snapshots of the numerical simulations showing the ligand2 propagation in an array of hexagonal cells after induction of this ligands in four cells in the middle of the array.

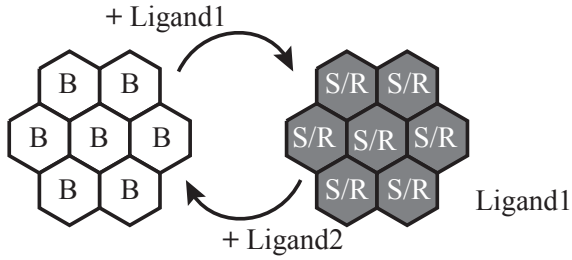

Figure 2.19 Signaling states involved in the transitions outlined in each ligand propagation event, as described in Fig. 2.18. Propagation of ligand1 involves the transition from a homogeneous state of cells mutually blocking signal activity (B) which could be activated by ligand1 to a homogeneous state of cells sending and receiving signaling (S/R).

cell type is associated to a different signaling state. The signaling states that arise can be briefly described as

1. S: Signal sending cells with high levels of the signaling ligand (ligand1) and low levels of ligand2 (which acts as a partial agonist)[15].
2. B/R: Signal blocking and receiving cells. These cells have high levels of the signal and the partial agonist (ligand2) and low levels of ligand1. In this cell type, the high activity levels of the partial agonist can block signal activity in a neighboring cell type with high levels of ligand1 (for instance in Fig. 2.21 in the middle panel).
3. R: Signal receiving cells. These cells have intermediate to high activity levels of the signal, and low levels of the ligands.

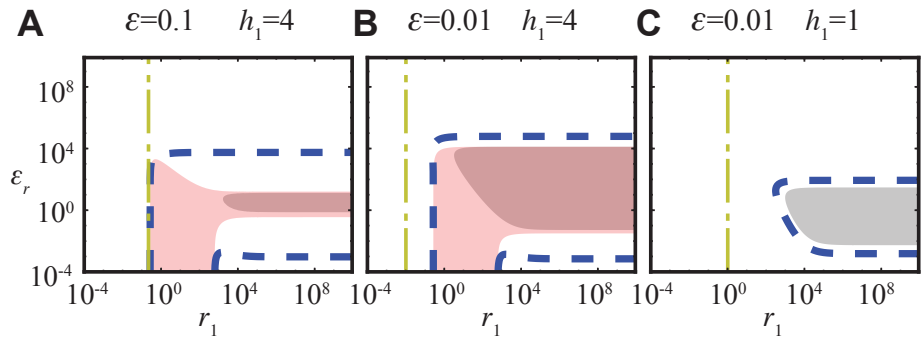

Figure 2.20 Periodic patterning driven cooperatively by the two ligands. Regime of spontaneous pattern formation when ligand1 is repressed by the signal and ligand2 is activated, as described in Fig. 2.16B, in the parameter space ε_r and r_1. Ligand2 acts as a partial agonist of the signal in the region at the right of the yellow-dashed line. The diagrams depict ligand pattern formation either when ligand1 is able to drive it when expressed in isolation (i.e., panels A and B for $h_1 = 4$) or not (i.e., panel C for $h_1 = 1$).

We reasoned that this behavior (i.e., the enhancement of the functional response) can be explained by the cooperation between the type of lateral regulation that each ligand is mediating. For instance, in the case described in Fig. 2.16A, both ligands are acting in lateral induction (i.e., $R_{s,\langle l_1\rangle}R_{l_1,s} > 0$ and

[15]Note that in each case, S cells have at least one neighboring cell type R, which means that S is truly acting as signal sending.

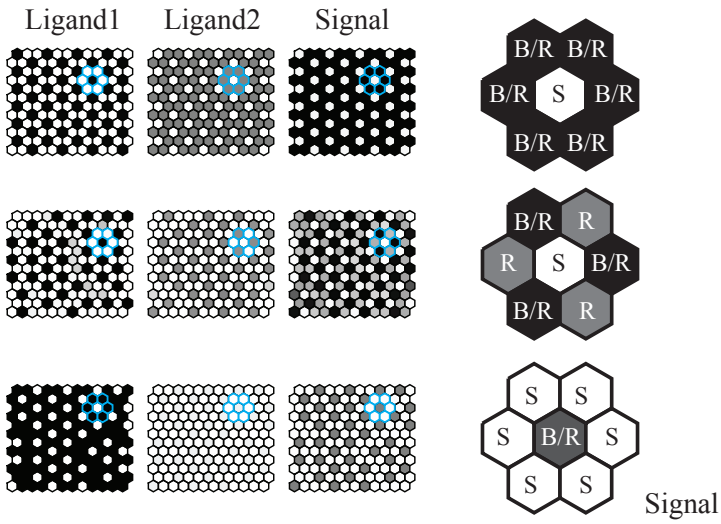

Figure 2.21 Types of patterned states that arise in the regime of trans-inhibition when ligand1 is repressed and ligad2 is activated by Notch. Snapshots of the numerical simulations showing the steady patterned states for each species. Parameter values are $\varepsilon = 10^{-2}$, $r_1 = 10^4$ and (top) $\varepsilon_r = 10^{-3}$, (middle) $\varepsilon_r = 10$ and (bottom) $\varepsilon_r = 5 \cdot 10^4$. (Right) Representation of the signaling states in a cluster of cells withing the arrays described in the snapshots (edges highlighted in blue). Signaling states are represented in terms on the levels of the signal activity. Cells can be signal blocking and receiving (B/R), signal sending (S) or signal receiving (R).

$R_{s,\langle l_2\rangle} R_{l_2,s} > 0$) when ligand2 behaves as a partial agonist[16]. Since both ligands mediate the same type of lateral regulation, the functional response associated to that type of regulation is cooperatively facilitated. We found that the cooperation between ligands can be sufficiently strong to drive a concerted functional response even when it cannot be driven by either ligand expressed in isolation[17] (Figs. 2.17C and 2.20C). In terms of the magnitude of the lateral regulation mediated by each ligand (for instance, in the regulatory scenario described by Fig. 2.16B), we can have that $R_{s,\langle l_1\rangle} R_{l_1,s} > -2$ and $R_{s,\langle l_2\rangle} R_{l_2,s} > -2$, but $R_{s,\langle l_1\rangle} R_{l_1,s} + R_{s,\langle l_2\rangle} R_{l_2,s} < -2$ such that patterning can arise. In this regard,

[16] In previous sections we have shown that the type of lateral regulation in which ligand2 is acting can change when this ligand behaves as a partial agonist.

[17] We have assumed $h_1 = 1$ in the cases shown in Figs. 2.17C and 2.20C, such that ligand1 is not able to drive neither ligand propagation nor periodic patterning when expressed in isolation, respectively.

despite the lateral regulation mediated by each ligand is not sufficiently strong to drive patterning, when co-expressed the functional response can arise.

Taken together, our results show that ligands driving opposing responses when expressed in isolation can cooperate to drive a concerted response when co-expressed, which correspond to the type of respond driven by the stronger ligand when expressed in isolation. This type of functional response is different from that expected in the one ligand scenario because (i) it can be robust to over-expression of ligand1 and (ii) it produces signaling states involving the partial agonist (i.e., B states), which can only arise in the two ligands scenario.

2.3.3.2 Cooperation between ligands to drive pattern formation involves faster patterning dynamics

We studied the patterning dynamics associated to the systems driving periodic pattern formation studied in previous sections. Briefly, the systems driving patterning that we analyze in this section are[18]

1. one ligand, which is repressed by Notch signaling (Fig. 2.1),
2. two ligands equally repressed by Notch, where ligands signal with the same efficiency (i.e., $\varepsilon = 1$) and they use independent resources to signal (Fig. 2.3A),
3. two ligands equally repressed by Notch, where ligands signal with the same efficiency (i.e., $\varepsilon = 1$) and they use shared resources to signal (Fig. 2.3B),
4. two ligands oppositely regulated, which signal differently such that ligand2 acts as a partial agonist (i.e., $\varepsilon < 1$) and ligands used shared resources to signal (Fig. 2.20B).

Therefore, in 2 and 3 ligands can drive redundantly pattern formation upon co-expression, but in 4 the co-expression of the ligands enables cooperative patterning.

[18]The system in which both ligands are activated by Notch signaling can drive pattern formation when ligand2 acts as a partial agonist. This system has not been taken into account in this section because the distribution of ligand1 and the signal is not comparable to that arising in the one ligand scenario.

To address the patterning dynamics we used the results of the linear stability analysis in the homogeneous steady state and numerical simulations of the dynamics on arrays of hexagonal cells. From the linear stability analysis (Appendix A for $v = 1$), the growing rate of the fastest growing mode (i.e., for $\Omega_{\frac{1}{3},\frac{2}{3}} = \Omega_{\frac{2}{3},\frac{1}{3}} = -0.5$)[19] reads

$$\lambda_{\text{Max}} = -1 + \sqrt{-\frac{1}{2}(R_{s,\langle l_1\rangle} R_{l_1,s} + R_{s,\langle l_2\rangle} R_{l_2,s})} \tag{2.18}$$

This rate predicts the exponential growth of the periodic perturbations about the homogeneous stationary state, in the linear regime. Hence this rate can be useful as a first estimate of the time scale of patterning initiation. We evaluated this rate in the parameter space ε_r and r_1, for the systems described above. According to the obtained values of λ_{Max}, we found that periodic patterning is expected to arise faster when there is cooperation between ligands to a response than in the case in which patterning is a redundant response (Fig. 2.22A-C).

Using numerical simulations we corroborated this tendency. We defined an order parameter for the non-dimensional values of ligand1 activity (l_1) in a perfect array of hexagonal cell as

$$\Theta(t) = \frac{1}{N}\sum_{i=1}^{N}\left|l_{1,i}(t) - \langle l_{1,i}(t)\rangle\right| \tag{2.19}$$

where i labels the cell within the array, N is the total number of cells and $\langle l_{1,i}(t)\rangle = \frac{1}{\omega}\sum_{j\in NN} l_{1,j}(t)$ is the ligand l_1 activity averaged over the Nearest Neighbors of cell i, as defined above. We evaluated the characteristic patterning time, which is the time when the patterned state of the array is approximately the same as that in the final time of the simulation (t_f). This characteristic patterning time is defined as the time t_p for which the following condition meets

$$\left(\underbrace{\left|1 - \frac{\Theta(t)}{\Theta(t_f)}\right|}_{\kappa} \leq 10^{-3}\right) \forall_{t\geq t_p} \tag{2.20}$$

[19]This mode corresponds to the periodic perturbations that can drive a lateral inhibition-like periodic patterning. Details on the linear stability analysis are shown in Appendix A.

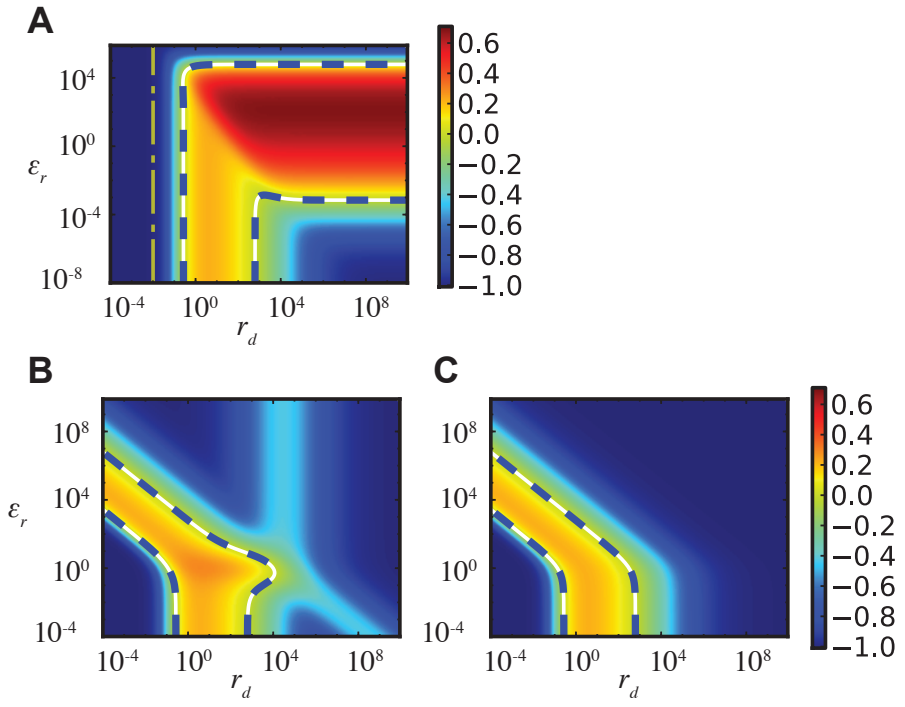

Figure 2.22 Patterning dynamics driven by co-expressing ligands in the linear regime. Heat maps showing the growing rate of the perturbations in the homogeneous state (λ_{Max}) when A) ligands are antagonistically regulated by Notch, signal differently and share resources for signaling (as described in Fig. 2.20B), B) when ligands are both repressed by Notch, have the same signaling efficiency (i.e., $\varepsilon = 1$) and use independent resources to signal (as described in Fig. 2.3C) or C) when ligands are both repressed by Notch, have the same signaling efficiency (i.e., $\varepsilon = 1$) and use shared resources to signal (as described in Fig. 2.3D). Color scale is the same for the three cases.

where $\Theta(t_f)$ is the value of the parameter order at the final time of the simulation, $t_f = 500$ a.u. This condition was evaluated at each time step t_j, having $t_j < t_f$. These simulations were done assuming parameter values $r_1 = 100$ and $\varepsilon_r = 1$ in all cases except the case in which there is one ligand only, where we assumed $\varepsilon_r = 0$. Numerical details on the simulations can be found in Appendix B.

We found that the four models described above exhibit disparity in their characteristic patterning time, but a hierarchy between the systems can be drawn (Fig. 2.23). In the model in which oppositely regulated ligands that signal differently (i.e., $\varepsilon < 1$) cooperate, patterning arises faster, in accordance to the

prediction in the linear regime (Fig. 2.22). Interestingly, when the two ligands are repressed by the signal and are equally efficient at signaling (i.e., $\varepsilon = 1$) the dynamics is different depending on whether they use independent resources to signal or not. When they do, the patterning dynamics is faster than in the case in which there is only one ligand repressed by the signal (Figs. 2.23). If ligands use shared resources to signal, then the patterning dynamics is slower than in the case of one ligand. We observed this behavior when the initial conditions of the signal correspond to the homogeneous stationary levels plus random perturbations (while the initial conditions of the ligands are the stationary levels without perturbations), but also in the case when the initial conditions of the ligands and the signal correspond to the homogeneous stationary levels plus random perturbations (Fig. 2.23).

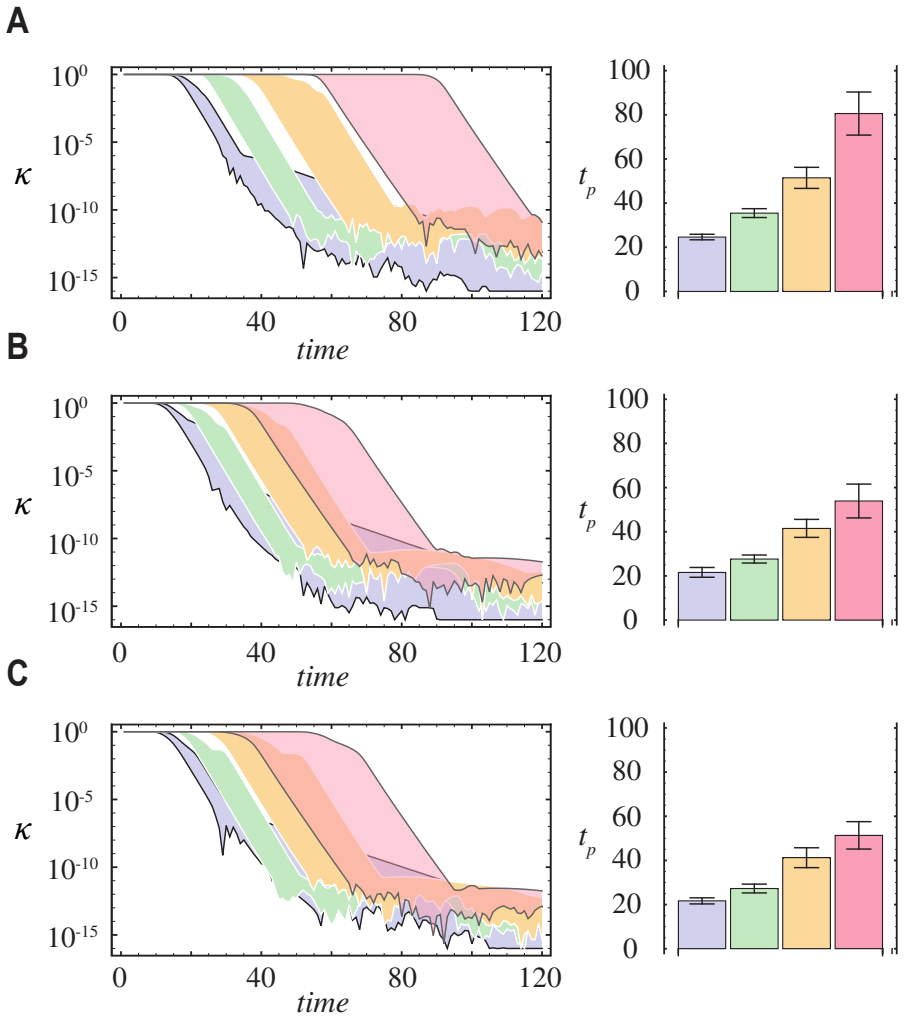
A
B
C
10^{0}
10^{-5}
10^{-10}
10^{-15}
κ
0
40
80
120
time
100
80
60
40
20
0
t_p

Figure 2.23 ***(previous page)*** Patterning dynamics driven by co-expressing ligands inferred from numerical simulations. Ensemble of 25 simulations showing the time course of $\kappa = \left|1 - \frac{\Theta(t)}{\Theta(t_f)}\right|$ (left side of condition 2.20) as a characterization of the patterning dynamics of the four scenarios described in the text, i.e, (i) ligands oppositely regulated by Notch (purple), (ii) ligands equivalently regulated by Notch using independent resources (green) and (iii) shared (red) resources to signal and (iv) one single ligand repressed by Notch (orange). In each scenario the simulations were done using different initial conditions (see Appendix B for details). Average values of the patterning time (t_p) evaluated according to condition 2.20 are shown in the bar diagrams of the right. The color code of the bars is the same as the code for the time courses in the left. Initial conditions of the simulations were set by random perturbations about the homogeneous steady state as described in Appendix B. These perturbations were induced on the initial levels of A) only ligand1 (i.e., the initial levels of ligand2 and the signal are not subject to perturbations), B) only the signal (i.e., the initial levels of the ligands are not subject to perturbations) or C) all the species, i.e., the ligand(s) and the signal.

Taken together, these results show that co-expressing a weak signaling ligand (activated by Notch) acting as a partial agonist can drive a faster patterning dynamics than the case in which co-expressed equivalent ligands drive patterning redundantly. Although intuition could suggest that Notch signaling could enhance more efficiently a specific response by co-expressing two equivalent ligands which expressed in isolation each can mediate such specific response, our results suggest that a better mechanism in terms of patterning dynamics can be to co-express antagonistically regulated ligands where one of them can act as a partial agonist of the signal.

2.3.4 Oppositely regulated ligands can drive oscillations

In the previous sections, the activation of the signal is triggered by the ligands following a Michaelis-Menten-like behavior. However, the activation of the signal mediated by the ligands could be sharper due to different processes not being taken into account explicitly here, e.g., cis-inhibition [Sprinzak et al., 2011]. In this section we address which functional response arises in the regulatory scenario in which there are two ligands oppositely regulated by Notch signaling, which in turn trigger signaling with Hills coefficients > 1. Assuming that ligand1 and ligand2 are repressed and activated by Notch signaling, respectively (Fig. 2.24A), the dynamic equations read

$$\begin{aligned}
\frac{\mathrm{d}s_i}{\mathrm{d}t} &= \frac{r_1\langle l_{1,i}\rangle^{h_{s1}} + \varepsilon\varepsilon_r r_1\langle l_{2,i}\rangle^{h_{s2}}}{1 + r_1\langle l_{1,i}\rangle^{h_{s1}} + \varepsilon_r r_1\langle l_{2,i}\rangle^{h_{s2}}} - s_i \\
\frac{\mathrm{d}l_{1,i}}{\mathrm{d}t} &= v\left(\frac{1}{1 + b_1 s_i^{h_1}} - l_{1,i}\right) \\
\frac{\mathrm{d}l_{2,i}}{\mathrm{d}t} &= v\left(\delta_l + (1-\delta_l)\frac{b_2 s_i^{h}}{1 + b_2 s_i^{h_2}} - l_{1,i}\right)
\end{aligned} \tag{2.21}$$

For the calculations presented in this section we assumed parameter values similar to those used in previous sections, $b_1 = 10^4$, $b_2 = 1$, $r_1 = 95$, $r_2 \equiv \varepsilon_r r_1 = 15$ and $\varepsilon = 0.9$. The main difference in these values is that the cooperativity in the activation of the signal is higher than before, i.e., $h_{s1} = h_{s2} = 4$. We evaluated the system dynamics by numerical integration of Eqns. 2.21 in an array of hexagonal cells imposing periodic boundary conditions. Details of the numerical simulations are described in Appendix B.

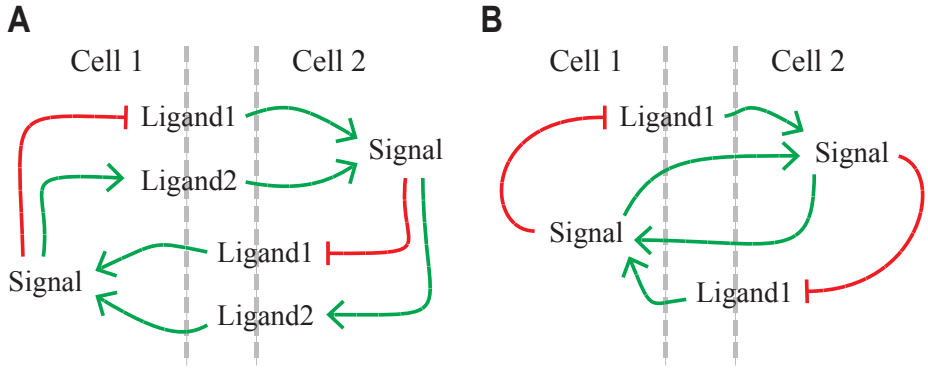

Figure 2.24 Antagonistic ligands driving oscillations. A) Schematic representation of the functional interactions between ligands and the signal in a system in which both ligands effectively activate the signal in neighboring cells. Transcriptional regulation of the ligands is represented as described in previous figures. B) The same as A, but for the case in which there is only one ligand taken into account explicitly. High levels of the signal activity drive high levels of the signal in the neighboring cell.

We found that oscillations around a patterned state can arise in this scenario (Fig. 2.25). Because of this, the signaling states are not fixed but can change in time (Fig. 2.26A), i.e., a cell can act as signal sending during a period of time, and then change to signal receiving spontaneously. In this regard, the initial condition can favor the differentiation of a given cell in one particular direction,

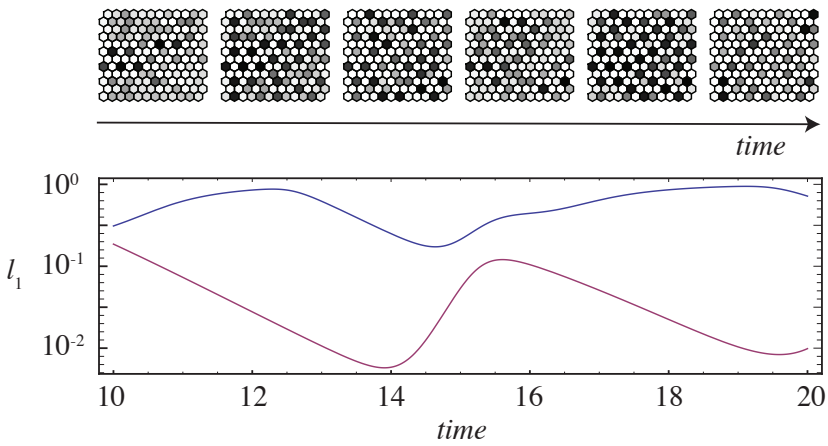

Figure 2.25 Oscillatory dynamics of the inter-cellular signaling system (short time). (Top) Snapshots of the numerical simulations showing the oscillations of the patterned state in the cell array, from 10 a.u. to 20 a.u.. The levels of activity of ligand1 are represented in gray scale as described for previous figures. (Bottom) Time course of the levels of ligand1 in two neighboring cells within they array of hexagonal cells described in top.

but only initially since this signaling state can be reversed spontaneously even at late times (Fig. 2.26A, B). We found that oscilations can also arise in a system in which ligands use independent resources to signal (Fig. 2.26C).

The novel oscillatory functional response seems to arise from an instability of the inhomogenoeus (patterned) state. Therefore, the theoretical framework developed in previous sections, which has focused on the analysis of the homogeneous state, cannot be used to address the emergence of these oscillations. Hence, we proposed a simplified version of this system, with less dynamical variables, in order to facilitate the analysis of the inhomogeneous states. We assumed a system of only two cells in mutual interaction. In this simplified model, the activation of the signal activity in one cell occurs by the activity levels of the ligand and the signal in the neighboring cell (Fig. 2.24B). Accordingly, the production of the ligand is repressed by the signal activity. Taking into account these regulatory interactions, the dynamic equations read

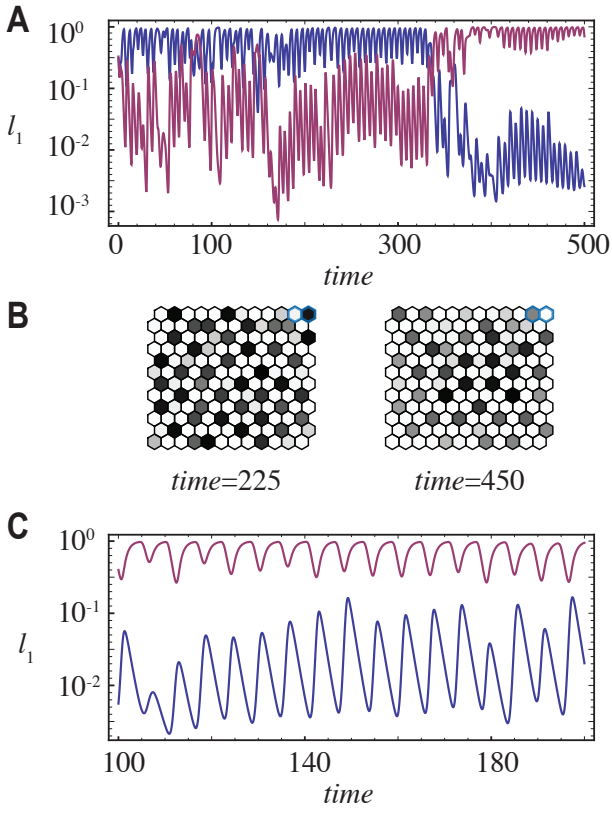

Figure 2.26 Oscillatory dynamics of the inter-cellular signaling system (long time). A) Time course of the levels of ligand1 (l_1) in the two neighboring cells (highlighted in B), where the levels of the ligands are represented in logarithmic scale. B) Snapshots of the numerical simulations showing the change of signaling state of two neighboring cells (light-blue). C) Time course of the levels of ligand1 in two neighboring cells within an array of hexagonal cells, as described in A, but in the case in which ligands use independent resources to signal.

$$\begin{aligned} \frac{\mathrm{d}s_i}{\mathrm{d}t} &= \frac{r_1 l_{1,j}^{h_{s1}} + r_2 s_j^{h_{s2}} \varepsilon}{1 + r_1 l_{1,j}^{h_{s1}} + r_2 s_j^{h_{s2}}} - s_i \\ \frac{\mathrm{d}l_{1,i}}{\mathrm{d}t} &= v \left(\frac{1}{1 + b_1 s_i^{h_1}} - l_{1,i} \right) \end{aligned} \tag{2.22}$$

where $i = 1$ and $j = 2$ for cell 1 and $i = 2$ and $j = 1$ for cell 2.

Using this approach we described the phase portrait of the system. We found that an oscillatory behavior around inhomogeneous states (i.e., $s_i \neq s_j$ in the

steady state) coexists with a homogeneous stable state (Fig. 2.29A). In this regard, when the initial conditions are the same in the two cells, they evolve to the homogeneous state. If small fluctuations are considered then the dynamics evolves towards one of the two oscillatory states. We also corroborate that oscillations require high Hills coefficient to arise (Fig. 2.29A-C)

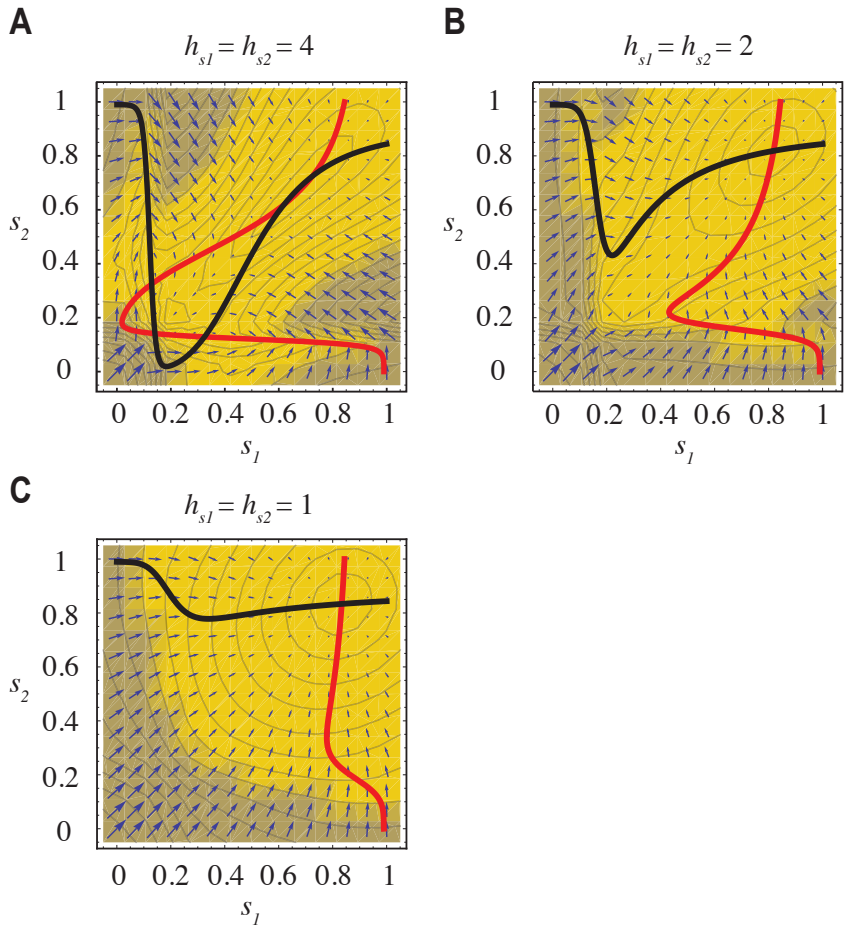

Figure 2.27 Oscillation of the inhomogeneous state in the two cells system. A-C) Phase portrait showing the nullclines for the signal dynamics in each cell (black and red curves) for different cooperativity coefficients (h_{s1} and h_{s2}) as indicated in each panel. In the vector field, the size of each vector represent the magnitude of the flow discontinually while the color and the contour lines stands for continuous variations in the magnitude of flow.

Mutual activation of the signal between cells is governed by r_2 when $\varepsilon \approx 1$. When this mutual activation drives signal activity significantly (i.e., $r_2 \gg r_1$) it

is expected to generate a regime of lateral induction consistent to that described in previous sections. In contrast, when the mutual activation is not significant (i.e., $r_2 \ll r_1$) then it is expected that the circuit of lateral inhibition mediated by ligand1 governs the systems response. In this regard, a transition from lateral induction to lateral inhibition can arise by changing the relation between r_2 and r_1 (i.e., $\frac{r_1}{r_2}$). This type of transition has been described in many developmental scenarios (see discussion below). We reproduced this transition using numerical simulations of Eqns. 2.22, from high to low values of r_2. We found that for high levels of r_2 (i.e., $r_2 \approx r_1$) equivalent cells with low levels of the signal can evolve to a homogeneous state characterized by higher levels (Fig. 2.28A). As the value of r_2 decreases (while the value of r_1 is maintained constant, i.e., $r_2 < r_1$), the oscillatory dynamics arises (Fig. 2.28B). Finally, when the value of r_2 is very low compared to r_1, cells adopt stationary opposed states, as occurs in the case of lateral inhibition mediated by one ligand (Fig. 2.28C). We concluded that the oscillatory regime of the inhomogeneous state can arise as an intermediary state between lateral induction and lateral inhibition (Fig. 2.28).

Finally, we analyzed this simplified model to identify the underlying mechanism driving the oscillations. We found that (i) low signal activity levels in cell 1 induce a repression on the signal in cell 2, but (ii) for increasing activity levels of the signal in cell 1 the signal becomes activated in cell 2 (Fig. 2.29A). We reasoned, that the mutual regulation of the activity of the signal between the two cells is mediated by an incoherent feedforward loop (Fig. 2.29B). A key aspect of this kind of loop is that the thresholds of the antagonistic effects (i.e., activation and inhibition) should be different such that each type of regulation takes place for different levels of the signal activity.

In the cases studied in previous sections, when ligands were co-expressed and they were equally efficient at signaling (i.e., $\varepsilon = 1$), they either disrupted each others response or they drive a redundant state. However, these results show that equally strong signaling ligands can drive other functional responses when co-expressed (assuming high Hills coefficients). Given that the partial agonist is not involved in the emergence of oscillations, this type of response can arise either if ligands use shared or independent resources to signal.

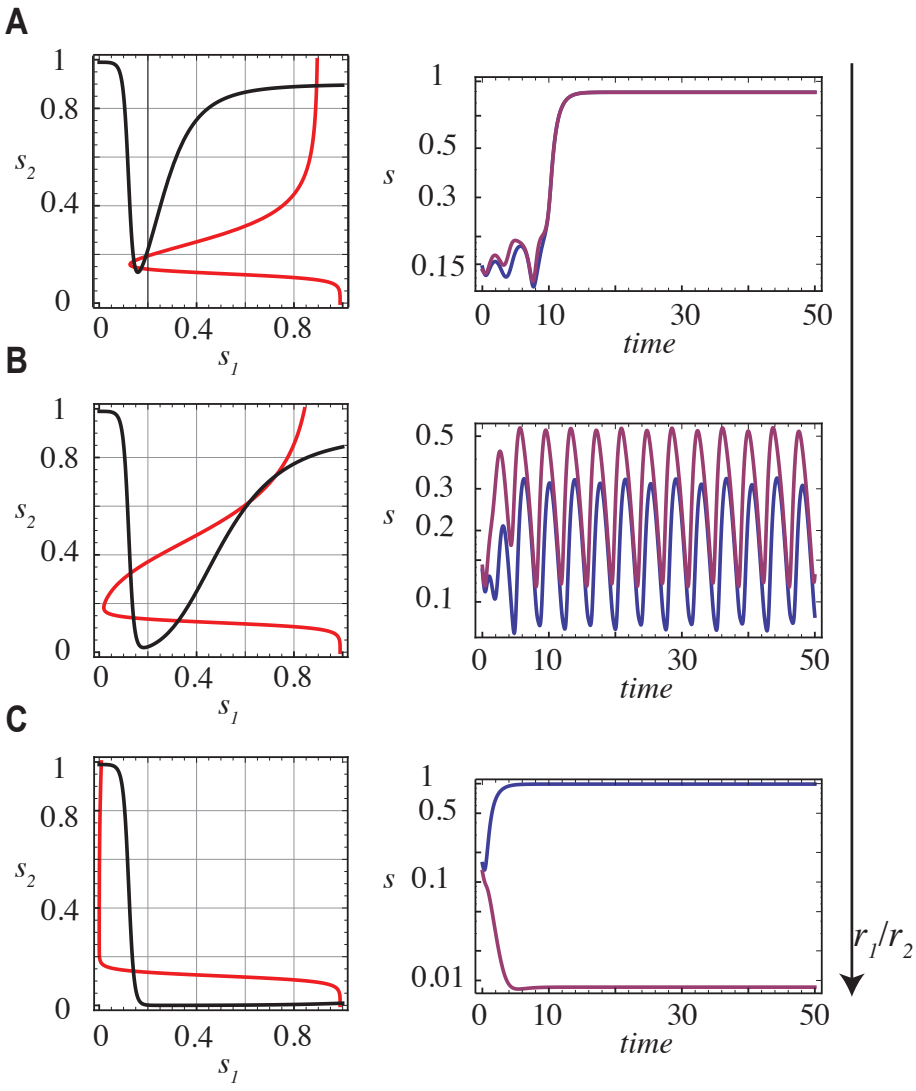

Figure 2.28 Functional response of the two cell system for decreasing levels of the mutual trans-activation of the signal (r_2). Phase portrait (left) and time course of the levels of the signal (right) of the system of two cells described by Eqns. 2.22. The phase portrait describe the nullclines for the signal in cell1 (red) and cell2 (black) and the fixed points corresponds to the intersection of both nullclines. The analysis describes the outcomes of the system for different values of r_2 (setting $r_1 = 95$ constant): A) Bistability of homogeneous states by lateral induction (for $r_2 = 100$), B) oscillations about the inhomogeneous states mediated by the incoherent feedforward loop (for $r_2 = 15$) and C) opposing cell differentiation between the two cells mediated by lateral inhibition (for $r_2 = 0.01$).

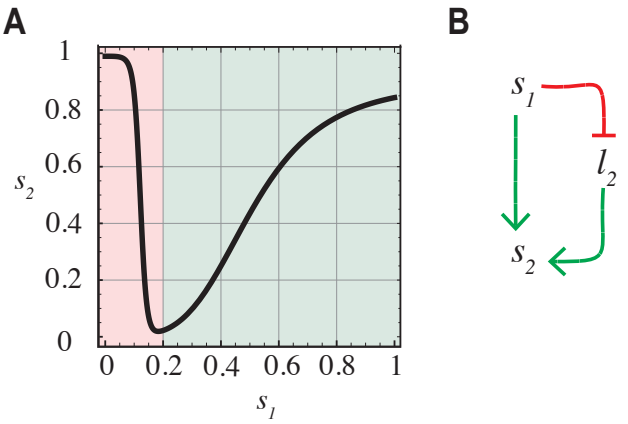

Figure 2.29 Oscillation of the inhomogeneous state in the two cells system. A) Nullcline of the dynamics of the signal in cell 2 extracted from Fig. 2.29A showing that the signal in cell 2 has two regimes of regulation by the signal in cell 1, inhibition and activation. B) Schematic representation of the incoherent feed forward loop mediated by two antagonistic interactions leading to first repression and then activation of the signal.

2.3.5 The inner ear as a case of study

Notch signaling has shown essential during specification and differentiation of hair cells (HC) in mammals[20]. At the stage of HC differentiation and patterning in the mammalian inner ear, cells co-express three different ligands, Jagged1 (Jag1), Jagged2 (Jag2) and Delta1 (Dl1) which are distinctly regulated by Notch. The transcription of Jag2 and Dl1 is repressed by Notch signaling [Brooker et al., 2006, Kiernan et al., 2005] while the transcription of Jag1 is activated [Kiernan et al., 2001]. It has been shown that these ligands expressed in the inner ear only need to bind to one receptor type (Notch1) to trigger signaling, despite there are two isoforms of Notch expressed at this developmental stage. *In vitro* and *in vivo* experiments have shown that these ligands can activate Notch signaling at different levels, depending partially on post-transcriptional modifications on Notch receptor, such as glycosylation [Hicks et al., 2000, Yang et al., 2005, Zhang et al., 2000].

Extending the framework developed in previous sections, in this section we addressed the regime of periodic pattern formation when Notch signaling is

[20] We described in more detail the role of Notch signaling in different context during development and differentiation in Metazoa in the Introduction.

triggered by three ligands, as in the specific context of HC patterning and differentiation in the mammalian inner ear. Based on the regulatory interactions of Notch signaling on the ligands activity, we proposed a model of Notch signaling with three co-expressed ligands, Jag2 (l_1), Dl1 (l_2) and Jag1 (l_3), such that the dynamics in cell i reads

$$\begin{aligned}
\frac{\mathrm{d}s_i}{\mathrm{d}t} &= \frac{r_1\langle l_{1,i}\rangle + \varepsilon_1 r_2\langle l_{2,i}\rangle + \varepsilon_2 r_3\langle l_{3,i}\rangle}{1 + r_1\langle l_{1,i}\rangle + r_2\langle l_{2,i}\rangle + r_3\langle l_{3,i}\rangle} - s_i \\
\frac{\mathrm{d}l_{1,i}}{\mathrm{d}t} &= v\left(\frac{1}{1+b_1 s_i^{h_1}} - l_{1,i}\right) \\
\frac{\mathrm{d}l_{2,i}}{\mathrm{d}t} &= v\left(\frac{1}{1+b_2 s_i^{h_2}} - l_{2,i}\right) \\
\frac{\mathrm{d}l_{3,i}}{\mathrm{d}t} &= v\left(\delta_l + (1-\delta_l)\frac{b_3 s_i^{h_3}}{1+b_3 s_i^{h_3}} - l_{3,i}\right)
\end{aligned} \tag{2.23}$$

where ε_1 and ε_2 stand for the efficiency of signaling of Dl1 and Jag1 with respect to Jag2 (respectively), as discussed for the two ligands model.

The details on the linear stability analysis for this models are described in Appendix A. The condition for which the homogeneous steady state is linearly unstable to inhomogeneous small perturbations, leading to the formation of patterned states reads

$$R_{s,\langle l_1\rangle} R_{l_1,s} + R_{s,\langle l_2\rangle} R_{l_2,s} + R_{s,\langle l_3\rangle} R_{l_3,s} \leq -2\,. \tag{2.24}$$

We confirmed that the patterns follow the same periodicity of that described by experiments, implementing numerical simulations of the dynamic equations 2.23. We analyzed the model 2.23 to adress some puzzling phenotypes that arise in this regulatory scenario[21].

First puzzling phenotype. HC periodic patterning arises when there are antagonistically regulated ligands being co-expressed. How can a single response arise in a context in which there are ligands expected to drive opposing responses

[21] The parameter values related to Jag1 dynamics were chosen such that (i) Jag1 signaling efficiency is lower than that of Jag2 and (ii) Jag1 expressed alone is able to drive bistability of homogeneous states and ligand propagation.

(i.e., Jag1 is expected to drive ligand propagation while Jag2 and Dl1 are expected to drive periodic patterning)? Interestingly, it has been shown *in vivo* that Jag1 helps to mediate proper HC patterning [Zine et al., 2000]. In agreement with these experiments, our previous analysis suggested that antagonistic ligands can cooperate to drive the response of the strong signaling ligand. We obtained the same kind of behavior in our three ligands model. In particular, we found that Jag2 and Jag1 can cooperate to drive hair cell patterning when Jag1 acts as a weak signaling ligand compared to Jag2 (Fig. 2.30). This cooperation is enhanced as the signaling efficiency of Jag1 decreases (Fig 2.30A, B). Notice Jag1 can be a stronger signaling ligand than Dl1 (i.e. $\frac{\varepsilon_1}{\varepsilon_2} < 1$) and still cooperate to drive periodic patterning (Fig. 2.30B).

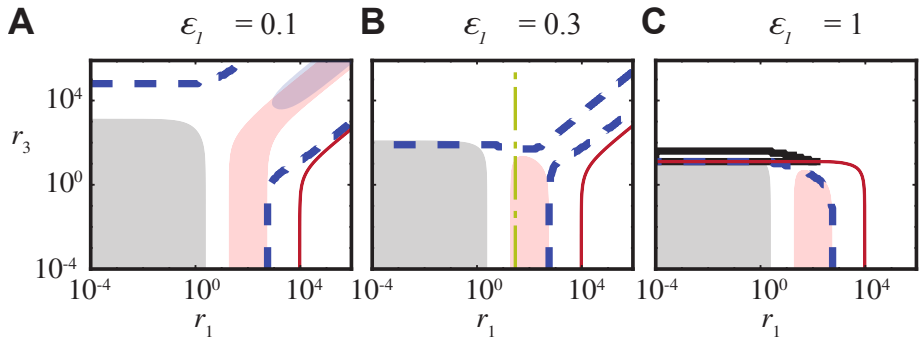

Figure 2.30 Regime of spontaneous hair cell (HC) patterning for the system with three ligands, in the parameter space r_3 and r_1. Spontaneous HC patterning occurs in the regions inside the blue-dashed line. Gray and red regions indicate in which case either Dl1 or Jag2 drives the patterning, respectively. We say that Dl1 or Jag2 can drive patterning when $R_{s,\langle l_2\rangle} R_{l_2,s} < -2$ or $R_{s,\langle l_1\rangle} R_{l_1,s} < -2$, respectively (see Appendix A for more details in the analysis). Jag1 and Dl1 can act as partial agonists of the signal at the right of the solid-red and the dashed-yellow lines, respectively. The value of the signaling efficiency of Jag1 (i.e., ε_2) is described in each panel. The signaling efficiency of Dl1 is set constant, $\varepsilon_1 = 0.75$.

Table 2.1 Summary of the values of the signaling efficiency of Dl1 and Jag1 in Fig. 2.31

Panel	ε_1	ε_2
A	0.75	0.3
B	0.1	0.3
C	0.5	0.3

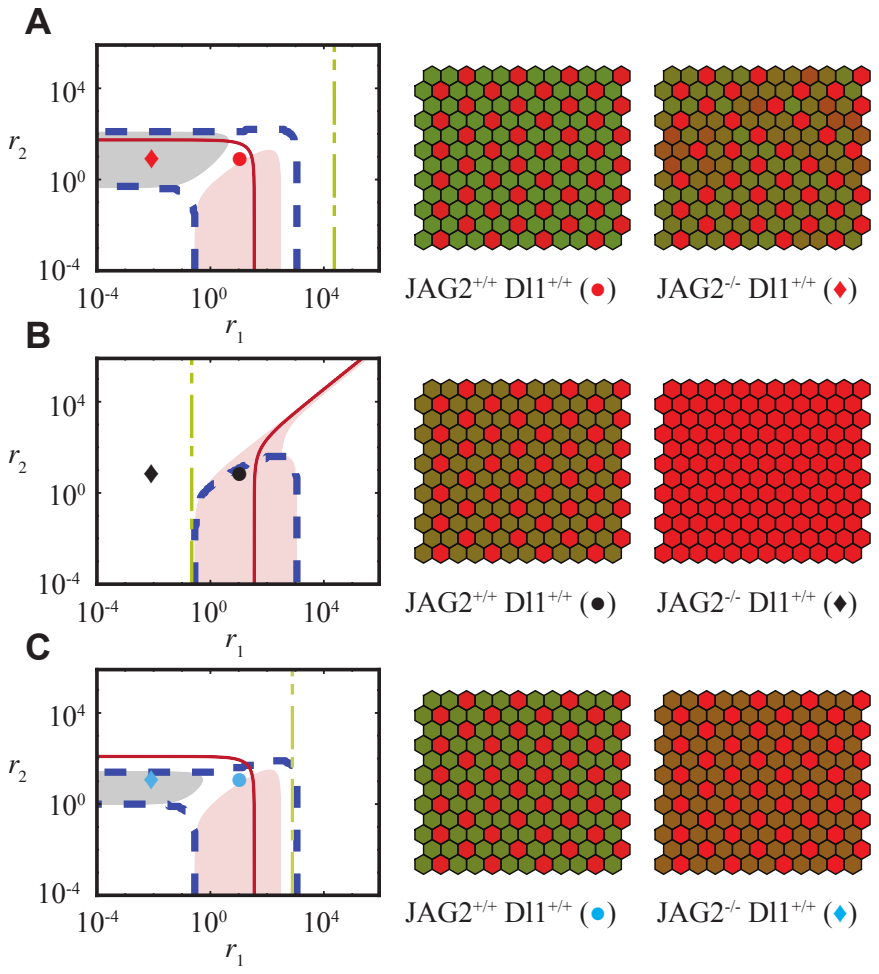

Figure 2.31 Regime of predicted Hair Cell patterning when Jag2, Dl1 and Jag1 are co-expressed. (A-C, left) Regions of spontaneous pattern formation in the parameter space r_1 and r_2. (A-C, right) Snapshots of numerical simulation showing hair cell patterning. Representation of each cell type (i.e., hair cells and supporting cells) depends on the levels of the signal, such that low levels entail hair cell differentiation (shown in red) while high levels entails supporting cell differentiation (shown in green). In each scenario, simulations corresponds to the case in which Jag2 and Dl1 are co-expressed (circles) or to the case when only Dl1 is binding to Notch1 (diamonds), depicted in the diagrams of the left. Co-expression with Jag1 is assumed in all the cases (i.e., $r_3 = 10$). The value of the of the parameter used in the simulations and the diagrams are $b_1 = b_2 = 10^4$, $b_3 = 1$ and $h_1 = h_2 = h_3 = 4$. The rest of the parameters are described in table 2.1.

Second puzzling phenotype. In the mammalian cochlea there are two different types of HC, inner hair cells (iHC) and outer hair cells (oHC), both organized in a salt-and-pepper patterned state. However, it is not clear why iHC and oHC patterning respond differently upon the loss of function of Jag2. Periodic patterning in iHC but not in oHC is disrupted after the impaired expression of Jag2 [Zhang et al., 2000]. Our analysis suggests that Dl1 could be acting as a weak signaling ligand compared to Jag2 in iHC but not in oHC[22]. Therefore, Jag2 and Dl1 can drive HC patterning redundantly in oHC (Fig. 2.31A), while in the iHC only the strong signaling ligand (Jag2) can drive patterning expressed in isolation (Fig. 2.31B). Assuming that the strength of signaling triggered by Dl1 is substantially low ($\varepsilon_1 = 0.1$), when the levels of Jag2 are depleted (i.e., $r_1 \ll 1$) there is no ligand in the system able to drive periodic patterning. In this regard, our results suggest that oHC have two equivalently strong signaling ligands (Jag2 and Dl1), both able to drive patterning, while iHC only have one strong ligand (Jag2). This assertion seems consistent with a recent study *in vivo* showing that supporting cells in contact with hair cells have lower signal activity in inner tissues than in outer tissues [Liu et al., 2013].

Third puzzling phenotype. Lunatic fringe (Lfng) is a glycosyl-transferase that modifies Notch post-translationally, adding glycosyl groups at extracellular domains [Panin et al., 1997]. This glycosylation can affect either the binding rate of the ligands to Notch [Hicks et al., 2000], or the signaling efficiency associated to each ligand after binding [Yang et al., 2005]. It has been shown that neither loss of function of Lfng nor simultaneous loss of function of Jag2 and Lfng can drive iHC pattern disruption [Zhang et al., 2000]. Then, if loss of function of Lfng alone does not have any phenotypic effect, why does it restore patterning after loss of function of Jag2? Our analysis suggests that loss of function of Lfng could make Dl1 and Jag2 equivalently strong signaling ligands in iHC such that they become redundant at driving patterning (Fig. 2.31C). Hence, our model supports the idea that Lfng can be partially mediating the differences in signaling between Jag2 and Dl1, making Dl1 to act as a weak signaling ligand in iHC.

Taken together, the results of this section show that the theoretical framework developed along the chapter can be used to understand experimental phenotypes that appear contradictory from the one ligand scenario standpoint. They

[22]This conclusion follows from the analysis of our model and is in agreement with the interpretation of the phenotypes done by the authors in [Yang et al., 2005].

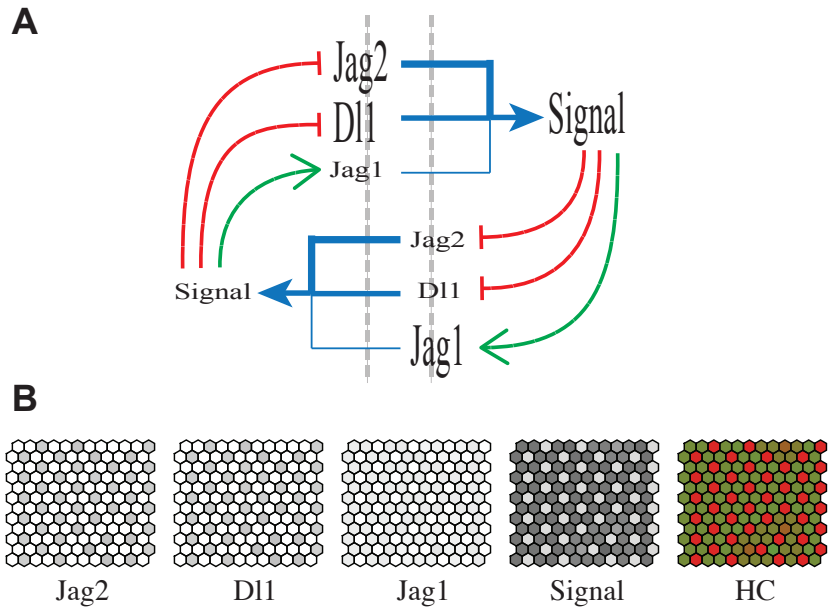

Figure 2.32 Signaling states driven by 3 co-expressed. A) Schematic representation of the functional relations within the circuit of lateral inhibition driving Hair Cell patterning. Font size describe the activity levels of the Jag1, Jag2, Dl1 and the signal, while green and red arrows stand for the transcriptional regulation of the ligands by Notch. B) Snapshots showing the patterned steady state of the numerical simulations for each species. The non-dimensional levels of the ligands and the signal are depicted in gray scale, as described for previous figures.

also stand out the modularity of the properties described in previous sections. Note that the behavior observed when three ligands are co-expressed can be understood as the response of two independent two-ligands systems. On the one hand, there is redundancy between Dl1 and Jag2. On the other hand, there is cooperation between Jag1 and Jag2 driving HC patterning. This suggests that the outcomes observed *in vivo* can be due to different functional interactions between ligands, and because of this some impaired phenotypes may seem contradictory when they are analyzed from the one ligand scenario framework.

2.4 Discussion

The coordinated outcome of cell-to-cell communication mediated by Notch signaling has been commonly guided by what to be expected from a single ligand acting. Single-ligand mediated responses have been thoroughly addressed computationally and it is known that the stationary response depends crucially on how Notch signaling regulates the transcription of the ligand: periodic patterning when the ligand is repressed and ligand propagation when the ligand is activated [Collier et al., 1996, Matsuda et al., 2012, 2015, Owen et al., 2000, Petrovic et al., 2014, Wearing et al., 2000, Webb and Owen, 2004]. Yet, there are several developmental scenarios in which multiple different ligands are expressed and all activate Notch signaling. A relevant question therefore is what functional response can be expected when two ligands are co-expressed. Mathematical modeling becomes a powerful tool to address this question because of the nonlinear coupling between the regulatory circuits mediated by each ligand. The results outlined along this chapter revealed three different scenarios in which the response driven by two co-expressing ligands cannot be envisaged from the one ligand scenario. The signaling states that arises in each scenario also depart from those formed when there is only one ligand triggering Notch signaling. Finally, we show that functional interactions between ligands driving specific responses can be modular.

Another relevant aspect of Notch signaling is that it can drive cells to have distinct signaling states. This has been classified in terms of the activity of a single ligand and of Notch signaling. Using the terminology by Sprinzak et al. [Sprinzak et al., 2011], periodic patterning in lateral inhibition drives few cells with high ligand activity and no signal (termed signal Sending cells, S) to be surrounded by cells with low ligand and high signal activities (termed signal Receiver cells, R). Lateral induction in turn drives all cells in a mixed S/R state, that has both high ligand and signal activity [Boareto et al., 2015] (Fig. 2.2C). Recently, the functional response of lateral induction has been defined in theoretical terms as a single S/R homogeneous state [Boareto et al., 2015]. When analyzing our results at the light of which signaling states arise when two ligands are acting, we found that additional signaling states can be defined when ligands signal with different efficiency while sharing resources. These additional states provide an explanation for patterns found during inner ear development, where cells with one (strong signaling) ligand type are surrounded by cells with

another type of (weak signaling) ligand and have high Notch signaling activity [Petrovic et al., 2014]. We term signal Blocking cells (B) those that have activity of a weak signaling ligand can act as a partial agonist and hence performs trans-inhibition. Therefore, Blocking cells can have both high ligand activities but release little signaling because the weak ligand prevents the stronger ligand from signaling by competing with it for limited resources. Blocking (or trans-inhibitory) cells have been also proposed to be in other contexts where different Notch ligands are [Benedito et al., 2009, Gama-Norton et al., 2015]. In addition, we find that different spatial ordering of the signaling states can occur. For instance, S/R cells can be surrounded by all S/R cells [Boareto et al., 2015] or be mixed with B/R cells.

Throughout the development of neural-sensory organs of vertebrates, transitions from lateral induction to lateral inhibition have been proposed to occur in developing tissues [Daudet and Lewis, 2005, Hartman et al., 2010, Millimaki et al., 2007, Petrovic et al., 2014, Zine, 2003]. First, a group of cells specify a prosensory domain by lateral induction. Then, some cells of that group differentiate as sensory cells while the other differentiate as supporting tissue by lateral inhibition. How these transitions can happen? From the classical paradigm of lateral regulation mediated by one ligand, one would expect these transitions take place only by the sequential non-overlapping action of single, antagonistic, ligands. However, it has been reported that these transitions can involve the co-expression of ligands and not the sequential expression of single ligands separately [Daudet and Lewis, 2005, Petrovic et al., 2014, Zine, 2003]. In the context of the transition occurring during avian inner ear development, we have previously shown that it can take place when the ligand that is incorporated during the transition (Dl1) is a stronger signaling ligand that is antagonistically regulated with respect to the ligand that is acting in a previous lateral induction stage (Jag1) [Petrovic et al., 2014]. Our results herein suggest additional ways through which transitions between lateral induction and lateral inhibition responses can be envisaged, by pinpointing under which conditions these responses arise when several ligands are present. The results show that the strength of trans-interactions and the relative signaling efficiency of the ligands control, among other factors, whether lateral induction or lateral inhibition responses arise. We also found that when the activation of the signal involves high Hill exponents an intermediary state between ligand propagation and periodic patterning can arise, i.e., oscillations of the patterned state. Oscillations

associated to Notch signaling have been described in different scenarios during development, and they seem to be necessary to maintain a proper cell number by proliferation before cell differentiation occurs. In this regard, within the context of the formation of the sensory organs, lateral induction can drive the specification and restriction of the pro-sensory domains, while the oscillations could maintain cells undifferentiated and proliferating, before lateral inhibition acts driving the irreversible differentiation. The feedforward loop between neighboring cells, mediated by two ligands oppositely regulated by Notch which trigger the signal each when co-expressed, is a novel mechanism that underlies the oscillatory dynamics of the patterned state. To our knowledge, we are the first describing this type of response associated to a feedforward loop of an intercellular signaling system. Whether this type of oscillations occur *in vivo* remains to be determined.

Herein, we have not considered additional levels of complexity in the Notch signaling pathway, such as ligand-independent Notch signaling [Baron, 2012, Cornell and Eisen, 2005, Hori et al., 2012, Shimizu et al., 2014, Wilkin et al., 2008] or cis-interactions, wherein ligands can bind the Notch receptor in the same cell preventing its signaling [Fiuza et al., 2010, Sakamoto et al., 2002, Sprinzak et al., 2010]. Whereas multiple mechanisms of Notch activation and its related trafficking have been shown to be fundamental to provide canalizing phenotypes in *Drosophila*, which are robust to temperature variation [Shimizu et al., 2014, 2001], cis-inhibition results in the enhancement of patterning mediated by lateral inhibition [Barad et al., 2010, Formosa-Jordan and Ibañes, 2014, Sprinzak et al., 2011]. Cis-inhibition might be expected to be detrimental to lateral induction driving ligand propagation because the ligand is activated by the signal. Intriguingly, it has been shown that negatively regulated ligands perform more cis-inhibition than those being activated by Notch signaling when the glycosyltransferase Fringe is acting [LeBon et al., 2014]. This suggests whether cis-inhibition may be ligand-modulated to enhance the performance of the ligand. Recently, a theoretical study has indeed proposed that cis-inhibition reduces the bistable region generated by lateral induction and that can be detrimental for ligand pulse propagation in a tissue [Lakhanpal, 2014].

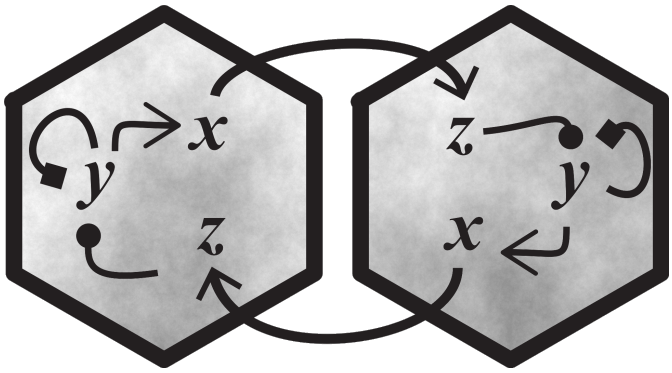

"Would you rather be Einstein or Shakespeare? I'm not sure whose genius is the more awesome. I come, hesitantly, to believe we need both science and story to make sense of a universe in which we agents, part of the universe, get on with our embodied know-how, we who strut and fret our hour upon the stage."

S. A. Kauffman

Chapter 3

Lateral inhibition and self-activation of Atoh1

3.1 Introduction: Lateral inhibition in the developing inner ear

3.1.1 Atoh1 drives hair cell differentiation

In *Drosophila*, atonal is a basic Helix Loop Helix transcription factor required for the specification and determination of sensory organs [Jarman et al., 1995]. The vertebrate homolog, Atoh1 [Akazawa et al., 1995], is necessary and sufficient to drive sensory hair cells (HC) differentiation [Bermingham et al., 1999]. Cells that fail to activate Atoh1 differentiate as non-sensory supporting cells (SC) in the inner ear [Bermingham et al., 1999, Cafaro et al., 2007, Kelley, 2006]. In the approach presented in this chapter we assumed that high levels of Atoh1 entails differentiation as HC. In contrast, cells with low activity levels of Atoh1 are assumed to differentiate as SC.

Atoh1 is a key element in the regulatory pathway of Notch signaling. Atoh1 is known to directly promote the transcription of Delta1 (Dl1) and also its own transcription (reviewed in Zine [2003]). In turn, it is repressed by Notch

signaling (Fig. 3.1) ([Zheng et al., 2000] and reviewed in Zine [2003]). The self-activation motif within the inhibitory pathway mediated by Notch signaling is recurrent among vertebrates and *Drosophila* [Lubensky et al., 2011, Millimaki et al., 2007, Neves et al., 2013b].

In a previous work, in which I was involved in the numerical and computational analysis, we studied the effect of the miss-expression of Jagged1[1] during HC differentiation and patterning in the inner ear of the chick [Petrovic et al., 2014]. In this work we proposed a model in which Dl1 and Jagged1 are co-expressed and they trigger Notch signaling by binding to the same receptor. Our analysis suggested that the self-activation of Atoh1 can make HC patterning robust to gain and loss of function of Jagged1. Motivated by our results [Petrovic et al., 2014], here we explored the effect of the self-activation of Atoh1 to miss-expression of Dl1. In particular, we address whether self-activation of Atoh1 can explain recent *in vivo* phenotypes which involve miss-expression of Dl1 [Chrysostomou et al., 2012]. For the sake of simplicity, here we studied a simplified model in which only Dl1 is expressed, unlike the model in Petrovic et al. [2014].

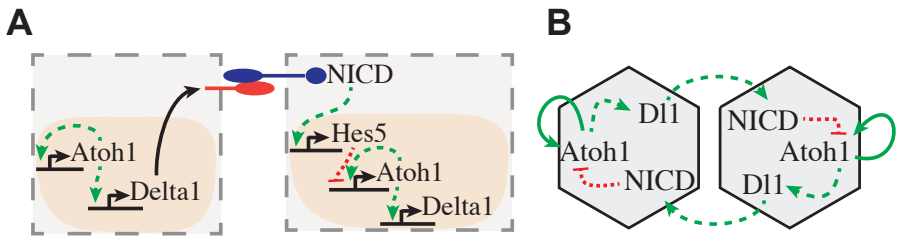

Figure 3.1 Schematic representation of the Notch signaling with self-activation of Atoh1. A) Representation of the regulatory topology between two adjacent cells. The dashed arrows represent transcriptional regulation. Green arrows stand for activation and red blunt arrows stand for repression. B) Representation of the simplified topology of mutual lateral inhibition between two neighboring cells as assumed in our modeling scheme. Atoh1 activates the transcription of Dl1 in the same cell, while Dl1 activates Notch signaling in the neighboring cell. Within or modeling framework, high levels of Atoh1 activity induce HC differentiation.

[1] In this context, Jagged1 is another Notch ligand which is transcriptionally activated by the signal and can mediate lateral induction when expressed in isolation, as discussed in Chapter 2.

3.1.2 Hair cell differentiation and patterning can be robust to miss-expression of Delta1 *in vivo*

Chrysostomou et al. [2012] evaluated the role of Dl1 in the developing inner ear of the chick at the onset of HC differentiation and patterning. Dl1 is transcriptionaly repressed by Notch signaling and hence is thought to mediate lateral inhibition at this stage of differentiation in the inner ear [Brooker et al., 2006, Daudet and Lewis, 2005, Kiernan et al., 2005]. The authors induced the controlled expression of Dl1 by electroporation (EP) of exogenous Dl1. This type of experiments enable cells to express Dl1 independently of the levels of Atoh1, which is known to regulate Dl1 expression (Fig. 3.1). In their experiments they found that [Chrysostomou et al., 2012]:

1. EP at low densities promote HC differentiation of the electroporated cells (Fig. 3.2A).
2. EP at high densities disrupts HC patterning and differentiation. In this regard, there is no HC differentiation within clusters where most cells express exogenous Dl1 (Fig. 3.2B). However, there can be some cases in which HC differentiation is observed adjacent to cells expressing exogenous Dl1 (Fig. 3.2B).

These observations are in agreement with the expected role of Dl1 acting in lateral inhibition. Dl1 can induce HC differentiation in cis (i.e., in the cell expressing Dl1), but inhibits HC differentiation in trans (i.e., in cells adjacent to that expressing Dl1). However, the fact that in some cases HC differentiation can be robust to inhibition by Dl1 (Fig. 3.2B) seems to be contradictory with the classic model of lateral inhibition. In this chapter we address two models of lateral inhibition and evaluate which of these models (if any) can account for the aforementioned experimental phenotypes.

3.1.3 Statement of the problem

The experimental phenotypes described by Chrysostomou et al. [2012] suggest that there might be other factors relevant for HC differentiation in the inner ear of the chick. In this chapter we ask *whether the self-activation of Atoh1*

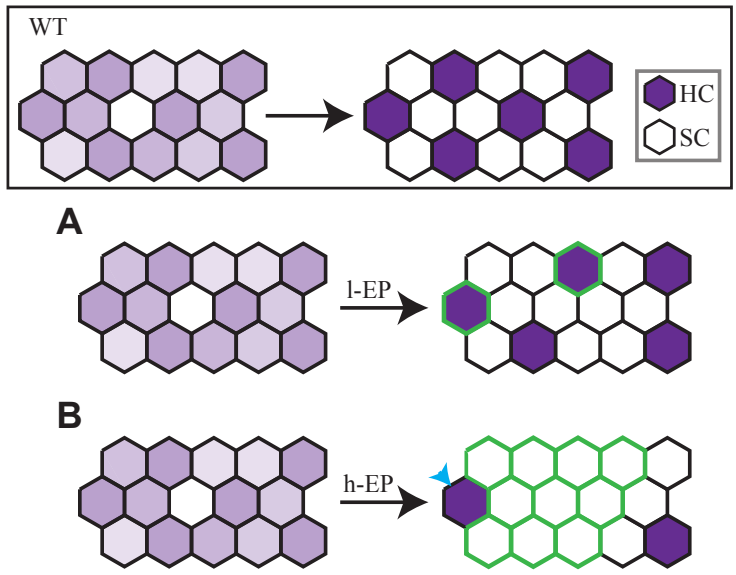

Figure 3.2 Our schematic summary of results of the *in vivo* experiments in the inner ear of the chick [Chrysostomou et al., 2012]. Wild type situation (WT) represents the expected cell fate adoption within a cell array, from a prosensorial state (array in the left) to a HC patterned state (array of the right). The scenarios described below are assumed to evolve from the same initial state as in the case of the WT. HCs and SCs are represented in purple and white, respectively. A) HC differentiation promoted in a cell after low density electroporation of exogenous Dl1 (l-EP), which is expected to differentiate as supporting cell in the WT situation. B) Pattern disruption after high density electroporation of exogenous Dl1 (h-EP). Cells that express exogenous Dl1 are represented by green edges. In this situation there is also the case where hair cell differentiation can be robust to inhibition by (exogenous) Dl1 (cell pointed by the blue arrow head).

can mediate HC differentiation robust to miss-expression of Dl1. Motivated by our previous work where we show that self-activation of Atoh1 can make HC differentiation robust to miss-expression of Jagged1 [Petrovic et al., 2014], we propose a model of lateral inhibition which takes into account explicitly the self-activation loop on Atoh1 transcription and evaluate *whether this model can account for the robustness of HC differentiation to miss-expression of Dl1*, as described by Chrysostomou et al. [2012].

3.2 Modeling approach

Taking into account the regulatory relations between the Notch signal (NICD), Atoh1 and Dl1 described in Fig. 3.1B, we propose two phenomenological models depending on whether Atoh1 promotes its own transcription or not. When it does not, the dynamics of cell i can be modeled as

$$\begin{aligned}
\frac{\mathrm{d}s_i}{\mathrm{d}t} &= \frac{\langle d_i \rangle}{1+\langle d_i \rangle} - s_i \\
\frac{\mathrm{d}a_i}{\mathrm{d}t} &= v\left(\beta_a \underbrace{\frac{1}{1+b_a s_i^{ha1}}}_{\text{NICD inhibition}} - a_i\right) \\
\frac{\mathrm{d}d_i}{\mathrm{d}t} &= v\left(\beta_d \frac{a_i}{\theta_d + a_i} - d_i\right)
\end{aligned} \tag{3.1}$$

where s, a and d stand for the activity levels of the signal, Atoh1 and Dl1, respectively, and $\langle d_i \rangle$ is the coupling between neighboring cells. In addition, we have that β_x is the rate of production of species $x = a$ for Atoh1 or $x = d$ for Dl1. θ_d is the threshold of activation of Dl1 and $\left(\frac{1}{b_a}\right)^{\frac{1}{h_{a1}}}$ is the threshold of inhibition of Atoh1[2]. h_{a1} is the cooperativity coefficients related to the processes of inhibition of Atoh1. Hereafter we will refer to this model as simple lateral inhibition model (LI).

When Atoh1 promotes its own transcription, the dynamics of cell i can be modeled as

[2]The model studied in this Chapter considers explicitly the dynamics of Atoh1 activity. Therefore the inhibition of Dl1 by the signal occurs indirectly through inhibition on Atoh1 activity, in contrast to the model described in Chapter 2 where the signal activity directly repressed the ligand activity. In addition, this non-dimensional version of Notch signaling is different since the dynamics of the signal activity has no free parameter.

$$\begin{aligned}
\frac{\mathrm{d}s_i}{\mathrm{d}t} &= \frac{\langle d_i \rangle}{1+\langle d_i \rangle} - s_i \\
\frac{\mathrm{d}a_i}{\mathrm{d}t} &= v\left(\beta_a \underbrace{\frac{1}{1+b_a s_i^{ha1}}}_{\text{NICD inhibition}}\left(1+\underbrace{\alpha\frac{a_i^{ha2}}{\theta_a^{ha2}+a_i^{ha2}}}_{\text{Atoh1 self-activation}}\right) - a_i\right) \\
\frac{\mathrm{d}d_i}{\mathrm{d}t} &= v\left(\beta_d \frac{a_i}{\theta_d + a_i} - d_i\right)
\end{aligned} \tag{3.2}$$

where θ_a and h_{a2} are the threshold of activation and the cooperativity coefficient of the self-activation of Atoh1 and α is related to the weight of the self-activation. Hereafter we will refer to this model as lateral inhibition with self-activation model (SA)[3].

For the results of the simulations shown in the following sections, we used the non-dimmensional parameter values: $\theta_d = 0.1$, $\theta_a = 0.1$, $b_a = 5 \cdot 10^4$, $\beta_d = 10^2$, $\beta_a = 1$, $h_{a1} = h_{a2} = 4$ and $\alpha = 10^6$ unless otherwise stated. With these parameter values the LI and SA models are expected to drive periodic patterning since (i) Atoh1 is sufficiently sensitive to the inhibition mediated by NICD (i.e., $\frac{1}{b_a} \ll 1$), (ii) the Hills coefficient associated to the inhibition of Atoh1 activity is high[4] and (iii) the strength of activation of NICD mediated by the ligand is sufficiently high (i.e., the maximal activity level of the ligand follows $\beta_d \gg 1$). In addition, the parameter values used in the SA model make that the self-activation term is more relevant than the inhibition term when the former is *on* (i.e., $\beta_a \frac{\alpha}{b_a} \gg 1$). Hence, if the self-activation is taking place (for instance, if $a > \theta_a$ in the SA model) then this term is expected to dominate over the inhibition mediated by NICD.

[3] When $\alpha = 0$ then Eqn. 3.1 and Eqn. 3.2 are the same.

[4] Notice that for $h_{a1} = 1$ patterning is not expected to arise, as discussed in Chapter 2.

3.3 Results

3.3.1 The outcome of the two models to miss-expression of Dl1 induced after differentiation is opposite

We compared the behavior of the LI and SA models in the *wild type* scenario (i.e., without miss-expression of Dl1) by numerical simulations of Eqns. 3.1 and 3.2 within a perfect array of hexagonal cells of size 6×6. At this level of coupling between neighboring cells, we assumed $\langle d_i \rangle \equiv \frac{1}{\omega} \sum_{j \in NN} d_j$ in Eqns. 3.1 and 3.2, as the average ligand activity in the $\omega = 6$ Nearest Neighboring cells. In addition, we assumed periodic boundary conditions.

We evaluated the time at which 6 cells, within the array of 6×6 cells, have differentiated as HC. As indicated above, HC differentiation is dictated by the levels of Atoh1. Therefore we assumed that cells with high activity levels of Atoh1 differentiate as HC. High activity levels are considered relative to the activation threshold of Dl1 mediated by Atoh1. When the activity levels of Atoh1 in cell i (a_i) follow $\left(\frac{a_i}{\theta_d}\right)^{h_d} > 1$ then we say that they are sufficiently high and this cell is assumed to differentiate as HC. In particular, we assumed cells have differentiated as HC when their activity levels of Atoh1 are above 0.5.

We found that the time of differentiation of the first HCs is similar in both models, being slightly faster in the SA model (Fig. 3.3A). In addition, we found that the number of HCs produced at the steady state was the same in both models (Fig. 3.3B). In this regard, self-activation of Atoh1 does not change the proportion of HCs within the array and neither the periodicity of the patterning with respect to the LI model (Fig. 3.3C).

In order to evaluate the response of the models to miss-expression of Dl1, we induced the expression of exogenous Dl1 (d_{ex}), i.e., Dl1 whose transcription is not regulated by the levels of Atoh1. The dynamics of d_{ex} in cell i follows a constant production rate and a linear degradation, according to

$$\frac{\mathrm{d}d_{ex,i}}{\mathrm{d}t} = \beta_{d-ex} - d_{ex,i} \tag{3.3}$$

In this regard, we say that cell i expresses exogenous Dl1 when $\beta_{d-ex} > 0$ in that cell. We assumed that d_{ex} can activate Notch similarly to endogenous Dl1

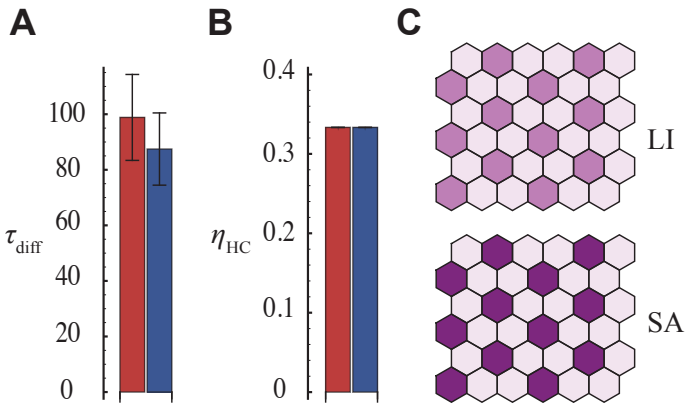

Figure 3.3 Hair cell differentiation dynamics and patterning in the LI and SA models. A) Average time of differentiation (τ_{diff}) for the LI (red bars) and SA (blue bars) models. This time is calculated by numerical simulations of the Eqns. 3.1 and 3.2 for the LI and the SA model, respectively, in arrays of 6×6 hexagonal cells imposing periodic boundary conditions. Differentiation time corresponds to the time at which the first 6 HC are differentiated within the array, which is inferred from the activity levels of Atoh1. When the are sufficiently high (> 0.5) then the cell is assumed to differentiate as HC. B) Average proportion of cells differentiated as HC in the cell array for the LI (red bars) and SA (blue bars) models at the steady state. This proportion is determined for the arrays as described in A, by evaluating the total number of HC formed at the steady state with respect to the total number of cells in the array. The average values in A and B were inferred from 50 simulations. Each simulation was done using different initial conditions as described in Appendix B. C) Snapshots of the numerical simulations showing the periodicity of the patterned state that arises in the LI and the SA models. The color of the cells depends on their levels of Atoh1 activity (following a linear scaling), being purple the highest and white the lowest activity levels. These two states correspond to HCs and SCs, respectively.

(i.e., the Dl1, d, that is under the regulation of Atoh1). Therefore, the signal dynamics in cell i when exogenous Dl1 activity is taken into account reads

$$\frac{\mathrm{d}s_i}{\mathrm{d}t} = \frac{\langle d_i \rangle + \langle d_{ex,i} \rangle}{1 + \langle d_i \rangle + \langle d_{ex,i} \rangle} - s_i \tag{3.4}$$

We induced the expression of d_{ex} either before (τ_1) or after (τ_2) HC differentiation (Fig. 3.4). Electroporations were done at different densities such that the proportion of cells expressing d_{ex} could be low (ρ_1) or high (ρ_2).

In the case of low density electroporation (ρ_1), we induced d_{ex} in one cell chosen randomly within the array and then evaluated whether this cell differentiates

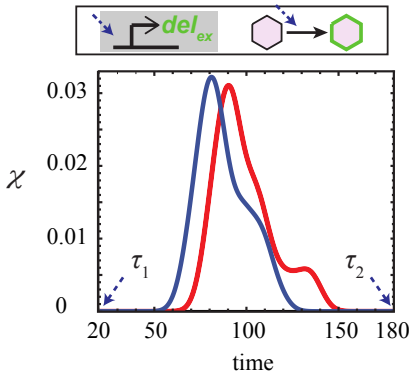

Figure 3.4 *In silico* electroporation with exogenous Dl1. (Top) Schematic representation of the induction of del_{ex} and (Bottom) probability density function of the time of differentiation(i.e., τ_{diff}) for the SA (blue) and the LI (red) models. We used Mathematica function "SmoothHistogram" to compute the probability (χ) for which the differentiation of six cells occurred at a given time. The probabilities were inferred from 50 simulations, in arrays of 6×6 hexagonal cells imposing periodic boundary conditions. Each simulation was done using different initial conditions as described in Appendix B. The induction time of exogenous Dl1 (del_{ex}) in the following essays is $\tau_1 = 20$ or $\tau_2 = 180$.

as HC or not by measuring the activity levels of Atoh1 in this cell at the steady state. We run 50 simulations using different initial conditions and selecting a different cell for electroporation each simulation. From these data we determined what is the probability of the electroporated cell to differentiate as HC after the electroporation is done (η_{ind-HC})[5]. We found that the electroporated cell always differentiate as HC in both models (i.e., $\eta_{ind-HC} = 1$) when the electroporation occurs at early times before differentiation, i.e., at τ_1 (Fig. 3.5). The situation is very different when the electroporation is induced at late times after differentiation, i.e., at τ_2. In this case, the electroporated cell has high propensity to be a HC at the steady state in the LI model, but not in the SA model (Fig. 3.5).

In the case of electroporations at higher density (ρ_2), the expression of d_{ex} within the array is induced such that most of the cells are in contact with at least one cell expressing d_{ex} according to

[5] When $\rho_1 = \frac{1}{36}$, then η_{ind-HC} is defined as the number of times that the electroporated cell differentiates as HC along the simulations over the total number of simulations (50).

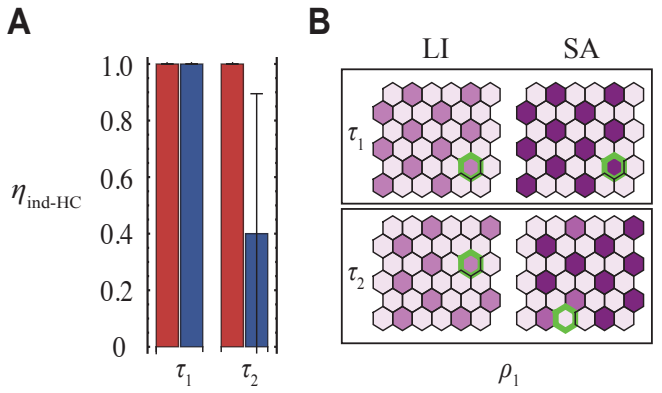

Figure 3.5 Effect of exogenous Dl1 expression (del_{ex}) in cell fate determination for the LI and SA models, at low density of electroporation ($\rho_1 = \frac{1}{36}$). A) Probability of HC differentiation of the cell expressing d_{ex} (η_{ind-HC}), in the SA (blue bars) and the LI (red bars) models, for $\rho_1 = \frac{1}{36}$ density of electroporation, induced at early ($\tau_1 = 20$) and late ($\tau_2 = 180$) times. B) Snapshots of the steady state of one simulation of the LI (left arrays) and SA (right arrays) models. The cell expressing d_{ex} in each array is represented with green edges. Cell coloring depends linearly on the levels of Atoh1. In each case, thetime of d_{ex} induction is indicated by the corresponding τ value in each panel.

$$\rho = 1 - (1 - \rho_{\text{av}})^{\frac{1}{6}} \tag{3.5}$$

where ρ is the density of electroporation and ρ_{av} is the given percentage of cells that is in contact with at least one cell expressing exogenous Delta1. In this case of high density of electroporation, we evaluated the proportion of HC differentiation within the array (η_{HC}), i.e., the number of HC differentiated at the steady state with respect to the total number of cells in the array.

We found that if the expression of d_{ex} is induced early before differentiation at τ_1, HC patterning is disrupted. Hence, the fraction of HC in the tissue decreases for both models (Fig. 3.6A). again, the situation is very different when the electroporation is induced after differentiation, at τ_2. In this case, we found that HC differentiation and patterning is disrupted in the LI, but not in the SA model (Fig. 3.6A, B). In the SA model the proportion of HC after electroporation is the same as in the case without electroporation (Figs. 3.6A and 3.3B).

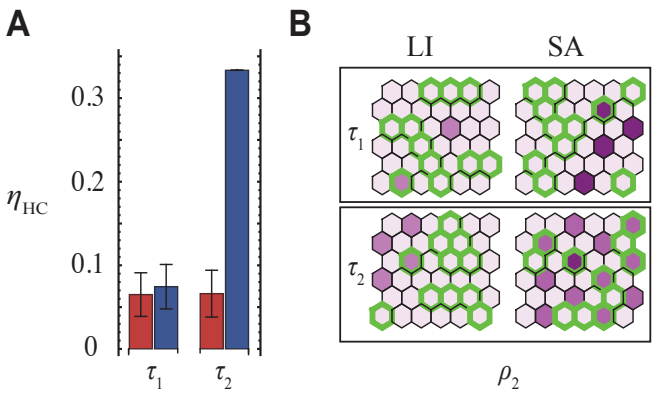

Figure 3.6 Effect of exogenous Dl1 expression (del_{ex}) in HC patterning for the LI and SA models, at high density of electroporation ($\rho_2 = \frac{11}{36}$). A) Average value of the proportion of cells that differentiate as HC (η_{HC}) in the SA (blue bars) and the LI (red bars) models after induction of d_{ex} at high density of electroporation, $\rho_2 = \frac{11}{36}$. Electroporations were done at early ($\tau_1 = 20$) and late ($\tau_2 = 180$) times. B) Snapshots of the steady state of one simulation of the LI (left arrays) and SA (right arrays) models. Color code for electroporation and differentiation as in Fig. 3.5.

Our results of the electroporations done at τ_2 suggest that trans-differentiation events can occur, i.e., transitions in cell fate from HC to SC, which are evident in the LI model. To determine whether trans-differentiation events arise at low density electropotarions is more difficult from Figs. 3.5 and 3.6 since the number of HC is not expected to change by electroporations at this density level. Hence, we quantify these trans-differentiation events in each model by measuring the levels of Atoh1 activity in each cell before the induction of d_{ex} done at τ_2 (i.e., at a time large enough to enable cells to differentiate *naturally*) and at the steady state (when cells have had enough time differentiate after the electroporation). Quantification of the trans-differentiation events was done using a trans-differentiation coefficient (N_{Td}) defined as the number of trans-differentiation events of each type[6] taking place. We found that in the SA model there are no trans-differentiation events taking place. Once a cell adopts a cell fate it persists despite external inhibitory signals mediated by d_{ex} are introduced (Fig. 3.7). In contrast, in the LI model both types of trans-differentiation occurred, i.e., from HC to SC and from SC to HC (Fig. 3.7). This suggests that

[6]Notice that trans-differentiation events could arise either by transitions from HC to SC or by transitions from SC to HC.

the robustness that we observed in the SA model after induction of d_{ex} could be due to stiffness in the cell fate commitment.

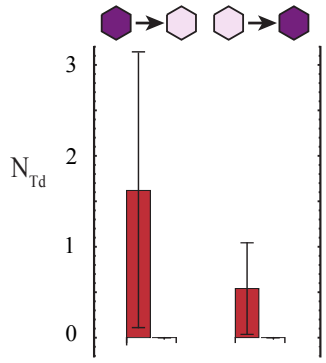

Figure 3.7 Trans-differentiation events after d_{ex} induction in the LI and SA models. Average value of the coefficient of each type of trans-differentiation (i.e., N_{Td}, where trans-differentiation can be from HC to SC or from SC to HC) after d_{ex} induction at $\tau_2 = 180$ and low density of EP ($\rho_1 = \frac{1}{36}$), for the SA (blue bars) and the LI (red bars) models.

Taken together, these results show that the self-activation of Atoh1 can modulate the response of the system to miss-expression of Dl1 specially when cell differentiation has occurred. In the following sections we devise the mechanisms underlying this modulation.

3.3.2 Cell-autonomous multistability can drive irreversible differentiation and robust periodic patterning

In this section we studied the LI and SA models (Eqns. 3.1 and 3.2) in simpler scenarios of cell coupling. Our aim in this section is to explain why the two models (LI and SA) produce opposite outputs after the miss-expression of Dl1. We analyzed three different scenarios of cell coupling: (i) no coupling (single cell), (ii) coupling between two adjacent cells and (iii) cell coupling between hexagonal cells using a simplification of a perfect array. We focused in the description of the stationary states that arises in each scenario and their stability to miss-expression of Dl1.

3.3.2.1 The self-activation of Atoh1 can drive irreversible HC differentiation

We addressed the differentiation of a single cell interacting with a fixed source of external Dl1 (Fig. 3.8). In this case, the value of $\langle d_1 \rangle$ in the term of signal production in Eqns. 3.1 and 3.2 is assumed to be a free parameter, termed Del_{ext}, and therefore there is no feedback associated to cell coupling. In this scenario of a single cell we addressed which stable steady states arise in the LI (Fig. 3.8A) and in the SA models (Fig. 3.8B) for variable levels of $\langle d_1 \rangle = Del_{ext}$.

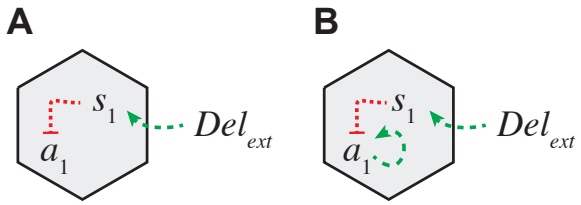

Figure 3.8 Dl1-Notch regulation in the one cell scenario. Schematic representation of the regulatory interactions occurring A) when there is no self-activation of Atoh1 (LI model) and B) when there is (SA model), in the scenario of a single cell interacting with external Dl1 (Del_{ext}). Green arrows represent activation, while red-blunt arrows represent repression.

We found that in the LI model there is a single stable steady state whose characteristics are dictated by the activity levels of Del_{ext} (Fig. 3.9A). When the level of Del_{ext} is low, the activity levels of Atoh1 in the cell are high and induce HC differentiation. In contrast, at higher levels of Del_{ext} the activity levels of Atoh1 decrease and hence the cell is assumed to differentiate as SC (Fig. 3.9A). Therefore, increasing the levels of external Dl1 (Del_{ext}) induces differentiation as SC.

In contrast, the SA model exhibits two stable steady states when the activity levels of Del_{ext} are high. These states are characterized by high and low levels of Atoh1 which can be associated to differentiation as HC and SC, respectively (Fig. 3.9B). In this regard, in the SA model there can be HC differentiation despite the presence of an external inhibition (given by Del_{ext}), while in the LI model when the cell is subjected to inhibition it can only differentiate as SC (Fig.3.9).

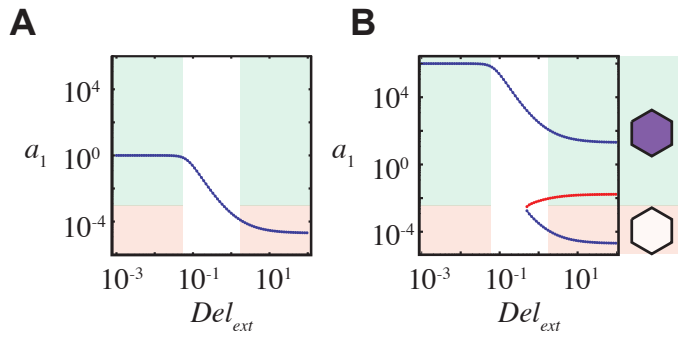

Figure 3.9 Stable steady states of Atoh1 activity in the one cell scenario. Stationary states of Atoh1 in the cell (a_1) shown in logarithmic scale as a function of Del_{ext} (set as a free parameter) for A) the LI model and B) the SA model. Stable and unstable states are shown in blue and red, respectively. Low (orange region) and high (green region) levels of a_1 are assumed to entail cell differentiation as SC and HC, respectively.

We also evaluated which steady states arise in a system of two coupled cells for both models (Fig. 3.10). In this scenario, Notch signaling is mutually regulated between cells, being

$$\begin{aligned} \frac{\mathrm{d}s_1}{\mathrm{d}t} &= \frac{d_2}{1+d_2} - s_1 \\ \frac{\mathrm{d}s_2}{\mathrm{d}t} &= \frac{d_1}{1+d_1} - s_2 \end{aligned} \tag{3.6}$$

the dynamics of the Notch signaling activity in cell 1 and cell 2, respectively.

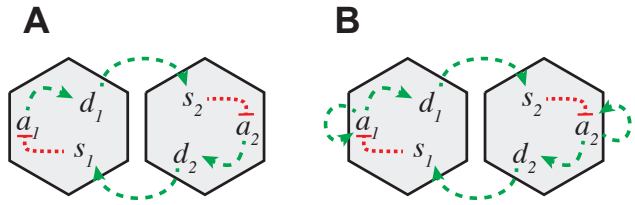

Figure 3.10 Dl1-Notch regulation in the two coupled cells scenario. Schematic representation of the regulatory interactions in (A) the model of simple lateral inhibition (LI) and in (B) the model of lateral inhibition with self-activation of Atoh1 (SA), in the scenario of two coupled cells. Green arrows represent activation, while red-blunt arrows represent repression.

We evaluated the steady states (and their basins of attraction) that arise in both models, using numerical simulations. As initial conditions for Atoh1 activity in each cell we took each value within the grid a_1 and a_2, where a_1 and a_2 are the activity levels of Atoh1 in cell 1 and cell 2 respectively. These initial conditions were perturbed randomly, and upon the perturbation the dynamics was computed deterministically. We assumed the same initial conditions in both cells for the activity levels of Notch signaling and Dl1 ($s_1 = s_2 = 0.45$ and $d_1 = d_2 = 0$). These values approximately correspond to the expected intermediate levels of Notch signaling and low to null levels of Dl1 expression at the onset of HC differentiation.

We found that the positive feedback loop mediated by Dl1 acting in lateral inhibition in the LI model can drive the formation of two stable steady states, as expected (Fig. 3.11A). These states are opposite in terms of the cell fate that each cell adopt. In one of these states the levels of Atoh1 activity are high in cell 1 and low in cell 2, driving HC and SC differentiation, respectively. In the other steady state the cell fates are inverted such that cell 1 differentiates as SC while cell 2 differentiates as HC (Fig. 3.11C). Notice that the cell that initially has higher levels of Atoh1 activity tends to differentiate as HC, hence preventing its neighbor from differentiating as HC.

We found that these steady states producing opposite cell fates between cells also arise in the SA model (Fig. 3.11B). Interestingly, there is another steady state that arises in this model in which both cells have high levels of Atoh1 activity and hence they are both expected to differentiate as HCs (Fig. 3.11B, C).

To address the effect of miss-expression of Dl1 on HC differentiation in this scenario (two cells coupled), we induced the expression of exogenous Dl1 (d_{ex}), in cell 1 only. We assumed initial conditions such that cell 1 differentiates as SC and cell 2 as HC, i.e., the initial levels of Atoh1 activity are higher in cell 2 than in cell 1 and the initial levels of the signal and Dl1 are the same for both cells. After cell differentiation, we induced the expression of d_{ex} only in cell 1[7], by assuming $\beta_{d-ex} = 1$ in cell 1 and $\beta_{d-ex} = 0$ in cell 2, and then we evaluated the system dynamics from that point. We found that in the LI model the induction of d_{ex} in cell 1 entails a switching in cell differentiation, i.e., cell 1 trans-differentiates from SC to HC while cell 2 trans-differentiates from HC to

[7]Notice that SC are not expected to express Dl1 [Fekete and Wu, 2002].

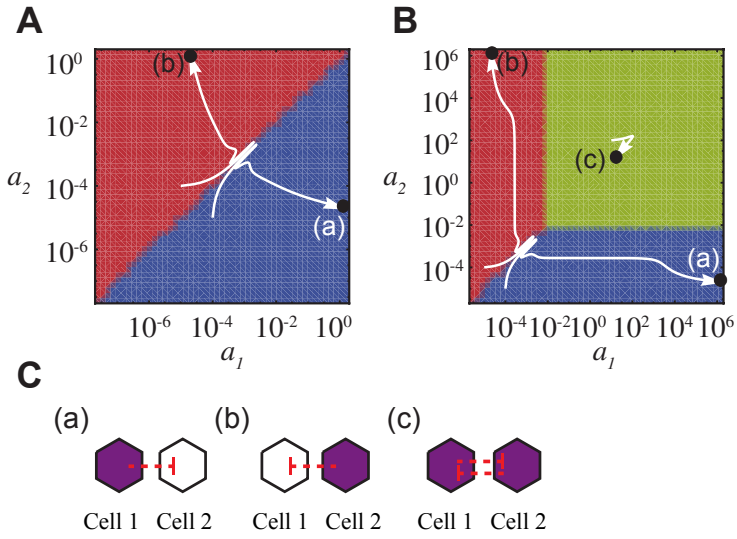

Figure 3.11 Stable steady states in the two coupled cells scenario. Steady states (gray dots) and basins of attraction of each steady state (colored regions) occurring in (A) the LI model and (B) the SA model, when evaluated in the two-coupled cells scenario (Fig. 3.10). White arrows depict the temporal evolution of two different initial conditions towards different steady states. In each case, the steady state is label according to the levels of Atoh1 activity in the cells, as described in C. Initial condition of NICD and Dl1 are $s = 0.45$ and $d = 0$ in both cells equally. C) Schematic representation of the differentiation states of two interacting cells. Each scenario is described in terms of the levels of Atoh1 activity (a) in the cells (color), and in terms of the inhibitory capacity (red blunt arrows). (a) Cell 1 differentiates as HC and cell 2 as SC. (b) Cell 1 differentiates as SC and cell 2 as HC. (c) The two cells differentiate as HC, with the same levels of Atoh1 activity (a).

SC (Fig. 3.12A). In contrast, in the SA model there was no trans-differentiation events taking place after induction of d_{ex}, in agreement with our previous results (Figs. 3.12B and 3.7).

We evaluated the steady states and their basins of attraction in the scenario of two coupled cells, when exogenous Dl1 (d_{ex}) transcription is active in cell 1 but not in cell 2. We found that the multistability driven by the positive feedback loop driven by lateral inhibition is lost in the LI, but no in the SA model (Fig. 3.12C, D). In the SA model, three steady states prevail despite the steady expression of d_{ex} in cell 1 (i.e., setting $\beta_{d-ex} = 1$ in cell 1 but not in cell 2).

In the SA model the asymmetric production Dl1 (i.e., having $\beta_{d-ex} = 1$ in cell 1 but not in cell 2) makes the cell fate induction to be asymmetric for low activity levels of Atoh1 in both cells (compare Figs. 3.11B and 3.12D for a_1, $a_2 \ll 1$). Hence, at the onset of HC differentiation (i.e., for a_1, $a_2 \ll 1$) the miss-expression of Dl1 is expected to bias HC differentiation in the SA model. This result is consistent with the results shown in Fig. 3.5 at τ_1, where miss-expression of Dl1 affected cell differentiation in both models equally.

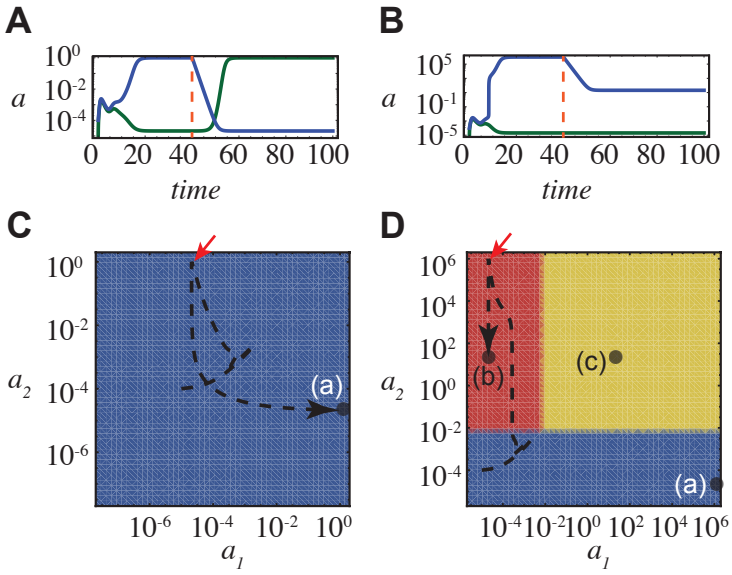

Figure 3.12 Induction of d_{ex} in cell 1 after cell 2 differentiates into HC. Time course of the activity levels of Atoh1 in cell 1 (green) and cell 2 (blue) for A) the LI model and B) the SA model. The initial conditions are chosen such that the cell 1 and cell 2 differentiate as SC and HC, respectively (i.e., $at_1 < at_2$). At $time = 40$ (vertical dashed line) the transcription of exogenous Dl1 (d_{ex}) is activated in cell 1 only. Steady states and basins of attraction of each steady state in C) the LI model and D) the SA model, in the case in which the transcription of exogenous Dl1 (d_{ex}) is active in cell 1 but not in cell 2. The black-dashed lines depict the trajectories described in A and B for each model. States a–c as described in Fig. 3.11C.

These results show that when self-activation of Atoh1 is taking place, HC differentiation becomes numb to inhibition by Dl1 (Fig. 3.12B, D). This can be expected from the parameter values we have chosen, where the self-activation (when taking place) is stronger than the inhibition by NICD (i.e., $\beta_a \frac{\alpha}{b_a} \gg 1$). This hierarchy in Atoh1 regulation can explain the irreversibility in cell differentiation shown in Fig. 3.5 for the SA model, but not for the LI model. Because

of this ireversibility, no trans-differentiation events are expected to take place in the SA model, as shown in Fig. 3.7. In summary, self-activation of Atoh1 can drive robust multistability such that HC differentiation becomes irreversible to inhibition by Dl1. In the following section we explore whether this robust multistability can be extended to higher levels of cell coupling.

3.3.2.2 The self-activation of Atoh1 drives robust HC periodic patterning

Nascent HCs organize in a salt-and-pepper pattern where typically one HC is surrounded by six SCs, while one SC is surrounded by three HCs and three SCs (Fig. 3.13) [Goodyear and Richardson, 1997]. This spatial organization defines a particular periodicity of the patterning. In this section we addressed the emergence of patterned states with this specific periodicity and the response of these patterns to homogeneous exogenous expression of Dl1.

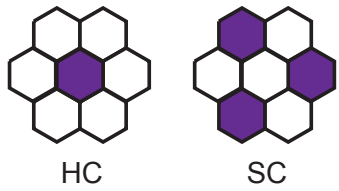

Figure 3.13 Spatial organization of HCs and SCs within a cluster of hexagonal cells surrounding the HC (left) and the SC (right), respectively.

To analyze the scenario of cell coupling within an array of hexagonal cells, we used a simplification which describes the dynamics of two different cell types[8]. In this simplified approach, the cell coupling is different for each cell type. It is important to remark that in this context cell types are defined in terms of the type of neighboring cells each cell has and their spatial disposition in the array, i.e., each cell type has a different coupling. Specifically, cell type II has only one type of neighboring cells while cell type I has two types of neighbors (Fig.

[8]This approach has been used previously to address exact solutions of patterned states as described in [Formosa-Jordan and Ibañes, 2009].

3.14). This approach is based on the periodicity of HC patterning in arrays of hexagonal cells (Figs. 3.13 and 3.14)[9].

Given this difference in the cell coupling between the two cell types, the signal dynamics in cell type I and cell type II reads

$$\begin{aligned} \frac{\mathrm{d}s_1}{\mathrm{d}t} &= \frac{\frac{1}{2}\left(d_1+d_2\right)}{1+\frac{1}{2}\left(d_1+d_2\right)} - s_1 \\ \frac{\mathrm{d}s_2}{\mathrm{d}t} &= \frac{d_1}{1+d_1} - s_2 \end{aligned} \tag{3.7}$$

respectively.

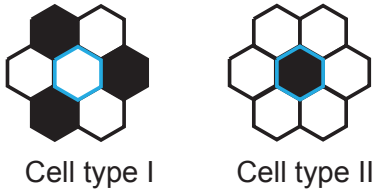

Figure 3.14 Cartoon of the reduced cell type model. Schematic representation of the two cell types described by the reduced model in the patterned state. Each cell type corresponds to the cell in the middle of the array, drawn with blue edges. Notice that the cell types are defined by the cell coupling and not by the activity level of any of the species.

Numerical evaluation of the two models in this scenario revealed that a stable patterned state can arise in both models (LI and SA), which is compatible with the HC and SC patterned state that arises in the inner ear [Goodyear and Richardson, 1997] (Fig. 3.15A, B). In terms of the periodicity and the cell coupling of the patterned state that arises, HC are compatible with cell type II and SC with cell type I (Fig. 3.15C). In the two models a state also arises in which both cell types have low levels of Atoh1 activity, and hence differentiate as SC (state d in Fig. 3.15A, B). Notice that this state is stable when it comes to a deterministic dynamics, but it might be not expected so when small random fluctuations would be taking place because this state is close to the borderline separating the two basins of attraction.

[9]Notice that in this scenario when the dynamics evolves towards a state in which $a_1 = a_2$, then we say that the system settles at a homogeneous steady state. In contrast, if the dynamics evolves towards a state in which $a_1 \neq a_2$ then we say that the system settles at a patterned state with the specific period $\frac{1}{3}$ and $\frac{2}{3}$.

Interestingly, we found an additional steady state arising in the SA model in which both cell types have high levels of Atoh1 activity and hence they differentiate as HC (state c in Fig. 3.15B). In this model there is also a stable patterned state in which the proportion of HC and SC is inverted, i.e., there is 33% of SCs and 66% of HCs (state b in Fig. 3.15B, C).

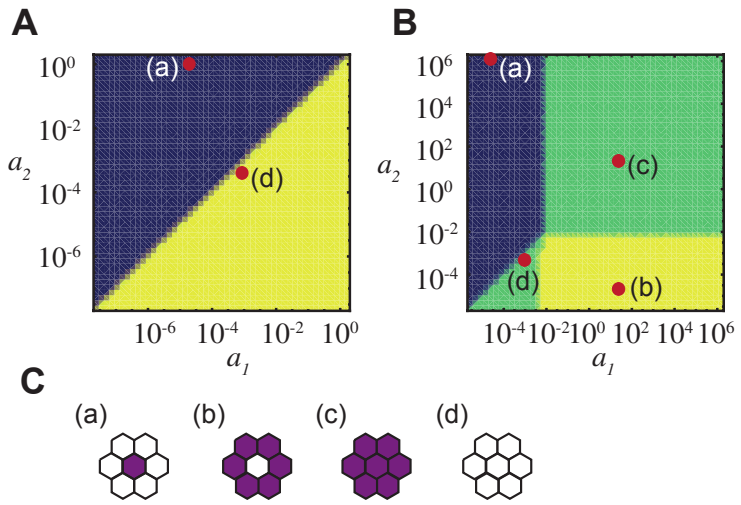

Figure 3.15 Cell fate determination in the reduced model of hexagonal cells. Steady states of Atoh1 activity in cell type I (a_1) and cell type II (a_2) (red dots) and basins of attraction of each steady state (colored regions) occurring in A) the LI and B) the SA models. In each case, the steady state is labelled according to the levels of Atoh1 activity of each cell type, as described in C. C) Schematic representation of the steady states of cell type I (cell in the center of the array) and cell type II (neighboring cells), in terms of the levels of Atoh1 activity (a). (a) Patterned state in which cell type I and cell type II differentiate as HC and SC, respectively. (b) Patterned state in which cell type I and cell type II differentiate as SC and HC, respectively. (c) Homogeneous state in which both cell types differentiate as HC. (d) Homogeneous state in which both cell types differentiate as SC.

To evaluate the response of the HC patterned states to miss-expression of Dl1, we induced the expression of d_{ex} in both cell types such that $\beta_{d-ex} = 1$ equally for cell type I and cell type II (Fig. 3.16A). We found that the homogeneous expression of d_{ex} in the LI model leads the formation of a single stable homogeneous state in which both cell types have low levels of Atoh1 activity and hence differentiate as SC (Fig. 3.16A). Therefore, HC patterning is disrupted in this model. In contrast, in the SA model the HC patterned state prevails after the homogeneous expression of d_{ex} (Fig. 3.16B). In addition, the induction of d_{ex}

expression stabilizes the homogeneous state of SC arising in the SA model (state d in Fig. 3.16B).

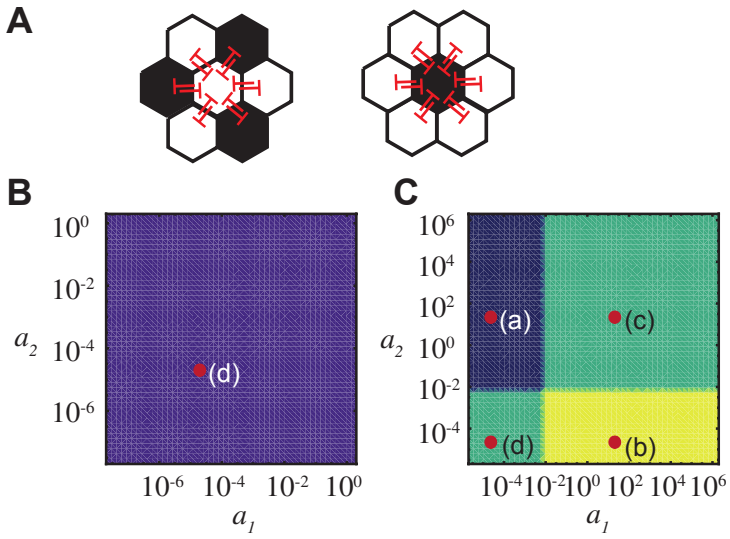

Figure 3.16 Periodic patterning when Dl1 is homogeneously expressed. A) Schematic representation of the two cell types described by the reduced model, both expressing exogenous Dl1 (d_{ex}) denoted by red-blunted arrows. Steady states and basins of attraction of each steady state occurring in B) the LI model and C) the SA model, as described in Fig. 3.15, but when both cell types express exogenous Dl1 (d_{ex}), which is not regulated by Atoh1 activity, as represented in A.

The reduced model (3.7) is an approximation to the dynamics of a cell array in which the cell coupling is the same along the tissue. In this regard, it is only useful to understand the dynamics of a cell array in which the stationary pattern that arises is perfect. Taking into account this consideration, our analysis suggests that HC patterning states can be robust to homogeneous over-expression of Dl1. This is in agreement with the results shown in Fig. 3.6 where HC patterning is robust to high density electroporation of exogenous Dl1 in the SA model only. Notice also that if the homogeneous expression of Dl1 is assumed to occur in a scenario that simulates the onset of HC differentiation (i.e., for a_1, $a_2 \ll 1$) then HC patterning is prevented because the system evolves towards a stable state of SC only (state d in Fig. 3.16C). This is in agreement with the results shown in Fig. 3.6 where both models responded equally to miss-expression of Dl1 when the electroporations are done before cell differentiation occurred (i.e., at τ_1).

Taken together, these results suggest that the SA model can drive multistability and periodic HC patterning which can be robust to miss-expression of Dl1. Our analysis predicted that in the scenario of an array of coupled hexagonal cells, once a pattered state is formed it is not disrupted by the homogeneous expression of Dl1. This behavior does not arise without the self-activation of Atoh1.

3.3.3 Self-activation of Atoh1 can account for reported *in vivo* phenotypes

In this section we take a closer look to the role of Dl1 during HC differentiation in the inner ear of the chick. As explained above, recent *in vivo* experiments confirmed the role of Dl1 during HC differentiation and patterning acting in lateral inhibition [Chrysostomou et al., 2012]. The results described in previous sections show that lateral inhibition with self-activation of Atoh1 can explain this behavior. In the SA model, HC cell differentiation is not disrupted by miss-expression of Dl1. However, the experimental results showed that this robustness arises only in some cases, but in most cases the induction of exogenous Dl1 disrupts HC differentiation. In this section we provide an explanation to these data using the framework developed in previous sections.

3.3.3.1 The model with self-activation of Atoh1 can account for the role of Dl1 mediating lateral inhibition in the inner ear of the chick

To account for the effect of miss-expression of Dl1 on HC patterning in large arrays of hexagonal cells, we integrated the dynamics of Eqns. 3.1 and 3.2, where we defined $\langle d_i \rangle \equiv \frac{1}{\omega} \sum_{j \in NN} d_j$, as the average ligand activity in the $\omega = 6$ Nearest Neighboring cells, as described above. Details of the simulations can be found in Appendix B.

We induced the expression of exogenous Dl1 (d_{ex}) at the onset of HC differentiation (Fig. 3.17A), by assuming that $\beta_{d-ex} = 1$ in cells randomly chosen

within the array. These *in silico* electroporations[10] (EP) were done at different densities such that the 25% ($\rho_1 = 0.05$), the 50% ($\rho_2 = 0.1091$), the 75% ($\rho_3 = 0.206$) or the 90% ($\rho_4 = 0.318$) of the cells are in contact with at least one cell expressing exogenous Dl1 (d_{ex}). *In vivo* experiments were done using two types of EP [Chrysostomou et al., 2012]. In the first type, the electroporated cell express the exogenous Dl1 independently of its activity levels of NICD. In the second type, the EP cell only expresses exogenous Dl1 if the activity levels of NICD are high [Chrysostomou et al., 2012]. Hence, we proposed two types of EP based on these *in vivo* experiments (Fig. 3.17B). In our *in silico* EP type II, we assumed that when the activity levels of Notch signaling are sufficiently high to inhibit Atoh1 activity in the absence of self-activation (i.e., $s > b^{-\frac{1}{h_{a1}}}$) then the cell expresses the exogenous Dl1 if electroporated.

In the *in vivo* experiments, the response of the tissue to both types of electroporation was similar [Chrysostomou et al., 2012]. Likewise, we found that the response of the models (LI and SA) was similar to both types of EP (Figs. 3.18 and 3.19). First we evaluated the propensity of the electroporated cells to differentiate as HC (η_{ind-HC}) after the EP. We found that for low densities of EP the electroporated cells have high propensity to differentiate as HC, but this ratio (η_{ind-HC}) decreases as the density of the electroporation increases (Figs. 3.18A-a and 3.19A-a). This behavior is similar in both models (LI and SA) and is in agreement with the role of Dl1 promoting HCs differentiation in cis (Fig. 3.2A).

We also evaluated the proportion of HC within the array (η_{HC}) after the EP, following the same method described previously. We found that the proportion of HCs within the array (η_{HC}) decreases for increasing density of EP (Figs. 3.18A-b and 3.19A-b). This behavior is observed similarly in both models and is in agreement with the role of Dl1 inhibiting HC differentiation in trans (Fig. 3.2B), i.e., as there are more cells expressing (exogenous) Dl1, there is less HC differentiation.

By visual inspection of the snapshots of the simulation we found that in both models (LI and SA) there are highly EP regions where HC differentiation was prevented, which can account for the decrease in the proportion of HC diferentiation after highly dense EP (red arrows in Figs. 3.18B and 3.19B). Interestingly,

[10] In this context, we refer to the induction of exogenous Dl1 as *in silico* electroporations. See previous sections for details on how we model the expression of exogenous Dl1.

we found that there can be HC differentiation adjacent to cells expressing exogenous Dl1 (blue arrows in Figs. 3.18B and 3.19B), but only in the SA model. This explains why the decrease in HC proportion was more significant for the LI than for the SA model. This also fits with the *in vivo* experiments showing that HC differentiation can be robust to inhibition by Dl1 (Fig. 3.2B) [Chrysostomou et al., 2012].

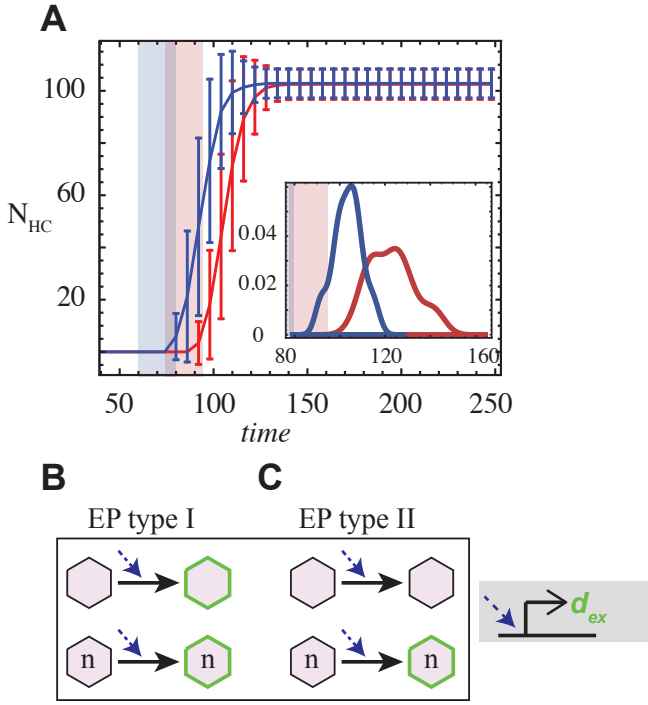

Figure 3.17 Differentiation of HCs on large arrays of hexagonal cells. A) Time course of HC differentiation in the SA (blue curve) and LI (red curve) models. Simulations were done on arrays of 18×18 hexagonal cells imposing periodic boundary conditions. The time course shows the average value (and the standard deviation) of the total HCs formed in the array (N_{HC}), corresponding to 45 independent simulations. The expected HCs number for arrays of this size is $\frac{1}{3}(18 \times 18) = 108$. The shadowed regions indicate the time frame at which the induction of exogenous Dl1 (d_{ex}) was done (blue and red frames correspond to SA and Li models, respectively). The results of these electroporations are presented in Figs. 3.18 and 3.19. Inset: Probability density function of the time of differentiation, τ_{diff} of the first 18 HCs, for the SA (blue) and the LI (red) models. B) Schematic representation of the two type of electroporations done in the simulations. The electroporated cell expresses exogenous Dl1 (green edges) independently of whether the levels of signal activity are high (n) or not in that cell. C) Only the electroporated cell with high levels of signal activity (n) can express exogenous Dl1.

Chrysostomou et al. [2012] showed that HC differentiation adjacent to cells expressing exogenous Dl1 was not facilitated by cis inhibition. The authors showed that these HCs had high activity levels of Notch signaling and hence cis inhibition was not likely to be taking place. In the line of these experiments, we evaluated the proportion of HC having high levels of NICD ($\eta_{HC-NICD}$), according to

$$\eta_{HC-NICD} = \frac{N_{HC-NICD}}{N_{HC}} \tag{3.8}$$

where $N_{HC-NICD}$ is the number of HC with high levels of NICD and N_{HC} is the number of HC within the array. We found that the proportion of HCs with high levels of NICD ($\eta_{HC-NICD}$) was zero for any density of electroporation in the LI but not in the SA model (Figs. 3.18A-c and 3.19A-c).

Taken together, our results show that only the SA model can account for all the phenotypes described reported by Chrysostomou et al. [2012] (Fig. 3.2), despite they might seem contradictory from the standpoint of lateral inhibition without self-activation of Atoh1, i.e., the role of Dl1 as an inhibitor of HC differentiation in trans is in conflict with the fact that some HCs can differentiate adjacent to other cells expressing Dl1. Hence, the model of simple lateral inhibition (LI) is not sufficient to account for the role of Dl1 in the developing inner ear at the onset of HC differentiation. We propose that Atoh1 self-activation can be the missing piece in this regulatory scaffold.

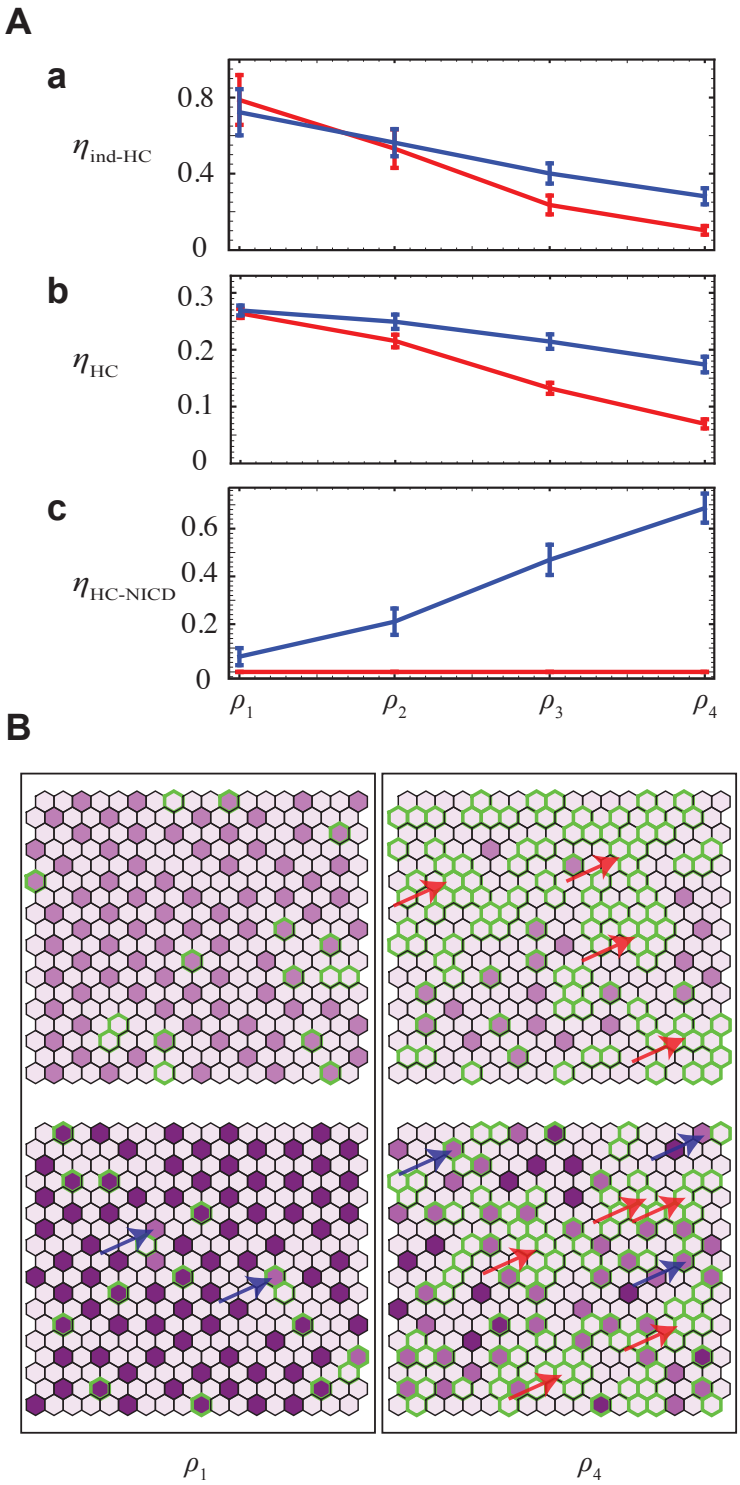
A
a
$\eta_{\text{ind-HC}}$
0.8
0.4
0
b
η_{HC}
0.3
0.2
0.1
0
c
$\eta_{\text{HC-NICD}}$
0.6
0.4
0.2
0
ρ_1
ρ_2
ρ_3
ρ_4
B
ρ_1
ρ_4

Figure 3.18 ***(previous page)*** Miss-expression of Dl1 trough type I electroporation in large arrays of hexagonal cells. Results of the LI (red) and SA (blue) models at EP densities $\rho_1 = 0.05$, $\rho_2 = 0.1091$, $\rho_3 = 0.206$ and $\rho_4 = 0.318$ for (a) the average value of EP cells that differentiate as HC (η_{HC}), (b) the average proportion of the cells array that differentiate as HC in the steady state and (c) the average proportion of HCs with high activity levels of NICD at the steady state. Averages values in a-c were obtained from 30 simulations done in arrays of 18×18 cells imposing periodic boundary conditions and different initial conditions. B) Snapshots of the steady state of one simulation of the LI model (left in each box) and the SA model (right in each box), for densities of cells expressing exogenous Dl1 (cells with green edges) ρ_1 and ρ_4. Red arrows point clusters of cells all expressing d_{ex}, where there is no HC differentiation. Blue arrows points HC differentiating adjacent to cells expressing d_{ex}.

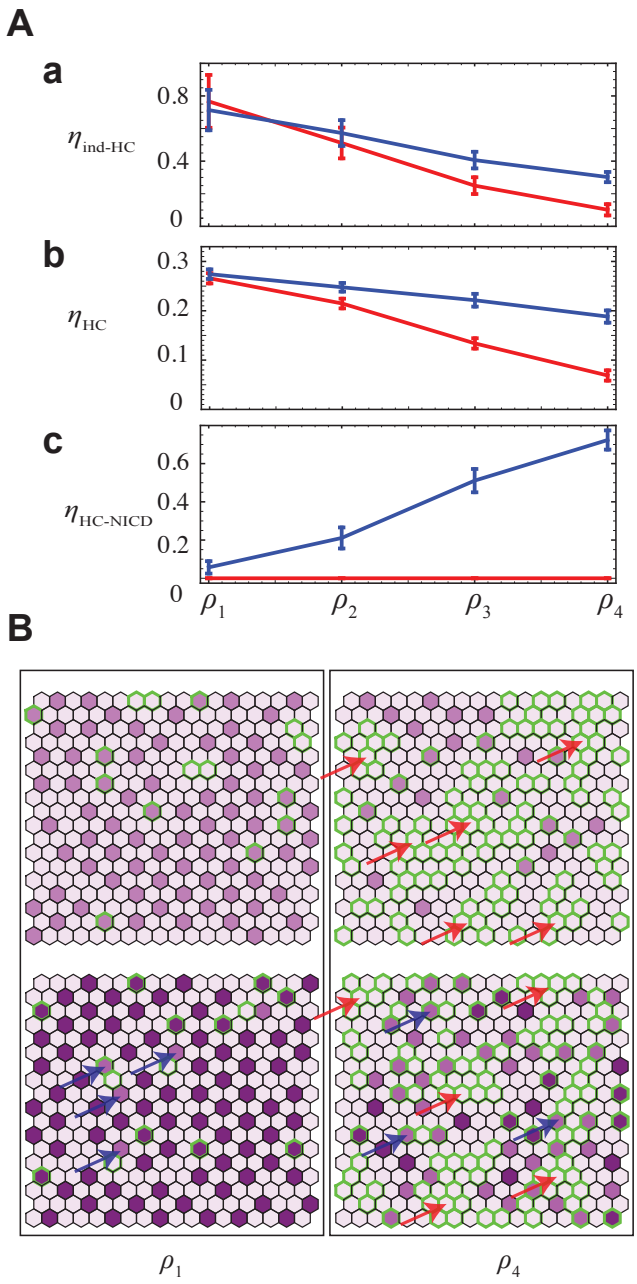
A
a
$\eta_{\text{ind-HC}}$
0.8
0.4
0
b
η_{HC}
0.3
0.2
0.1
0
c
$\eta_{\text{HC-NICD}}$
0.6
0.4
0.2
0
ρ_1
ρ_2
ρ_3
ρ_4
B
ρ_1
ρ_4

Figure 3.19 ***(previous page)*** Miss-expression of Dl1 trough type II electroporation in large arrays of hexagonal cells. Results of the LI (red) and SA (blue) models at EP densities $\rho_1 = 0.05$, $\rho_2 = 0.1091$, $\rho_3 = 0.206$ and $\rho_4 = 0.318$ for (a) the average value of EP cells that differentiate as HC (η_{HC}), (b) the average proportion of the cells array that differentiate as HC in the steady state and (c) the average proportion of HCs with high activity levels of NICD at the steady state. Averages values in a-c were obtained from 30 simulations done in arrays of 18×18 cells imposing periodic boundary conditions and different initial conditions. B) Snapshots of the steady state of one simulation of the LI model (left in each box) and the SA model (right in each box), for densities of cells expressing exogenous Dl1 (cells with green edges) ρ_1 and ρ_4. Red arrows point clusters of cells all expressing d_{ex}, where there is no HC differentiation. Blue arrows points HC differentiating adjacent to cells expressing d_{ex}.

3.3.3.2 Errors in patterning can be explained by low Notch signaling at the onset of differentiation

During the differentiation of the avian basilar papilla, transient contacts between nascent HCs are observed [Goodyear and Richardson, 1997]. Although immature, these cells express molecular markers of HCs and are morphologically recognizable as well. The LI model cannot account for HC-to-HC physical contacts because mutual inhibition between two adjacent cells results in the inhibition of the HC phenotype. In contrast, we show that in the SA model two adjacent cells can differentiate both as HCs (Fig. 3.11B). However, in that scenario the cells required initial high levels of Atoh1 activity simultaneously, which is not the case at the onset of HC differentiation where cells have initially low levels of Atoh1. Therefore we asked under which conditions two neighboring cells can both differentiate as HCs if the initial activity levels of Atoh1 are low in these cells.

We found that neighboring cells can differentiate both as HCs when they both have initial low levels of Atoh1 activity if in contrast their initial levels of Notch signal are sufficiently low (Fig. 3.20A). Using numerical simulations on arrays of hexagonal cells, we confirmed that the propensity of HC-to-HC contacts (ζ) is higher when the initial activity levels of Notch (s_0) are low (Fig. 3.20B). Notice that a small reduction in the initial levels of the signal activity (i.e., for $s_0 \approx 0.3$), almost every HC is in contact with another HC (i.e., $\zeta \approx 0.8$ in Fig. 3.20B inset b). Altogether, our analysis shows that the SA model can account for transient errors in patterning as observed in the developing *basilar papilla* of the chick [Goodyear and Richardson, 1997]. According to this model,

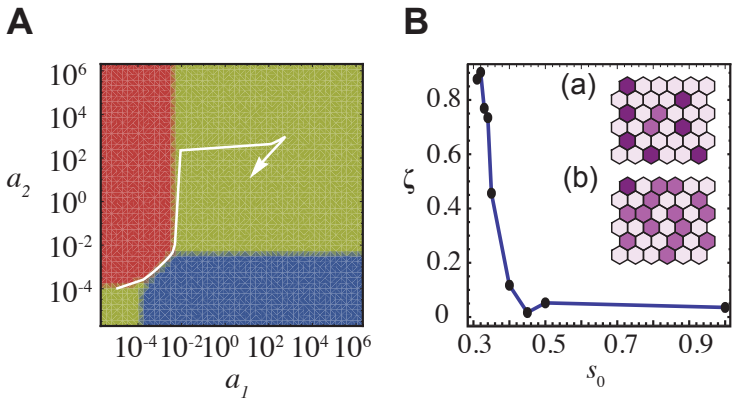

Figure 3.20 Errors in patterning by contacts between adjacent. A) Basins of attraction of each steady state occurring in the system of two coupled cells in the SA model. The basins of attraction of each steady states are labeled according to Fig. 3.11C. As initial conditions for the signal and Dl1 we set $s_0 = 0.25$ and $d_0 = 0$, respectively. Note that this initial condition for the signal is lower to that considered in previous sections. The white trajectory describes the evolution of an initial condition with low levels of Atoh1 activity in both cells, to a state in which both cell differentiate as HCs. B) Average ratio of HC-to-HC contacts with respect to the total number of HC in the tissue (ζ) as a function of the initial levels of the signal (s_0). The average at each point was calculated from 10 simulations in an array of 6×6 cells, taking as initial conditions for Atoh1 and Dl1 activity $a = 10^{-5}$ and $d = 10^{-2}$, respectively. Snapshots of the cell arrays corresponding to one of the simulations taking a) $s_0 = 1$ and b) $s_0 = 0.31$.

small clusters of cells with low activity levels of Notch signaling can result in differentiation of adjacent HCs.

3.4 Discussion

In this chapter we addressed the effect of Atoh1 transcriptional self-activation on the response of cell systems to miss-expression of Dl1. Transcriptional self-activation entails the formation of a cell-autonomous positive feedback loop. It is well known that when this regulatory feedback is sufficiently strong, it can drive bistability of the levels of the gene product, i.e., the protein levels can be either in OFF or ON states (Fig. 3.21) [Alon, 2006]. In addition, mutual lateral inhibition between neighboring cells can also entail a positive feedback loop (Fig. 3.1B) [Collier et al., 1996]. In this regard, the results presented here show how these two feedback loops interact functionally in terms of the

effect of the self-activation of Atoh1 on the outputs driven Dl1 acting in lateral inhibition, i.e., alternative cell-fate modulation and periodic patterning.

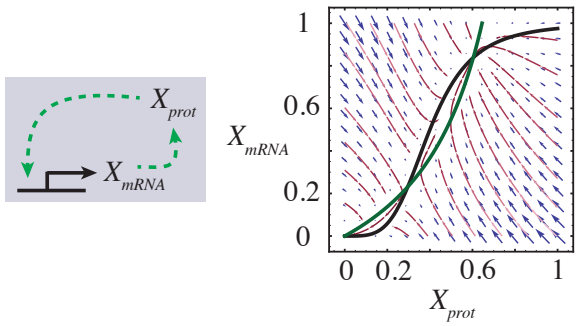

Figure 3.21 Bistability driven by a self-activation loop. (Left) Schematic representation of the transcriptional regulation of a gene X. mRNA of the gene translates into the protein which in turn promotes the transcription of the gene, leading to mRNA production. (Right) Phase portrait and vector flow of the system described in left, using a simple mathematical representation in which the protein promotes the transcription of the gene through a Michaelis-Menten like function (green curve) while the translation process follows a Hills like function with Hill coefficient 4 (black curve).

We found that these two mechanisms (lateral inhibition and self-activation of Atoh1) underlying multistability are combined, cell HC differentiation and patterning can be robust to miss-expression of Dl1. This robustness arises because self-activation of Atoh1 makes differentiated HCs numb to external sources of inhibition by seting multiple steady states. The maintenance of these HCs after miss-expression of Dl1 guaranties the maintenance the patterned state because they maintain their neighboring SCs differentiated as such. This mechanism devised from our modeling approach seems to fit better with recent *in vivo* experiments in the developing inner ear of the chick [Chrysostomou et al., 2012] than the model of simple lateral inhibition (i.e., when self-activation of Atoh1 is not considered explicitly).

Other mechanisms that could explain the robustness that some differentiated HCs exhibit to inhibition by external Dl1 are cis inhibition [Jacobsen et al., 1998, Schweisguth, 2004, Sprinzak et al., 2010] and/or the expression of Numb [Eddison et al., 2000, Frise et al., 1996, Rhyu et al., 1994].

In cis inhibition, Dl1 can bind to Notch receptor in the same cell and thereby it prevents Notch signaling to be activated by Dl1 in neighboring cells [Jacobsen

et al., 1998]. Therefore, a cell can be in contact with other cells expressing Dl1, but Notch signaling is not triggered because Dl1 in that cell is blocking the Notch receptors. However, Chrysostomou et al. [2012] showed that differentiated HCs that were in contact with other cells expressing exogenous Dl1 have high levels of Notch signaling activity. This strongly suggests that cis inhibition cannot be taking place significantly because Notch signaling is not prevented in the HCs adjacent to the cells expressing exogenous Dl1. Numb is a conserved factor among vertebrates and *Drosophila* [Eddison et al., 2000] and its expression occurs asymmetrically in dividing cells during development [Rhyu et al., 1994]. In *Drosophila* this asymmetry favors the adoption of sensory cell fate such that the cell expressing higher levels of *numb* differentiates as a sensory precursor. Numb can act as a repressor of Notch by direct binding to NICD and promoting is endocytosis and degradation [Frise et al., 1996, Jafar-Nejad et al., 2002, McGill and McGlade, 2003]. In this regard, when Numb is active then Notch signaling could be activated by external Dl1 but it will be degraded by the action of Numb, reducing the activity levels of Notch signaling. However, the *in vivo* experiments described above revealed high Notch signaling activity, and therefore signal degradation is not expected to be noticeably promoted by Numb. In addition, a recent study has shown that Numb does not behave as a strong inhibitor of Notch signal in the developing inner ear of the chick, and therefore is not involved in cell fate specification associated to Notch signaling [Eddison et al., 2015]. In contrast, the mechanism of Atoh1 self-activation can account for these observations, reconciling the two roles of Dl1 mediating lateral inhibition (i.e., inhibiting HC differentiation in trans) with the fact that some HCs can differentiate despite having high Notch signaling activity levels. Whether this self-activation effectively accounts for this robustness remains to be elucidated experimentally.

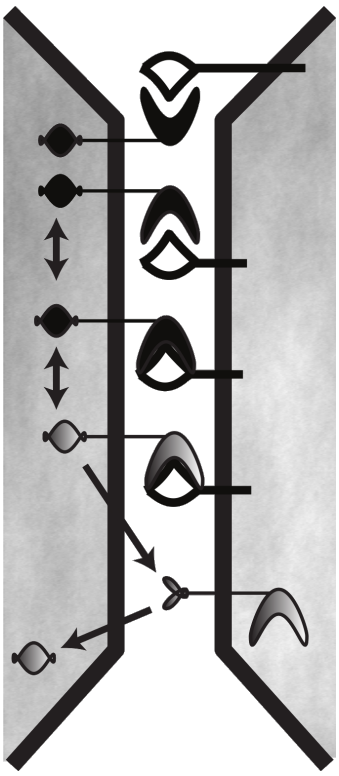

"Siempre es levemente siniestro volver a los lugares que han sido testigos de un instante de perfección."

Ernesto Sabato, Sobre héroes y tumbas

Chapter 4

Characterization of the differential signaling efficiency between co-expressed Notch ligands

4.1 Introduction

Canonical Notch signaling is activated by ligands binding to Notch receptor at the cell membrane (for a review see Kopan and Ilagan [2009]). This interaction generates a ligand–receptor complex which undergoes a cascade of proteolytic events, resulting in the cleaving and releasing of the cytoplasmic portion of Notch. This portion translocates to the nucleus where it can act as a regulator of gene transcription (reviewed in Fortini [2009], Kopan and Ilagan [2009]). Notch receptor can bind to different types of ligands, and each type can activate the signaling equivalently by means of the same biochemical scaffold [Fortini, 2009, Kopan and Ilagan, 2009]. The rate of signaling that can be activated by each type of ligand can be different [Hicks et al., 2000, Petrovic et al., 2014, Yang et al., 2005].

Fringe *glycosyltransferases*[1] are known to modify Notch receptor post-translationaly [Bruckner et al., 2000]. Fringe proteins can regulate the binding rate of the ligands with the receptor (i.e., their affinity) [Bruckner et al., 2000, Hicks et al., 2000, Panin et al., 1997, Shimizu et al., 2001, Taylor et al., 2014]. Increasing the binding rate of a type of ligand to Notch receptor can increase the signal activity level mediated by that ligand type[2]. For instance, Lunatic Fringe is known to enhance the rate of signaling of Delta1 by increasing the affinity of binding to Notch receptor [Taylor et al., 2014, Yang et al., 2005].

Ligand–receptor complex formation is the first step on the processes of Notch signaling activation and therefore it is expected that a high affinity value can lead to a high signaling level. However, there are additional processes taking place upon ligand–receptor binding [Kopan and Ilagan, 2009]. Because of this, it can be expected that the signaling activation mediated by the ligands might be affected by other processes other than the binding affinity. *In vitro* experiments have shown that Lunatic Fringe can decrease the levels of signaling activation of Jagged1 without affecting the binding affinity of Jagged1 to Notch receptor [Yang et al., 2005]. In this regard, Jagged1 can bind to Notch in the same proportion but the levels of signaling activation becomes lower when Notch is glycosylated.

4.1.1 Statement of the problem

Taking into account these *in vitro* experiments we ask *how can different steps along Notch signaling activation be changed in order to affect the amount of signal produced by the ligands upon binding to Notch receptor*? We proposed a simple model of Notch signaling activation taking into account two different ligands. Using this model we analyzed in which way different steps other than ligand–receptor binding can affect the signaling rate of the ligands.

We defined the signaling efficiency of the ligands and we show that when ligands have different efficiency of signaling then the ligand with lower efficiency can trans-inhibit the formation of the signal. In the last part of this Chapter

[1] Glycosyltransferases are enzymes that attach sugar groups on their substrates, which in this case is the Notch receptor.

[2] Such increase in signal activity level can be noticeable only if the receptor is not saturated by the ligand.

we studied a model which takes into account cis-interactions between the ligands and the receptor and we show how this type of interactions can drive a differential signaling efficiency between the ligands.

4.2 Modeling approach

4.2.1 Model with trans-interaction only. Reactions

As a first approach, we studied a system in which we considered only trans-interactions between the ligands and the receptor in a system of two adjacent cells. We assumed that one cell expresses the ligands and the other cell expresses only the receptor. Hence, signaling activation is assumed to occurr only in the last cell. In accordance with previous notation [Sprinzak et al., 2011], the first cell can be termed *signal-sending* cell and the other *signal-receiving* cell (Fig 4.1).

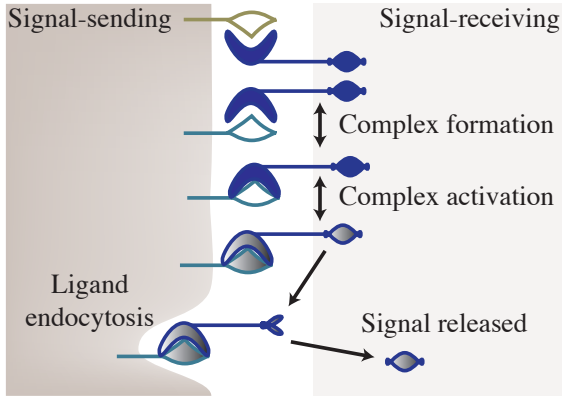

Figure 4.1 Schematic representation of the two cell scenario. The signal-receiving cell expresses the receptor, which binds to the ligand types expressed in the signal-sending cell. Upon binding, there is a complex formation step. This complex can transit (reversibly) a conformational change, resulting in an activated state of the complex. Upon this change, receptor cleavage occurs which depends on ligand endocytosis in the signal-sending cell.

We assumed that there are two ligand types (L_i, taking $i = 1$ or $i = 2$ for ligand1 or ligand2, respectively) which can bind reversibly to Notch receptor (R), leading to the formation of a complex (C_i), according to

$$L_i + R \underset{k_{\mathrm{u,i}}}{\overset{k_{\mathrm{b,i}}}{\rightleftarrows}} C_i \tag{4.1}$$

where $k_{\mathrm{b,i}}$ and $k_{\mathrm{u,i}}$ represent the binding and unbinding coefficients, specific of each ligand type. In turn, the complex C_i follows a reversible conformational change, to an activated state C_i^*, according to

$$C_i \underset{k_{\mathrm{ba,i}}}{\overset{k_{\mathrm{fo,i}}}{\rightleftarrows}} C_i^*. \tag{4.2}$$

We assumed that when the ligand-receptor complex is this active state (C_i^*) then it is able to interact with the cleaving enzyme E[3].

Notch signaling activation requires two consecutive cleaving processes mediated by ADAM and $\gamma-$secretase (reviewed in Kopan and Ilagan [2009]). We have simplified these cleaving steps to just one cleaving process mediated by a single enzyme. Assuming a Michaelis-Menten like behavior, we proposed that the active complex can bind reversibly to a cleaving enzyme (E), which is assumed to be the same for both complexes types (i.e., C_1^* and C_2^*). After binding, there is the formation of an intermediary complex ($C_{E,i}^*$), from which the signal (S) is formed according to

$$C_i^* + E \underset{k_{\mathrm{eu,i}}}{\overset{k_{\mathrm{eb,i}}}{\rightleftarrows}} C_{E,i}^* \xrightarrow{\varepsilon_i} S + E. \tag{4.3}$$

We assumed that this intermediary complex ($C_{E,i}^*$) only degrades upon signaling, which is an irreversible process with constant rate (ε_i). In turn, we assumed that (i) the ligands and the receptor are produced with constant rates α_{li} ($i = 1$ and $i = 2$ for ligand1 and ligand2, respectively) and α_r respectively, and (ii) the ligands, the receptor, the complexes and the signal, degrade according to

[3]It has been shown that this conformational change is mediated by a pulling force exerted by the endocytosis of the ligand after binding to Notch [Glittenberg et al., 2006, Gordon et al., 2015, Meloty-Kapella et al., 2012, Parks et al., 2000].

$$
\begin{aligned}
L_i &\xrightarrow{\gamma_{L_i}} \emptyset \\
R_i &\xrightarrow{\gamma_{R_i}} \emptyset \\
C_i &\xrightarrow{\gamma_{C_i}} \emptyset \\
C_i^* &\xrightarrow{\gamma_{C_i^*}} \emptyset \\
S &\xrightarrow{\gamma_{C_i^*}} \emptyset
\end{aligned}
\tag{4.4}
$$

where γ_x represents the constant rate of degradation of x.

4.2.2 Model with trans-interaction only. Dynamic equations

Taking into account the reactions described before, we can write the dynamical system of equations for the receptor, the ligands, the complexes and the signal, which reads[4]

$$
\begin{aligned}
\frac{\mathrm{d}R}{\mathrm{d}t} &= \alpha_r + C_1 k_{\mathrm{u1}} + C_2 k_{\mathrm{u2}} - R\left(\gamma_R + L_1 k_{\mathrm{b1}} + L_2 k_{\mathrm{b2}}\right) \\
\frac{\mathrm{d}L_1}{\mathrm{d}t} &= \alpha_{l1} + C_1 k_{\mathrm{u1}} - L_1\left(R k_{\mathrm{b1}} + \gamma_{L1}\right) \\
\frac{\mathrm{d}L_2}{\mathrm{d}t} &= \alpha_{l2} + C_2 k_{\mathrm{u2}} - L_2\left(R k_{\mathrm{b2}} + \gamma_{L2}\right) \\
\frac{\mathrm{d}C_1}{\mathrm{d}t} &= R L_1 k_{\mathrm{b1}} + C_1^* k_{\mathrm{ba1}} - C_1\left(k_{\mathrm{u1}} + k_{\mathrm{fo1}} + \gamma_{\mathrm{C1}}\right) \\
\frac{\mathrm{d}C_2}{\mathrm{d}t} &= R L_2 k_{\mathrm{b2}} + C_2^* k_{\mathrm{ba2}} - C_2\left(k_{\mathrm{u2}} + k_{\mathrm{fo2}} + \gamma_{\mathrm{C2}}\right) \\
\frac{\mathrm{d}C_1^*}{\mathrm{d}t} &= C_1 k_{\mathrm{fo1}} + C_{E,1}^* k_{\mathrm{eu1}} - C_1^*\left(k_{\mathrm{ba1}} + E k_{\mathrm{eb1}} + \gamma_{\mathrm{C}_1^*}\right) \\
\frac{\mathrm{d}C_2^*}{\mathrm{d}t} &= C_2 k_{\mathrm{fo2}} + C_{E,2}^* k_{\mathrm{eu2}} - C_2^*\left(k_{\mathrm{ba2}} + E k_{\mathrm{eb2}} + \gamma_{\mathrm{C}_2^*}\right) \\
\frac{\mathrm{d}C_{E,1}^*}{\mathrm{d}t} &= C_1^* E k_{\mathrm{eb1}} - C_{E,1}^*\left(k_{\mathrm{eu1}} + \varepsilon_1\right) \\
\frac{\mathrm{d}C_{E,2}^*}{\mathrm{d}t} &= C_2^* E k_{\mathrm{eb2}} - C_{E,2}^*\left(k_{\mathrm{eu2}} + \varepsilon_2\right) \\
\frac{\mathrm{d}S}{\mathrm{d}t} &= C_{E,1}^* \varepsilon_1 + C_{E,2}^* \varepsilon_2 - S\gamma_S
\end{aligned}
\tag{4.5}
$$

[4]Notice that these reactions only consider production–degradation and binding–unbinding processes, i.e., the dynamics of the species does not account for diffusion.

For simplicity, we assumed that the total amount of the cleaving enzyme (E_{Tot}) is conserved. Therefore, the levels of free enzyme can be written as $E = E_{Tot} - (C^*_{E,1} + C^*_{E,2})$.

4.2.3 Model with cis-interactions

Cis-interactions between Notch ligands and receptor are well known to occur and they have been described in different contexts [Glittenberg et al., 2006, Jacobsen et al., 1998]. Cis-interactions occur when the ligand bind to the receptor in the same cell. These interactions do not trigger signaling activity, and hence they are said to drive cis-inhibition of Notch signaling [Jacobsen et al., 1998]. Within our modeling framework, we included cis-interactions both in the signal sending and in the signal receiving cell by setting that the receptor is present in the two interacting cells. However, the complex-processing pathway has been omitted in the signal sending cell. Therefore, the receptor in each cell (R_j) can interact with ligands in the neighboring cell (as described in the previous section), but also with ligands in the same cell ($L_{j,i}$) according to

$$L_{j,i} + R_j \underset{k_{\mathrm{uci}}}{\overset{k_{\mathrm{bci}}}{\rightleftarrows}} C_{c,(j,i)} \tag{4.6}$$

where $k_{\mathrm{bc,i}}$ and $k_{\mathrm{uc,i}}$ are the binding and unbinding coefficients in cis. Notice that now we have introduced two subindexes for the ligand to indicate the cell in which it is located (subindex j) and the type of ligand it is (subindex i).

We assumed that cis-interactions do not drive signaling activity, i.e., the complexes $C_{c,(j,i)}$[5] do not undergo conformational changes as occurred for the complexes formed in trans.

Hence, considering this type of interactions we can write the dynamics of the ligands, the receptor and the cis-complexes in cell j as

[5]Notice that these interactions can occur between ligand1 (for $i = 1$) or ligand2 (for $i = 2$) and the receptor in each cell j

$$
\begin{aligned}
\frac{\mathrm{d}R_j}{\mathrm{d}t} &= \alpha_r + C_1 k_{\mathrm{u1}} + C_2 k_{\mathrm{u2}} + C_{c,(j,1)} k_{\mathrm{uc1}} + C_{c,(j,2)} k_{\mathrm{uc2}} - \\
&\quad - R\left(\gamma_R + L_{i,1} k_{\mathrm{b1}} + L_{i,2} k_{\mathrm{b2}} + L_{j,1} k_{\mathrm{bc1}} + L_{j,2} k_{\mathrm{bc2}}\right) \\
\frac{\mathrm{d}L_{j,1}}{\mathrm{d}t} &= \alpha_{l1} + C_1 k_{\mathrm{u1}} + C_{c,(j,1)} k_{\mathrm{uc1}} - \\
&\quad - L_1\left(R_i k_{\mathrm{b1}} + R_j k_{\mathrm{bc1}} + \gamma_{L1}\right) \\
\frac{\mathrm{d}L_{j,2}}{\mathrm{d}t} &= \alpha_{l2} + C_2 k_{\mathrm{u2}} + C_{c,(j,2)} k_{\mathrm{uc2}} - \\
&\quad - L_2\left(R_i k_{\mathrm{b2}} + R_j k_{\mathrm{bc2}} + \gamma_{L2}\right) \\
\frac{\mathrm{d}C_{c,(j,1)}}{\mathrm{d}t} &= R_j L_{j,1} k_{\mathrm{bc1}} - C_{c,(j,1)}\left(k_{\mathrm{uc1}} + \gamma_{\mathrm{C1}}\right) \\
\frac{\mathrm{d}C_{c,(j,2)}}{\mathrm{d}t} &= R_j L_{j,2} k_{\mathrm{bc2}} - C_{c,(j,2)}\left(k_{\mathrm{uc2}} + \gamma_{\mathrm{C2}}\right)
\end{aligned}
\tag{4.7}
$$

The dynamical equations for the remaining variables (i.e., the trans-complexes, the complex-processing variables and the signal) do not change by considering cis-interactions, and hence they are the same as in Eqns. 4.5. Then, the dynamics of the signal-sending cell is described by the first five equations in 4.5 Eqns. together with 4.7, whereas the dynamics of the signal-receiving cell is described by Eqns. 4.5 and 4.7.

4.2.4 Model assumptions

4.2.4.1 Parameter values

In the following we briefly motive our choice on the parameter values.

We assumed that the production and degradation rates for the receptor are such that in the absence of binding and unbinding to the ligands, the expected concentration of free receptor in the membrane is $\sim 10^3$ units of concentration (u.c.). We assumed two different scenarios depending on whether the ligand1 can saturate the receptor when expressed in isolation, such that $\alpha_{l1} = \frac{10^2}{2} \cdot \alpha_r$, i.e., the expected concentration of the ligand is higher than that of the receptor in the absence of binding and unbinding events. In contrast, in the second scenario we assumed that ligand1 does not saturate the receptor and then $\alpha_{l1} = 10^{-1} \cdot \alpha_r$. We also assumed that ligands and receptor degrade at the same rate,

while the signal degrades five times faster, in accordance with a previous work [Boareto et al., 2015].

We assumed that the ligand–receptor and complex–enzyme binding rates are much higher than the unbinding rates, such that the binding equilibrium constants are in the order of $\sim 10^5$ (u.c.)$^{-1}$. This is consistent with a scenario of nearly irreversible binding processes [Sprinzak et al., 2010]. Likewise, the rates of conformational changes of the ligand–receptor complexes are assumed such that in equilibrium the formation of the active complex state is favored (i.e., the equilibrium constant of activation is on the order of $\sim 10^3$). We assumed that the binding rates are two orders of magnitude higher than the signaling rates (i.e., ε_i), but in turn these signaling processes are irreversible. Taking into account these considerations, we described the parameter values used along the simulations in Table 4.1. We assumed as arbitrary unit of time (a.u.t.) the inverse of the degradation rate of the receptor, γ_r (Table 4.1).

Parameter	Value	Units
α_r	10^3	$(\text{a.u.t.})^{-1}$
γ_{L1}, γ_{L2}	1	$(\text{a.u.t.})^{-1}$
γ_s	5	$(\text{a.u.t.})^{-1}$
k_{u1}, k_{u2}	10^{-3}	$(\text{a.u.t.})^{-1}$
k_{b1}, k_{b2}	10^2	$(\text{u.c.})^{-1}(\text{a.u.t.})^{-1}$
k_{ba1}, k_{ba2}	10^{-1}	$(\text{a.u.t.})^{-1}$
k_{fo1}	10^2	$(\text{a.u.t.})^{-1}$
k_{eu1}, k_{eu2}	10^{-3}	$(\text{a.u.t.})^{-1}$
k_{eb1}	10^2	$(\text{u.c.})^{-1}(\text{a.u.t.})^{-1}$
ε_1, ε_2	1	$(\text{a.u.t.})^{-1}$

Table 4.1 Parameter values for the numerical simulations. The value of the parameters not listed in this table are depicted in the corresponding figure captions below.

Along the simulations we assumed positive initial conditions for the ligands ($L_1(t=0) = L_2(t=0) = 10$) and the receptor ($R(t=0) = 100$), but zero for the rest of the variables. An exception is made for the results shown in Figs. 4.7 and 4.8, where the initial levels of the ligands are zero.

4.2.4.2 Relative signaling efficiency between ligands

The concentration of the signal can be written as a function of the production rate of the ligands and the receptor, according to

$$S = s(\alpha_r, \alpha_{l1}, \alpha_{l2}) \tag{4.8}$$

Hence, we say that the maximal concentration of the signal driven by ligand1 when expressed in isolation is $s(\alpha_r, \alpha_{l1}, 0)$, such that $\frac{\alpha_{l1}}{\alpha_r} \gg 1$, i.e., the ligand is expected to saturate the receptor as long as the binding equilibrium constant is sufficiently high. According to this, we defined the relative signaling efficiency of ligand2 with respect to ligand1 (ε_s) as the ratio between the concentration of the signal driven by each ligand in isolation

$$\varepsilon_s = \frac{s(\alpha_r, 0, \alpha_{l2})}{s(\alpha_r, \alpha_{l1}, 0)} \tag{4.9}$$

In order to evaluate Eqn. 4.9 when Notch receptor is saturated by each ligand, we assumed that (i) $\alpha_{li} = \frac{1}{2}\alpha_r 10^2$ for $i = 1$ and $i = 2$ corresponding to ligand1 and ligand2, respectively, and (ii) the value of the binding rates of the ligands to Notch receptor ($k_{\mathrm{b}1}$ and $k_{\mathrm{b}2}$) are sufficiently high to promote binding over unbinding (as described in Table 4.1).

4.3 Results

In the first part of this section we show how the signaling efficiency of the ligands can be modulated by the parameters associated to the complex-processing pathway. We also explore how is the signal activity when the two ligand types have different signaling rates. In the last part, we show that cis-interactions can modulate the signaling rate of the ligand types.

4.3.1 Complex-processing is essential to modulate the relative signaling efficiency between ligands

It has been shown that Fringe can change the levels of Notch signal activation mediated by Notch ligands without changing their binding affinity to Notch receptor [Yang et al., 2005]. A plausible mechanism by which this type of modifications could arise is that the ligand-receptor complex dissociates by the pulling force exerted upon the endocytosis of the ligand. Because of this, the complex could not be processed by the cleaving enzymes and hence signaling is prevented. This mechanism has been proposed earlier, based on experimental observations [Yang et al., 2005], although it has not been confirmed to occur *in vivo*.

We first explored how changing the values of the parameters associated to the ligand–receptor complex processing can affect the relative signaling efficiency between ligands (ε_s). To do so, we evaluated the value of ε_s for different values of the parameters that control the complex-processing pathway specific to ligand2 (i.e., k_{fo2} and k_{eb2}). We considered two different scenarios in which the enzyme can be a limiting resource for signaling or not assuming low and high concentration levels of the enzyme, respectively.

We found that both parameters k_{fo2} and k_{eb2} can change the value of the relative signaling efficiency (ε_s) in the scenario in which the enzyme is a limiting resource (Fig. 4.2A). Particularly, for constant low values of k_{eb2}, the relative efficiency increases with k_{fo2} close to its maximal value $\varepsilon_s \approx 1$ when $k_{\text{fo2}} = k_{\text{fo1}}$. However, for a constant high value of k_{eb2}, the value of ε_s remains constant (and close to maximal) with respect to the increasing values of k_{fo2}. We found a similar behavior in the scenario in which the concentration of the enzyme is high, such that ε_s increases with k_{fo2} close to its maximal value $\varepsilon_s \approx 1$ when $k_{\text{fo2}} = k_{\text{fo1}}$ (Fig. 4.2B). Interestingly, the dependence of the value of ε_s on k_{fo2} was the same for both high and low values of k_{eb2} (notice that the squares and the triangles overlap in Fig. 4.2B).

Notice that the value of ε_s is higher when the concentration of the enzyme is low than when it is high. We reasoned that in the first scenario ($E_{Tot} = 10$) the ligands saturate the enzyme such that the complexes associated to each ligand can bind to all the available enzyme despite having slower rates of processing. Hence, the expected concentration of the active complex bound to the enzyme

follows $C^*_{E,i} \approx E_{Tot}$, assuming that the binding rate k_{ebi} is sufficiently high. Accordingly, the expected concentration of the signal in the stationary state follows $s^{st} = \frac{1}{\gamma_s} E_{Tot}$, as confirmed numerically in Fig. 4.2A (inset). Because of this, the differences in the signaling efficiency between ligands become lower. This is not the case for the scenario in which the concentration of the enzyme is high. In this scenario, the limiting resource is the receptor and hence differences in complex processing are relevant for the value of ε_s. Furthermore, since the enzyme is very abundant, the binding rate of the active complex to the enzyme is not expected to affect the relative efficiency (4.2B).

Taken together, these results show that the processing rates can affect the signaling efficiency of the ligands such that the less efficient ligand is the one for which the dynamics of processing of the complexes is slower.

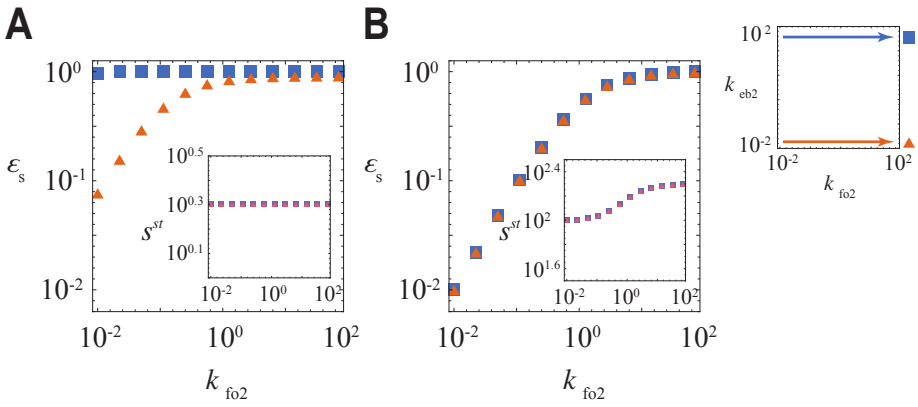

Figure 4.2 Relative signaling efficiency of ligand2 with respect to ligand1 (ε_s) for A) low ($E_{tot} = 10$) and B) high ($E_{tot} = 10^6$) concentration of the enzyme. The evaluation was done assuming high and low constant values of k_{eb2} (10^2 and 10^{-2}), as schematized in the diagram on the right, where blue and orange arrows represent the path corresponding to the squares and triangles respectively. Degradation rates for the complexes are $\gamma_C = \gamma_{C*} = 1$. Insets: Concentration of the signal at the stationary state $s^{st} = s(\alpha_r, \alpha_{l1}, \alpha_{l2})$, assuming $\alpha_{l1} = \alpha_{l2} = \frac{1}{2}10^5$ and $\alpha_r = 10^3$, as a function of k_{fo2}. Squares and triangles correspond to high and low values of k_{eb2}.

4.3.2 Low values of the relative signaling efficiency can drive trans-inhibition of the signal by over-expression of the less efficient ligand

Our previous results suggest that having a less efficient signaling ligand might not have a remarkable effect on the concentration of the signal at the stationary state (insets Fig. 4.2). In that case, the signal concentration is evaluated when both ligands are expected to be equally abundant (i.e., $\alpha_{l1} = \alpha_{l2}$). To determine the effect of having a less efficient ligand when the ligands are present at different concentrations, we evaluated the concentration of the signal at the stationary state (s^{st}) when only ligand1 is expressed and then tested how this concentration changes upon a second ligand becomes to be expressed. We studied the case in which the second ligand is equally efficient at signaling (i.e., $k_{\text{eb2}} = k_{\text{eb1}}$ and $k_{\text{fo2}} = k_{\text{fo1}}$) and the case in which the complexes of the second ligand are processed at slower rates (i.e., $k_{\text{eb2}} = 10^{-4} \cdot k_{\text{eb1}}$ and $k_{\text{fo2}} = 10^{-4} \cdot k_{\text{fo1}}$). Notice that in this last case, we have that $\varepsilon_s < 1$ according to Fig. 4.2A.

We found that when both ligands are equally efficient at signaling then the concentration of the signal at the stationary state increases noticeably upon the over-expression of the second ligand, if the receptor is not already saturated by ligand1 (triangles in Fig. 4.3A). If the receptor was initially saturated, then the signal activity levels at the stationary state do not change much upon ligand2 over-expression (squares in Fig. 4.3A). In contrast, we found that if the complexes associated to the second ligand are processed slowly compared to those associated to ligand1, then the over-expression of ligand2 reduces the concentration of the signal at the stationary state (Fig. 4.3B). This occurred independently of whether the receptor was initially saturated by ligand1 or not. Yet, the concentration of the signal decreases when the expected abundance of ligand2 is similar to that of the receptor, i.e., for $\alpha_{l2} \approx \alpha_r$ (Fig. 4.3B).

Since the effect of the ligands is due to trans-interactions between the ligand and Notch receptor, hereafter we say that ligand2 trans-inhibits the formation of the signal at the stationary state.

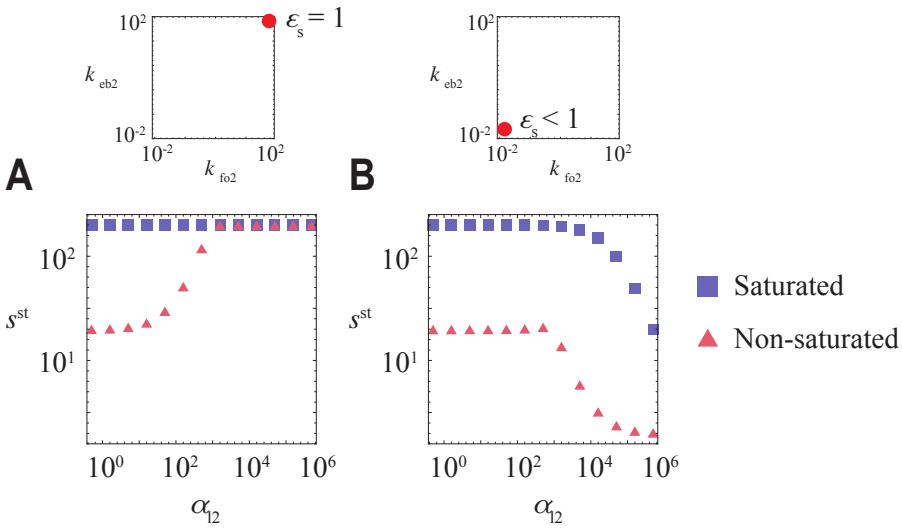

Figure 4.3 Concentration of the signal in the stationary state as a function of the production rate of ligand2. A) Ligands are equally efficient at signaling, as schematized in the diagram on the top (i.e., $k_{\text{eb2}} = k_{\text{eb1}}$ and $k_{\text{fo2}} = k_{\text{fo1}}$ corresponding to $\varepsilon_s = 1$). B) Ligand2 is less efficient at signaling than ligand1 due to slower rates of complex-processing (i.e., $k_{\text{eb2}} = k_{\text{eb1}}10^{-4}$ and $k_{\text{fo2}} = k_{\text{fo1}}10^{-4}$ corresponding to $\varepsilon_s < 1$). Squares represent the case in which the receptor is already saturated by ligand1 (i.e., $\alpha_r = 10^3$ and $\alpha_{l1} = \frac{1}{2}10^5$) and the triangles the case in which it is not (i.e., $\alpha_r = 10^3$ and $\alpha_{l1} = 10^2$). Degradation rates for the complexes are $\gamma_C = \gamma_{C*} = 1$ and the concentration of the enzyme is high, $E_{tot} = 10^6$.

4.3.3 Differential signaling efficiency only arises when intermediary complexes degrade

Despite our model is a simplification of the Notch signaling pathway, it still has too many variables and parameters which make difficult the analysis of the underlying mechanism by which the less efficient ligand mediates trans-inhibition of the signal.

In our scheme of reactions (Fig. 4.4A), we identify three main processes:

- complex formation,
- complex processing and signaling and
- leaking by complex degradation

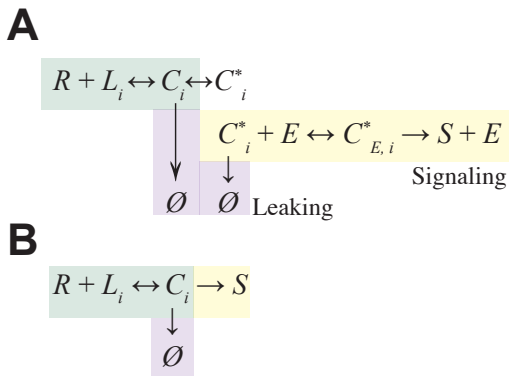

Figure 4.4 Complex formation, processing and leaking pathways during signal activation. Schematic representation of the reactions taking place in A) the extended model (Reactions 4.6, 4.2 and 4.3) and B) the simplified model (Reactions 4.10). Each module is framed with a different color; Ligand-receptor complex formation in green, complex-processing and signalling in yellow and intermediary complex degradation (leaking) in purple.

Based on these processes, we proposed a simpler version of the model (Fig. 4.4B). The reactions taking place in this minimal system are

$$\begin{aligned} L_i + R \underset{k_{\mathrm{u,i}}}{\overset{k_{\mathrm{b,i}}}{\rightleftarrows}} C_i \xrightarrow{\varepsilon_i} S \\ C_i \xrightarrow{\gamma_{C_i}} \emptyset \end{aligned} \tag{4.10}$$

for $i = 1$ and $i = 2$, corresponding to ligand1 and ligand2, respectively. Assuming signal and receptor degradation, as well as constant production of the receptor and the ligands, we can derive dynamic equations analogous to Eqns. 4.5. From these equations we can easily derive an expression for the concentration of the signal in the stationary state, which reads

$$s^{st} = \frac{\alpha_r}{\gamma_s} \frac{\epsilon_1 L_1^{st} \hat{K}_{\mathrm{b1}} + \epsilon_2 L_2^{st} \hat{K}_{\mathrm{b2}}}{1 + L_1^{st} \hat{K}_{\mathrm{b1}} + L_2^{st} \hat{K}_{\mathrm{b2}}} \tag{4.11}$$

where

$$\begin{aligned} \hat{k}_{\mathrm{bi}} &= \frac{k_{\mathrm{bi}}(\gamma_{C_i} + \varepsilon_i)}{k_{\mathrm{ui}} + \gamma_{C_i} + \varepsilon_i} \\ \epsilon_i &= \frac{\varepsilon_i}{\varepsilon_i + \gamma_{C_i}} \end{aligned} \tag{4.12}$$

Notice from these expressions that the maximal signal concentration driven by ligand1 and ligand2 at the stationary state, when each ligand is expressed in isolation, is ϵ_1 and ϵ_2, respectively. Hence, the relative signaling efficiency of ligand2 with respect to ligand1 in the stationary state can be written as

$$\varepsilon_s \equiv \frac{\epsilon_2}{\epsilon_1} = \frac{1 + \frac{\gamma_{C_1}}{\varepsilon_1}}{1 + \frac{\gamma_{C_2}}{\varepsilon_2}}. \tag{4.13}$$

From Eqn. 4.13 we argued that ligand2 is expected to be less efficient at signaling than ligand1 (i.e., $\varepsilon_s < 1$) if its associated coefficient between complex-degradation and complex-processing is higher than that associated to ligand1, i.e., $\frac{\gamma_{C_2}}{\varepsilon_2} > \frac{\gamma_{C_1}}{\varepsilon_1}$. Hence, complex degradation is necessary, but not sufficient, in order to have a differential signaling efficiency between ligands.

Back to our full-length model, we evaluated the value of ε_s as a function of the degradation rate of the active complexes, γ_{C^*}. Notice that this rate is the same for both ligand types (Eqns. 4.5). Numerical calculations were done when the processing of the complexes associated to ligand2 is slower than that associated to ligand1 (i.e., $k_{\mathrm{eb2}} = 10^{-4} \cdot k_{\mathrm{eb1}}$ and $k_{\mathrm{fo2}} = 10^{-4} \cdot k_{\mathrm{fo1}}$) in two different regimes of enzyme abundance. In addition, we explored the case in which the degradation rate of the non-active complex (γ_C) is either high or low.

We found that when the enzyme is a limiting resource then the value of ε_s decreases for increasing values of γ_{C*} (Fig. 4.5A). Interestingly, when the value of the degradation rates of the complexes is low ($\gamma_{C*} = \gamma_C = 10^{-2}$) then both ligands are expected to be equally efficient at signaling, i.e., $\varepsilon_s \approx 1$, despite having different rates of complex-processing (Fig. 4.5A). In addition, we found that when the enzyme is not a limiting resource (i.e., $E_{Tot} \gg \alpha_r$) then the value of ε_s only depends on γ_C (Fig. 4.5B). Hence, in both regimes of enzyme levels (i.e., for low and high E_{Tot}) the relative signaling efficiency in the stationary state is expected to be < 1 when at least one of the rates of degradation is sufficiently high (Fig. 4.5). These numerical results show that a positive degradation rate

of the complexes is necessary in order that ligands can have a differential signaling efficiency in the stationary state, as predicted by the analysis of a simplified model (Eqn. 4.13).

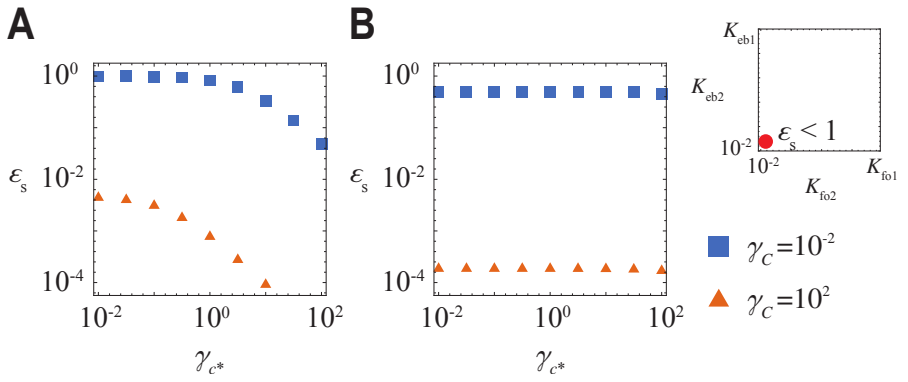

Figure 4.5 Relative signaling efficiency (ε_s) at the stationary state as a function of the rate of active complexes degradation (γ_{C^*}). A) Low enzyme levels ($E_{tot} = 10$) and B) high enzyme levels ($E_{tot} = 10^6$), when the dynamics of complex-processing is slower for ligand2 than for ligand1, as shown in the diagram of the right ($k_{\text{eb2}} = 10^{-4} \cdot k_{\text{eb1}}$ and $k_{\text{fo2}} = 10^{-4} \cdot k_{\text{fo1}}$). The blue squares and the orange triangles show the case in which the rate of degradation of the non-active complex is low ($\gamma_C = 10^{-2}$) and high ($\gamma_C = 10^2$), respectively.

In addition, we evaluated the stationary concentration of the signal (s^{st}) mediated by ligand1 and then tested how it changes when ligand2 becomes to be co- and over-expressed. We assumed that the complexes associated to ligand2 are processed slower than those associated to ligand1, i.e., $k_{\text{eb2}} = 10^{-4} \cdot k_{\text{eb1}}$ and $k_{\text{fo2}} = 10^{-4} \cdot k_{\text{fo1}}$, in a scenario in which the enzyme is not a limiting resource. In addition, we assumed that complexes degrade fast or slowly, i.e., $\gamma_{C^*} = \gamma_C = 10^2$ or $\gamma_{C^*} = \gamma_C = 10^{-2}$, respectively. Hence, the expected values of the relative signaling efficiency are $\varepsilon_s \approx 10^{-0.2}$ and $\varepsilon_s \approx 10^{-4}$ for low and high complexes degradation rates, respectively (Fig. 4.5B).

We found that when complex degrade fast, the stationary concentration of the signal decreases upon over-expression of ligand2 (Fig. 4.6A). Notice that this occurs independently of whether the receptor is initially saturated by ligand1 or not. In contrast, when complexes degrade slowly, the over-expression of ligand2 can drive signal activation or a mild reduction of the signal activity levels depending on whether the receptor is or it is not saturated by ligand1,

respectively (Fig. 4.6B). This mild reduction is expected since ligand2 is still slightly less efficient at signaling than ligand1 ($\varepsilon_s \approx 10^{-0.2}$).

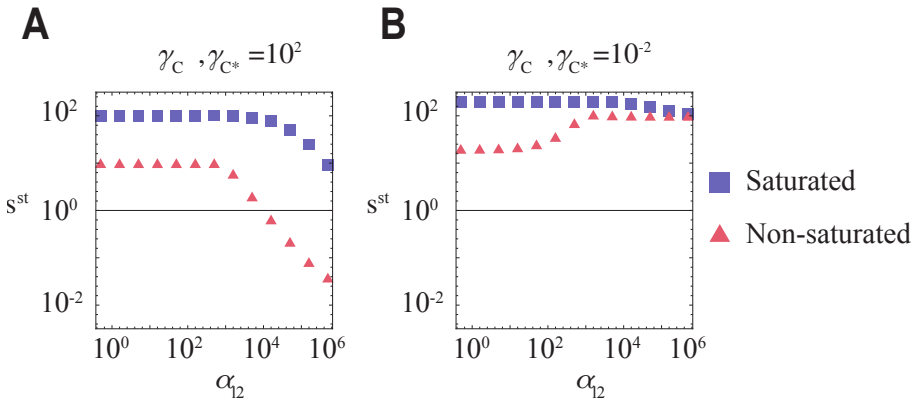

Figure 4.6 Concentration of the signal at the stationary state as a function of the production rate of ligand2 (variable complexes degradation). A) Complexes degrade with a high rates, $\gamma_{C^*} = \gamma_C = 10^2$. B) Complexes degrade slowly, $\gamma_{C^*} = \gamma_C = 10^{-2}$. In A and B the dynamics of complex-processing for ligand2 is slower than for ligand1,according to $k_{\text{eb2}} = 10^{-4} \cdot k_{\text{eb1}}$ and $k_{\text{fo2}} = 10^{-4} \cdot k_{\text{fo1}}$, and we assumed high concentration of the enzyme, $E_{tot} = 10^6$. Squares represent the case in which the receptor is already saturated by ligand1 (i.e., $\alpha_r = 10^3$ and $\alpha_{l1} = \frac{1}{2}10^5$) and the triangles the case in which it is not (i.e., $\alpha_r = 10^3$ and $\alpha_{l1} = 10^2$).

Taken together, our results show that the relative signaling efficiency between ligands depends critically on the coefficient between the complex-degradation and complex-processing associated to each ligand. When there is not enough degradation of the complexes then the signaling efficiency of the ligands in the stationary state is expected to be approximately the same (i.e., $\varepsilon_s \approx 1$), despite they might have different rates of complexes-processing. Accordingly, ligand2 (whose complexes are processed slower than those of ligand1) is not expected to trans-inhibit the formation of the signal when degradation rate of the complexes is low.

4.3.4 The role of the ligand with slower dynamics of complex-processing can change in time

Our previous results showed that if the intermediary complexes degrade slowly, compared to how the complexes are processed for ligand1, then the ligand2 does

not act as trans-inhibitor of the signal at the stationary state. However, it is not clear whether this role can be different at transient states.

In this section we evaluated the concentration of the signal, at early and late times, as a function of the production rate of ligand2 (α_{l2}) in the case in which the dynamics of the complexes-processing associated to ligand2 is slower than that associated to ligand1 (i.e., $k_{\text{eb2}} = 10^{-4} \cdot k_{\text{eb1}}$ and $k_{\text{fo2}} = 10^{-4} \cdot k_{\text{fo1}}$) and the degradation of the complexes occurs slowly for both ligands (i.e., $\gamma_{C^*} = \gamma_C = 10^{-2}$). In addition, we studied the scenarios in which the enzyme is a limiting resource or not.

We found that when the concentration of the enzyme is low, the expression of ligand2 does not have an effect on the concentration of the signal (Fig. 4.7A). We reasoned that since the enzyme is the limiting factor (and not the receptor) then the expected concentration of the signal is $s^{st} = \frac{1}{\gamma_s} E_{Tot}$ (as discussed above)[6]. However, when the concentration of the enzyme is high then ligand2 acts as an activator of the signal (Fig. 4.7A). This is in agreement with our previous results that show that when the degradation of the complexes occurs slowly, then the role of ligand2 as trans-inhibitor is less prone to arise.

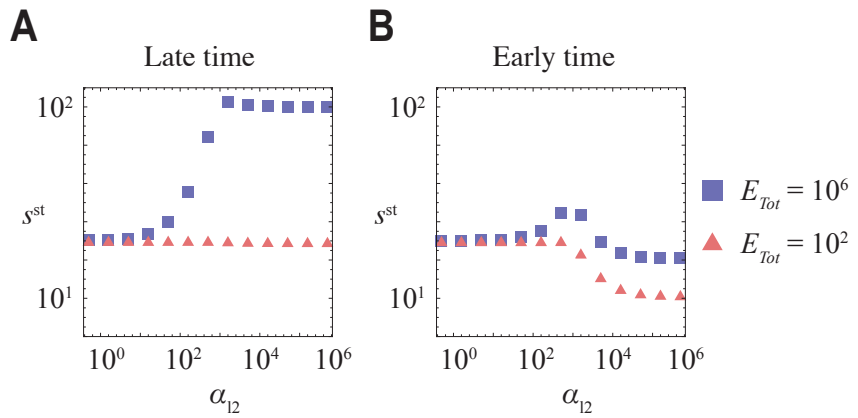

Figure 4.7 Concentration of the signal as a function of the production rate of ligand2, evaluated at early and late times. A) Late times, $t = 10^6$. B) Early times, $t = 10^6$. For A and B the complexes are assumed to degrade slowly (i.e., $\gamma_{C^*} = \gamma_C = 10^{-2}$) and the receptor is assumed to be non-saturated by ligand1 (i.e., $\alpha_r = 10^3$ and $\alpha_{l1} = 10^2$). Squares and triangles represent the case in which the enzyme levels are high ($E_{Tot} = 10^6$) and low ($E_{Tot} = 10^2$), respectively.

[6] Assuming that the production rates of the ligands are sufficiently high, as is the case in Fig. 4.7.

In contrast, we found that at early times the ligand2 can act as trans-inhibitor of the signal (Fig. 4.7B). Notice that this trans-inhibition is stronger when the concentration of the enzyme is lower (triangles in Fig. 4.7B). Finally, we explored the role of ligand2 on signal activity at different times of simulation and for different levels of enzyme concentration. To do so, we evaluated the coefficient between the concentration of the signal ($s\left(\alpha_r, \alpha_{l1}, \alpha_{l2}\right)$) when the rate of production of both ligands is the same (i.e., $s\left(10^3, 10^2, 10^2\right)$) and the concentration of the signal when ligand2 becomes over-expressed (i.e., $s\left(10^3, 10^2, \frac{1}{2}10^5\right)$):

$$f_s = \frac{s(10^3, 10^2, 10^2)}{s(\alpha_r = 10^3, 10^2, \frac{1}{2}10^5)} \tag{4.14}$$

Notice that when $f_s < 1$, ligand2 is said to trans-inhibit the formation of the signal, i.e., upon over-expression of ligand2 the concentration of the signal decreases.

We found that for intermediate to high levels of the enzyme ($E_{Tot} \geq 10^2$) a change of role can arise along the time dynamics, i.e., for early times the ligand trans-inhibits the formation of the signal, but at later times it acts as an activator (Fig. 4.8). These results show that the ligand for which the intermediary complexes are processed slowly can act as a trans-inhibitor of the signal transiently, despite both ligands are equally efficient at signaling at the stationary state (i.e., $\varepsilon_s = 1$) due to slow rates of complex degradation.

4.3.5 The less efficient signaling ligand sequesters the receptor and enhances its degradation

As previously shown, when ligands have different rates of complex-processing then a differential signaling efficiency between the ligands can arise at the stationary state. However, it is not clear why the ligand with the slower processing dynamics can act as a trans-inhibitor of the signal.

Since the concentration of the receptor is a limiting factor for signaling, we studied whether the occupancy of the receptor by each ligand results affected when ligands have a different dynamics of complex-processing, such that $\varepsilon_s < 1$. To do so, we evaluated the relative occupancy of the receptor by ligand2 with

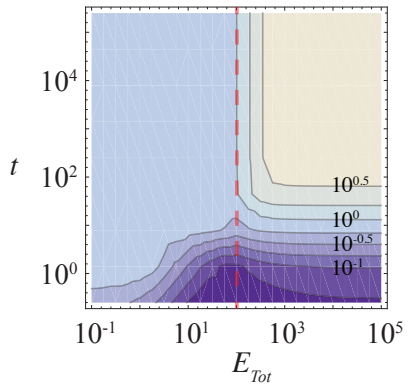

Figure 4.8 Effect of over-expression of ligand2 on the concentration of the signal for variable time of evaluation and enzyme concentration. Numerical calculation of the coefficient of the activity levels of the signal when the levels of ligand2 are high and low, f_s. Ligand2 is expected to act as a trans-inhibitor of the signal when $f_s < 1$. At the right of the red-dashed line the role of ligand2 is expected to change from trans-inhibition to trans-activation as the dynamics evolve. Initial conditions for the receptor are 100 and 0 for the two ligands.

respect to that of ligand1 (σ) as a function of the production rate of ligand2 α_{l2}.

We defined σ as

$$\sigma = \frac{\varsigma_2}{\varsigma_1} \tag{4.15}$$

where $\varsigma_i = C_i^{st} + C_i^{*st} + C_{E,i}^{*st}$ is the amount of ligand i bound to the receptor in the stationary state. We studied the case in which the receptor is saturated by ligand1 and when it is not.

We found that the stationary relative occupancy of the receptor by this ligand increases monotonically for increasing values of α_{l2} when the receptor is saturated by the ligand and when it is not (Fig. 4.9A, B). Interestingly, this behavior is independent of whether ligands have different signaling efficiency (due to a different dynamics of complex-processing) or not (Fig. 4.9A, B). This suggests that the role of ligand2 as trans-inhibitor of the signal does not involve a change in the fraction of the receptor bound to each ligand. Hence, we explored whether there are differences in the concentration of the different complexes associated

to each ligand. Specifically, we focused on the relative concentration of active complex bound to the enzyme associated to ligand2 ($C^{*st}_{E,2}$) with respect to that associated to ligand1 in the stationary state, $C^{*st}_{E,1}$, $\zeta = \frac{C^{*st}_{E,2}}{C^{*st}_{E,1}}$.

Interestingly, in this case we found that when ligands signal differently ($\varepsilon_s < 1$) the relative amount of stationary active receptor bound to each ligand type is significantly different (Fig. 4.9C, D). We found that the stationary concentration of active complex bound to the enzyme associated to ligand2 is much lower than that associated to ligand1 when $\varepsilon_s < 1$ (Fig. 4.9C, D). These type of differences still arise when the enzyme is not a limiting resource, but they becomes smaller as expected. Notice that there is a sudden increase in the value of ζ when ligand2 begins to saturate the receptor (i.e., for $\alpha_{l2} > \alpha_r$), in the scenario in which ligand1 does not saturate Notch receptor (Fig. 4.9C). This increase correlates with the decrease in the concentration of the signal in the stationary state (s^{st}), upon over-expression of ligand2 (Fig. 4.9C).

These results show that the fraction of receptor occupied by each ligand is not affected when they have different signaling efficiency. However, the concentration of each type of intermediary complexes can be different between ligand types when $\varepsilon_s < 1$. In particular, we found that the levels of active complex bound to the enzyme associated to ligand2 are lower compared to the other ligand (i.e., $\zeta \ll 1$). These results suggest that the slower ligand can act as a signal inhibitor by *sequestering* the receptor in complexes that make part of the leaking pathway. Therefore, if there is no leaking pathway (i.e., no degradation of the complexes), then these complexes end up transforming as signal such that the efficiency of the ligand would be the same independently of its complex-processing dynamics. This can explain why it is necessary to have complexes degradation in order to generate a differential signaling efficiency between the ligands.

4.3.6 Cis-interactions can modulate the value of the relative signaling efficiency between ligands

Cis-interactions between Notch and ligands in the same cell typically do not trigger signaling activation leading to cis-inhibition [del Álamo et al., 2011], i.e., the ligand binding to Notch in cis prevents signaling by ligands that could bind to that receptor in trans. This suggest that the efficiency of signaling of the

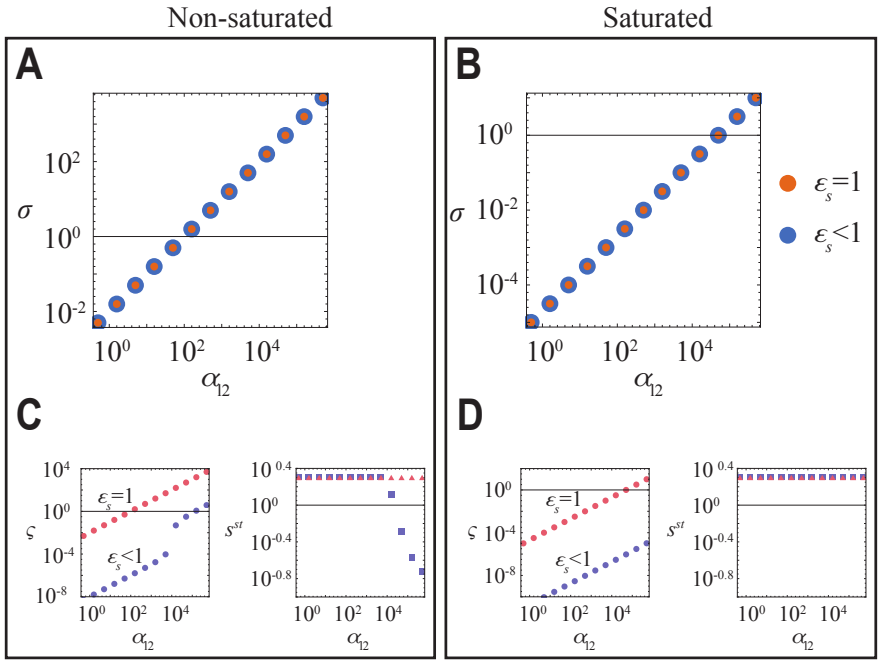

Figure 4.9 Receptor occupancy at the stationary state with and without a differential signaling efficiency between the ligands. Relative occupancy of Notch receptor between ligand2 and ligand1 (σ) as a function of the production rate of ligand2 (α_{l2}) when A) the receptor is not saturated by ligand1 (i.e., $\alpha_{l1} = 10^2$ and $\alpha_r = 10^3$) and B) when it is (i.e., $\alpha_{l1} = \frac{1}{2}10^5$ and $\alpha_r = 10^3$). Blue and orange circles represent the case in which ligand2 is less efficient than ligand1 at signaling (due to a slower dynamics of complex-processing) and the case in which both ligands are equally efficient, respectively. C, D) Relative abundance of the active complex bound to the enzyme, associated to ligand2 with respect to that associated to ligand1 (ζ) and concentration of the signal as a function of the production rate of the ligand2 (α_{l2}) [left and right, respectively]. Color code in both diagrams indicates whether ligands are equally efficient at signaling or not. In C the receptor is not saturated by ligand1 while in D it is. The concentration of the enzyme in A-D is $E_{Tot} = 10$.

ligand can be affected by cis-interactions. In this section we address whether these rates can induce a differential signaling efficiency when cis-interactions are taking place.

We evaluated the relative signaling efficiency of ligand2 with respect to ligand1 (ε_s) for variable values of k_{bt2} and k_{bc2}. We assumed that the efficiency of signaling of the ligands is the same at the complex-processing stage (i.e., $k_{\mathrm{eb1}} = k_{\mathrm{eb2}}$ and $k_{\mathrm{fo1}} = k_{\mathrm{fo2}}$), and that the enzyme is not a limiting resource (i.e., $E_{Tot} = 10^5$). We also assumed that the propensity of ligand1 to bind to Notch in trans is higher than in cis (i.e., $k_{\mathrm{bt1}} = 10^2$ and $k_{\mathrm{bc1}} = 1$).

We found that the value of ε_s decreases when the propensity of ligand2 to bind to Notch in cis is higher than in trans (Fig. 4.10). Interestingly, we have that $\varepsilon_s < 1$ when $\frac{k_{\mathrm{bc2}}}{k_{\mathrm{bt2}}} > 10^{-2}$ (notice that $\frac{k_{\mathrm{bc1}}}{k_{\mathrm{bt1}}} = 10^{-2}$).

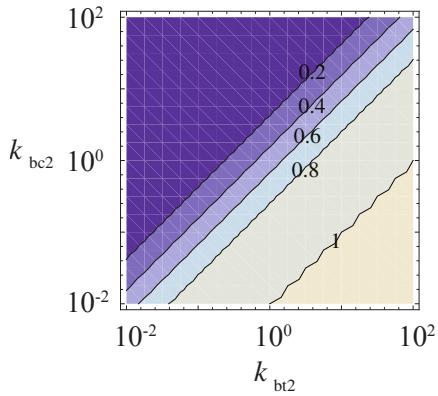

Figure 4.10 Relative signaling efficiency at the stationary state (ε_s) as a function of the binding rates of ligand2 to the receptor in cis (k_{bc2}) and trans (k_{bt2}). Parameter values for trans and cis-interactions of ligand1 are $k_{\mathrm{bt1}} = 10^2$ and $k_{\mathrm{bc1}} = 1$, respectively. We assumed high concentration of the enzyme ($E_{Tot} = 10^5$) although similar results were found assuming lower levels of concentration.

In addition, we evaluated the concentration of the signal in the signal-receiving cell at the stationary state, as a function of the production rate of ligand2 (α_{l2}), when the ligand1 is also expressed with a constant rate of production[7]. We assumed that ligand2 has a higher tendency to bind in cis than ligand1 (i.e., $k_{\mathrm{bc1}} = 1$ and $k_{\mathrm{bc2}} = 10^3$), although they both assumed to bind to Notch equally

[7]This production rate is assumed to be the same for both signal-sending and signal-receiving cells.

in trans (i.e., $k_{\mathrm{bt1}} = k_{\mathrm{bt2}} = 10^2$). As in previous sections, we studied the cases in which the enzyme is a limiting resource or not.

We found that the concentration of the signal decreases upon over-expression of ligand2 equivalently for high and low levels of the enzyme (Fig. 4.11). This behavior is more noticeable when the receptor is saturated by ligand1. In this case, the concentration of the signal decreases monotonically for increasing values of α_{l2} (Fig. 4.11B). Taken together, these results show that the binding rate of the ligands to Notch receptor in trans or in cis can modulate the signaling efficiency of each ligand, which in turn can reflect on the concentration of the signal at the stationary state.

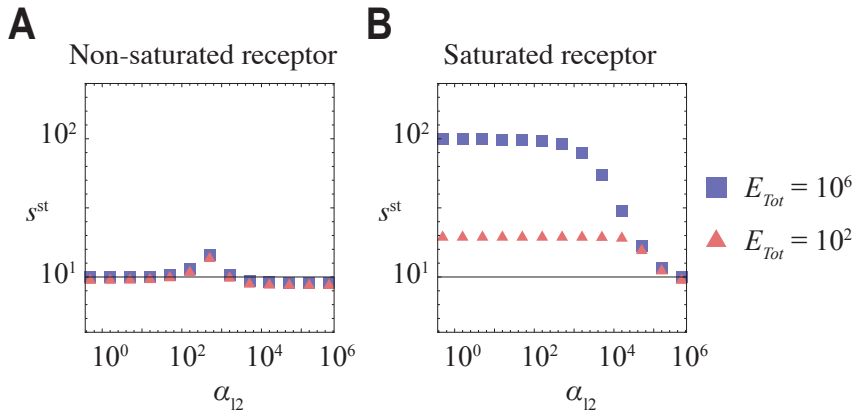

Figure 4.11 Concentration of the signal at the stationary state (s^{st}) as a function of the production rate of ligand2 in a model with cis-interactions. A) The receptor is not saturated by ligand1 (i.e., $\alpha_{l1} = 10^2$ and $\alpha_r = 10^3$). B) Ligand1 saturates the receptor (i.e., $\alpha_{l1} = \frac{1}{2}10^5$ and $\alpha_r = 10^3$). Squares and triangles represent the cases in which the levels of the enzyme are high ($E_{Tot} = 10^6$) and low ($E_{Tot} = 10^2$), respectively. Cis and trans interactions are such that ligand2 has higher propensity to bind to Notch in cis than in trans (i.e., $k_{\mathrm{bc2}} = 10^3$ and $k_{\mathrm{bt2}} = 10^2$) while ligand1 has higher propensity to bind in trans than in cis (i.e., $k_{\mathrm{bc1}} = 1$ and $k_{\mathrm{bt1}} = 10^2$).

4.4 Discussion

In this Chapter we have studied a model of Notch signal activation, which considers explicitly a series of steps associated to ligand–receptor complex formation and processing before signaling. From this analysis we grasp which steps

are necessary for the emergence of a differential signaling efficiency between ligands. When ligands signal differently, the less efficient signaling ligand can trans-inhibit the formation of the signal. As we shown in Chapter 2, this type of behavior can drive unexpected responses in arrays of hexagonal cells.

Our results show that the differential efficiency between ligands at the stationary state is expected to arise when the rates for complex processing associated to each ligand type are different. Interestingly, we found that a leaking path is necessary to change the efficiency of signaling of the ligands. When the complexes are not subject to degradation, then the ligands have the same efficiency of signaling independently of their rates of complex processing. In this regard, it is not sufficient that the complex-processing pathway associate to each ligand works differently (i.e., at different dynamic rates), but they need to involve receptor loss due to degradation when it is bound to the ligand. Our analysis suggests that it is not necessary that the degradation of the complexes, associated to each type of ligand, are different in order to have a differential signaling efficiency. The difference in efficiency comes from the time that the receptor is *exposed* to the leaking path. The slower the complex-processing path associated to one ligand type works, then the longer the receptor is going to be expose to the leaking path (i.e., the ligand type will be less efficient at signaling).

It can be argued that degradation rates of the complexes could be much slower compared to the rates of complex-processing. In this regard, the leaking path can be neglected and hence the differential efficiency between ligands is not expected to arise. However, we show that a ligand type can trans-inhibit the formation of the signal transiently over time when there is no degradation of the complexes.

It has been shown that Fringe proteins can modulate the signaling levels triggered by Notch ligands, either by changing the binding rates of the ligands to Notch [Bruckner et al., 2000, Panin et al., 1997, Taylor et al., 2014] or without affecting these binding rates [Yang et al., 2005]. Our results pinpoint at which steps Fringe could be acting and drive a distinct efficiency. We also found that modulation of the binding rates in cis and trans can drive the formation of a differential efficiency of signaling between ligands. Interestingly, it has been shown that Fringe can modulate the affinity of cis-interactions in a similar way as trans interactions are modulated [LeBon et al., 2014]. It remains to be tested

whether the effect of Fringe on cis and trans interactions can drive the differential signaling efficiency predicted by our model.

Chapter 5

Conclusions

5.1 Overview

In this Thesis we have presented a theoretical approach to analyse different aspects of inter-cellular communication mediated by Notch signaling. This is one of the few signaling systems driving coordinated responses during the development of Metazoan [Artavanis-Tsakonas et al., 1999, Gridley, 1997, Guruharsha et al., 2012, Lai, 2004, Louvi and Artavanis-Tsakonas, 2006]. Notch signaling comprises a complex network of interactions ranging from ligand–receptor interactions at the cell membrane, to regulation of genetic transcription in the nucleus [Kopan and Ilagan, 2009]. Despite this complexity, simple abstractions have been devised in order to account for the coordinated differentiation events driven by Notch signaling. These models have been important to propose mechanisms by which inter-cellular communication mediated by Notch can drive coordinated responses, e.g., salt-and-pepper pattern formation (for review see [Shaya and Sprinzak, 2011]).

We aimed to account for two relevant aspects of Notch signaling: activation by several ligands and considering additional steps of the signaling cascade (i.e., the self-activation of Atoh1). Our analysis is based on theoretical and numerical studies of simple models of lateral regulation, inspired mainly in the model of Collier et al. [1996]. We analyzed these models at transient and stationary states, using mathematical and computational tools. We mainly used

linear stability analysis of the homogeneous stationary states to determine the emergence of spatially coordinated responses, and numerical integration of the deterministic dynamics to evaluate the spatial outcome of each variable. Despite its simplicity, our modeling framework is useful to produce working hypothesis that could be tested in the laboratory.

The results obtained from our analysis are summarized below.

5.2 Summary of the results

5.2.1 Two co-expressed ligands can drive functional responses

In Chapter 2 we studied which functional responses arise when there are two co-expressed ligands triggering Notch signaling. The functional responses we focused were salt-and-pepper patterning and ligand propagation. We also considered the response of single homogeneous solutions but did not termed those states as functional. Co-expression of ligands has been reported in several developmental scenarios. Yet, few theoretical studies have focused on this topic [Boareto et al., 2015, de Back et al., 2013, Petrovic et al., 2014]. These studies, and in particular the one in which we participated [Petrovic et al., 2014], showed that the response achieved by two ligands driving signaling is not just the addition of of what is expected for each ligand expressed in isolation. To investigate the effect of co-expressing ligands we analyzed a wide variety of possible scenarios.

We addressed the cases in which ligands can either share resources to signal or not. These resources can be for instance the Notch receptor, which in turn can be a limiting resource or not. In addition, we considered that ligands can be equally efficient signaling or not. This efficiency of signaling is related to the maximal amount of signal that each ligand is able to activate when it is expressed in isolation. We also explored all the possible transcriptional regulatory scenarios, i.e., ligands equivalently or antagonistically regulated by Notch (either being activated or repressed by the signal). Finally, the functional outcome was evaluated as a function of the capability each ligand has to induce

Notch signaling, which depends on its abundance and its affinity rto bind to notch, among other factors.

Our results show that when ligands are equally efficient at signaling and they are equivalently regulated by Notch, then the functional response that arises is redundantly driven by the two ligands, i.e., it can arise when each of the ligands is expressed in isolation or when they are co-expressed. Interestingly, in this scenario any of the ligands can be detrimental to the response. If one of the ligands results over-expressed then the overall response is disrupted.

In the case in which there is a differential signaling efficiency between the ligands, then the less efficient signaling ligand can act as a partial agonist of the signal. This only occurred in the model in which ligands use shared resources to signal. In this model two different types of behavior arise. One behavior occurred when both ligands are equivalently regulated by Notch. In this scenario, the functional response of the system is opposite to that expected from the type of regulation the ligands are subjected to. For instance, two ligands activated by the signal are predicted to mediate periodic pattern formation, when the expected response is ligand propagation (which is the response expected from each ligand expressed in isolation). The other behavior occurred when ligands are antagonistically regulated by the signal. In this scenario, the functional response that arises corresponds to that expected from the type of regulation of the stronger signaling ligand, but it is driven cooperatively by the two ligands. We reasoned that these two behaviors arise because the type of lateral regulation that the weaker signaling ligand mediates when expressed in isolation is the opposite than when it is co-expressed with the stronger ligand, i.e., when the weaker signaling ligand acts as a partial agonist of the signal.

Finally, we have shown that additional responses can arise when two Notch ligands are co-expressed. In particular, antagonistically regulated ligands can drive oscillations about the periodic patterned state. Interestingly, this type of response arises as an intermediary state between ligand propagation and periodic patterning[1]. Despite some of our results are in agreement with reported experimental phenotypes, others still lack of corroboration by *in vivo* experimentation.

[1]This type of transition between these two states is observed during the development of sensory organs.

5.2.2 Lateral inhibition with self-activation of Atoh1 can drive robust hair cell differentiation

In Chapter 3 we proposed a model of lateral inhibition mediated by Dl1 in which the self-activation of the transcription factor Atoh1, which is a transcriptional activator of Dl1, was considered explicitly. We studied this model in different scenarios (one cell, two coupled cells and two-dimensional arrays of hexagonal cells) in order to address the effect of Atoh1 self-activation on the two relevant biological outputs: the differentiation induced (either as hair cell or supporting cell) and the periodic distribution of the distinct differentiation states. Despite self-activation of Atoh1 is a recurrent motif among vertebrates and *Drosophila*, it is typically neglected in modeling approaches.

A previous study [Petrovic et al., 2014] showed that Atoh1 self-activation can make robust the differentiation upon the expression of a ligand activated by Notch signaling (Jag1). Recent results have shown that hair cells differentiation can be robust to activation of Dl1 ligand which instead is inhibited by Notch signal [Chrysostomou et al., 2012]. We addressed whether Atoh1 self-activation can explain this kind of robustness as well, as in the case of Jag1. We found that in our model of lateral inhibition with self-activation of Dl1 HC differentiation can be robust to inhibition by Dl1. This property arises due to the multistability driven by the self-activation of Atoh1 which mediates a positive feedback loop additional to that mediated by the circuit of lateral inhibition with feedback. Interestingly, *in vivo* electroporations of Dl1 in the developing inner ear of the chick have shown that in some cases cells can differentiate adjacent to other cells expressing Dl1. These observations seem to be contradictory with the model of lateral inhibition, but not with our model. Particularly, our results show that *in silico* electroporations of Dl1 can lead to impaired HC differentiation, but occasionally some cells differentiate as HC despite being inhibited by adjacent cells expressing Dl1.

We argued that our model fits better with recent *in vivo* experiments in the inner ear of the chick [Chrysostomou et al., 2012] than the traditional model of lateral inhibition, in which the self-activation of Atoh1 is neglected. Other mechanisms that could account for the robustness of HC differentiation to miss-expression of Dl1 have been discarded experimentally [Chrysostomou et al., 2012, Eddison et al., 2015].

5.2.3 Emergence of the differential efficiency between two ligands on Notch signaling activation

In Chapter 4 we addressed which aspects of the Notch pathway could drive a differential signaling efficiency[2] between the ligands, when co-expressing ligands are triggering Notch. These results can be seen as complementary to those obtained in Chapter 2, where we studied the functional responses driven by a partial agonist, i.e., a less efficient signaling ligand that is expected to inhibit the formation of the signal. To do so, we studied a model of signaling activation in which we detail a minimal set of regulatory steps. Despite simple, this model is describes with more detail the activation pathway of Notch signal than in the models proposed in previous chapters. The steps considered for signal activation are 1) Ligand–receptor binding and unbinding, 2) ligand–receptor complexes processing, which includes conformational changes of the complex[3] and proteolytic cleavage, and 3) signal formation. We found that ligands can have a different signaling efficiency when the complex processing pathway associated to each ligand is different. Interestingly, our analysis revealed that complex degradation is a necessary condition for the emergence of a differential efficiency between ligands. We reasoned that this degradation constitutes a leaking path for the receptor, which remains active the time that the receptor is bound to the ligand. Therefore, the leaking path associated to the ligand that processes the complex slower will be active longer.

When there is a differential signaling efficiency between ligands then the less efficient ligand can trans-inhibit formation of the signal. Hence, the role of the ligand on signal activation (i.e., whether it is an activator or an inhibitor) can be modulated by its signaling efficiency, when it is co-expressed with a second ligand type. Interestingly, our results show that this role can change along the dynamics. Hence, at transient stages the ligand can act as a trans-inhibitor, but at the stationary state it can act as an activator.

We also have shown that cis interactions can be a source of differential efficiency between ligands. By the framework developed in this chapter, we argued that the emergence of a differential efficiency between ligands can be modulated

[2] As in Chapter 2, we say that ligands have different efficiency of signaling when the expected signaling activity levels each ligand drives when expressed in isolation is different.

[3] These changes can be induced by ligand endocytosis [Meloty-Kapella et al., 2012, Nichols et al., 2007].

Fringe proteins. Fringe can change the binding rates of the ligands to Notch (both in cis and trans), but also can change the rate of signaling associated to each ligand type without altering their binding rates [LeBon et al., 2014, Yang et al., 2005].

5.3 Future perspectives

As most theoretical works, this Thesis leaves several open questions to be addressed experimentally. Of special relevance to us is the determination *in vivo* of the functional response driven by equivalently regulated ligands, in a scenario in which one of these ligands act as a partial agonist. Our analysis predicts that the response arising would be opposite to that expected from the regulation of the ligands. However, there are no reported phenotypes yet that can fit this prediction. This does not imply that the aforementioned type of response can not arise in the lab. Our analysis suggests that when ligands are co-expressed, the overall response of the system cannot be envisaged from the traditional model of one ligand triggering Notch signaling. Hence, we expect that our results help to clarify experimental evidences that could be in conflict with this traditional view of Notch signaling.

Another appealing hypothesis that remains to be tested *in vivo* is whether Atoh1 self-activation is the underlying mechanism of the robustness exhibit by some HC upon miss-expression of Dl1. We have established a collaboration with the group of Proff. Fernando Giráldez, at Universidad Pompeu Fabra, to approach this subject. The ongoing research so far has focused in the determination of the regulatory mechanism of Atoh1 transcription in the inner ear of the chick.

This Thesis also has opened questions that can be addressed from a computational and mathematical approach. One of these questions is about the regime in which the oscillatory response arises when Notch signaling is triggered by two ligands. A first approach revealed that oscillations can be an intermediary state between lateral induction and lateral inhibition. Transitions between lateral induction and lateral inhibition occur in developing sensory organs. Because of this we argue that a complete characterization of this oscillatory regime can be important to understand sensory organs specification and differentiation. Given that this oscillatory state arises from an unstability of the patterned state, the

theoretical framework used in this thesis does not provide a clear answer to where the oscillatory regime arises.

Appendix A

Linear stability analysis

In this Appendix we briefly describe the derivation of the conditions for linear stability of the homogeneous state used in Chapter 2, for the case of one, two and three ligands triggering Notch signaling. In that Chapter the models describe signaling only in two steps: the signal activity and the ligand activity. For this type of models the derivations for the one ligand and the two ligands scenarios can be found in [Collier et al., 1996] and [Formosa Jordan, 2013, Petrovic et al., 2014] respectively and are here included for the sake of completeness. We generalized the analysis for the case of three ligands.

A.1 Linear stability analysis: One ligand

We assumed a bidimensional array of $L \times M$ hexagonal cells, in which the state of the cells is described by two variables, the levels of the ligand (l) and the levels of the signal (s) activities. We also assumed periodic boundary conditions[1].

In this system, the dynamic equations for a cell reads

$$\begin{aligned} \frac{\mathrm{d}s_{j,k}}{\mathrm{d}t} &= f_s(\langle l_{j,k} \rangle) - s_{j,k} \\ \frac{\mathrm{d}l_{j,k}}{\mathrm{d}t} &= \left(f_l(s_{j,k}) - l_{j,k}\right) v \end{aligned} \tag{A.1}$$

[1] This is important for the *ansatz* on the type of solutions, as will be described below.

where the subindexes describe the position of the cell within the bidimensional array. f_s and f_l are regulatory functions, described explicitly in Chapter 2 (notice that in Chapter 2 only a subindex is used to label the cell). For the sake of generality, we describe the analysis without specification on the particular type of functions used. In addition, we define

$$\langle l_{j,k} \rangle \equiv \frac{1}{\omega} \sum_{n,m \in NN} l_{n,m} \tag{A.2}$$

as the average level of the ligand in the ω Nearest Neighboring cells (NN) of cell $l_{j,k}$. Since we assumed that the array is composed by perfect hexagonal cells, then we have that $\omega = 6$.

We studied the stability of a stationary homogeneous state (s^{st}, l^{st}), for which the following conditions are met:

$$\begin{aligned} & l_{j,k} = l^{st},\ s_{j,k} = s^{st}\ \forall_{j,k} \\ & \frac{\mathrm{d}s^{st}}{\mathrm{d}t} = f_s(l^{st}) - s^{st} = 0 \\ & \frac{\mathrm{d}l^{st}}{\mathrm{d}t} = \left(f_l(s^{st}) - l^{st}\right) v = 0\,. \end{aligned} \tag{A.3}$$

We assumed small perturbations ($\sigma_{j,k}$, $\zeta_{j,k}$) about the homogeneous steady state

$$\begin{aligned} s_{j,k}(t) &= s^{st} + \sigma_{j,k}(t) \\ l_{j,k}(t) &= l^{st} + \zeta_{j,k}(t) \end{aligned} \tag{A.4}$$

such that $\sigma_{j,k}(t=0) \ll s^{st}$ and $\zeta_{j,k}(t=0) \ll l^{st}$. By replacing (A.4) in (A.1), we can make a linear approximation of the dynamics of the perturbations, which reads

$$\begin{aligned} \frac{\mathrm{d}\sigma_{j,k}}{\mathrm{d}t} &\approx \left.\frac{\partial F_s}{\partial \langle l_{j,k} \rangle}\right|_{s^{st},l^{st}} \langle \zeta_{j,k} \rangle + \left.\frac{\partial F_s}{\partial s_{j,k}}\right|_{s^{st},l^{st}} \sigma_{j,k} \\ \frac{\mathrm{d}\zeta_{j,k}}{\mathrm{d}t} &\approx \left.\frac{\partial F_l}{\partial s_{j,k}}\right|_{s^{st},l^{st}} \sigma_{j,k} + \left.\frac{\partial F_l}{\partial l_{j,k}}\right|_{s^{st},l^{st}} \zeta_{j,k} \end{aligned} \tag{A.5}$$

where we defined

$$\begin{aligned} F_s\left(\langle l_{j,k}\rangle, s_{j,k}\right) &\equiv f_s(\langle l_{j,k}\rangle) - s_{j,k} \\ F_l\left(l_{j,k}, s_{j,k}\right) &\equiv \left(f_l(s_{j,k}) - l_{j,k}\right) v\,, \end{aligned} \tag{A.6}$$

corresponding to the right side of Eqn. A.1, and where the condition of stationarity of the homogeneous state (Eqn. A.3) is taken into account. In addition, we defined

$$\begin{aligned} R_{s,\langle l\rangle} &= \left.\frac{\partial F_s}{\partial \langle l_{j,k}\rangle}\right|_{s^{st},l^{st}} \\ R_{l,s} &= \frac{1}{v}\left.\frac{\partial F_l}{\partial s_{j,k}}\right|_{s^{st},l^{st}} \end{aligned} \tag{A.7}$$

Hence, dynamic equations for the perturbations (A.5) can be written as

$$\begin{aligned} \frac{\mathrm{d}\sigma_{j,k}}{\mathrm{d}t} &= \frac{1}{\omega} R_{s,\langle l\rangle} \sum_{n,m\in NN} \zeta_{n,m} - \sigma_{j,k} \\ \frac{\mathrm{d}\zeta_{j,k}}{\mathrm{d}t} &= \left(R_{l,s}\sigma_{j,k} - \zeta_{j,k}\right) v\,. \end{aligned} \tag{A.8}$$

The solutions of this linear system (A.8) are of the type

$$\begin{aligned} \sigma_{j,k}(t) &= \sum_{\overline{p}} \sum_{\overline{q}} \beta^{s}_{\overline{p},\overline{q}} e^{2\pi i(\overline{p}j+\overline{q}k)} e^{\alpha_{\overline{p},\overline{q}}t} \\ \zeta_{j,k}(t) &= \sum_{\overline{p}} \sum_{\overline{q}} \beta^{l}_{\overline{p},\overline{q}} e^{2\pi i(\overline{p}j+\overline{q}k)} e^{\alpha_{\overline{p},\overline{q}}t} \end{aligned} \tag{A.9}$$

where $\overline{p} = \frac{p}{L}$ and $\overline{q} = \frac{q}{M}$, for $p = 1, 2, ...L$ and $q = 1, 2, ...M$, are the coupled discrete modes of the perturbations, i.e., the wavelength of the perturbations is $\frac{2\pi}{\overline{p}}$, $\frac{2\pi}{\overline{q}}$ in the bidimensional array. $\beta^{s}_{\overline{p},\overline{q}}$ and $\beta^{l}_{\overline{p},\overline{q}}$ are constants for the coupled modes $\overline{p}$, $\overline{q}$. In turn, $\alpha_{\overline{p},\overline{q}}$ is the growing rate of the corresponding mode $\overline{p}, \overline{q}$. This kind of solution for (A.8) can be assumed since we are imposing periodic boundary conditions (see, for instance, [Cross and Greenside, 2009]).

By replacing (A.9) in (A.8) we obtain that

$$\begin{aligned}\alpha_{\overline{p},\overline{q}}\beta^{s}_{\overline{p},\overline{q}} &= R_{s,\langle l\rangle}\Omega_{\overline{p},\overline{q}}\beta^{l}_{\overline{p},\overline{q}} - \beta^{s}_{\overline{p},\overline{q}} \\ \alpha_{\overline{p},\overline{q}}\beta^{l}_{\overline{p},\overline{q}} &= vR_{l,s}\beta^{s}_{\overline{p},\overline{q}} - v\beta^{l}_{\overline{p},\overline{q}}\end{aligned} \tag{A.10}$$

where

$$\begin{aligned}\Omega_{\overline{p},\overline{q}} &\equiv \frac{1}{6}\left(e^{2\pi i\overline{p}} + e^{-2\pi i\overline{p}} + e^{2\pi i\overline{q}} + e^{-2\pi i\overline{q}} + e^{2\pi i(\overline{p}-\overline{q})} + e^{-2\pi i(\overline{q}-\overline{p})}\right) = \\ &= \frac{1}{3}\left(\cos 2\pi\overline{p} + \cos 2\pi\overline{q} + \cos 2\pi(\overline{p}+\overline{q})\right)\end{aligned} \tag{A.11}$$

arises from the coupling between cells (i.e., from $\langle\zeta_{j,k}\rangle$)[2]. Writing $\vec{\beta}_{\overline{p},\overline{q}} = \begin{pmatrix}\beta^{s}_{\overline{p},\overline{q}} \\ \beta^{l}_{\overline{p},\overline{q}}\end{pmatrix}$ we have that

$$\alpha_{\overline{p},\overline{q}}\vec{\beta}_{\overline{p},\overline{q}} = \Lambda\vec{\beta}_{\overline{p},\overline{q}} \tag{A.12}$$

where

$$\Lambda = \begin{pmatrix}-1 & R_{s,\langle l\rangle}\Omega_{\overline{p},\overline{q}} \\ vR_{l,s} & -v\end{pmatrix} \tag{A.13}$$

In this case of two state variables per cell, the dimension of matrix Λ is two. For larger systems (i.e., having more state variables per cell) the dimension of this matrix becomes larger, as will be described below. However, the analysis shown up to here is equivalent.

Linear matrix Λ has two eigenvalues $\alpha^{(1)}_{\overline{p},\overline{q}}$ and $\alpha^{(2)}_{\overline{p},\overline{q}}$, which define the growing rate of the perturbations with periodicity modes $\overline{p}$ and $\overline{q}$. To obtain these eigenvalues, we solve the characteristic equation given by

$$\det(\Lambda - \alpha_{\overline{p},\overline{q}}I) = 0 \tag{A.14}$$

where I is the identity matrix of dimension two. This equation is a second order polynomial and therefore the solutions are

[2]Here we just replace (A.9) in $\sum_{n,m\in NN}\zeta_{n,m}$.

$$\begin{aligned}\alpha_{\overline{p},\overline{q}}^{(1)} &= -\frac{1}{2}(v+1) + \frac{1}{2}\sqrt{(v+1)^2 - 4v\left(1 - R_{s,\langle l\rangle}R_{l,s}\Omega_{\overline{p},\overline{q}}\right)} \\ \alpha_{\overline{p},\overline{q}}^{(2)} &= -\frac{1}{2}(v+1) - \frac{1}{2}\sqrt{(v+1)^2 - 4v\left(1 - R_{s,\langle l\rangle}R_{l,s}\Omega_{\overline{p},\overline{q}}\right)}\end{aligned} \tag{A.15}$$

The homogeneous stationary state (s^{st}, l^{st}) is linearly stable to perturbations with a given periodic mode $\overline{p},\overline{q}$ if $Re(\alpha_{\overline{p},\overline{q}}) < 0$, i.e., the growing rate of this type of perturbation is negative and therefore it decreases exponentially in time. There is any value of $\overline{p},\overline{q}$ for which $Re(\alpha_{\overline{p},\overline{q}}) > 0$, then the homogeneous state is linearly unstable.

Notice that $Re\left(\alpha_{\overline{p},\overline{q}}^{(2)}\right) \leq 0$ independently of the modes $\overline{p},\overline{q}$. In contrast, $Re(\alpha_{\overline{p},\overline{q}}^{(1)})$ can be either negative or positive depending on the sign of $1-R_{s,\langle l\rangle}R_{l,s}\Omega_{\overline{p},\overline{q}}$ (> 0 or < 0, respectively), which depends on the modes $\overline{p},\overline{q}$ through the term $\Omega_{\overline{p},\overline{q}}$ and of the sign of $R_{s,\langle l\rangle}R_{l,s}$[3]. Since $R_{s,\langle l\rangle}R_{l,s}\Omega_{\overline{p},\overline{q}}$ is a linear function of $\Omega_{\overline{p},\overline{q}}$, then $Re\left(\alpha_{\overline{p},\overline{q}}^{(1)}\right)$ is maximal at either end of the range of $\Omega_{\overline{p},\overline{q}}$, i.e., for $\Omega_{\overline{p},\overline{q}} = -0.5$ or $\Omega_{\overline{p},\overline{q}} = 1$ (see Eqn. A.11). In particular, for $R_{s,\langle l\rangle}R_{l,s} < 0$, maximal $Re\left(\alpha_{\overline{p},\overline{q}}^{(1)}\right)$ arises for $\Omega_{\overline{p},\overline{q}} = -0.5$, whereas if $R_{s,\langle l\rangle}R_{l,s} > 0$, maximal $Re\left(\alpha_{\overline{p},\overline{q}}^{(1)}\right)$ occurs for $\Omega_{\overline{p},\overline{q}} = 1$.

$\Omega_{\overline{p},\overline{q}} = -0.5$ corresponds to the pair of coupled modes $\overline{p} = \frac{1}{3}$, $\overline{q} = \frac{2}{3}$ and $\overline{p} = \frac{2}{3}$, $\overline{q} = \frac{1}{3}$, while $\Omega_{\overline{p}\overline{q}} = 1$ corresponds to the mode $\overline{p} = \overline{q} = 1$. As indicated above, these are the modes that drive the maximal value of $Re(\alpha_{\overline{p},\overline{q}}^{(2)})$, and hereafter we name them the fastest growing modes in the linear regime. But, what do these fastest growing modes say about the stability homogeneous steady state (s^{st}, l^{st})? When the homogeneous steady state becomes unstable to small perturbations, the system is expected to evolve to a state with the periodicity related to these modes.

When the fastest growing modes are $\overline{p} = \frac{1}{3}$, $\overline{q} = \frac{2}{3}$ and $\overline{p} = \frac{2}{3}$, $\overline{q} = \frac{1}{3}$ and the stationary state is linearly unstable, the system is expected to evolve to a periodic patterned state. Let us consider first the coupled modes $\overline{p} = \frac{1}{3}$, $\overline{q} = \frac{2}{3}$ along the first six cells in the horizontal axis of the cell array (i.e., $j = 1$ and $k = 1, 2, 3...6$). The value of the perturbation in these cells has a common factor, which is $\beta_{\overline{p},\overline{q}}^{s}e^{\alpha_{\overline{p},\overline{q}}t}$ and what is different is the value of the spatial exponential, which reads

[3]In Chapter 2, we termed lateral inhibition the situation in which $R_{s,\langle l\rangle}R_{l,s} < 0$ and lateral induction the situation in which $R_{s,\langle l\rangle}R_{l,s} > 0$.

$$
\begin{aligned}
e^{2\pi i\left(1\frac{1}{3}+1\frac{2}{3}\right)} &= e^{2\pi i(1)} \\
e^{2\pi i\left(1\frac{1}{3}+2\frac{2}{3}\right)} &= e^{2\pi i\left(\frac{5}{3}\right)} \\
e^{2\pi i\left(1\frac{1}{3}+3\frac{2}{3}\right)} &= e^{2\pi i\left(\frac{7}{3}\right)} \\
e^{2\pi i\left(1\frac{1}{3}+4\frac{2}{3}\right)} &= e^{2\pi i(3)} \\
e^{2\pi i\left(1\frac{1}{3}+5\frac{2}{3}\right)} &= e^{2\pi i\left(\frac{11}{3}\right)} \\
e^{2\pi i\left(1\frac{1}{3}+6\frac{2}{3}\right)} &= e^{2\pi i\left(\frac{13}{3}\right)} \\
e^{2\pi i\left(1\frac{1}{3}+7\frac{2}{3}\right)} &= e^{2\pi i(5)}
\end{aligned}
\tag{A.16}
$$

Hence, the value of the perturbation every three cells is the same, i.e., $\sigma_{1,1} = \sigma_{1,4} = \sigma_{1,7} = ...$[4]. Following an analogous procedure, it can be easily shown that the other pair of coupled modes (i.e., $\overline{p} = \frac{2}{3}$, $\overline{q} = \frac{1}{3}$) which grows equally fast, guaranties that the value of the perturbation in the two in-between cells is the same, i.e., $\sigma_{1,2} = \sigma_{1,3} = \sigma_{1,5} = \sigma_{1,6} = ...$ Taken together, this analysis indicates that the fastest growing modes $\overline{p} = \frac{1}{3}$, $\overline{q} = \frac{2}{3}$ and $\overline{p} = \frac{2}{3}$, $\overline{q} = \frac{1}{3}$ correspond to a periodic pattern composed of two different cell types, arranged spatially in a specific manner (that characteristic of the salt-and-pepper pattern of lateral inhibition).

In contrast, when the fastest growing mode is $\overline{p} = \overline{q} = 1$, then the value of the perturbation is independent of the position of the cell within the array, i.e., the value of $\sigma_{j,k}$ and $\zeta_{j,k}$ does not change with j, k. In this case, the fastest growing mode $\overline{p} = \overline{q} = 1$ corresponds to a homogeneous state.

Back to the stability analysis, the homogeneous stationary state is expected to be stable to perturbations with wave numbers $\overline{p}$, $\overline{q}$ when $1 - R_{s,\langle l\rangle} R_{l,s} \Omega_{\overline{p},\overline{q}} > 0$. Hence, the homogeneous stationary state is expected to be stable to any kind of perturbation (i.e., setting $\Omega_{\overline{p},\overline{q}} = -0.5$ and $\Omega_{\overline{p},\overline{q}} = 1$) in the linear regime when

$$
-2 < R_{s,\langle l\rangle} R_{l,s} < 1 \tag{A.17}
$$

When $R_{s,\langle l\rangle} R_{l,s} \leq -2$ then the homogeneous state becomes unstable and the fastest growing modes are $\overline{p} = \frac{1}{3}$, $\overline{q} = \frac{2}{3}$ and $\overline{p} = \frac{2}{3}$, $\overline{q} = \frac{1}{3}$. Therefore, in this situation periodic patterned states are expected to arise. In Chapter 2 these

[4]The same holds for the value of the perturbation on the levels of the ligand

regions are enclosed by the dashed-blue lines. Accordingly, when there are two homogeneous steady states for which Eqn. A.17 is met then we expect a *ligand propagation* process between these two states upon a non-linear perturbation[5]. In Chapter 2 these regions are enclosed by the solid-black lines.

A.2 Stability of the homogeneous state in the two and three ligands-scenario

The previous analysis can be extended to the case in which two ligands trigger Notch signaling. In this case, the dynamics of the system reads

$$\begin{aligned}
\frac{\mathrm{d}s_{j,k}}{\mathrm{d}t} &= \underbrace{f_s(\langle l1_{j,k}\rangle, \langle l2_{j,k}\rangle) - s_{j,k}}_{F_s} \\
\frac{\mathrm{d}l1_{j,k}}{\mathrm{d}t} &= \underbrace{\left(f_{l1}(s_{j,k}) - l1_{j,k}\right) v}_{F_{l1}} \\
\frac{\mathrm{d}l2_{j,k}}{\mathrm{d}t} &= \underbrace{\left(f_{l2}(s_{j,k}) - l2_{j,k}\right) v}_{F_{l2}}
\end{aligned} \tag{A.18}$$

where we have assumed that the value of v is the same for ligand1 and ligand2.

Analogously to the analysis presented in the previous section, we can write $\vec{\beta}_{\overline{p},\overline{q}} = \begin{pmatrix} \beta^{s}_{\overline{p},\overline{q}} \\ \beta^{l1}_{\overline{p},\overline{q}} \\ \beta^{l2}_{\overline{p},\overline{q}} \end{pmatrix}$ and hence

$$\alpha_{\overline{p},\overline{q}}\vec{\beta}_{\overline{p},\overline{q}} = \Lambda\vec{\beta}_{\overline{p},\overline{q}} \tag{A.19}$$

where

$$\Lambda = \begin{pmatrix} -1 & R_{s,\langle l1\rangle}\Omega_{\overline{p},\overline{q}} & R_{s,\langle l2\rangle}\Omega_{\overline{p},\overline{q}} \\ vR_{l_1,s} & -v & 0 \\ vR_{l_2,s} & 0 & -v \end{pmatrix} \tag{A.20}$$

[5] We confirmed this association between bistability and ligand propagation by numerical simulations, as described in Appendix B.

The definition of $R_{s,\langle li\rangle}$ and $R_{li,s}$ is analogous to that described previously for the one ligand-scenario, i.e.,

$$\begin{aligned} R_{s,\langle l_1\rangle} &= \left.\frac{\partial F_s}{\partial\langle l1_{j,k}\rangle}\right|_{s^{st},l_1^{st},l_2^{st}} \\ R_{s,\langle l2\rangle} &= \left.\frac{\partial F_s}{\partial\langle l2_{j,k}\rangle}\right|_{s^{st},l_1^{st},l_2^{st}} \\ R_{l_1,s} &= \left.\frac{1}{v}\,\frac{\partial F_{l1}}{\partial s_{j,k}}\right|_{s^{st},l_1^{st},l_2^{st}} \\ R_{l_2,s} &= \left.\frac{1}{v}\,\frac{\partial F_{l2}}{\partial s_{j,k}}\right|_{s^{st},l_1^{st},l_2^{st}} \end{aligned} \tag{A.21}$$

In this case of two ligands, the characteristic equation $\alpha_{\overline{p},\overline{q}}\vec{\beta}_{\overline{p},\overline{q}} = \Lambda\vec{\beta}_{\overline{p},\overline{q}}$ has three solutions

$$\begin{aligned} \alpha^{(1)}_{\overline{p},\overline{q}} &= -\frac{1}{2}(v+1) + \frac{1}{2}\sqrt{(v+1)^2 - 4v\left(1 - \left(R_{s,\langle l_1\rangle}R_{l_1,s} + R_{s,\langle l_2\rangle}R_{l_2,s}\right)\Omega_{\overline{p},\overline{q}}\right)} \\ \alpha^{(2)}_{\overline{p},\overline{q}} &= -\frac{1}{2}(v+1) - \frac{1}{2}\sqrt{(v+1)^2 - 4v\left(1 - \left(R_{s,\langle l_1\rangle}R_{l_1,s} + R_{s,\langle l_2\rangle}R_{l_2,s}\right)\Omega_{\overline{p},\overline{q}}\right)} \\ \alpha^{(3)}_{\overline{p},\overline{q}} &= -v \end{aligned} \tag{A.22}$$

While the real part of the last two eigenvalues is always negative, $Re\left(\alpha^{(1)}_{\overline{p},\overline{q}}\right)$ is expected to be negative when $1-\left(R_{s,\langle l_1\rangle}R_{l_1,s} + R_{s,\langle l_2\rangle}R_{l_2,s}\right)\Omega_{\overline{p},\overline{q}} > 0$. As in the one ligand-scenario, $\alpha^{(1)}_{\overline{p},\overline{q}}$ becomes first positive at the limits of the range of $\Omega_{\overline{p},\overline{q}}$, which is defined equally by Eqn. A.11. However, in this case there are two terms $R_{s,\langle l_1\rangle}R_{l_1,s}$ and $R_{s,\langle l_2\rangle}R_{l_2,s}$ defining the sign of $\left(R_{s,\langle l_1\rangle}R_{l_1,s} + R_{s,\langle l_2\rangle}R_{l_2,s}\right)\Omega_{\overline{p},\overline{q}}$. Notice that these terms despite being associated to each ligand are not independent of the other ligand. For instance, $R_{l_1,s}$ is associated to ligand1, but it depends on the value of ligand1 and ligand2 in the stationary state (see Eqns. A.21)[6]. Hence, the homogeneous stationary state is expected to be stable to any kind of small perturbations in the linear regime when

[6]The interpretation of each of these terms is discussed in Chapter 2.

$$-2 < R_{s,\langle l_1\rangle} R_{l_1,s} + R_{s,\langle l_2\rangle} R_{l_2,s} < 1 \tag{A.23}$$

is met. When $R_{s,\langle l_1\rangle} R_{l_1,s} + R_{s,\langle l_2\rangle} R_{l_2,s} < 0$, then the fastest growing modes are $\overline{p} = \frac{1}{3}$, $\overline{q} = \frac{2}{3}$ and $\overline{p} = \frac{2}{3}$, $\overline{q} = \frac{1}{3}$. Accordingly, when $R_{s,\langle l_1\rangle} R_{l_1,s} + R_{s,\langle l_2\rangle} R_{l_2,s} > 0$, then the fastest growing mode is $\overline{p} = \overline{q} = 1$. The implications of the unstabilization of the homogeneous state by perturbations characterized by these modes follows as described in the previous section.

Finally, in the case of three ligands activating Notch signaling the Λ matrix reads

$$\Lambda = \begin{pmatrix} -1 & R_{s,\langle l_1\rangle}\Omega_{\overline{pq}} & R_{s,\langle l_2\rangle}\Omega_{\overline{pq}} & R_{s,\langle l_3\rangle}\Omega_{\overline{pq}} \\ vR_{l_1,s} & -v & 0 & 0 \\ vR_{l_2,s} & 0 & -v & 0 \\ vR_{l_3,s} & 0 & 0 & -v \end{pmatrix} \tag{A.24}$$

such that there are four eigenvalues, but only three are different

$$\begin{aligned} \alpha^{(1)}_{\overline{p},\overline{q}} &= -\frac{1}{2}(v+1) + \\ &\quad + \frac{1}{2}\sqrt{(v+1)^2 - 4v\left(1 - \left(R_{s,\langle l_1\rangle} R_{l_1,s} + R_{s,\langle l_2\rangle} R_{l_2,s} + R_{s,\langle l_3\rangle} R_{l_3,s}\right)\Omega_{\overline{p},\overline{q}}\right)} \\ \alpha^{(2)}_{\overline{p},\overline{q}} &= -\frac{1}{2}(v+1) - \\ &\quad - \frac{1}{2}\sqrt{(v+1)^2 - 4v\left(1 - \left(R_{s,\langle l_1\rangle} R_{l_1,s} + R_{s,\langle l_2\rangle} R_{l_2,s} + R_{s,\langle l_3\rangle} R_{l_3,s}\right)\Omega_{\overline{p},\overline{q}}\right)} \\ \alpha^{(3)}_{\overline{p},\overline{q}} &= \alpha^{(4)}_{\overline{p},\overline{q}} = -v \end{aligned} \tag{A.25}$$

Again, the homogeneous steady state is stable if

$$1 - \left(R_{s,\langle l_1\rangle} R_{l_1,s} + R_{s,\langle l_2\rangle} R_{l_2,s} + R_{s,\langle l_3\rangle} R_{l_3,s}\right)\Omega_{\overline{p},\overline{q}} > 0 \tag{A.26}$$

Hence, we can summarize the condition of linear stability of the homogeneous steady state as

$$\chi_r \Omega_{\overline{p},\overline{q}} < 1 \tag{A.27}$$

such that the homogenous stationary state is stable to any kind of small perturbation in the linear regime when

$$-2 < \chi_r \Omega_{\overline{p},\overline{q}} < 1 \tag{A.28}$$

where $\chi_r = \sum_{i \in r} R_{s,\langle l_i \rangle} R_{l_i,s}$, for $r = (1, 2, 3)$ different ligand types activating Notch signaling. When condition A.27 is met, the homogeneous steady state is expected to be stable to perturbations with modes $\overline{p}$, $\overline{q}$.

Appendix B

Details on numerical analysis and simulations

In this appendix we briefly describe details of the numerical method implemented for addressing the regimes of spontaneous patterning and ligand propagation, and the details of the numerical simulations, corresponding to the results shown in Chapter 2.

We also describe the details of the numerical simulations done in Chapter 3 to calculate the basins of attraction of the steady states.

B.1 Phase diagrams

The phase diagrams shown in Chapter 2 were calculated in the homogeneous steady state (for definition of this homogeneous steady state see Eqns. A.3). To compute those states we used a custom-made program for root-finding, which implements the bisection method, adapted from a previous version done by Pau Formosa-Jordan. The program makes a logarithmic span within the interval in which the root is expected, in order to improve the resolution of the method.

In the following we briefly describe the regions composing the phase diagrams.

1. Regions where spontaneous patterning is expected to arise, i.e., $\chi_r \leq -2$. These regions are encompassed by dashed-blue lines in the diagrams[1].

2. Regions in which the system has two stable steady states, i.e., there are two homogeneous stationary states for which $-2 < \chi_r < 1$ is met. These regions are encompassed by the solid-black line.

3. Regions in which lateral regulation mediated by ligand1 is sufficiently strong to drive patterning, i.e., $R_{s,\langle l_1 \rangle} R_{l_1,s} < -2$. These regions are depicted in red. The analogous regions for ligand2 (i.e., the regions in which $R_{s,\langle l_2 \rangle} R_{l_2,s} < -2$) are depicted in gray[2]. In the case of three ligands, the region where the third ligand (Jag1 in that context) is sufficiently strong to drive patterning (i.e., $R_{s,\langle l_3 \rangle} R_{l_3,s} < -2$) is shown in light blue.

In addition, we calculated the critical line which defines the role of ligand2 on signal activity[3],

$$\varepsilon - \frac{r_1^{(c)} l_1^{st}}{r_1^{(c)} l_1^{st} + 1} = 0 \tag{B.1}$$

where l_1^{st} is the activity level of ligand1 at the homogeneous steady state and $r_1^{(c)}$ is the critical value of r_1 for which the previous condition is met. In this regard, for $r_1 < r_1^{(c)}$ and $r_1 > r_1^{(c)}$ ligand2 is said to activate and repress the signal in the homogeneous steady state, respectively. This is represented by a dashed-yellow line.

B.2 Numerical simulations

We performed numerical integration of the dynamics in order to account for the dynamical behavior of ligand propagation and periodic patterning and also to account for the steady state levels of the ligands and the signal activity.

[1] For a definition of χ_r see Appendix A.

[2] Note that despite ligand1 or ligand2 can be sufficiently strong to drive patterning, this functional response could not arise. This is because even if one of the ligands is promoting patterning individually (i.e., $R_{s,\langle l_1 \rangle} R_{l_1,s} < -2$ or $R_{s,\langle l_2 \rangle} R_{l_2,s} < -2$), the overall lateral regulation could not be sufficiently strong to mediate the response, i.e., $\chi_2 > -2$. For instance, this is the case for the results shown in Fig. 2.9B.

[3] This condidion can be easily derive from setting $R_{s,\langle l_2 \rangle} = 0$ in Eqn. A.21

Numerical integration of the dynamics was done using NDSolve function of Mathematica 8.0 on a perfect hexagonal grid of 12×12 cells, imposing periodic boundary conditions. Time step of integration was variable between 0.001 and 0.05 chosen by default by the Mathematica function. Integration was done up to the final non-dimensional time 500 a.u.. Initial conditions for each dynamical variable x in each i cell was $x_i(t = 0) = x^{st}(1 + 0.2 \cdot (0.5 - \eta))$, where x^{st} is the stationary homogeneous solution, as described in Appendix A, and η is a random uniform number between 0 and 1 generated using the Mathematica function RandomReal.

The activity levels of the ligands and the signal in the snapshots are represented in linear gray scale, where white corresponds to low levels and black to high levels. The same scale was used for ligands and the signal activities,

This type of simulations were also used in the study of cell arrays in Chapter 3. In this case, simulations were done on arrays of 6×6 and 18×18 cells. Cell coloring for the simulation snapshots was made based on the Atoh1 activity levels in the cells. We used a continuous linear scale of different tones of purple to match the *in vivo* experiments done by Chrysostomou et al. [2012]. Hence, cells with high Atoh1 activity levels are shown in purple (which we assumed to differentiate as HC) while cells with low levels of Atoh1 are shown in light purple-white (which are assumed to differentiate as SC).

The simulations for the results shown in Chapter 4 were done using Mathematica NDSolve function. Further details as initial conditions and time of simulation are described in the Chapter.

B.3 Basins of attraction

In Chapter 3 we used numerical simulations to calculate stable steady states and their basins of attraction in a system of two coupled cells and in a reduced model which impose a specific cell coupling simulating an array of hexagonal cells, as described in the Chapter main text. Numerical integration of the dynamic equations was done using custom-made programs following a forth order Runge-Kutta method. Final time of simulation was 250 a.u. and the time step size of the method was 0.01. We used this custom programs due to faster performance was necessary. Briefly, we assumed as initial conditions for Atoh1

in cell 1 and cell 2 (or cell type I and cell type II) the values in the grid a_1 and a_2. The initial levels of Delta1 and NICD were the same for both cells (or cell types) as described in the main text of the Chapter. Numerical integration of the dynamics was evaluated for each point of the grid (a_1 and a_2), and those initial conditions evolving to the same stationary state were represented with the same color. We defined these regions to be the basins of attraction of each steady state.

B.4 Numerical corroboration of the phase diagrams

We used numerical simulations to corroborate the phase diagrams obtained from theoretical analysis in Chapter 2 . The exact points of the diagrams at which the corroborations were done are summarized in the following tables. Simulations were done at each point, where the rest of the parameter are specified in the main text of the chapter. By visual inspection we determined the observed behavior, which can be either, periodic patterning (Pat), ligand propagation (LP) or an absence of functional response (i.e., single homogeneous state, H). These corroborations were done using Mathematica NDSolve function, as described above (assuming a final time of simulations $t = 500$ a.u..). To address periodic patterning, we induced small random perturbations about the homogeneous stationary state, as described above. To address ligand propagation, we induced a non-linear perturbation in the homogeneous stationary state. This perturbations consisted in increasing the levels of the ligand in a small clusters of cells in the array. The size of this cluster in most cases was four cells, but in other cases (not specified) larger sizes of the cluster was needed in order to see the ligand propagation.

Table B.1 Numerical corroboration of Fig. 2.3C

r_1	ε_r	output
0.1	10^{-4}	H
1	10^{-4}	Pat
10	10^{-4}	Pat
500	10^{-4}	Pat
10^3	10^{-4}	H
$5 \cdot 10^3$	10^{-4}	H
0.1	10^{-1}	H
1	10^{-1}	Pat
10	10^{-1}	Pat
500	10^{-1}	Pat
10^3	10^{-1}	Pat
$5 \cdot 10^3$	10^{-1}	H
0.1	1	H
1	1	Pat
10	1	Pat
500	1	Pat
10^3	1	Pat
$5 \cdot 10^3$	1	Pat

Table B.2 Numerical corroboration of Fig. 2.12A

r_1	ε_r	output
0.1	10^{-4}	H
0.5	10^{-4}	Pat
10	10^{-4}	Pat
500	10^{-4}	Pat
10^3	10^{-4}	H
10	100	Pat
10	800	Pat/LP
10	$5 \cdot 10^3$	LP
10	10^4	H
10^4	100	H
10^4	500	H
10^4	$5 \cdot 10^3$	LP
10^4	10^4	H
10^8	100	H
10^8	500	H
10^8	$5 \cdot 10^3$	LP
10^8	10^4	H

Table B.3 Numerical corroboration of Fig. 2.12B

r_1	ε_r	output
0.5	10^{-4}	H
1	10^{-4}	LP
10	10^{-4}	LP
90	10^{-4}	LP
500	10^{-4}	H
100	10	LP
100	100	Pat
100	10^3	LP
100	$5 \cdot 10^3$	H
10^4	10	H
10^4	100	Pat
10^4	10^3	LP
10^4	$5 \cdot 10^3$	H
10^8	10	H
10^8	100	Pat
10^8	10^3	LP
10^8	$5 \cdot 10^3$	H

Table B.4 Numerical corroboration of Fig. 2.17B

r_1	ε_r	output
5	10^{-8}	H
20	10^{-8}	LP
500	10^{-8}	LP
10^3	10^{-8}	H
20	50	LP
20	10^3	H
500	10^{-3}	LP
500	10^{-2}	LP
500	1	H*
500	0.1	LP*
500	10	LP*
10^8	10^{-3}	H
10^8	10^{-2}	LP
10^8	10^2	LP
10^8	10^3	H

Table B.5 Numerical corroboration of Fig. 2.20B

r_1	ε_r	output
0.1	10^{-8}	H
1	10^{-8}	Pat
10	10^{-8}	Pat
500	10^{-8}	Pat
10^3	10^{-8}	Pat
500	10^{-3}	Pat
10^8	10^{-3}	Pat
1	10	Pat
10	10	Pat
500	10	Pat
10^3	10	Pat
10^8	10	Pat
500	10^4	Pat
10^8	10^4	Pat
500	10^4	H
10^8	10^4	H

Appendix C

Resumen

A continuación presentamos un breve resumen de los resultados originales presentados en esta Tesis y las perspectivas que se plantean a partir de ellos. Estos resultados son el producto de cuatro años de investigación llevados a cabo bajo la supervisión y asesoría de la Dra. Marta Ibañes Miguez y la tutoría del Profesor José María Sancho Herrero. A ambos quiero expresar mi más sincero agradecimiento por su dedicación en estos años de formación y trabajo académico.

Adicionalmente, quiero manifestar mi agradecimiento al Dr. Pau Formosa-Jordan por su colaboración y guía, especialmente durante los primeros años del doctorado. Junto a él estudiamos y discutimos el contenido presentado en los Capítulos 2 y 3. Asimismo, aprovecho para expresar mi agradecimiento al Profesor Fernando Giraldez de la Universidad Pompeu Fabra y a su grupo de investigación en el Parque de Investigación Biomédica de Barcelona. Junto a ellos discutimos los resultados presentados en los Capítulos 2 y 3 de esta Tesis.

C.1 Introducción

C.1.1 Contexto biológico

La comunicación inter-celular es un mecanismo mediante el cual las células interactúan y median respuestas coordinadas. Este proceso es de gran importancia durante el desarrollo, ya que la coordinación en los eventos de división y

diferenciación entre células es vital para la apropiada formación del organismo.

Existen diferentes tipos de comunicación intercelular. En esta Tesis nos hemos enfocado en estudiar la señalización yuxtacrina, en la cual las células se comunican mediante proteínas localizadas en la membrana celular. Debido a esta característica, la señalización yuxtacrina es un tipo de comunicación inter-celular de "corto alcance", en el cual una célula sólo se comunica con sus vecinas adyacentes. Sin embargo, este tipo de señalización es capaz de generar respuestas de "largo alcance". Cómo se genera este tipo de respuestas mediante interacciones locales, es una pregunta de gran interés tanto en física de sistemas alejados del equilibrio como en biología del desarrollo.

C.1.2 Aproximación matemática

La modelización matemática de los sistemas de señalización es cada vez más una herramienta relevante para entender procesos de coordinación y auto-organización durante el desarrollo de Metazoos.

Aunque existen diferentes ejemplos de señalización yuxtacrina, en esta Tesis nos hemos enfocado en el estudio de la vía de señalización de Notch. Notch es un receptor de membrana que al unir a su ligando, localizado en la membrana de células vecinas, libera una señal al citoplasma (señal de Notch) que posteriormente se traslada al núcleo donde regula la actividad transcripcional. Entre los diferentes genes que regula, la señal de Notch puede activar o reprimir la transcripción de los genes de los ligandos que unen a Notch en primera instancia. Este mecanismo establece un "feedback" en la activación de la señal de Notch entre células vecinas.

Modelos matemáticos de la vía de Notch han permitido establecer como éste tipo de señalización yuxtacrina puede mediar respuestas de largo alcance a nivel de tejidos, como por ejemplo la formación de patrones "salt-and-pepper" observados en tejidos y órganos neuro-sensoriales de vertebrados (Fig. C.1A) o la propagación expansiva de un estado de diferenciación celular (Fig. C.1B). Puesto que la vía de Notch es muy intrincada, se ha utilizado diferentes grados de abstracción de ésta vía con el fin de entender diferentes aspectos de las respuestas y estados que puede mediar a nivel inter-celular. En esta Tesis aplicamos esta estrategia para estudiar tres aspectos específicos asociados a Notch:

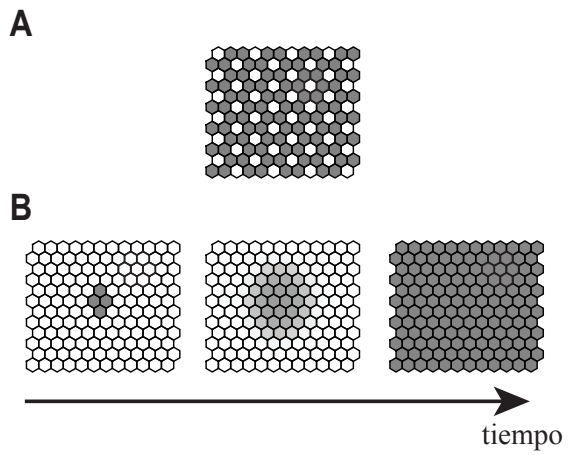

Figure C.1 Respuestas en un tejido mediadas por la vía de Notch. A) Patrón periódico salt-and-pepper. En gris y blanco se muestran dos tipos celulares diferentes. B) Propagación expansiva de un estado celular. La propagación ocurre desde un estado 1 (células blancas) hacia un estado 2 (células grises) tras una perturbación en el tejido (células grises en medio del array de la izquierda).

1. ¿Qué estados o respuestas surgen cuando Notch es activado por dos o más tipos de ligando diferentes?

2. ¿Qué efecto tiene la auto-activación de un gen asociado con la diferenciación celular y que es regulado por la señal de Notch, en la respuesta inter-celular mediada por la vía de Notch?

3. ¿Qué procesos pueden modular la eficiencia con la que un ligando activa la señal de Notch?

A continuación detallamos cada uno de estos frentes. En la Tesis, cada frente corresponde a un capítulo en la sección de resultados.

C.2 Resumen de los resultados y conclusiones

C.2.1 Respuestas funcionales en un sistema de comunicación inter-celular mediada por dos ligandos

C.2.1.1 Motivación

A nivel de tejido, hay dos tipos de estados o respuesta mediados por la vía de Notch, a saber, la formación de patrones salt-and-pepper y la propagación expansiva de un estado de diferenciación celular (Fig. C.1). Cuando Notch es activado por un único ligando, se ha establecido que cada tipo de respuesta es debido al tipo de regulación que Notch ejerce sobre la transcripción de ese ligando. Por lo tanto, cuando la transcripción del ligando es reprimida por la señal de Notch, se espera que se produzca un estado de patrón salt-and-pepper. Por el contrario, cuando la transcripción del ligando es activada por Notch, se espera la propagación expansiva de un estado de diferenciación celular.

Es bien sabido que Notch puede ser activado por diferentes tipos de ligando. Adicionalmente, se ha observado que en diferentes contextos durante el desarrollo de metazoos, diferentes tipos de ligando se co-expresan. Esto sugiere un escenario en el cual Notch pueda estar siendo activado por dos o más tipos de ligando a la vez. Puesto que (i) cada tipo de ligando que se co-expresa puede estar regulado de manera diferente por Notch y (ii) cada tipo de ligando puede tener una tasa efectiva de señalización diferente, ¿qué estados o respuestas surgen cuando Notch es activado por dos o más tipos de ligando diferentes?

C.2.1.2 Aproximación y resultados

Para estudiar este problema llevamos a cabo el análisis de un modelo de regulación Notch-ligandos en un tejido de células hexagonales. Para la formulación del modelo asumimos que el estado de cada célula puede ser descrito por tres variables (el nivel de actividad de los ligandos y el nivel de actividad de la señal de Notch), y consideramos funciones fenomenológicas para describir la regulación de la actividad de cada ligando, así como la activación de la señal de Notch. De esta forma, nuestro modelo es lo suficientemente sencillo para

hacer una análisis matemático de la estabilidad lineal de los estados estacionarios. Dicho análisis nos permite predecir en qué condiciones surge cada tipo de respuesta, i.e., la formación de patrones salt-and-pepper o la propagación expansiva de una estado de diferenciación celular. Por tanto, exploramos el espacio de parámetros del sistema para determinar el régimen en el que surge cada tipo de respuesta, las cuales corroboramos mediante simulaciones numéricas.

Estudiamos dos escenarios de activación de la señal de Notch. En uno, los ligandos usan recursos independientes para activar la señal. En el otro, los ligandos comparten recursos. Este último es compatible con el caso en el cual los dos tipos de ligando unen al mismo receptor Notch, tal como se ha observado *in vivo*. Para cada escenario estudiamos el caso en el que los tipos de ligando señalizan con la misma eficiencia (i.e., la tasa de señal máxima inducida por cada ligando cuando éste está expresado de manera aislada) o con eficiencia diferente. Asimismo, en cada escenario estudiamos diferentes tipos de regulación sobre los ligandos, i.e., ambos ligandos regulados equivalentemente (ya sean activados o inhibidos) y ambos ligandos regulados de forma opuesta (un tipo activado y el otro tipo inhibido).

Nuestros resultados muestran que cuando ambos tipos de ligando tienen la misma eficiencia de señalización, el régimen para el cual surge cada tipo de respuesta es el mismo en ambos escenarios (recursos independientes y recursos compartidos). Así, la formación de patrones salt-and-pepper bien puede estar mediada por cada ligando inhibido por la señal o por los dos simultáneamente y equivalentemente para la propagación expansiva de un estado de señalización celular. En este sentido, decimos que la respuesta del sistema está mediada de forma redundante por ambos tipos de ligando.

Sin embargo, cuando los dos tipos de ligando señalizan con diferente eficiencia, tal que uno de ellos es muy poco eficiente (i.e., su máxima tasa de señalización es muy baja comparada con la del otro ligando) entonces los resultados son muy diferentes para cada escenario. Primero, cuando los ligandos usan recursos independientes encontramos que el régimen de cada respuesta corresponde a aquel que esperaríamos en el caso en el que hay un único ligando. Puesto que la eficiencia de señalización del ligando es equivalente a la contribución del ligando para la formación de la señal y por tanto cuando ésta es muy baja se puede interpretar como que este ligando no está expresado.

Por otro lado, en el escenario en el que los ligandos usan recursos compartidos para señalizar, la eficiencia de señalización del ligando no es equivalente a la contribución del ligando para la formación de la señal. Cuando el ligando menos eficiente se co-expresa con el otro ligando, entonces ocurre una disminución en el nivel de señal de Notch que se produce. Por lo tanto, este ligando tiene un efecto negativo sobre la actividad de la señal. Este comportamiento hace que se generen respuestas inesperadas en el tejido. Principalmente, encontramos dos tipos de comportamiento. En el primero, el ligando menos eficiente produce un tipo de respuesta que no puede generar ninguno de los dos tipos de ligando expresados de manera aislada. Por ejemplo, cuando ambos ligandos son activados por la señal, el ligando menos eficiente facilita la formación de patrones salt-and-pepper. En el segundo, el ligando menos eficiente facilita la respuesta mediada por el otro ligando, pese a que esta respuesta puede ser incompatible con el tipo de regulación a la que está sujeto el ligando menos eficiente. Por ejemplo, encontramos que cuando el ligando menos eficiente es inhibido por la señal de Notch, mientras que el otro ligando es activado, entonces la respuesta de este último resulta altamente promovida si se compara con el caso en el que sólo hay un ligando expresado.

En resumen, nuestros resultados muestran que cuando la integración de estímulos ocurre de manera no aditiva (i.e., como en el escenario en el que los ligandos usan recursos independientes para señalizar) surgen propiedades emergentes en el sistema.

C.2.2 Inhibición lateral mediada por la vía de Notch y auto-activación de Atoh1

C.2.2.1 Motivación

Cuando la señal de Notch reprime la transcripción de su ligando, se dice que este ligando actúa mediando la inhibición lateral. Un ligando de este tipo es Delta1 (Dl1). Dl1 se expresa durante la etapa de diferenciación y maduración de células sensoriales en el oído interno de los vertebrados. La señal de Notch inhibe la transcripción de Dl1 mediante la represión directa de Atoh1. Atoh1 es un gen proneural necesario para la diferenciación de células sensoriales. Además,

Atoh1 activa la transcripción de Dl1 y su propia transcripción, de tal manera que genera un circuito de auto-regulación positiva.

Pese a que la auto-activación de Atoh1 se conserva en vertebrados y en Drosophila, típicamente los modelos de la vía de Notch no suelen tener en cuenta este diseño de auto-activación. Por lo tanto, nos preguntamos ¿qué efecto tiene la auto-activación de Atoh1 en la respuesta inter-celular mediada por la vía de Notch?

C.2.2.2 Aproximación y resultados

Para estudiar este problema, analizamos un modelo matemático considerando de forma explicita la dinámica de Atoh1. Estudiamos dos escenarios en los que tenemos en cuenta o no el motivo de auto-activación de Atoh1 y para diferentes niveles de acoplamiento entre células.

En todos los niveles de acoplamiento encontramos que en el caso con auto-activación de Atoh1 hay mayor multiestabilidad en el sistema, que cuando no hay auto-activación. Esto podría esperarse debido a que el motivo de auto-activación en si mismo (i.e., sin la inhibición lateral) implica bistabilidad. Una consecuencia de esta multiestabilidad añadida es que la diferenciación celular puede ser irreversible ante perturbaciones sobre los niveles de Dl1. Este resultado es novedoso ya que el modelo de inhibición lateral sin auto-activación de Atoh1 es sensible a sobre-expresión de Dl1. Cuando Dl1 se expresa de manera no controlada, se rompe el feedback y en consecuencia la formación de patrón asociada a la inhibición lateral no ocurre. Sin embargo, cuando hay auto-activación de Aoth1 el patrón periódico que se forma por inhibición lateral puede ser robusto a la sobre-expresión de Dl1. El mantenimiento del patrón ante perturbaciones en Dl1 ocurre debido a que la diferenciación de las células sensoriales se hace irreversible con la auto-activación.

Nuestro análisis permite entender resultados experimentales *in vivo* en los que se observa que ocasionalmente las células sensoriales no son inhibidas pese a que hay exceso de Dl1 en su entorno.

C.2.3 Estudio de un modelo detallado de la activación de la señal de Notch

C.2.3.1 Motivación

Los resultados descritos en el Capítulo 2 muestran la respuesta de un sistema en el que la señal de Notch es activada por dos tipos de ligando diferentes. Allí mostramos que cuando estos ligandos tienen diferente eficiencia de señalización, definiendo la eficiencia como la tasa máxima de señal producida por cada ligando cuando se expresa de forma aislada, surgen estados emergentes que no se esperan del escenario en el cual la señal de Notch es activada por un único ligando. Por tanto, nos preguntamos ¿qué procesos pueden modular la eficiencia con la que un ligando activa la señal de Notch?

El receptor Notch está sujeto a diversas modificaciones pos-transcripcionales. En particular, la glicosilación de Notch mediada por las proteínas Fringe se ha asociado a cambios en la tasa de señalización inducida por ligandos. El efecto de dicha glicosilación sobre la tasa de señalización inducida por cada tipo de ligando puede ser diferente. Además, se ha visto que Fringe puede modular el nivel de señal de Notch activado por cada tipo de ligando de forma dependiente o independiente de la afinidad de los ligandos por el receptor de Notch.

En el Capítulo 4 estudiamos los procesos que podrían estar implicados en el cambio de eficiencia de señalización, y que a su vez podrían estar siendo modulados por Fringe.

C.2.3.2 Aproximación y resultados

A diferencia de capítulos anteriores, en el Capítulo 4 proponemos un modelo en el cual describimos la activación de la señal de Notch mediada por dos ligandos con más detalle. Nos hemos enfocado en describir (i) la formación del complejo receptor-ligando y (ii) el procesamiento de dicho complejo hasta que se genera la señal de Notch. Básicamente , el procesamiento del complejo consiste en un cambio conformacional del complejo y la proteólisis del mismo, lo cual permite que se libere la porción citoplasmática que corresponde con la señal de Notch. Adicionalmente, consideramos interacciones en cis, i.e., la unión de los ligandos al receptor de Notch en una misma célula. Utilizamos este modelo para estudiar

la producción de señal mediada por los ligandos cuando el procesamiento de los complejos receptor-ligando es diferente para cada tipo de ligando, y cuando cada tipo de ligando une de forma diferente a Notch en cis y en trans. Este estudio lo llevamos a cabo en un sistema de dos células, tal que sólo en una de ellas se procesa el complejo para la producción de la señal.

Nuestros resultados muestran que cuando el procesamiento del complejo es más lento para uno de los ligandos, entonces su eficiencia de señalización en el estado estacionario (definida anteriormente) es más baja con relación al otro ligando. Una baja eficiencia de señalización relativa conduce a una disminución en el nivel de señal tras la sobre-expresión del ligando menos eficiente. Llamamos a este proceso "trans-inhibición" de la señal debido a que dicha inhibición ocurre por interacciones en trans (i.e., entre el receptor y el ligando de células diferentes). Nuestro análisis muestra que los cambios en la eficiencia de señalización ocurren sólo si hay degradación de los estados intermedios del complejo a lo largo de su procesamiento. Sin degradación, la eficiencia del ligando en el estado estacionario no cambia pese a que el procesamiento del complejo asociado sea muy lento.

Adicionalmente, encontramos que el rol del ligando, i.e., si es activador o inhibidor de la formación de la señal, puede cambiar en el tiempo. Así, un ligando que en el estado estacionario se espera que actúe como activador de la señal, puede actuar como inhibidor en estadios transitorios. Finalmente, nuestro análisis muestra que las interacciones en cis pueden modificar la eficiencia de señalización asociada a un tipo de ligando. Puesto que las interacciones en cis no conducen a la activación de la señal, la sobre-expresión de un ligando que une más en cis que otro conduce a una disminución en el nivel de señal de Notch producida.

Bibliography

J. Adam, A. Myat, I. Le Roux, M. Eddison, D. Henrique, D. Ish-Horowicz, and J. Lewis. Cell fate choices and the expression of notch, delta and serrate homologues in the chick inner ear: parallels with drosophila sense-organ development. *Development*, 125(23):4645–4654, 1998.

C. Akazawa, M. Ishibashi, C. Shimizu, S. Nakanishi, and R. Kageyama. A mammalian helix-loop-helix factor structurally related to the product of drosophila proneural gene atonal is a positive transcriptional regulator expressed in the developing nervous system. *Journal of Biological Chemistry*, 270(15):8730–8738, 1995.

B. Alberts, D. Bray, K. Hopkin, A. Johnson, J. Lewis, M. Raff, K. Roberts, and P. Walter. *Essential cell biology*. Garland Science, 2013.

U. Alon. *An introduction to systems biology: design principles of biological circuits*. CRC press, 2006.

P. Andersen, H. Uosaki, L. T. Shenje, and C. Kwon. Non-canonical notch signaling: emerging role and mechanism. *Trends in cell biology*, 22(5):257–265, 2012.

Å. Apelqvist, H. Li, L. Sommer, P. Beatus, D. J. Anderson, T. Honjo, M. H. de Angelis, U. Lendahl, and H. Edlund. Notch signalling controls pancreatic cell differentiation. *Nature*, 400(6747):877–881, 1999.

S. Artavanis-Tsakonas, M. D. Rand, and R. J. Lake. Notch signaling: cell fate control and signal integration in development. *Science*, 284(5415):770–776, 1999.

O. Barad, D. Rosin, E. Hornstein, and N. Barkai. Error minimization in lateral inhibition circuits. *Science signaling*, 3(129):ra51, 2010.

M. Baron. Endocytic routes to notch activation. In *Seminars in cell & developmental biology*, volume 23, pages 437–442. Elsevier, 2012.

B. L. Bassler. Small talk: cell-to-cell communication in bacteria. *Cell*, 109(4): 421–424, 2002.

R. Benedito, C. Roca, I. Sörensen, S. Adams, A. Gossler, M. Fruttiger, and R. H. Adams. The notch ligands dll4 and jagged1 have opposing effects on angiogenesis. *Cell*, 137(6):1124–1135, 2009.

N. A. Bermingham, B. A. Hassan, S. D. Price, M. A. Vollrath, N. Ben-Arie, R. A. Eatock, H. J. Bellen, A. Lysakowski, and H. Y. Zoghbi. Math1: an essential gene for the generation of inner ear hair cells. *Science*, 284(5421): 1837–1841, 1999.

W. J. Blake, M. Kærn, C. R. Cantor, and J. J. Collins. Noise in eukaryotic gene expression. *Nature*, 422(6932):633–637, 2003.

M. Boareto, M. K. Jolly, M. Lu, J. N. Onuchic, C. Clementi, and E. Ben-Jacob. Jagged–delta asymmetry in notch signaling can give rise to a sender/receiver hybrid phenotype. *Proceedings of the National Academy of Sciences*, page 201416287, 2015.

R. Brooker, K. Hozumi, and J. Lewis. Notch ligands with contrasting functions: Jagged1 and delta1 in the mouse inner ear. *Development*, 133(7):1277–1286, 2006.

K. Bruckner, L. Perez, H. Clausen, and S. Cohen. Glycosyltransferase activity of fringe modulates notch-delta interactions. *Nature*, 406(6794):411–414, 2000.

J. Cafaro, G. S. Lee, and J. S. Stone. Atoh1 expression defines activated progenitors and differentiating hair cells during avian hair cell regeneration. *Developmental Dynamics*, 236(1):156–170, 2007.

A. B. Chitnis. The role of notch in lateral inhibition and cell fate specification. *Molecular and Cellular Neuroscience*, 6(4):311–321, 1995.

E. Chrysostomou, J. E. Gale, and N. Daudet. Delta-like 1 and lateral inhibition during hair cell formation in the chicken inner ear: evidence against cis-inhibition. *Development*, 139(20):3764–3774, 2012.

M. Cohen, M. Georgiou, N. L. Stevenson, M. Miodownik, and B. Baum. Dynamic filopodia transmit intermittent delta-notch signaling to drive pattern refinement during lateral inhibition. *Developmental cell*, 19(1):78–89, 2010.

J. R. Collier, N. A. Monk, P. K. Maini, and J. H. Lewis. Pattern formation by lateral inhibition with feedback: a mathematical model of delta-notch intercellular signalling. *Journal of Theoretical Biology*, 183(4):429–446, 1996.

R. A. Cornell and J. S. Eisen. Notch in the pathway: the roles of notch signaling in neural crest development. In *Seminars in cell & developmental biology*, volume 16, pages 663–672. Elsevier, 2005.

M. Cross and H. Greenside. *Pattern formation and dynamics in nonequilibrium systems*. Cambridge University Press, 2009.

N. Daudet and J. Lewis. Two contrasting roles for notch activity in chick inner ear development: specification of prosensory patches and lateral inhibition of hair-cell differentiation. *Development*, 132(3):541–551, 2005.

W. de Back, J. X. Zhou, and L. Brusch. On the role of lateral stabilization during early patterning in the pancreas. *Journal of The Royal Society Interface*, 10 (79):20120766, 2013.

D. del Álamo, H. Rouault, and F. Schweisguth. Mechanism and significance of cis-inhibition in notch signalling. *Current Biology*, 21(1):R40–R47, 2011.

P. Doherty, J. Cohen, and F. S. Walsh. Neurite outgrowth in response to transfected n-cam changes during development and is modulated by polysialic acid. *Neuron*, 5(2):209–219, 1990.

B. D'souza, A. Miyamoto, and G. Weinmaster. The many facets of notch ligands. *Oncogene*, 27(38):5148–5167, 2008.

M. Eddison, I. Le Roux, and J. Lewis. Notch signaling in the development of the inner ear: lessons from drosophila. *Proceedings of the National Academy of Sciences*, 97(22):11692–11699, 2000.

M. Eddison, S. J. Weber, L. Ariza-McNaughton, J. Lewis, and N. Daudet. Numb is not a critical regulator of notch-mediated cell fate decisions in the developing chick inner ear. *Frontiers in cellular neuroscience*, 9, 2015.

F. Fagotto and B. M. Gumbiner. Cell contact-dependent signaling. *Developmental biology*, 180(2):445–454, 1996.

D. M. Fekete and D. K. Wu. Revisiting cell fate specification in the inner ear. *Current opinion in neurobiology*, 12(1):35–42, 2002.

A. Fischer and M. Gessler. Delta–notch—and then? protein interactions and proposed modes of repression by hes and hey bhlh factors. *Nucleic acids research*, 35(14):4583–4596, 2007.

U.-M. Fiuza, T. Klein, A. M. Arias, and P. Hayward. Mechanisms of ligand-mediated inhibition in Notch signaling activity in Drosophila. *Dev Dyn*, 239 (3):798–805, Mar 2010. doi: 10.1002/dvdy.22207.

P. Formosa Jordan. *Pattern formation through lateral inhibition mediated by Notch signaling*. PhD thesis, Universitat de Barcelona, 04 2013.

P. Formosa-Jordan and M. Ibañes. Diffusible ligand and lateral inhibition dynamics for pattern formation. *Journal of Statistical Mechanics: Theory and Experiment*, 2009(03):P03019, 2009.

P. Formosa-Jordan and M. Ibañes. Competition in notch signaling with cis enriches cell fate decisions. *PloS one*, 9(4):e95744, 2014.

P. Formosa-Jordan, M. Ibañes, S. Ares, and J.-M. Frade. Lateral inhibition and neurogenesis: novel aspects in motion. *International Journal of Developmental Biology*, 57(5):341–350, 2013.

M. E. Fortini. Notch signaling: the core pathway and its posttranslational regulation. *Developmental cell*, 16(5):633–647, 2009.

E. Frise, J. A. Knoblich, S. Younger-Shepherd, L. Y. Jan, and Y. N. Jan. The drosophila numb protein inhibits signaling of the notch receptor during cell-cell interaction in sensory organ lineage. *Proceedings of the National Academy of Sciences*, 93(21):11925–11932, 1996.

L. Gama-Norton, E. Ferrando, C. Ruiz-Herguido, Z. Liu, J. Guiu, A. B. M. M. K. Islam, S.-U. Lee, M. Yan, C. J. Guidos, N. López-Bigas, T. Maeda, L. Espinosa, R. Kopan, and A. Bigas. Notch signal strength controls cell fate in the haemogenic endothelium. *Nature Communications*, 6:8510, 2015. ISSN 2041-1723. doi: 10.1038/ncomms9510. URL http://www.nature.com/doifinder/10.1038/ncomms9510.

M. C. Gibson, A. B. Patel, R. Nagpal, and N. Perrimon. The emergence of geometric order in proliferating metazoan epithelia. *Nature*, 442(7106):1038–1041, 2006.

D. S. Glass, X. Jin, and I. H. Riedel-Kruse. Signaling delays preclude defects in lateral inhibition patterning. *Physical Review Letters*, 116(12):128102, 2016.

M. Glittenberg, C. Pitsouli, C. Garvey, C. Delidakis, and S. Bray. Role of conserved intracellular motifs in serrate signalling, cis-inhibition and endocytosis. *The EMBO journal*, 25(20):4697–4706, 2006.

R. Goodyear and G. Richardson. Pattern formation in the basilar papilla: evidence for cell rearrangement. *The Journal of neuroscience*, 17(16):6289–6301, 1997.

W. R. Gordon, B. Zimmerman, L. He, L. J. Miles, J. Huang, K. Tiyanont, D. G. McArthur, J. C. Aster, N. Perrimon, J. J. Loparo, et al. Mechanical allostery: evidence for a force requirement in the proteolytic activation of notch. *Developmental cell*, 33(6):729–736, 2015.

P. Gray and S. Scott. Sustained oscillations and other exotic patterns of behavior in isothermal reactions. *The Journal of Physical Chemistry*, 89(1):22–32, 1985.

J. B. Green and J. Sharpe. Positional information and reaction-diffusion: two big ideas in developmental biology combine. *Development*, 142(7):1203–1211, 2015.

T. Gridley. Notch signaling in vertebrate development and disease. *Molecular and Cellular Neuroscience*, 9(2):103–108, 1997.

K. Guruharsha, M. W. Kankel, and S. Artavanis-Tsakonas. The notch signalling system: recent insights into the complexity of a conserved pathway. *Nature Reviews Genetics*, 13(9):654–666, 2012.

C. Haddon, Y.-J. Jiang, L. Smithers, and J. Lewis. Delta-notch signalling and the patterning of sensory cell differentiation in the zebrafish ear: evidence from the mind bomb mutant. *Development*, 125(23):4637–4644, 1998.

N. Haines and K. D. Irvine. Glycosylation regulates notch signalling. *Nature reviews Molecular cell biology*, 4(10):786–797, 2003.

W. A. Harris. Cellular diversification in the vertebrate retina. *Current opinion in genetics & development*, 7(5):651–658, 1997.

B. H. Hartman, T. A. Reh, and O. Bermingham-McDonogh. Notch signaling specifies prosensory domains via lateral induction in the developing mammalian inner ear. *Proceedings of the National Academy of Sciences*, 107(36): 15792–15797, 2010.

C. Hicks, S. H. Johnston, et al. Fringe differentially modulates jagged1 and delta1 signalling through notch1 and notch2. *Nature Cell Biology*, 2(8):515–520, 2000.

K. Hori, A. Sen, T. Kirchhausen, and S. Artavanis-Tsakonas. Regulation of ligand-independent notch signal through intracellular trafficking. *Communicative & integrative biology*, 5(4):374–376, 2012.

T. L. Jacobsen, K. Brennan, A. M. Arias, and M. Muskavitch. Cis-interactions between delta and notch modulate neurogenic signalling in drosophila. *Development*, 125(22):4531–4540, 1998.

H. Jafar-Nejad, K. K. Norga, and H. J. Bellen. Numb:"adapting" notch for endocytosis. *Developmental cell*, 3(2):155–156, 2002.

A. P. Jarman, Y. Sun, L. Y. Jan, and Y. N. Jan. Role of the proneural gene, atonal, in formation of drosophila chordotonal organs and photoreceptors. *Development*, 121(7):2019–2030, 1995.

M. K. Jolly, M. Boareto, M. Lu, O. Jose'N, C. Clementi, and E. Ben-Jacob. Operating principles of notch–delta–jagged module of cell–cell communication. *New Journal of Physics*, 17(5):055021, 2015.

E. Karsenti. Self-organization in cell biology: a brief history. *Nature Reviews Molecular Cell Biology*, 9(3):255–262, 2008.

S. A. Kauffman. Self-organization, selective adaptation, and its limits: a new pattern of inference in evolution and development. *Neutral Models in Biology, ed. M. Nitecki, A. Hoffman*, pages 56–89, 1987.

S. A. Kauffman. *The origins of order: Self organization and selection in evolution*. Oxford University Press, USA, 1993.

M. W. Kelley. Regulation of cell fate in the sensory epithelia of the inner ear. *Nature Reviews Neuroscience*, 7(11):837–849, 2006.

A. E. Kiernan, N. Ahituv, H. Fuchs, R. Balling, K. B. Avraham, K. P. Steel, and M. H. de Angelis. The notch ligand jagged1 is required for inner ear sensory development. *Proceedings of the National Academy of Sciences*, 98 (7):3873–3878, 2001.

A. E. Kiernan, R. Cordes, R. Kopan, A. Gossler, and T. Gridley. The notch ligands dll1 and jag2 act synergistically to regulate hair cell development in the mammalian inner ear. *Development*, 132(19):4353–4362, 2005.

H. Kitano. Systems biology: a brief overview. *Science*, 295(5560):1662–1664, 2002.

H. Kitano et al. *Foundations of systems biology*. MIT press Cambridge, 2001.

S. Kondo and T. Miura. Reaction-diffusion model as a framework for understanding biological pattern formation. *science*, 329(5999):1616–1620, 2010.

R. Kopan and M. X. G. Ilagan. The canonical notch signaling pathway: unfolding the activation mechanism. *Cell*, 137(2):216–233, 2009.

E. C. Lai. Notch signaling: control of cell communication and cell fate. *Development*, 131(5):965–973, 2004.

A. Lakhanpal. *Experimental and theoretical studies of Notch signaling-mediated spatial pattern.* Dissertation (Ph.D.), California Institute of Technology., 2014.

P. J. Lanford, Y. Lan, R. Jiang, C. Lindsell, G. Weinmaster, T. Gridley, and M. W. Kelley. Notch signalling pathway mediates hair cell development in mammalian cochlea. *Nature genetics*, 21(3):289–292, 1999.

L. LeBon, T. V. Lee, D. Sprinzak, H. Jafar-Nejad, and M. B. Elowitz. Fringe proteins modulate notch-ligand cis and trans interactions to specify signaling states. *eLife*, 3:e02950, 2014.

J.-M. Lehn. Toward self-organization and complex matter. *Science*, 295(5564): 2400–2403, 2002.

E. B. Lewis. A gene complex controlling segmentation in drosophila. In *Genes, Development and Cancer*, pages 205–217. Springer, 1978.

Z. Liu, Z. Liu, B. J. Walters, T. Owen, R. Kopan, and J. Zuo. In vivo visualization of notch1 proteolysis reveals the heterogeneity of notch1 signaling activity in the mouse cochlea. *PloS one*, 8(5):e64903, 2013.

F. Livesey and C. Cepko. Vertebrate neural cell-fate determination: lessons from the retina. *Nature Reviews Neuroscience*, 2(2):109–118, 2001.

A. Louvi and S. Artavanis-Tsakonas. Notch signalling in vertebrate neural development. *Nature Reviews Neuroscience*, 7(2):93–102, 2006.

D. K. Lubensky, M. W. Pennington, B. I. Shraiman, and N. E. Baker. A dynamical model of ommatidial crystal formation. *Proceedings of the National Academy of Sciences*, 108(27):11145–11150, 2011.

L. J. Manderfield, F. A. High, K. A. Engleka, F. Liu, L. Li, S. Rentschler, and J. A. Epstein. Notch activation of jagged1 contributes to the assembly of the arterial wall. *Circulation*, 125(2):314–323, 2012.

L. Marcon and J. Sharpe. Turing patterns in development: what about the horse part? *Current opinion in genetics & development*, 22(6):578–584, 2012.

T. Marquardt and P. Gruss. Generating neuronal diversity in the retina: one for nearly all. *Trends in neurosciences*, 25(1):32–38, 2002.

J. Massague and A. Pandiella. Membrane-anchored growth factors. *Annual review of biochemistry*, 62(1):515–541, 1993.

M. Matsuda, M. Koga, E. Nishida, and M. Ebisuya. Synthetic signal propagation through direct cell-cell interaction. *Science signaling*, 5(220):ra31, 2012.

M. Matsuda, M. Koga, K. Woltjen, E. Nishida, and M. Ebisuya. Synthetic lateral inhibition governs cell-type bifurcation with robust ratios. *Nature communications*, 6, 2015.

M. A. McGill and C. J. McGlade. Mammalian numb proteins promote notch1 receptor ubiquitination and degradation of the notch1 intracellular domain. *Journal of Biological Chemistry*, 278(25):23196–23203, 2003.

L. Meloty-Kapella, B. Shergill, J. Kuon, E. Botvinick, and G. Weinmaster. Notch ligand endocytosis generates mechanical pulling force dependent on dynamin, epsins, and actin. *Developmental cell*, 22(6):1299–1312, 2012.

M. B. Miller and B. L. Bassler. Quorum sensing in bacteria. *Annual Reviews in Microbiology*, 55(1):165–199, 2001.

B. B. Millimaki, E. M. Sweet, M. S. Dhason, and B. B. Riley. Zebrafish atoh1 genes: classic proneural activity in the inner ear and regulation by fgf and notch. *Development*, 134(2):295–305, 2007.

H. Momiji and N. A. Monk. Oscillatory notch-pathway activity in a delay model of neuronal differentiation. *Physical Review E*, 80(2):021930, 2009.

A. Morrison, C. Hodgetts, A. Gossler, M. H. de Angelis, and J. Lewis. Expression of delta1 and serrate1 (jagged1) in the mouse inner ear. *Mechanisms of development*, 84(1):169–172, 1999.

G. B. Müller and S. A. Newman. *Origination of organismal form: beyond the gene in developmental and evolutionary biology*. MIT Press, 2003.

J. D. Murray. *Mathematical Biology. II Spatial Models and Biomedical Applications {Interdisciplinary Applied Mathematics V. 18}*. Springer-Verlag New York Incorporated, 2001.

J. Neves, C. Parada, M. Chamizo, and F. Giráldez. Jagged 1 regulates the restriction of sox2 expression in the developing chicken inner ear: a mechanism for sensory organ specification. *Development*, 138(4):735–744, 2011.

J. Neves, G. Abelló, J. Petrovic, and F. Giraldez. Patterning and cell fate in the inner ear: a case for Notch in the chicken embryo. *Development, growth & differentiation*, dec 2012. ISSN 1440-169X. URL papers://30dd8192-3a85-4010-af1a-3e33b620a902/Paper/p7337.

J. Neves, G. Abelló, J. Petrovic, and F. Giraldez. Patterning and cell fate in the inner ear: a case for notch in the chicken embryo. *Development, growth & differentiation*, 55(1):96–112, 2013a.

J. Neves, I. Vachkov, and F. Giraldez. Sox2 regulation of hair cell development: incoherence makes sense. *Hearing research*, 297:20–29, 2013b.

J. T. Nichols, A. Miyamoto, S. L. Olsen, B. D'Souza, C. Yao, and G. Weinmaster. Dsl ligand endocytosis physically dissociates notch1 heterodimers before activating proteolysis can occur. *The Journal of cell biology*, 176(4):445–458, 2007.

G. Nicolis, I. Prigogine, and G. Nocolis. *Exploring complexity*. WH Freeman & Company, 1989.

M. R. Owen, J. A. Sherratt, and H. J. Wearing. Lateral induction by juxtacrine signaling is a new mechanism for pattern formation. *Developmental biology*, 217(1):54–61, 2000.

K. Painter, P. Maini, and H. Othmer. Stripe formation in juvenile pomacanthus explained by a generalized turing mechanism with chemotaxis. *Proceedings of the National Academy of Sciences*, 96(10):5549–5554, 1999.

V. M. Panin, V. Papayannopoulos, R. Wilson, and K. D. Irvine. Fringe modulates notch-ligand interactions. *Nature*, 387(6636):908–912, 1997.

A. L. Parks, K. M. Klueg, J. R. Stout, and M. Muskavitch. Ligand endocytosis drives receptor dissociation and activation in the notch pathway. *Development*, 127(7):1373–1385, 2000.

B. M. Pers, S. Krishna, S. Chakraborty, S. Pigolotti, V. Sekara, S. Semsey, and M. H. Jensen. Effects of growth and mutation on pattern formation in tissues. *PloS one*, 7(11), 2012.

J. Petrovic, P. Formosa-Jordan, J. C. Luna-Escalante, G. Abelló, M. Ibañes, J. Neves, and F. Giraldez. Ligand-dependent notch signaling strength orchestrates lateral induction and lateral inhibition in the developing inner ear. *Development*, 141(11):2313–2324, 2014.

J. O. Pickles and W. R. van Heumen. Lateral interactions account for the pattern of the hair cell array in the chick basilar papilla. *Hearing research*, 145(1):65–74, 2000.

K. Preuße, L. Tveriakhina, K. Schuster-Gossler, C. Gaspar, A. I. Rosa, D. Henrique, A. Gossler, and M. Stauber. Context-Dependent Functional Divergence of the Notch Ligands DLL1 and DLL4 In Vivo. *PLOS Genetics*, 11(6): e1005328, 2015. ISSN 1553-7404. doi: 10.1371/journal.pgen.1005328. URL http://dx.plos.org/10.1371/journal.pgen.1005328.

I. Prigogine. Exploring complexity. *European Journal of Operational Research*, 30(2):97–103, 1987.

F. Radtke, A. Wilson, and H. R. MacDonald. Notch signaling in t-and b-cell development. *Current opinion in immunology*, 16(2):174–179, 2004.

M. S. Rhyu, L. Y. Jan, and Y. N. Jan. Asymmetric distribution of numb protein during division of the sensory organ precursor cell confers distinct fates to daughter cells. *Cell*, 76(3):477–491, 1994.

J.-Y. Roignant and J. E. Treisman. Pattern formation in the drosophila eye disc. *The International journal of developmental biology*, 53(5-6):795, 2009.

K. Sakamoto, O. Ohara, M. Takagi, S. Takeda, and K. Katsube. Intracellular cell-autonomous association of Notch and its ligands: A novel mechanism of Notch signal modification. *Dev Biol*, 241(2):313–326, Jan 2002. doi: 10.1006/dbio.2001.0517.

S. S. Saravanamuthu, C. Y. Gao, and P. S. Zelenka. Notch signaling is required for lateral induction of Jagged1 during FGF-induced lens fiber differentiation. *Developmental Biology*, 332(1):166–176, 2009. ISSN 00121606. doi: 10.1016/j.ydbio.2009.05.566. URL http://linkinghub.elsevier.com/retrieve/pii/S001216060900894X.

F. Schweisguth. Regulation of notch signaling activity. *Current biology*, 14(3): R129–R138, 2004.

O. Shaya and D. Sprinzak. From notch signaling to fine-grained patterning: Modeling meets experiments. *Current opinion in genetics & development*, 21 (6):732–739, 2011.

H. Shimizu, S. A. Woodcock, M. B. Wilkin, B. Trubenová, N. A. M. Monk, and M. Baron. Compensatory flux changes within an endocytic trafficking network maintain thermal robustness of notch signaling. *Cell*, 157(5):1160–74, May 2014. doi: 10.1016/j.cell.2014.03.050.

K. Shimizu, S. Chiba, T. Saito, K. Kumano, T. Takahashi, and H. Hirai. Manic fringe and lunatic fringe modify different sites of the notch2 extracellular region, resulting in different signaling modulation. *Journal of Biological Chemistry*, 276(28):25753–25758, 2001.

A. B. Singh and R. C. Harris. Autocrine, paracrine and juxtacrine signaling by egfr ligands. *Cellular signalling*, 17(10):1183–1193, 2005.

E. Smith and H. J. Morowitz. Universality in intermediary metabolism. *Proceedings of the National Academy of Sciences of the United States of America*, 101(36):13168–13173, 2004.

D. Sprinzak, A. Lakhanpal, L. LeBon, L. A. Santat, M. E. Fontes, G. A. Anderson, J. Garcia-Ojalvo, and M. B. Elowitz. Cis-interactions between notch and delta generate mutually exclusive signalling states. *Nature*, 465(7294): 86–90, 2010.

D. Sprinzak, A. Lakhanpal, L. LeBon, J. Garcia-Ojalvo, and M. B. Elowitz. Mutual inactivation of notch receptors and ligands facilitates developmental patterning. *PLoS computational biology*, 7(6):e1002069, 2011.

P. Stanley. Regulation of notch signaling by glycosylation. *Current opinion in structural biology*, 17(5):530–535, 2007.

S. H. Strogatz. *Nonlinear dynamics and chaos: with applications to physics, biology, chemistry, and engineering*. Westview press, 2014.

P. Taylor, H. Takeuchi, D. Sheppard, C. Chillakuri, S. M. Lea, R. S. Haltiwanger, and P. A. Handford. Fringe-mediated extension of o-linked fucose in the ligand-binding region of notch1 increases binding to mammalian notch ligands. *Proceedings of the National Academy of Sciences*, 111(20):7290–7295, 2014.

L. A. Timmerman, J. Grego-Bessa, A. Raya, E. Bertrán, J. M. Pérez-Pomares, J. Díez, S. Aranda, S. Palomo, F. McCormick, J. C. Izpisúa-Belmonte, et al. Notch promotes epithelial-mesenchymal transition during cardiac development and oncogenic transformation. *Genes & development*, 18(1):99–115, 2004.

A. M. Turing. The chemical basis of morphogenesis. *Philosophical Transactions of the Royal Society of London B: Biological Sciences*, 237(641):37–72, 1952.

K. L. VanDussen, A. J. Carulli, T. M. Keeley, S. R. Patel, B. J. Puthoff, S. T. Magness, I. T. Tran, I. Maillard, C. Siebel, Å. Kolterud, et al. Notch signaling modulates proliferation and differentiation of intestinal crypt base columnar stem cells. *Development*, 139(3):488–497, 2012.

H. Wearing, M. Owen, and J. Sherratt. Mathematical modelling of juxtacrine patterning. *Bulletin of Mathematical Biology*, 62(2):293–320, 2000.

S. D. Webb and M. R. Owen. Oscillations and patterns in spatially discrete models for developmental intercellular signalling. *Journal of mathematical biology*, 48(4):444–476, 2004.

M. Wilkin, P. Tongngok, N. Gensch, S. Clemence, M. Motoki, K. Yamada, K. Hori, M. Taniguchi-Kanai, E. Franklin, K. Matsuno, et al. Drosophila hops and ap-3 complex genes are required for a deltex-regulated activation of notch in the endosomal trafficking pathway. *Developmental cell*, 15(5): 762–772, 2008.

L.-T. Yang, J. T. Nichols, C. Yao, J. O. Manilay, E. A. Robey, and G. Weinmaster. Fringe glycosyltransferases differentially modulate notch1 proteolysis induced by delta1 and jagged1. *Molecular biology of the cell*, 16(2):927–942, 2005.

N. Zhang, G. V. Martin, M. W. Kelley, and T. Gridley. A mutation in the lunatic fringe gene suppresses the effects of a jagged2 mutation on inner hair cell development in the cochlea. *Current Biology*, 10(11):659–662, 2000.

J. L. Zheng, J. Shou, F. Guillemot, R. Kageyama, and W.-Q. Gao. Hes1 is a negative regulator of inner ear hair cell differentiation. *Development*, 127(21): 4551–4560, 2000.

G. Zimmerman, D. Lorant, T. McIntyre, and S. Prescott. Juxtacrine intercellular signaling: another way to do it. *American journal of respiratory cell and molecular biology*, 9(6):573–577, 1993.

A. Zine. Molecular mechanisms that regulate auditory hair-cell differentiation in the mammalian cochlea. *Molecular neurobiology*, 27(2):223–237, 2003.

A. Zine, T. R. Van De Water, and F. de Ribaupierre. Notch signaling regulates the pattern of auditory hair cell differentiation in mammals. *Development*, 127(15):3373–3383, 2000.